

A Thesis Submitted for the Degree of PhD at the University of Warwick

Permanent WRAP URL:

<http://wrap.warwick.ac.uk/108029>

Copyright and reuse:

This thesis is made available online and is protected by original copyright.

Please scroll down to view the document itself.

Please refer to the repository record for this item for information to help you to cite it.

Our policy information is available from the repository home page.

For more information, please contact the WRAP Team at: wrap@warwick.ac.uk

COORDINATION STUDIES OF THE HALIDES OF GROUPS (IV), (V) AND (VI)

By

STEVEN RONALD WADE B.Sc

Submitted to the University of Warwick in partial fulfilment of the
degree of Doctor of Philosophy.

September 1980



713013

To my Mother and Father

Parts of the work contained in this thesis have been published in the scientific literature with the following references:-

- S. R. Wade and G. R. Willey, *Inorg. Nucl. Chem. Lett.*, 1978, 14, 363.
- S. R. Wade and G. R. Willey, *Inorg. Chim. Acta*, 1979, 35, 61.
- S. R. Wade and G. R. Willey, *J. Less-Common. Met.*, 1979, 68, 105.
- S. R. Wade and G. R. Willey, *J. Inorg. Nucl. Chem.*, 1980, 42, 113.
- S. R. Wade and G. R. Willey, *Inorg. Chim. Acta*, 1980, in press.
- S. R. Wade and G. R. Willey, *J. Inorg. Nucl. Chem.*, 1980, in press.

ABSTRACT

The donor-acceptor chemistry of some Groups (IV), (V) and (VI) halides was investigated with a number of ligands.

Trimethylamine provided donor complexes with Hf (IV), Mo (V), Mo (II), As (III) and Sb (III) halides. With Cp_2TiCl_2 , MoOCl_4 and AuCl_3 trimethylamine was found to act as a reducing agent. The use of $\text{MCl}_4 \cdot 2\text{NMe}_3$ (M = Zr, Hf) adducts as intermediates in complex synthesis was briefly studied, and the Me_6tren adducts $(\text{MCl}_2\text{Me}_6\text{tren})^{2+}2\text{Cl}^-$ (M = Ti, Zr, Hf) isolated.

Hexamethylphosphoramide (HMPA) gave adducts with both M (IV) (M = Ti, Zr, Hf, Sn) and M (III) (M = Ti, V, Cr) chlorides. From the $\text{TiCl}_4/\text{HMPA}$ system, adducts of 2:1, 1:1 and 1:2 stoichiometries were isolated. $\text{CrCl}_3 \cdot 3\text{HMPA}$ was isolated as both fac and mer isomers. The $(\text{Me}_2\text{N})_x\text{Cl}_{3-x}\text{PS}$ (x = 1, 2, 3) series are much weaker donors than HMPA, although they provided a number of adducts with hard Lewis acids. Changes in the electronic structure of the phosphoryl and thiophosphoryl ligands that occur on complexation were examined by ^1H , ^{13}C , ^{31}P and IR spectroscopy.

$(\text{Me}_2\text{N})_2\text{CH}_2$ and bis(diphenylphosphino)methane gave 1:1 adducts with M(IV) halides. The dominant reaction in the $\text{CpTi}(\text{NMe}_2)_3$ and $\text{Cp}_2\text{Zr}(\text{NMe}_2)_2/\text{MX}_4$ systems, however, was group exchange to give the respective CpM halides. $\text{Me}_2\text{Si}(\text{NMe}_2)_2$ gave both 1:1 adducts (M (IV) = Ti, Zr, Hf, Sn) and group exchange (M = Si, Ge, Ti). The donor-acceptor chemistry of $\text{Me}_2\text{SiCl}(\text{NMe}_2)$ and $\text{Cl}_3\text{Ti}(\text{NMe}_2)$ was briefly studied, and was found to be dominated by disproportionation.

$(\text{CH}_2\text{O})_3$ and $(\text{CH}_2\text{S})_3$ act as weak monodentate donors towards hard M (IV) acids. Dynamic behaviour in the $\text{SnCl}_4 \cdot 2(\text{CH}_2\text{S})_3$ system was investigated by ^1H NMR and interpreted in terms of both ring inversion and donor-site interchange. $(\text{MeBNMe})_3$ was found to act as a bridging bidentate σ -donor in $(\text{MeBNMe})_3 \cdot 2\text{TiCl}_4$.

The substituted oxamides $(\text{CONHR})_2$ (R = Me, Et), thiooxamides $(\text{CSNHR})_2$ (R = Me, Et) and malonamide $\text{CH}_2(\text{CONHMe})_2$ act as chelating OO or SS donors towards MCl_4 (M = Ti, Sn). IR and ^1H NMR evidence suggests that the S donor ligands are more strongly bonded than their O counterparts.

C O N T E N T S

	<u>Page</u>
<u>ABSTRACT</u>	
<u>CHAPTER 1 - INTRODUCTION</u>	
1.1 The Early Transition Metals	1
1.2 Structure and Reactivity of the Early t-Metals	4
1.3 Coordination Chemistry of the Early t-Metals	20
1.4 Halides and Complexes of Group IVB and Group VB	28
 <u>CHAPTER 2 - COMPLEXES AND REACTIONS OF TRIMETHYLAMINE</u>	
2.1 Introduction	31
2.2 Reactions of HfX_4 ($\text{X} = \text{Br}, \text{I}$) and ZrCl_4 with NMe_3	34
2.3 Reactions of NMe_3 with Cp_2MCl_2 ($\text{M} = \text{Ti}, \text{Zr}, \text{Hf}$)	36
2.4 Reactions of NMe_3 with some Group VB Halides	37
2.5 NMe_3 Complexes of some Halides and Oxyhalides of Mo	40
2.5.1 Reactions of NMe_3 with MoCl_3 and MoCl_4	40
2.5.2 Reactions of MoOCl_3 , MoOCl_4 and NMe_3	42
2.6 Reactions of NMe_3 with Zirconium Trihalides	45
2.7 Reaction of NMe_3 with AuCl_3	46
2.8 Ligand Exchange Reactions of NMe_3 Complexes	47
2.8.1 Substitution reactions of $\text{MCl}_4 \cdot 2\text{NMe}_3$ ($\text{M} = \text{Zr}, \text{Hf}$)	47
2.8.2 Complexes of MCl_4 ($\text{M} = \text{Ti}, \text{Zr}, \text{Hf}$) with tren and Me_6tren	48
2.9 Experimental	51
 <u>CHAPTER 3 - COMPLEX CHEMISTRY OF DIMETHYLAMINO SUBSTITUTED PHOSPHINE CHALCONIDES</u>	
3.1 Introduction	62
3.2 Complexes of Hexamethylphosphoramide (HMPA)	68

	<u>Page</u>
3.2.1 Adducts of $(\text{NMe}_2)_3\text{PO}$ with MCl_4 ($\text{M} = \text{Ti}, \text{Sn}, \text{Zr}$ and Hf) and SnI_4	68
3.2.2 $\text{MCl}_3 \cdot 3\text{HMPA}$ complexes ($\text{M} = \text{Ti}, \text{V}, \text{Cr}$)	76
3.3.1 Complexes and reactions of $(\text{NMe}_2)_x\text{Cl}_{3-x}\text{PS}$ ($x = 1, 2, 3$) with metal chlorides	80
3.3.2 Complexes with SnCl_4 , ZrCl_4 , HfCl_4 and SbCl_5	81
3.3.3 Reaction of $(\text{NMe}_2)_2\text{ClPS}$ with BCl_3	93
3.4 Experimental	95

CHAPTER 4 - COMPLEXATION AND EXCHANGE REACTIONS OF SOME DIMETHYLAMINO SUBSTITUTED GROUP (IV) COMPOUNDS

4.1 Introduction	102
4.2 Complexes of $(\text{Me}_2\text{N})_2\text{CH}_2$ with MCl_4 ($\text{M} = \text{Ti}, \text{Sn}$), VCl_3 and $\text{CrCl}_3 \cdot 2\text{NMe}_3$	110
4.3 Reaction of bis(diphenylphosphino)methane (dpm) with TiCl_4	112
4.4.1 Exchange reactions between $\text{Me}_2\text{Si}(\text{NMe}_2)_2$ and MCl_4 ($\text{M} = \text{Si}, \text{Ge}$)	115
4.4.2 Exchange reaction between $\text{Me}_2\text{Si}(\text{NMe}_2)_2$ and TiCl_4	118
4.4.3 Mechanism of Si-N bond cleavage	119
4.5 Complexes of $\text{Me}_2\text{Si}(\text{NMe}_2)_2$ with MX_4 ($\text{M} = \text{Ti}, \text{Zr}, \text{Hf}, \text{X} = \text{Cl},$ $\text{M} = \text{Sn}, \text{X} = \text{Cl}, \text{Br}$)	121
4.6 Reactions of $\text{Me}_2\text{SiCl}(\text{NMe}_2)$ with MCl_4 ($\text{M} = \text{Sn}, \text{Ti}$)	125
4.7 Reaction of $\text{Cl}_3\text{TiNMe}_2$ with MCl_4 ($\text{M} = \text{Si}, \text{Ge}, \text{Sn}, \text{Ti}$) and Donor Solvents	127
4.8 Exchange Reactions between $\text{CpTi}(\text{NMe}_2)_3$ and $\text{Cp}_2\text{Zr}(\text{NMe}_2)_2$ with some Covalent Metal Tetrahalides	128
4.8.1 Reaction of Cp_2TiCl_2 with Me_2NLi	128
4.8.2 Reaction of $\text{CpTi}(\text{NMe}_2)_3$ and $\text{Cp}_2\text{Zr}(\text{NMe}_2)_2$ with MCl_4 ($\text{M} = \text{Si}, \text{Ge},$ $\text{Sn}, \text{Ti}, \text{Zr}, \text{Hf}$)	129
4.9 Experimental	131

CHAPTER 5 - SOME COMPLEX CHEMISTRY OF INORGANIC HETEROCYCLES

5.1	Introduction	146
5.1.1	Bonding in inorganic heterocycles	146
5.1.2	Donor chemistry of alternation heterocycles	150
5.2.1	Reactions of $(CH_2O)_3$ with MCl_4 ($M = Ti, Sn$) and $ZrCl_4 \cdot 2NMe_3$	153
5.2.2	Reaction of $(CH_2O)_3$ with $MCl_3 \cdot 2NMe_3$ ($M = V, Cr$)	154
5.3	Complexes of $(CH_2S)_3$ with Covalent Metal Chlorides	155
5.4	Reactions of $(Me_2SiO)_{3,4}$ with some Covalent Metal Halides	163
5.5	Complexes of Hexamethylborazine with Covalent Metal Halides	164
5.6	Comments on the Synthesis of $(R_2TiPR^*)_x$	167
5.7	Experimental	170

CHAPTER 6 - COMPLEXES OF SUBSTITUTED OXAMIDES, THIOOXAMIDES AND MALONAMIDES WITH METAL TETRAHALIDES

6.1	Introduction	176
6.2	Complexes of Substituted Oxamides, Thiooxamides and Malonamides with MCl_4 ($M = Ti, Sn$)	179
6.3	Experimental	186

APPENDIX A	189
------------	-----

APPENDIX B	197
------------	-----

REFERENCES	203-221
------------	---------

ACKNOWLEDGEMENTS

I would like to express my thanks to Dr G. R. Willey for his continued help and encouragement in the three years (1976-1979) during which the work described in this thesis was undertaken.

I would like to thank the technical staff of the University of Warwick for their assistance, in particular the glass-blowing department under the direction of Mr E. Burgess for an inexhaustible supply of 'pigs'. The contributions of Mr D. Rylance and Mlle. C. Mabillard who assisted in the work described in Chapter 6 as part of a third year project, are acknowledged.

A very special thankyou goes to Ms. Vicki Narbett for the typing of this manuscript.

A postgraduate award from the Science Research Council is also gratefully acknowledged.

T A B L E S

CHAPTER 1

Table 1.3.1	p.21	Classification of Bases
Table 1.3.2	p.21	Classification of Lewis Acids
Table 1.3.3	p.22	Heats of Formation of $MX_4 + 2L \rightarrow MX_4 \cdot 2L$ in Standard States
Table 1.4.1	p.29	Donor Numbers of some Selected Ligands

CHAPTER 2

Table 2.4.1	p.38	NMR Data for $MX_3 \cdot NMe_3$ and $MX_3 \cdot 2NMe_3$
-------------	------	---

CHAPTER 3

Table 3.1.1	p.64	Vertical Ionisation Energies for $(NMe_2)_x Cl_{3-x} PO(S)$
Table 3.1.2	p.65	Thermodynamic Data for $(Me_2N)_3PY + I_2$
Table 3.1.3	p.66	Selected σ -Phosphoryl Substituent Constants
Table 3.1.4	p.66	Thermodynamic Data for the Reaction $(NMe_2)_x Cl_{3-x} PO(S) + I_2 \rightleftharpoons (NMe_2)_x Cl_{3-x} PO(S) \cdot I_2$
Table 3.2.1	p.70	IR Spectra of M(IV) HMPA Adducts
Table 3.2.2	p.73	Low IR Spectra of some Sn (IV) Species
Table 3.2.3	p.74	NMR Data for M (IV) HMPA Complexes
Table 3.2.4	p.78	IR Spectra of M (III).HMPA Adducts
Table 3.3.1	p.83/4	IR Spectral Data of $(NMe_2)_3PS$ Complexes
Table 3.3.2	p.86/7	IR Spectral Data of $(NMe_2)_2ClPS$ Complexes
Table 3.3.3	p.89	1H and ^{31}P Spectra of the $(NMe_2)_3PS$ and $(NMe_2)_2ClPS$ Complexes. ($MeNO_2$ soln., $T = 298 K$)

CHAPTER 4

Table 4.1.1	p.104	IR Shifts of the $\nu(C-D)$ Band for some $CDCl_3$ /Amine Mixtures
-------------	-------	--

Table 4.1.2	p.104	Heats of Mixing for some CHCl_3 /Amine Systems
Table 4.1.3	p.105	^{13}C -H Coupling Constants for Selected Amines
Table 4.4.1	p.116	220 MHz ^1H NMR Chemical Shift Data for Various Silanes, Aminosilanes and Aminogermanes (2%, C_6D_6)
Table 4.5.1	p.124	^1H NMR Spectra of $\text{MX}_4\cdot\text{L}$ (220 MHz in C_6D_6) (Relative Intensities given in brackets)

CHAPTER 5

Table 5.8.1	p.157	IR Spectra of $(\text{CH}_2\text{S})_3$ Adducts
-------------	-------	---

CHAPTER 6

Table 6.2.1	p.181	Principle IR Bands of $\text{MCl}_4\cdot\text{B}$ Complexes
Table 6.2.2	p.184	^1H NMR Spectra of $\text{MCl}_4\cdot\text{B}$, $\text{CD}_3\text{NO}_2/\text{TMS}$ 90 MHz)
Table 6.2.3	p.185	^{13}C NMR Shift Data of the Ligands (a) CD_3OD and (b) CDCl_3
Table 6.3.1	p.188	Analytical Data of $\text{MCl}_4\cdot\text{B}$ Complexes

FIGURES

CHAPTER 1

Fig. 1.2.1	p.7	$M_6X_8(a)$ and $M_6X_{12}(b)$ Metal Cluster Centres
Fig. 1.2.2	p.9	Crystal Structure of $NbCl_5$
Fig. 1.2.3	p.10	Crystal Structure of $ZrCl_4$
Fig. 1.2.4	p.11	Structure of $NbCl_4$ (39)
Fig. 1.2.5	p.12	Structural Units of (a) β - $TiCl_4$ and (b) α , γ and δ $TiCl_3$
Fig. 1.2.6	p.14	Crystal Structure of Nb_3Cl_8
Fig. 1.2.7	p.15	Schematic Representation of a Sheet of $(MoCl_2)Cl_{8/2}$ Octahedra Showing Short (—) and long (---) Mo-Mo Bonds
Fig. 1.2.8	p.15	Crystal Structure of $MoBr_3$
Fig. 1.2.9	p.16	Structure of WCl_3 (50)
Fig. 1.2.10	p.17	The Cadmium Diiodide Structure
Fig. 1.2.11	p.18	Unit Cell of $CrCl_2$ Showing Short (2.39 Å) and Long (2.93 Å) Cr-Cl Bonds (53)
Fig. 1.2.12	p.19	Crystal Structure of $ZrCl$
Fig. 1.3.1	p.25	Crystal Structures of $TiCl_4 \cdot 2POCl_3$ (83) and $(TiCl_4 \cdot POCl_3)_2$ (87)
Fig. 1.3.2	p.27	Schematic Structure of $TiCl_4 \cdot 2diars$
Fig. 1.4	p.30	Usual Geometries of Group VB Halide Adducts

CHAPTER 2

Fig. 2.1.1	p.32	X-ray Structure of $CrCl_3 \cdot 2NMe_3$ (69, 78)
Fig. 2.4.1	p.39	Proposed Geometries of $AsBr_3 \cdot NMe_3$ and $SbX_3 \cdot 2NMe$ (X = Cl, Br)
Fig. 2.4.2	p.40	Proposed Structure of $SbX_3 \cdot NMe_3$ (X = Cl, Br)
Fig. 2.5.1	p.42	Possible Structures for $MoCl_2 \cdot 2NMe_3$

Fig. 2.5.2	p.43	Possible Structures of $\text{MoOCl}_3 \cdot 2\text{NMe}_3$
Fig. 2.7.1	p.47	Reaction Scheme for $\text{AuCl}_3 + \text{NMe}_3 \rightarrow \text{Au}$
Fig. 2.8.1	p.50	Proposed Structure of $\text{MCl}_4 \cdot \text{Me}_6\text{tren}$

CHAPTER 3

Fig. 3.1.1	p.63	X-ray Crystal Structures of $(\text{H}_2\text{N})_3\text{PO}$ and $(\text{Me}_2\text{N})_3\text{PSe}$
Fig. 3.2.1	p.72	Proposed Structures of $\text{TiCl}_4 \cdot 2\text{HMPA}$, $\text{TiCl}_4 \cdot \text{HMPA}$ and $2\text{TiCl}_4 \cdot \text{HMPA}$
Fig. 3.2.2	p.73	Possible Structures for $\text{SnCl}_4 \cdot \text{HMPA}$
Fig. 3.2.3	p.79	Proposed Structures of $\text{MCl}_3 \cdot 3\text{HMPA}$
Fig. 3.3.1	p.91	^1H NMR Spectra (220 MHz, CD_3NO_2 soln., rel. TMS) for $\text{SbCl}_5 \cdot (\text{NMe}_2)_3\text{PS} + (\text{NMe}_2)_3\text{PS}$ 1:1
Fig. 3.3.2	p.92	^1H NMR Spectra (220 MHz) of $\text{SbCl}_5 \cdot (\text{NMe}_2)_3\text{PS}$, CD_3NO_2 soln.
Fig. 3.3.3	p.93	^1H NMR Spectrum of $(\text{BCl}_2\text{NMe}_2)_2$, (CDCl_3 , 220 MHz)

CHAPTER 4

Fig. 4.1.1	p.103	Bonding Schemes for M-NR_2 Species
Fig. 4.1.2	p.106	Crystal Structure of $\text{TiCl}_3(\text{NET}_2)$ (268)
Fig. 4.2.1	p.112	Proposed Structure of $\text{MCl}_4 \cdot (\text{Me}_2\text{N})_2\text{CH}_2$ ($\text{M} = \text{Ti}, \text{Sn}$)
Fig. 4.3.1	p.113	Proposed Structure of $\text{TiCl}_4 \cdot \text{dpm}$
Fig. 4.3.2	p.114	^1H NMR Spectra (220 MHz, CD_3NO_2) of dpm and $\text{TiCl}_4 \cdot \text{dpm}$
Fig. 4.4.1a	p.119	'4-Centre' Mechanism
Fig. 4.4.1b	p.119	'Sommer-Type Mechanism'
Fig. 4.4.2	p.119	6 Coordinate Intermediate
Fig. 4.4.3	p.119	5 Coordinate Intermediate
Fig. 4.5.1	p.122	Proposed Structure of $\text{MX}_4 \cdot \text{Me}_2\text{Si}(\text{NMe}_2)_2$
Fig. 4.5.2	p.124	Possible Structures for $\text{MX}_4 \cdot \text{Me}_2\text{Si}(\text{NMe}_2)_2$

CHAPTER 5

Fig. 5.1.1	p.147	Schematic Diagram of Borazine Showing $\text{B} \rightarrow \text{N}$ σ -Donation, $\text{N} \rightarrow \text{B}$ π -Donation and Overall Charges on B and N
------------	-------	--

Fig. 5.1.2	p.148	Formation of Skeletal $d\pi-p\pi$ Bonds
Fig. 5.1.3	p.149	"Island" Model for Cyclophosphazines $(R_2PN)_3$
Fig. 5.1.4	p.151	Crystal Structure of $Cr(CO)_3 \cdot (EtNBu)_3$
Fig. 5.1.5	p.152	Proposed Structure of $(Me_2SiNH)_3MCl_3$, ($M = Ti, V$)
Fig. 5.3.1	p.156	Crystal Structure of $(CH_2S)_3$
Fig. 5.3.1	p.158	Crystal Structure of $SbCl_3 \cdot (CH_2S)_3$ (projection on xy plane)
Fig. 5.3.3	p.159	Proposed Structures of $MCl_4 \cdot 2L$ ($M = Sn, Ti$), $AuCl_3 \cdot L$ and $SbCl_5 \cdot L$
Fig. 5.3.4	p.160	s-Trithiane Showing Axial and Equatorial Protons
Fig. 5.3.5	p.160	Variable Temperature 1H NMR Spectra of $(CH_2S)_3$ (400 MHz, $CDCl_3$)
Fig. 5.3.6	p.160	Variable Temperature 1H NMR Spectra of $SnCl_4 \cdot 3(CH_2S)_3$ (220 MHz, $CDCl_3$)
Fig. 5.3.7	p.161	$SnCl_4 \cdot 2(CH_2S)_3$ Showing Magnetically Inequivalent Protons
Fig. 5.4.1	p.166	Proposed Structure of $2TiCl_4 \cdot HMB$

CHAPTER 6

Fig. 6.1.1	p.176	X-ray Crystal Structures of $(CONH_2)_2$ and $(CSNH_2)_2$
Fig. 6.1.2	p.177	Crystal Structure of N,N-dimethyldithiooxamide
Fig. 6.2.1	p.182	Proposed Structures of $MCl_4 \cdot B$
Fig. 6.2.2	p.183	Possible Isomers of $MCl_4 \cdot (Y_2C_2N_2(NR)_2)$

APPENDIX A

Fig. A1	p.192	Apparatus for the Preparation of MX_4 ($M = Hf$, $X = Cl, Br$, $M = Zr$, $X = Cl$)
Fig. A2	p.192	Furnace Tube

APPENDIX B

Fig. B1	p.197	Vacuum Line
Fig. B2	p.197	Solvent Still

Fig. B3	p.197	A 'pig'
Fig. B4	p.198	Single (a) and Double (b) Bomb Glass Reaction Vessels
Fig. B5a	p.198	Loading on the Vacuum Line
Fig. B5b	p.198	Extraction on the Vacuum Line
Fig. B6	p.201	UV Cell
Fig. B7	p.201	Conductivity Cell

ABBREVIATIONS

L	a monodentate Ligand
B	a bidentate Ligand
DETO	N,N'-diethyldithiooxamide
DEM	N,N'-diethylmalonamide
DEO	N,N'-diethyloxamide
diars	o-phenylenebisdimethylarsine
DMDTO	N,N'-dimethyldithiooxamide
DMO	N,N'-dimethyloxamide
dpm	Bis(diphenylphosphino)methane
Me ₆ tren	Tris(2-dimethylaminoethyl)amine
HMB	Hexamethylborazine
HMPA	Tris(dimethylamino)phosphine oxide
py	Pyridine
THF	Tetrahydrofuran
THT	Tetrahydrothiophene
tren	Tris(2-aminoethyl)amine

Abbreviations used in the description of IR Spectra:-

s	strong
m	medium
w	weak
br	broad
sh	shoulder

CHAPTER 1

INTRODUCTION

1. INTRODUCTION

The following introductory sections are concerned with the binary halides of the Ti, V and Cr subgroups, their structural chemistry and donor-acceptor properties in non-aqueous media. The halides of Groups IVB and VB play a less important role in terms of the subject matter of this thesis, and are therefore examined only in a general sense (Section 1.4) with the relevant chemistry being introduced to the text as and where appropriate.

1.1 The Early Transition Metals

The elements of groups IVA, VA and VIA exhibit many common properties, and are collectively known as 'the early transition metals'. All have relatively few electrons outside an inert gas configuration, and low effective nuclear charges. The resultant expansion in the size of the d-orbitals gives rise to low ionisation potentials, and the possibility of high oxidation states with no or few electrons. One class of compounds which tends to take full advantage of the possible range of oxidation states is the halides, this being particularly noticeable for the second and third row elements. The halides play an important part in early t-metal chemistry for a number of reasons. In high oxidation states they are often either monomeric, or possess weakly bonded lattices, and can thus provide a wide range of donor chemistry. This is in contrast to the early t-metal chalcogenides, for example, the chemistry of which is dominated by polymeric lattices and polyanions, both being unreactive in a donor-acceptor sense.

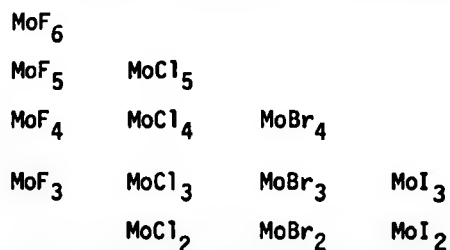
Another feature of early t-metal chemistry concerns metal-metal bonding. This phenomenon, conspicuous for the second and third row

elements has important repercussions for the coordination chemistry of the lower valence states, and is further discussed in Section 1.1.3.

In those halides where metal-metal bonding is not present, cleavage of the metal-halogen bond is unusually facile, and although this presents some technical problems in material handling, the inconvenience is more than offset by the extensive field of halo-substituted derivatives made possible by such reactions. The halides can, therefore, be utilised as synthetic precursors for a whole range of O, N, S, and P bonded species as well as in the rapidly expanding region of organometallic chemistry. Since the problems of hydrolysis and aerial oxidation have largely been overcome by the widespread introduction of high vacuum techniques, the early t-metal halides have become the focus of considerable attention, and several texts have appeared, the works of Canterford and Colton (1,2), Kepert (3) and Clark (4) being of note.

1.1.1 Occurrence of oxidation states of early t-metal halides

Despite the availability of much thermodynamic data (5), no simple pattern has yet emerged for the prediction of stable oxidation states either along a row (e.g. Ti, V, Cr) or down a group (e.g. Ti, Zr, Hf). One point that is fairly clear, however, is the ability of highly electronegative elements such as fluorine and oxygen to stabilise high oxidation states, whereas bromine and iodine favour low oxidation states. For example, the known stable binary halides of molybdenum consist of:-



MoF_2 and MoI_{4-6} are as yet unknown.

Similarly, although VCl_4 is thermally unstable, with slow decomposition to VCl_3 and chlorine being found even at room temperature, examples of stable V(IV) and V(V) species exist in the oxohalides V(IV)OCl_2 , V(V)OCl_3 and $\text{V(V)O}_2\text{Cl}$.

1.1.2 Metal-metal bonding in early t-metal halides

Metal-metal bonding is an important feature of early t-metal chemistry, dominating the structural (1.2) and complex (1.3) chemistry of the second and third row elements in low oxidation states. Kepert (3, 6, 7) and Vrieze (6) have reviewed the subject, and have summarised on an empirical basis the factors which tend to produce metal-metal bonding rather than mononuclear or halogen bridged species:

(a) High energies of atomisation and d-orbital overlap, both of which are favourable towards metal-metal bonding, are more pronounced for the early t-metals than for elements later in the d block. Thus metal-metal interactions are found in $\beta\text{-TiCl}_3$ but not VCl_3 or CrCl_3 , in HfCl_3 , TaCl_3 and WCl_3 but not OsCl_3 or IrCl_3 , in NbCl_4 and $\alpha\text{-MoCl}_4$ (marginally), but not in $\beta\text{-MoCl}_4$ or TcCl_4 . As these properties are enhanced in the second and third row elements, a similar trend is found on going down a particular group. For example, metal-metal bonding exists in TaCl_3 and NbCl_3 , but not VCl_3 , in TaCl_4 and NbCl_4 but not VCl_4 and in WCl_4 , with $\alpha\text{-MoCl}_4$ (marginal), but not $\beta\text{-MoCl}_4$.

(b) Metal-metal bonding is disfavoured by high oxidation states, where contracting d-orbitals and a reduction in the number of electrons available for m-m bonding are unfavourable influences. In addition, a high metal:halogen ratio would produce weakening of a projected m-m interaction on steric grounds. Examples of this phenomenon are numerous and exist in Ti, and all the second and third row elements of the first three periods.

(c) A decreasing lattice energy in the order $F > Cl > Br > I$ stabilises metal-metal bonding in the reverse order. It is, therefore, found that while m-m bonded bromo and iodo species are comparatively numerous, Nb_6F_{15} appears to be the sole example involving fluorine (6). An estimation of the relative capacities of F vs. I for m-m bonded species, purely on the basis of the number of known compounds, should be approached with caution, however, as F favours high oxidation states which are usually F bridged polymers for reasons examined in (b). However, the series MoX_3 ($X = F, Cl, Br, I$) does provide a valid example, with MoI_3 and $MoBr_3$ consisting of metal-metal bonded chains, $MoCl_3$ of chains of metal-metal bonded metal atom pairs, and MoF_3 showing no signs of any interaction at all.

1.2 Structure and Reactivity of Early T-Metal Halides

It is a generally held principle that the structure of the early t-metal halides plays an important role in their reactivity, with decreasing reactivity accompanying an increase in the polymeric nature of the metal halide. At a first approximation this behaviour can be rationalised simply in terms of the number of bonds

that have to be broken in order to achieve a mononuclear metal centre. A metal halide with a highly polymerised lattice would then be expected to be less vigorous in its reactions than that of a similar mononuclear or weakly associated species. With the Ti chlorides, for example, monomeric TiCl_4 is a strong acceptor, forming donor adducts with a large number of both strong and weak donors. The chloro-bridged structure of $\alpha\text{-TiCl}_3$, however, requires the use of stronger donors and more forcing conditions, while the donor chemistry of the even more highly polymerised TiCl_2 is minimal and poorly understood. The introduction into the lattice of a strong metal-metal interaction has a large influence on reactivity. Thus the metal-metal bonded β modification of TiCl_3 is not only chemically inert, but is capable of surviving an electrolytic oxidation-reduction cycle, apparently without change (8).

Despite this general correlation between structure and reactivity, it is impossible to predict the reactions of a particular metal halide purely on structural grounds. The factors involved are many and complex, and knowledge of some areas, particularly the nature of the reacting metal halide surface, is virtually non-existent.

1.2.1 Structural aspects

Structural data have now been obtained for the majority of the early t-metal halides, and from this work several points have emerged.

(a) Within a single oxidation state, species with either the same halide ions (Cl, Br, I) or with the same central metal atom

are often isostructural. Typically, only one example of each structural type has been studied by single crystal X-ray methods with the remainder of the group being confirmed as isomorphous by comparison of powder X-ray photographs.

(b) Many of the early t-metal halides exhibit polymorphism. This phenomenon can either take the form of metal-metal bonded vs. non-metal-metal bonded modifications as in β - and α - TiCl_3 respectively, or it can be a difference in halide ion packing (e.g. α , γ , and δ forms of TiCl_3). Modifications of the second type, present no change in the immediate environment of the metal ion, and there is no evidence for any difference in reactivity between polymorphs. Consequently, modifications of this type will be omitted from the text.

(c) The small size and high electronegativity of fluorine gives rise to metal fluorides which are atypical in both a chemical and a structural sense. As the fluorides have little direct relevance in terms of the subject matter of this dissertation, they have been excluded from the following sections. The fluorides have been the subject of several reviews (9-13).

(d) Recent studies have found that a number of metal halides previously thought to be of a simple composition are in fact non-stoichiometric, e.g. ZrCl_3 , ZrCl_2 and HfI_3 (14-16). The extent to which this phenomenon applies to the other metal halides has yet to be established.

(e) The lower halides of Nb, Ta, Mo and W are 'cluster' compounds, based on an octahedral arrangement of six strongly metal-metal bonded metal atoms. All the cluster compounds have halide ions either positioned above each face of the core octahedron, or bridging each edge, to give M_6X_8 and M_6X_{12} units respectively (Fig. 1.2.1).

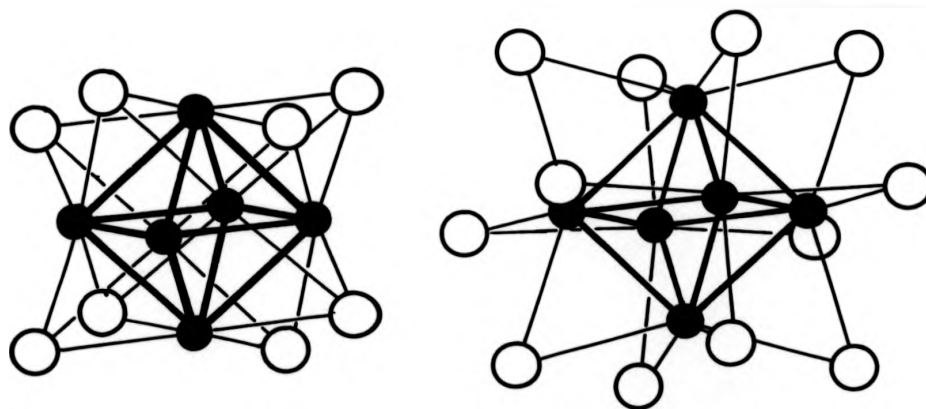


Fig. 1.2.1 M_6X_8 (a) and M_6X_{12} (b) Metal Cluster Centres

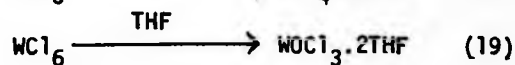
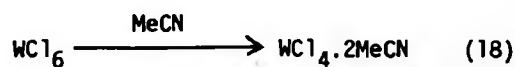
Additional halide ions can be bonded to the vertices of the M_6 core either in a terminal capacity, or be engaged in bridging to adjacent clusters. To simplify the description of such clusters, the formula is often written in the form:- (cluster core)(number of bridging halides/number of clusters bridged by each halide)(number of terminal halides). For example, ' $MoCl_{12}$ ' which has a Mo_6Cl_8 core +2 terminal

chlorine atoms +4 chlorine atoms each bridging to one other cluster would be described as $(\text{Mo}_6\text{Cl}_8)\text{Cl}_{4/2}\text{Cl}_2$. Similarly, WCl_3 (Fig. 1.2.9) would be $(\text{W}_6\text{Cl}_{12})\text{Cl}_6$. This nomenclature has also been applied to non-cluster metal-metal bonded compounds (e.g. MoCl_3 (Fig. 1.2.7) is $(\text{MoCl}_2)\text{Cl}_{8/2}$).

The following sections describe the structural chemistry by oxidation state:

Oxidation State VI

The volatile liquids MF_6 ($\text{M} = \text{Mo}$ and W) and crystalline solids MoCl_6 , WX_6 ($\text{X} = \text{Cl}, \text{Br}$) are the only known examples of the +6 state. In the solid state, the structures show a high degree of polymorphism, but all contain a metal atom in an octahedral monomeric environment (17). The hexahalides being coordinatively saturated have no well established coordination chemistry, but often give complexes as part of their reduction products, e.g.,



Oxidation State V

Of the known pentahalides, NbX_5 ($\text{X} = \text{Cl}, \text{Br}, \text{I}$) (20), TaX_5 ($\text{X} = \text{Cl}, \text{Br}, \text{I}$), MoCl_5 (21) and WX_5 ($\text{X} = \text{Cl}, \text{Br}$) (22) are all isostructural consisting in the solid state as MX_5 dimers, e.g. Fig. 1.2.2.

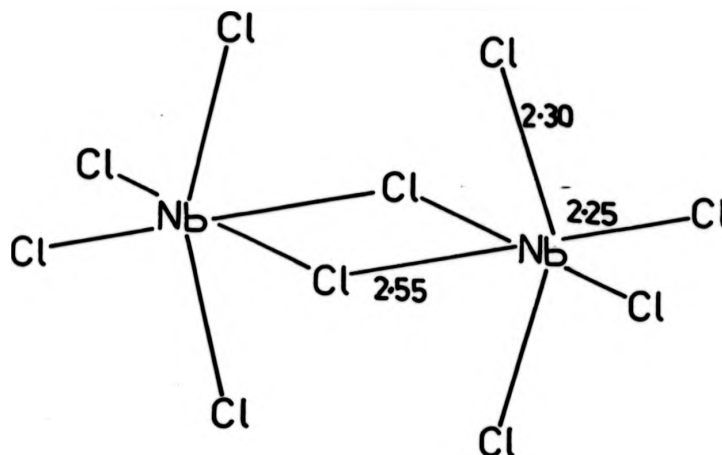


Fig. 1.2.2 Crystal Structure of NbCl_5 (20)

Distortion of the MX_6 octahedra occurs by mutual repulsion of the two Nb atoms from their octahedral centres. NbI_5 (23) and VF_5 (24) are more highly associated forming infinite halide bridged chains. All of the pentahalides are volatile, the gas phase structure being based on a monomeric trigonal bipyramidal unit (25).

Oxidation State IV

A wide range of structural chemistry is presented by the +4 state. It is also the highest oxidation state in which metal-metal bonding is of any significance. Titanium is the only first row element that forms thermally stable tetrahalides. TiCl_4 is a colourless fuming liquid, with a monomeric tetrahedral structure, both in the gas phase (26) and in solution (27) although Raman studies of the neat liquid indicate some association via chloride bridges (28). A monomeric structure was also found for the low melting point solids TiBr_4 (29, 30) and TiI_4 (30); the X-ray crystal structures show the lattice to consist of discrete TiX_4 units. VCl_4 is a brown fuming liquid which

slowly disproportionates to VCl_3 and Cl_2 at room temperature and rapidly on heating in vacuo (31). As with TiCl_4 a monomeric tetrahedral configuration is adopted in both solution and the gas phase, but here distortion occurs due to Jahn-Teller effects (32). VBr_4 is unstable, decomposing above -45°C while CrCl_4 has only been observed as a constituent of high temperature gas phase equilibria, and is unknown in the condensed phase.

The second and third row halides crystallise in only two basic structural types. ZrCl_4 , ZrBr_4 , HfCl_4 and HfBr_4 are isomorphous, the structure being typified by ZrCl_4 (Fig. 1.2.3) (33, 34).

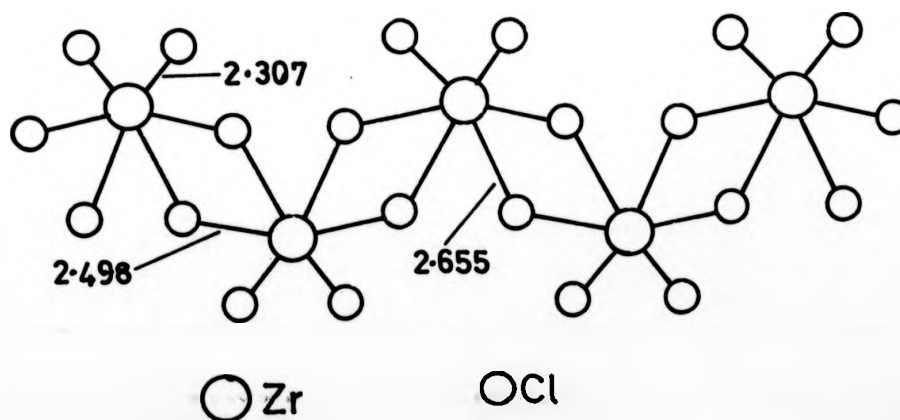


Fig. 1.2.3 Crystal Structure of ZrCl_4

Here, octahedrally coordinated Zr atoms each share two edges with adjacent octahedra via chloride bridges to form an infinite one-dimensional 'zig-zag' polymer. Variations in the bond lengths of the Zr-Cl bridges

between alternate octahedra are caused by distortions from ideal octahedral geometry rather than metal-metal bonding, which was eliminated on the basis of a value for the shortest Zr-Zr interatomic distance of 3.962 Å.

Crystalline ZrF_4 and HfF_4 have structures based on eight coordinate Zr or Hf. Each square antiprismatically coordinated Zr (Hf) is linked to neighbouring antiprisms through all eight vertices to form a three-dimensional solid (35).

In the gas phase, electron diffraction studies reveal the MX_4 ($\text{M} = \text{Zr}, \text{Hf}; \text{X} = \text{F}, \text{Cl}, \text{Br}, \text{I}$) polymers dissociate to give regular tetrahedral species as with the TiX_4 series (36-38).

The second structural type (Fig. 1.2.4) accounts for the solid phase chemistry of $\alpha\text{-MoCl}_4$, MoBr_4 , MX_4 ($\text{M} = \text{Nb}, \text{Ta}, \text{W}; \text{X} = \text{Cl}, \text{Br}$) all of which are isostructural (7, 39).

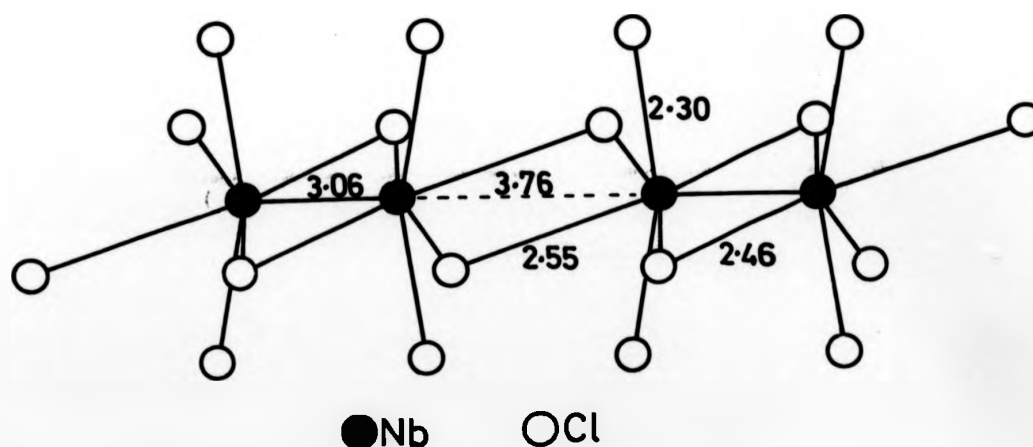


Fig. 1.2.4 Structure of NbCl_4 (37)

NbCl_4 consists of edge sharing octahedra forming an infinite chain, the Nb being displaced towards each other in alternate octahedra forming distinct Nb-Nb pairs, i.e. metal-metal bonding. NbI_4 (40) is structurally related, but alternate Nb-Nb distances of 3.31 and 4.36 Å were considered long, and the metal-metal interaction, therefore, weak.

MoCl_4 has also been obtained in a second β form (41). This was found to be related to $\alpha\text{-TiCl}_3$, having the same basic lattice, but with only three-quarters of the metal sites occupied. The Mo atoms are located in statistically disordered 'domains'. In each domain, half the metal sites are vacant in alternate layers to give alternating sheets composed of $(\text{Mo}_2\text{Cl}_6)^{2+}$ and MoCl_6^{2-} units. There is no evidence for any metal-metal bonding in the β modification.

Oxidation State III

In the +3 state all the early t-metals except vanadium and chromium exhibit metal-metal bonding in one or more modifications.

TiCl_3 has four modifications, all of which have been studied by Natta and coworkers (Fig. 1.2.5) (42).

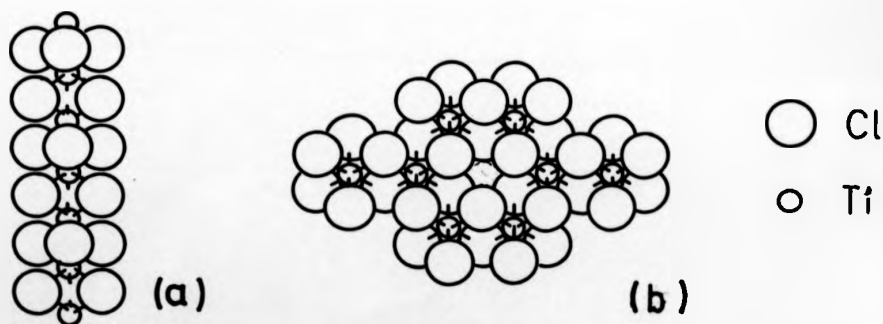


Fig. 1.2.5 Structural units of (a) $\beta\text{-TiCl}_3$ and (b) α , γ and $\delta\text{-TiCl}_3$

The mauve α , γ and δ forms are closely related forming layer lattices in which each Ti atom is octahedrally coordinated to six Cl atoms. In the α form the chloride ions are hexagonally close packed, and in the γ form cubically close packed. Prolonged grinding of either the α or γ forms results in δ -TiCl₃ which has a disordered lattice consisting statistically of 63% hexagonal close packing and 37% cubic close packing. The structure of the brown β metal-metal bonded form is quite different. As with α -TiCl₃, the Cl atoms are hexagonally close packed, but the Ti atoms are arranged in such a way that the structure can be considered as an infinite one-dimensional polymer formed by TiCl₆ octahedra sharing opposite faces. Although the Ti-Cl bond lengths in all four modifications are identical (2.45 - 2.46 Å), the Ti-Ti interatomic distance in the β form is much shorter (2.91 Å) than that found in the α , γ and δ forms (3.54 Å), equalling the Ti-Ti distance in metallic titanium.

TiBr₃ exists in both α and β forms, but TiI₃, ZrCl₃ (43), ZrBr₃ (44), ZrI₃ (45) and HfI₃ (45) are known only in the metal-metal bonded β modification.

VCl₃ is a mauve crystalline solid with an α -TiCl₃ type structure. VBr₃ forms continuous solid solutions with VCl₃ over the whole composition range, and is, therefore, considered as isomorphous with VCl₃ (3, 4). The isomorphous CrCl₃ and CrBr₃ structures (46) are made up of close packed halide sheets, with Cr atoms occupying two-thirds of the octahedral vacancies in every second layer to form repeating X/Cr/X 'sandwiches'.

Niobium and tantalum form no simple trihalides, $\text{MX}_{3.0}$ being only one constituent in a continuous phase between upper and lower limits (e.g. for 'NbCl₃', NbCl_{2.67} - NbCl_{3.13}). The lower limit correspond to M_3X_8 , the structure of which is known in the case of Nb₃Cl₈ (Fig. 1.2.6) (47, 48).

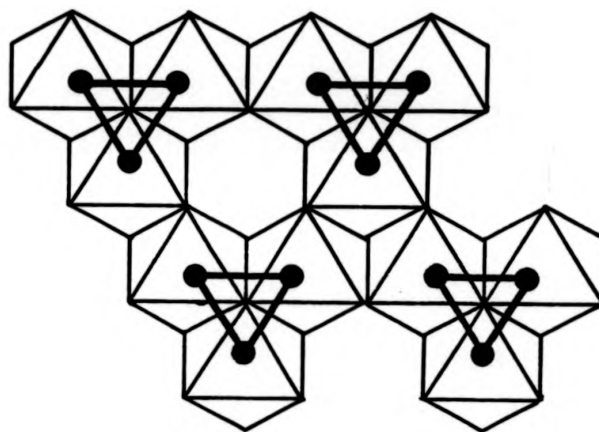


Fig. 1.2.6 Crystal Structure of Nb₃Cl₈

The main feature of this structure is a strongly metal-metal bonded Nb triangular cluster which occupies three out of four sites in a sheet composed of Cl octahedra. A niobium-niobium distance of 2.81 Å was found which is shorter than the metal-metal distance in NbCl₄ (3.06 Å) or in the metal itself (2.94 Å). Increasing the Nb:Cl ratio results in the disruption of the Nb₃ clusters to form diamagnetic Nb₂ units until an upper limit of NbCl_{3.13} is reached. Perhaps not surprisingly, there is no evidence for any coordination compounds with any of the 'MX₃' (M = Nb, Ta) series.

$\alpha\text{-MoCl}_3$ is related to both CrCl_3 and CrBr_3 , the structure (39) consisting of Mo atoms occupying two-thirds of the octahedral vacancies in a sheet of cubic close packed chloride ions. Metal-metal bonding between pairs of Mo atoms distorts the MoCl_3 octahedra, i.e. $\text{Mo}_2\text{Cl}_2\text{Cl}_{8/2}$ (Fig. 1.2.7). Consequently there is one short (2.77 \AA) and two long (3.71 \AA) Mo-Mo internuclear distances, as opposed to the three equal Cr-Cr internuclear distances in CrCl_3 or CrBr_3 .

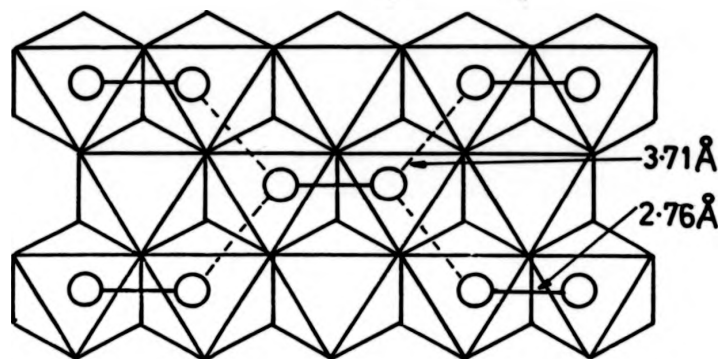


Fig. 1.2.7 Schematic Representation of a Sheet of $(\text{MoCl}_2\text{Cl}_{3/2})$ Octahedra Showing Short (—) and Long (---) Mo-Mo Bonds.

Instead of forming sheets of octahedra by edge bridging (as in MoCl_3), MoBr_3 (49) and MoI_3 (49) consist of infinite chains of MoX_6 octahedra sharing opposite faces with the two adjacent units, similar to $\beta\text{-TiCl}_3$. Metal-metal bonding between pairs of Mo atoms create Mo_2Br_6 units, i.e. $(\text{Mo}_2\text{Br}_3)\text{Br}_{6/2}$, as can be seen from the alternate short and long Mo-Mo bonds (Fig. 1.2.8).

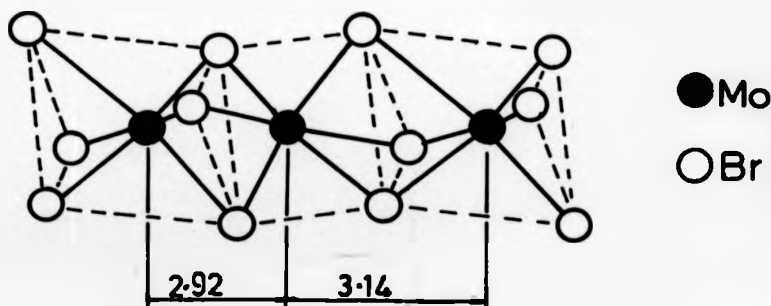


Fig. 1.2.8 Crystal Structure of MoBr_3

$\alpha\text{-MoCl}_3$ is related to both CrCl_3 and CrBr_3 , the structure (39) consisting of Mo atoms occupying two-thirds of the octahedral vacancies in a sheet of cubic close packed chloride ions. Metal-metal bonding between pairs of Mo atoms distorts the MoCl_3 octahedra, i.e. $\text{Mo}_2\text{Cl}_2\text{Cl}_{8/2}$ (Fig. 1.2.7). Consequently there is one short (2.77 \AA) and two long (3.71 \AA) Mo-Mo internuclear distances, as opposed to the three equal Cr-Cr internuclear distances in CrCl_3 or CrBr_3 .

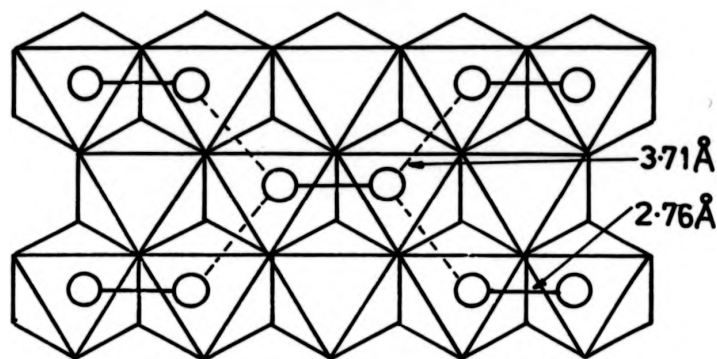


Fig. 1.2.7 Schematic Representation of a Sheet of $(\text{MoCl}_2)\text{Cl}_{3/2}$ Octahedra Showing Short (—) and Long (---) Mo-Mo Bonds.

Instead of forming sheets of octahedra by edge bridging (as in MoCl_3), MoBr_3 (49) and MoI_3 (49) consist of infinite chains of MoX_6 octahedra sharing opposite faces with the two adjacent units, similar to $\beta\text{-TiCl}_3$. Metal-metal bonding between pairs of Mo atoms create Mo_2Br_6 units, i.e. $(\text{Mo}_2\text{Br}_3)\text{Br}_{6/2}$, as can be seen from the alternate short and long Mo-Mo bonds (Fig. 1.2.8).

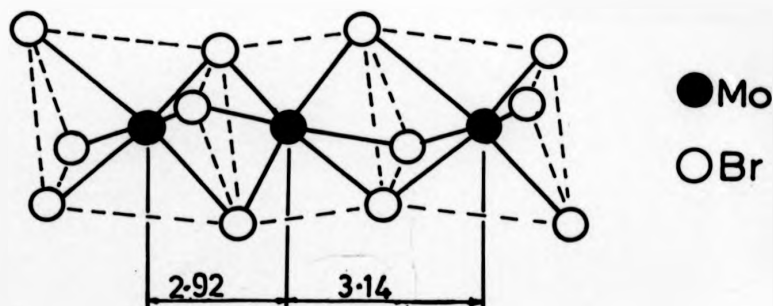


Fig. 1.2.8 Crystal Structure of MoBr_3

WCl_3 (50) and WBr_3 (51) are both cluster compounds. The trichloride (Fig. 1.2.9) contains a W_6 metal bonded octahedral core with twelve-edge bridging Cl atoms and six terminal Cl atoms, i.e. $(\text{W}_6\text{Cl}_{12})\text{Cl}_6$.

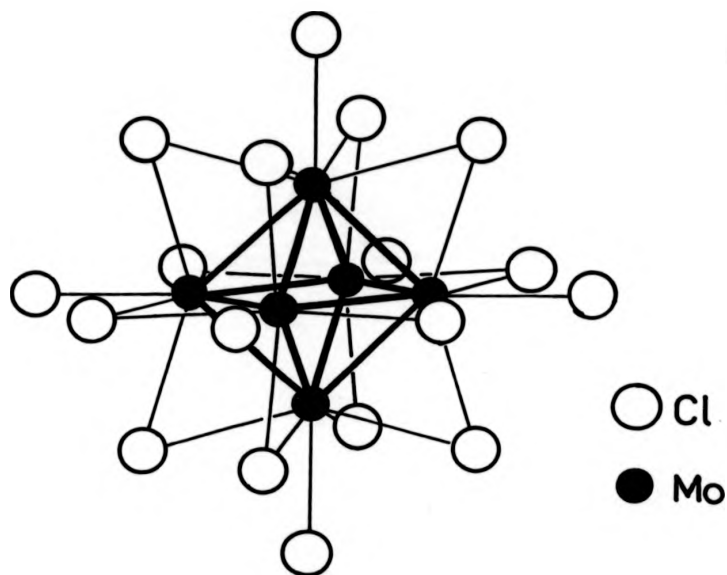


Fig. 1.2.9 Structure of WCl_3 (50)

' WBr_3 ' (51) is based on a $(\text{W}_6\text{Br}_8)^{6+}$ octahedral core with two bridging polybromide (Br_4^{2-}) groups per cluster, i.e. $(\text{W}_6\text{Br}_8)^{6+}(\text{Br}_4^{2-})_{4/2}\text{Br}_2$. WI_3 is isomorphous with MoBr_3 and MoI_3 . The stable cluster structures of WX_3 ($\text{X} = \text{Cl}, \text{Br}$) prevents the direct formation of coordination complexes, although reduction of complexes of the higher halides does provide a synthetic route to W(III) adducts (52).

Oxidation State II

The structures of the dihalides of titanium and vanadium all belong to the cadmium diiodide type (Fig. 1.2.10) (1, 3).

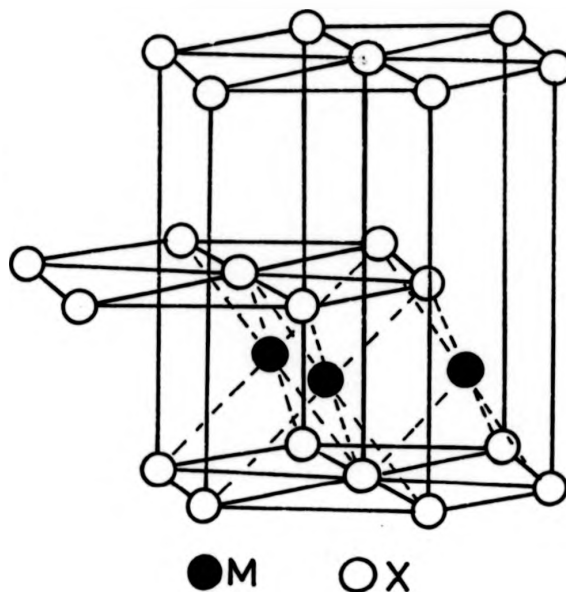


Fig. 1.2.10 The Cadmium Diiodide Structure

Sheets of close packed halide ions form planes with the metal atoms filling the octahedral sites between alternate pairs of layers.

The dihalides of chromium (F, Cl, Br, I) are related to a Rutile structure (3). At a first approximation the structure can be considered as four chromium atoms occupying octahedral vacancies between close packed halide sheets. Considerable distortion of the CrX_6 octahedra occurs, however, as a consequence of the Jahn-Teller effect, producing four short equatorial and two long axial Cr-X bonds (Fig. 1.2.11).

Little was known of the structural chemistry of the Zr and Hf dihalides until very recently, when Corbett and coworkers (16) succeeded in isolating pure samples of ZrCl_2 and the closely related non-stoichiometric $\text{Zr}_{1.05}\text{Cl}_2$. Both these compounds are based on a complex slab-like structure (16).

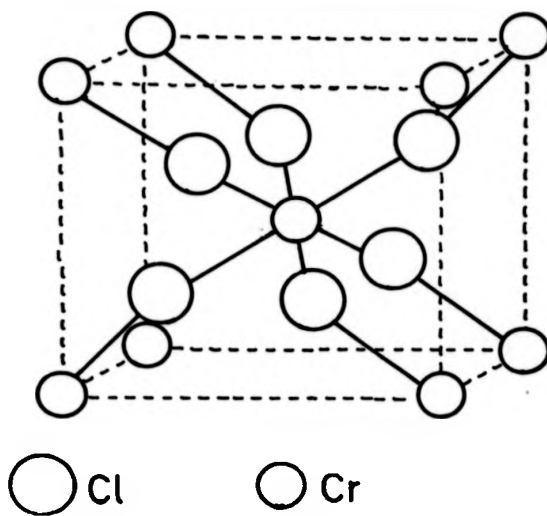


Fig. 1.2.11 Unit Cell of CrCl_2 Showing Short (2.39 \AA) and Long (2.93 \AA) Cr-Cl Bonds (53)

ZrI_2 provides the sole example of a neutral Group IVA cluster, the structure being based on an I bridged trigonal antiprism (Zr_6I_{12}) (54).

Niobium and tantalum form no true dihalides, instead giving a series of clusters based on $(\text{M}_6\text{X}_3)^{3+}$, $(\text{M}_6\text{X}_{12})^{2+}$, $(\text{M}_6\text{X}_{12})^{3+}$ and $(\text{M}_6\text{X}_{12})^{4+}$ with average metal oxidation states of 1.83, 2.33, 2.50 and 2.67 respectively. The chemistry of these compounds is extensive, and has been summarised (3, 6).

MX_2 ($\text{M} = \text{Mo}, \text{W}$; $\text{X} = \text{Cl}, \text{Br}, \text{I}$) are isomorphous. Structurally they are related to WCl_3 (Fig. 1.2.8), but with four meridional centrifugal halide atoms bridging to four adjacent clusters to form sheets, i.e. $(\text{M}_6\text{X}_8)\text{X}_{4/2}\text{X}_2$ (39). As with the niobium and tantalum clusters, oxidation yields a variety of cluster based compounds, depending on the conditions, e.g. $(\text{W}_6\text{Br}_8)\text{Br}_{4/2}\text{Br}_2 + \text{Br}_2 \rightarrow \alpha\text{-W}_6\text{Br}_{18}, \beta\text{-W}_6\text{Br}_{18}, \text{W}_6\text{Br}_{16}, \text{W}_6\text{Br}_{14}$ and W_6Br_{12} (3).

Rather surprisingly, the molybdenum and tungsten dihalides also have a coordination chemistry, which is discussed in Chapter 2.

Oxidation State I

ZrCl and HfCl appear to be the only monohalides known. The crystal structure (55) of ZrCl (Fig. 1.2.12) and that of the isomorphous HfCl show some rather remarkable features, including a Zr-Zr interatomic distance (3.09 \AA) which is considerably less than that in the twelve coordinate metal (3.19 \AA).

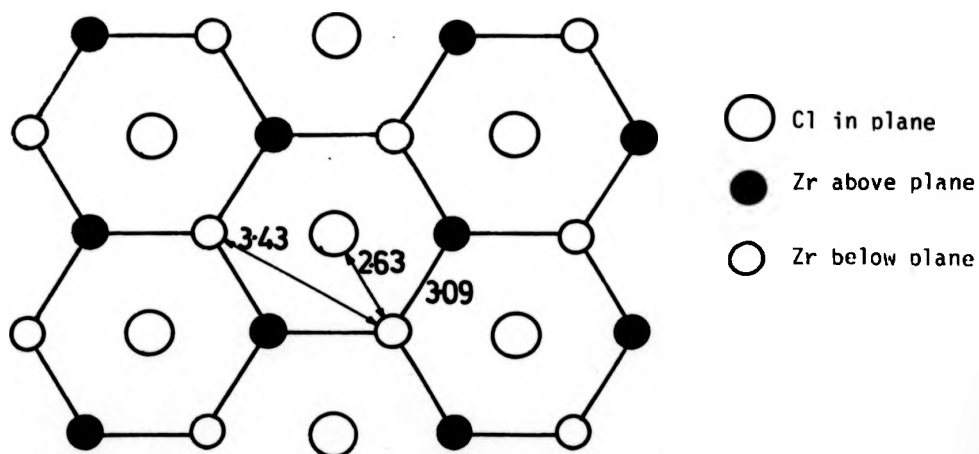


Fig. 1.2.12 Crystal Structure of ZrCl

The unique four layer structure (here presented as a projection on the 001 plane) consists of Cl-Zr-Zr-Cl stacked sheets, with each Zr atom having six in phase Zr neighbours (at 3.42 \AA), three Zr neighbours in the sheet below (at 3.09 \AA) and three Cl neighbours in the sheet above (at 2.63 \AA).

The monohalides have no known coordination chemistry, as might be expected from such a highly metal-metal bonded structure.

p block bases (N, O, F) which they called class A, and those species preferring to complex to second and third row donors (P, S, As, Se), called Class B. Pearson (58, 59) extended this idea, classifying bases in which the donor atom is at high electronegativity, low polarizability, and hard to oxidise as 'hard' (Class A) bases, and those of low electronegativity, high polarizability and easily oxidised as 'soft' (Class B) (Table 1.3.1).

HARD	SOFT	BORDERLINE
H_2O , OH^- , RO^- , R_2O	R_2S , RSH , RS^-	$\text{C}_6\text{H}_5\text{NH}_2$, $\text{C}_5\text{H}_5\text{N}$
ROH , PO_4^{3-} , SO_4^{2-}	SCN^- , R_3P , R_3As	N_3^- , Br^- , NO_2^- , N_2
Cl^- , F^-	I^- , CO , $(\text{RO})_3\text{P}$	
NH_3 , RNH_2 , N_2H_4	C_2H_4 , H^-	

Table 1.3.1 Classification of Bases

Lewis acids were likewise categorised by their affinity for either hard or soft bases (Table 1.3.2).

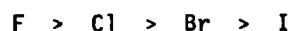
HARD	SOFT	BORDERLINE
H^+ , Li^+ , Na^+ , K^+	Cu^+ , Ag^+ , Au^+	Fe^{2+} , Co^{2+} , Ni^{2+} , Cu^{2+}
Cr^{3+} , Co^{3+} , Fe^{3+} , As^{3+}	Pd^{2+} , Cd^{2+} , Pt^{2+}	Pb^{2+} , Sn^{2+} , Sb^{3+} , Bi^{3+}
Si^{4+} , Sn^{4+} , Ti^{4+} , Zr^{4+} , Hf^{4+}	Tl^{3+} , BH_3 , GaCl_3	Rh^{3+} , BMe_3 , SO_2
WO^{4+} , VO^{2+} , MoO^{3+}	InCl_3 , I_2 , Br_2	GaH_3
BeMe_2 , BF_3 , B(OR)_3		
AlMe_3 , AlCl_3 , AlH_3		

Table 1.3.2 Classification of Lewis Acids

The character of an acid or base can be modified by changing the oxidation state. Thus Ni(0) is a soft acid, Ni(II) borderline, and Ni(IV) hard. Addition of soft ligands has the effect of softening the acceptor atom, so that whereas BF_3 is a typical hard Lewis acid, $\text{BH}_3(\text{B}_2\text{H}_6)$ is soft.

Having established the nature of both Lewis acids and Lewis bases, the stability of an acid-base complex can be described by the rule 'Hard acids prefer to bind to hard bases, and soft acids prefer to bind to soft bases'. This is a totally empirical correlation.

Inspection of Table 1.3.2 reveals that the early t-metals, where present, are all hard, and the preference for donor atoms should thus be in the order:-



Little quantitative evidence exists to substantiate the expected trend, but it is a general observation that the number of known complexes with O and N donor atoms far outweighs those with soft donors. Chung and Westland (60) have, however, obtained thermochemical data for the reaction of THF and THT with some Group IV tetrahalides, which does illustrate the HSAB principle as in Table 1.3.3.

COMPLEX	$-\Delta H \text{ (KJ mol}^{-1}\text{)}$
$\text{ZrCl}_4 \cdot 2\text{THF}$	140.5 ± 2.0
$\text{ZrCl}_4 \cdot 2\text{THT}$	124.6 ± 3.8
$\text{ZrBr}_4 \cdot 2\text{THF}$	151.3 ± 1.7
$\text{ZrBr}_4 \cdot 2\text{THT}$	36.4 ± 1.7
$\text{HfCl}_4 \cdot 2\text{THF}$	144.6 ± 0.8
$\text{HfCl}_4 \cdot 2\text{THT}$	138.3 ± 0.8

Table 1.3.3 Heats of Formation of $\text{MX}_4 + 2\text{L} \rightarrow \text{MX}_4 \cdot 2\text{L}$
in Standard States

For HfCl_4 , the small difference in enthalpy between the reaction between THF and THT was seen in terms of Hf possessing more B (soft) character than Zr.

Several workers have attempted to explain the HSAB phenomenon, the π -bonding theory of Chatt (61) being particularly appropriate for metal ions. Here, the important feature of soft acids was the presence of loosely held outer d-electrons, which can form π -bonds with a ligand by donation into empty d-orbitals on soft bases such as P, S etc. Hard acids have tightly held outer electrons but empty d orbitals, which again, can form π -bonds by accepting electron density from a hard donor atom. A hard base/soft acid interaction would be disfavoured by the repulsion between the filled orbitals on both metal and ligand.

Care should be taken in applying the HSAB principle too strictly, as the predicted and experimental behaviour of a complex do not always coincide. For example, the complex $\text{TiCl}_4 \cdot 2$ thioxan (thioxan = $\text{S}(\text{CH}_2)_4\text{O}$) is S bonded rather than the O bonded isomer expected from HSAB (62).

1.3.2 Geometry of coordination complexes

The following section is intended as a brief introduction to the types of geometry encountered in this area of chemistry, with (where possible) verified examples of each class.

Low coordination numbers (<5)

There are no true three coordinate halide species, although a number of compounds of first row elements of the type MR_3 ($\text{R} = \text{NR}_2'$, SiMe_3 , $\text{CH}(\text{SiMe}_3)_2$, SR' , etc.) have been isolated via halide substitution reactions.

Four coordination is very rare, the VX_4^- ($\text{X} = \text{Cl}, \text{Br}$) ions observed by Clark (63), and the distorted tetrahedral $\text{CrX}_2 \cdot 2\text{Ph}_3\text{PO}$ ($\text{X} = \text{Br}, \text{I}$)

complexes prepared by Scaife (64) being amongst the few known examples.

5 coordination

Penta-coordinate complexes appear to be restricted to first row elements, possibly due to the increased size (and thus ability to attain higher coordination numbers) of the second and third row metals. A common factor in all of these complexes is the presence of a bulky ligand, such as NR_3 , PR_3 , SR_2 , etc. Antler and Laubengayer (65) isolated the first 5 coordinate complexes in 1955 by the reaction of TiCl_4 with NMe_3 , giving $\text{TiCl}_4 \cdot \text{NMe}_3$ or $\text{TiCl}_3 \cdot 2\text{NMe}_3$ depending on the reaction conditions. Fowles and coworkers (66-69) extended the trimethylamine series in both the +4 ($\text{TiBr}_4 \cdot \text{NMe}_3$ (67), $\text{VX}_4 \cdot \text{NMe}_3$ (66)) and +3 ($\text{TiBr}_3 \cdot 2\text{NMe}_3$ (67), $\text{HCl}_3 \cdot 2\text{NMe}_3$, $\text{M} = \text{V}$ (66), Cr (68)) states. These complexes are discussed in greater detail in Chapter 2. Further work by a number of groups has since produced 5 coordinate adducts with a variety of nitrogen (66, 70), phosphorus (71), arsenic (62), oxygen (72, 73) and sulphur (68, 70) donors.

Spectroscopic (74, 75) and crystallographic (69, 76-78) studies have confirmed a trigonal bipyramidal (D_{3h} or C_{3v}) structure in a number of instances, the ligand(s) occupying an axial position in each case. Steric compression prevents the occupation of adjacent sites, i.e. 1 axial + 1 equatorial or 2 equatorial, eliminating the possibility of geometric isomerism. The tendency to dimerise in the solid state forming 6 coordinate species has also been noted (68, 70). 5 coordinate species have been reviewed (79-81).

6 coordination

One of the dominant factors in early transition metal chemistry appears to be the tendency of metal ions to form octahedral or pseudo-

octahedral 6 coordinate species. Consequently this is the most common geometry, adopted by the large majority of early t-metal complexes. Examples can be found for all the early t-metals in a variety of oxidation states and stoichiometries.

For an adduct at general formula MX_yL_2 , when $x + y = 6$ an octahedral environment is obtained simply by the ligands occupying vacant sites on the metal ion, e.g. $MX_5 \cdot L$ (82), $MX_4 \cdot L_2$ (83, 84), MX_3L_3 (85) and MX_2L_4 (86). Complexes which are coordinatively unsaturated as monomers, i.e. $x + y < 6$, can achieve 6 coordination by halogen bridging, e.g. $(MCl_4 \cdot L)_2$, $M = Ti$, $L = POCl_3$ (87), $MeNO_2$ (88), $EtOAc$ (89), $M = W$, $L = Cl_3CCN$ (90), $(MX_4)_2L$ (91), $(MX_3L_2)_2$ (68, 70), $(MX_2L_2)_x$ (92).

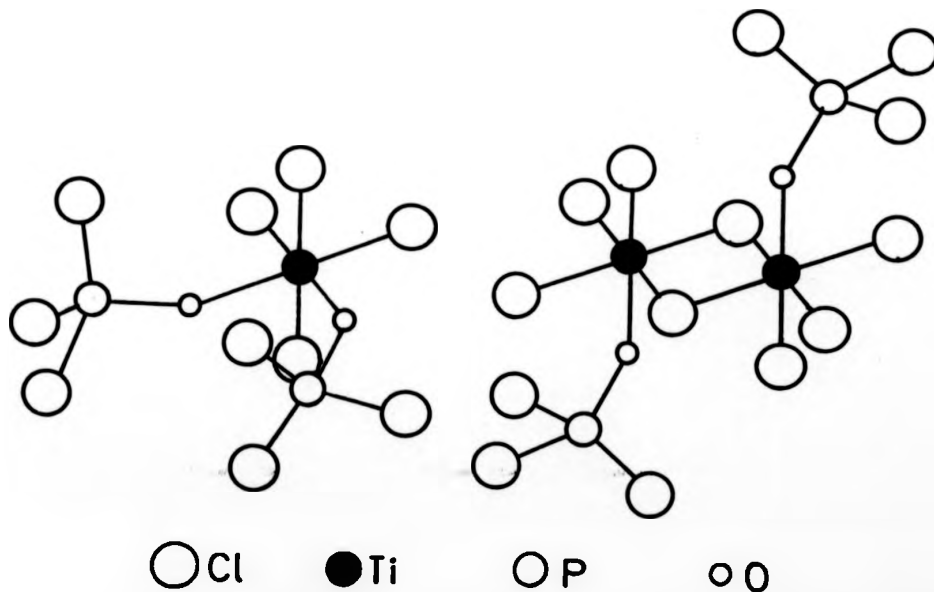


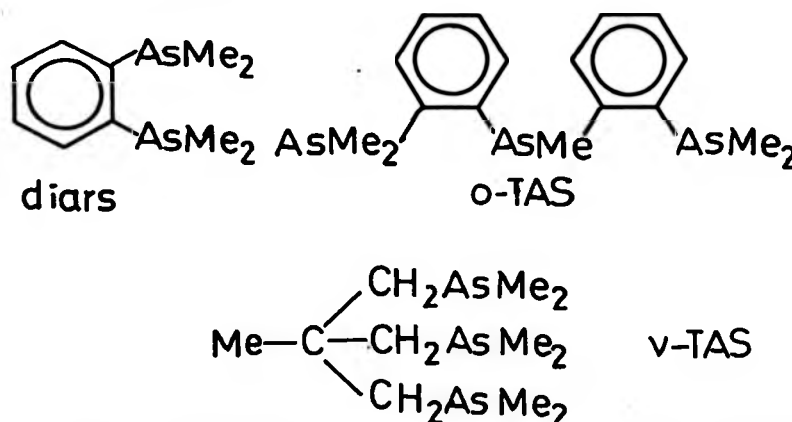
Fig. 1.3.1 Crystal Structures of $TiCl_4 \cdot 2POCl_3$ (83) and $(TiCl_4 \cdot POCl_3)_2$ (87)

When the number of ligands in a simple complex is two or more, geometrical isomerism can occur, e.g. cis $TiCl_4 \cdot 2POCl_3$ (83) and trans $WCl_4 \cdot 2py$ (84). In certain favourable instances, e.g. with the inert Cr^{3+} ion both isomers can be isolated, i.e. fac and mer $CrCl_3 \cdot 3L$,

$L = \text{NH}_3$ (93), THT (94), dien (95).

7 coordination

Theoretical aspects of 7 coordination have been examined by Kepert (3). A number of 7 coordinate adducts have been isolated with the polydentate arsine ligands o-phenylenebis(dimethylarsine)(diars), methylbis(o-dimethyarsinophenyl)arsine(o-TAS) and tris-1,1,1-(dimethylarsino methyl)ethane(v-TAS).



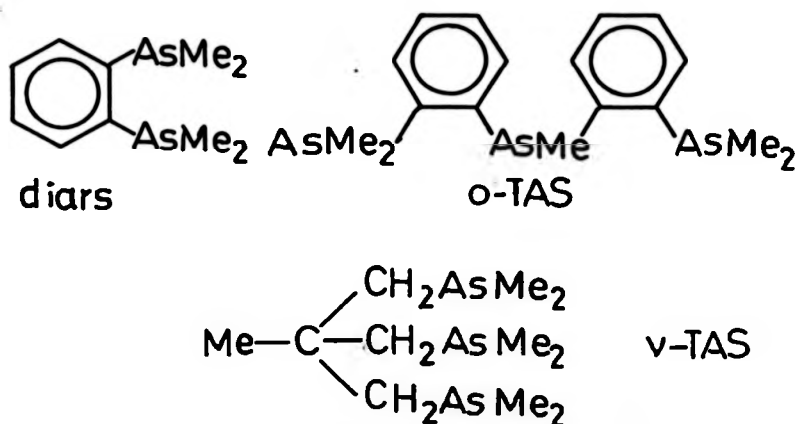
Clark and coworkers have prepared the 1:1 adducts $\text{MX}_5 \cdot \text{diars}$ ($M = \text{Nb}, \text{Ta}$, $X = \text{Cl}, \text{Br}$ (96); $M = \text{W}$, $X = \text{Cl}$ (97)), $\text{MCl}_4(\text{o-TAS})$ and $\text{MCl}_4(\text{v-TAS})$ ($M = \text{Ti}, \text{V}$) (98). These are diamagnetic and non-conducting. Equivalent AsMe signals in the ^1H NMR spectra were taken as evidence of 7 coordination. The possibility of a more common 6 coordinate structure with rapid exchange occurring in solution between free and coordinated donor sites (which would give an identical result to above) was, however, not discussed. Confirmatory X-ray, or variable temperature ^1H NMR studies on these species have yet to be carried out.

A number of potential 7 coordinate trimethylamine adducts have been isolated ($\text{WCl}_6 \cdot \text{NMe}_3$ (99), $\text{MCl}_5 \cdot 2\text{NMe}_3$ ($M = \text{Nb}$ (100), Ta (101), Mo (102)), $\text{WCl}_4 \cdot 3\text{NMe}_3$ (97)), but here the well established reducing properties of

$L = \text{NH}_3$ (93), THT (94), dien (95).

7 coordination

Theoretical aspects of 7 coordination have been examined by Kepert (3). A number of 7 coordinate adducts have been isolated with the polydentate arsine ligands *o*-phenylenebis(dimethylarsine)(diars), methylbis(*o*-dimethylarsinophenyl)arsine(*o*-TAS) and tris-1,1,1-(dimethylarsino methyl)ethane(*v*-TAS).



Clark and coworkers have prepared the 1:1 adducts $\text{MX}_5 \cdot \text{diars}$ ($M = \text{Nb}, \text{Ta}$, $X = \text{Cl}, \text{Br}$ (96); $M = \text{W}$, $X = \text{Cl}$ (97), $\text{MCl}_4(\text{o-TAS})$ and $\text{MCl}_4(\text{v-TAS})$ ($M = \text{Ti}, \text{V}$) (98). These are diamagnetic and non-conducting. Equivalent AsMe signals in the ^1H NMR spectra were taken as evidence of 7 coordination. The possibility of a more common 6 coordinate structure with rapid exchange occurring in solution between free and coordinated donor sites (which would give an identical result to above) was, however, not discussed. Confirmatory X-ray, or variable temperature ^1H NMR studies on these species have yet to be carried out.

A number of potential 7 coordinate trimethylamine adducts have been isolated ($\text{WCl}_6 \cdot \text{NMe}_3$ (99), $\text{MCl}_5 \cdot 2\text{NMe}_3$ ($M = \text{Nb}$ (100), Ta (101), Mo (102)), $\text{WCl}_4 \cdot 3\text{NMe}_3$ (97)), but here the well established reducing properties of

Trimethylamine (see Chapter 2) combined with the facile reduction undergone by many of the higher metal halides (2, 3) suggests a mixture of oxidation and reduction products to be a more appropriate formulation.

8 coordination

Studies by Clark, Nyholm, Lewis and coworkers with the bidentate ligand diars ($o\text{-C}_6\text{H}_4(\text{AsMe}_2)_2$) have now firmly established the 8 coordinate state for the early t-metals. Complexes of the type $\text{MX}_4 \cdot 2\text{diars}$ ($\text{M} = \text{Ti}$, $\text{X} = \text{Br}$, $\text{M} = \text{Zr}$, Hf , Nb , $\text{X} = \text{Cl}$, Br , $\text{M} = \text{V}$, $\text{X} = \text{Cl}$ (103-106)) were isolated and shown to be isomorphous with $\text{TiCl}_4 \cdot 2\text{diars}$, the crystal structure of which is known (Fig. 1.2.2) (103).

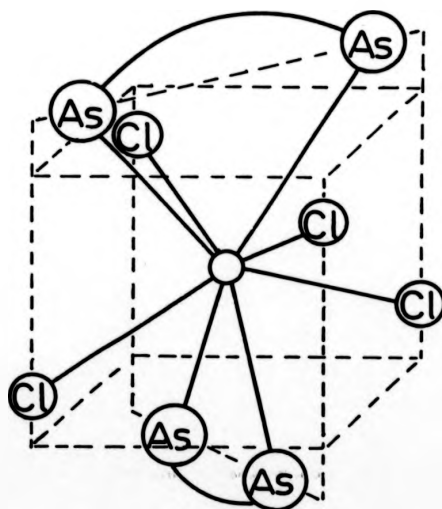


Fig. 1.3.2 Schematic Structure of $\text{TiCl}_4 \cdot 2\text{diars}$

Although $o\text{-C}_6\text{H}_4(\text{PMe}_2)_2$ (107) and $o\text{-C}_6\text{H}_4(\text{As}(\text{CD}_3)_2)_2$ (108) yielded similar 8 coordinate complexes, $o\text{-C}_6\text{H}_4(\text{AsEt}_2)_2$ (109), $o\text{-C}_6\text{H}_4(\text{PEt}_2)_2$ (110) and $o\text{-C}_6\text{H}_4(\text{AsMe}_2)(\text{NMe}_2)$ (108) gave only simple 1:1 6 coordinate adducts. Since the inductive properties of Et and CD_3 are approximately equal (108), it was concluded that the ability to give high coordination numbers lay

in the choice of donor atom, i.e. As or P, but not N, and the steric effects of the donor atom substituents (107-109).

1.4 Halides and Complexes of Groups IVB and VB

The halides of groups IVB and VB are, in general, weaker acceptors than their d-block counterparts. In particular, the halides of carbon, nitrogen and phosphorus show virtually no acceptor character at all, and consequently are omitted from the text.

The tetrahalides of Group IVB are either monomeric liquids (MCl_4 , $\text{M} = \text{Si, Ge, Sn, Pb, SiBr}_4$) or molecular solids (MBr_4 , $\text{M} = \text{Ge, Sn, MI}_4$, $\text{M} = \text{Si, Ge, Sn}$) (111). PbX_4 ($\text{X} = \text{Br, I}$) are unknown (111). In the +2 state the halides are more highly polymerised. SnX_2 ($\text{X} = \text{Cl, Br, I}$) and PbX_2 ($\text{X} = \text{Cl, Br}$) form layer lattices in which the metal atom can be considered as being 9 coordinate (111). GeX_2 ($\text{X} = \text{Cl, Br, I}$) (111) are of unknown structure and SiX_2 ($\text{X} = \text{Cl, Br}$) have only been observed in discharge experiments (112).

The acceptor properties of the IVB halides increase on descending the group. The ability to form donor complexes is roughly in the order:-

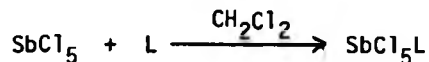


The Group IVB tetrahalides form both 1:1 and 1:2 adducts, the latter being more prevalent with the lower members of the group (113). Whereas, SiCl_4 forms mainly weakly bonded 5 coordinate 1:1 species, the complex chemistry of SnX_4 tends towards octahedral 1:2 adducts (113), and in many ways parallels that of the tetrahalides of the Ti subgroup. As with the early t-metals, $\text{SnX}_4 \cdot 2\text{L}$ adducts can exist as either cis ($\text{L} = \text{MeCN}$ (114), Me_2SO , POCl_3 (115), SeOCl_2 (116)) or trans ($\text{L} = \text{PEt}_3$ (117)) isomers (118).

Sn(II) and Pb(II) form a number of 1:1 and 1:2 complexes with a variety of donors, although little is known of the complex geometry (111). $\text{PbCl}_2 \cdot 2\text{thiourea}$ has been shown to contain 7 coordinate Pb (119).

For the Group VB halides the maximum possible oxidation state (+5) is only realised in the pentahalides SbF_5 , SbCl_5 and AsF_5 (120). AsCl_5 has no independent existence although some complexes have been isolated (121). All of the trihalides are known ($M = \text{As, Sb, Bi}$, $X = \text{F, Cl, Br, I}$), either as liquids (AsCl_3), or weakly associated solids (120, 122).

SbCl_5 is a powerful electron acceptor (123), and has been utilised by Gutmann and Wychera as a reference acid in constructing a series of relative ligand donor strengths (124). For the reaction:-



$$\text{donor number (DN)} = -\Delta H (\text{k cal mol}^{-1})$$

Some typical values are given in Table 1.4.1.

LIGAND	DN	LIGAND	DN
C_6H_6	0.1	Et_2O	19.2
MeNO_2	2.7	THF	20.0
POCl_3	11.7	Me_3PO	23.0
MeCN	14.1	py	33.1
Me_2CO	17.0	HMPA	38.8

Table 1.4.1 Donor Numbers of Some Selected Ligands

In the tervalent state, AsX_3 forms 1:1 and SbX_3 both 1:1 and 1:2 complexes (120). The existence of PX_3 adducts has been demonstrated at low temperatures (125). The stereochemistry of these adducts is complicated by the presence of a lone pair, which may (115, 126 - 128), or

may not (130, 131) be stereochemically significant. In the majority of cases however (129, 130), the lone pair has been found to be space filling, giving trigonal bipyramidal ($\text{AsCl}_3 \cdot \text{NMe}_3$ (126), $\text{SbCl}_3 \cdot \text{PhNH}_2$ (127), Fig. 1.4a) or square based pyramidal ($\text{SbCl}_3 \cdot 2\text{L}$, $\text{L} = \text{PhNH}_2$ (127), Ph_3AsO (115), $2\text{SbCl}_3 \cdot (1\text{-4-dithiane})$ (128), (Fig. 1.4b) geometries depending on the stoichiometry.

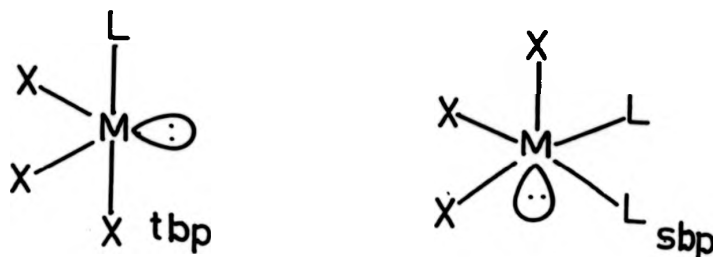


Fig. 1.4 Usual Geometries of Group VB Halide Adducts

CHAPTER 2

COMPLEXES AND REACTIONS OF TRIMETHYLAMINE

CHAPTER 2

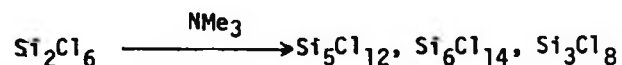
2.1 INTRODUCTION

Of the multitude of donor molecules that have been used as ligands towards transition metal halides, trimethylamine (N,N-dimethylmethaneamine) emerges as one of the most interesting, giving a wide range of both donor complexes, and chemical behaviour. Trimethylamine is a colourless gas at room temperature (b.p. 276.0K at 760 mm Hg) with a characteristic odour of decomposing fish (131). Consequently, all manipulations involving liquid NMe_3 have to be performed either at low temperatures, or under reduced pressure, the glass double ampoule bomb developed by Fowles and coworkers being particularly suited to this task (Appendix B).

The formation and chemistry of NMe_3 complexes is essentially governed by three factors:-

(a) Trimethylamine is a strong Lewis base, and acts as an electron donor towards a variety of metal, metalloidal and non-metal halides. A representative selection of the complexes formed includes: $\text{BX}_3 \cdot \text{NMe}_3$ ($\text{X} = \text{Cl}, \text{Br}, \text{I}$) (132); $\text{AlX}_3 \cdot \text{NMe}_3$ ($\text{X} = \text{Cl}, \text{Br}, \text{I}$) (133); $\text{M}(\text{CO})_5 \cdot \text{NMe}_3$ ($\text{M} = \text{Mo}, \text{W}$) (134); $\text{SeO}_3 \cdot \text{NMe}_3$ (135); Si_2H_6 , $\text{Si}_3\text{H}_8 \cdot \text{NMe}_3$ (136); $\text{SnX}_2 \cdot \text{NMe}_3$, $\text{SnX}_2 \cdot 2\text{NMe}_3$ ($\text{X} = \text{F}, \text{Cl}, \text{Br}, \text{I}$) (137) and $\text{MCl}_3 \cdot 2\text{NMe}_3$ ($\text{M} = \text{Ti}, \text{V}, \text{Cr}$) (77, 76, 69). Of particular interest are the Group IV halides SnX_4 ($\text{X} = \text{Cl}, \text{Br}, \text{I}$), SiF_4 , GeX_4 ($\text{X} = \text{Cl}, \text{Br}$) (113) and ZrCl_4 (138), which give complexes of both 1:1 and 1:2 stoichiometry. The stereochemistry of the 1:1 complexes is generally based on the trigonal bipyramid (C_{3v}), while that of the 1:2 complexes is octahedral in nature (74). TiX_4 ($\text{X} = \text{Cl}, \text{Br}$) gives only 1:1 adducts, reduction accompanying the addition of a second mole of trimethylamine.

With polychlorosilanes disproportionation rather than complexation occurs (139).



(b) The stereochemistry of NMe_3 complexes is dominated by the bulk of the ligand. Thus for 6 coordinate species there is a tendency to give trans geometries, e.g. trans $\text{SnI}_4 \cdot 2\text{NMe}_3$ (140), trans $\text{ZrX}_4 \cdot 2\text{NMe}_3$ ($\text{X} = \text{Cl}, \text{Br}$) (141). A more vivid example of the 'bulk' influences of NMe_3 is given by the complexes with MX_3 ($\text{M} = \text{Ti}, \text{V}, \text{Cr}, \text{X} = \text{Cl}, \text{Br}$). Here the effect of steric crowding overrides the electronic preferences of the metal ion, to produce the 5 coordinate $\text{MX}_3 \cdot 2\text{NMe}_3$ adducts. In the solid state, the complexes assume a monomeric, approximately (D_{3h}) symmetry, e.g. Fig.2.1.1.

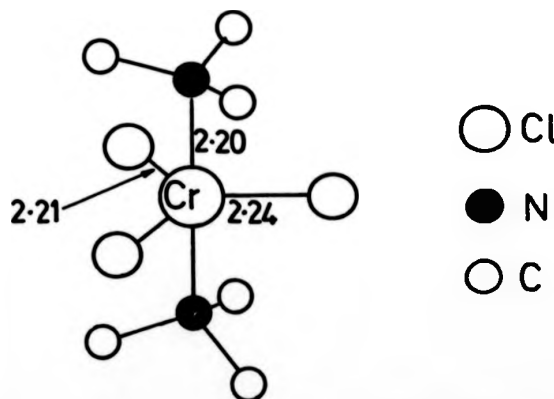


Fig. 2.1.1 X-ray Crystal Structure of $\text{CrCl}_3 \cdot 2\text{NMe}_3$ (69, 78)

Deviations from an ideal D_{3h} configuration are ascribed to Jahn-Teller distortion for $\text{TiBr}_3 \cdot 2\text{NMe}_3$ (77, 78) and $\text{CrCl}_3 \cdot 2\text{NMe}_3$ (69), and in the case of $\text{VCl}_3 \cdot 2\text{NMe}_3$ (for which Jahn-Teller distortion should not occur) to crystal packing forces (76).

A general instability of these adducts was found in all solvents except NMe_3 , decomposition occurring to give complexes of stoichiometry

$M_2Cl_6(NMe_3)_3$ (142). The confacial bioctahedral structure proposed for these species enables the metal ion to revert to the pseudo-octahedral configuration they invariably adopt with smaller, less bulky ligands (e.g. $MX_3 \cdot 3RCN$, $MX_3 \cdot 3THF$). The rates of decomposition for the $MCl_3 \cdot 2NMe_3$ ($M = Ti, V, Cr$) series have been measured in C_6H_6 solution at 298 K (142) and were found to vary in the order $Cr > V > Ti$. Decomposition of $CrCl_3 \cdot 2NMe_3$ is also noticeable in the solid phase, giving $(CrCl_3)_2(NMe_3)_3$ over a period of several months.

In addition to producing coordinative unsaturation, the steric properties of NMe_3 also give rise to a weakening of the metal ligand bond, making the $MX_3 \cdot 2NMe_3$ series useful intermediates for ligand exchange reactions. Use of such a synthetic route is particularly advantageous in the preparation of inert $Cr(III)$ (t_{2g}^3) complexes. Whereas NMe_3 displacement reactions have already been used to synthetic advantage with the $MCl_3 \cdot 2NMe_3$ complexes (143), the role of the octahedral $MX_4 \cdot 2NMe_3$ adducts in a similar capacity has yet to be established.

(c) Further to straightforward complexation, NMe_3 can also act as a reducing agent. One of the best known examples features the reduction of MX_4 ($M = Ti, V$) in excess NMe_3 to yield the tervalent $MX_3 \cdot 2NMe_3$ ($M = Ti, V$) species (65, 66). The analogous Zr (141) and Hf (144) tetrahalides under the same conditions yield only the simple 6 coordinate adducts $MCl_4 \cdot 2NMe_3$. Synthesis of the $MCl_3 \cdot 2NMe_3$ ($M = Ti, Cr$) complexes by direct reaction of MCl_3 with liquid NMe_3 also entails reduction, with formation of $MCl_2 \cdot NMe_3$ as a minor (1-2%) side reaction (145). Other examples are found in the reactions of NMe_3 with $MoCl_5$, WCl_6 (99) and $CuCl_2$ (146) giving $Mo(IV)$, $W(IV)$ and $Cu(I)$, respectively.

The identification of the trimethylamine oxidation products has been the subject of considerable effort. Most workers agree that the reduction

process proceeds by a radical route. Kiesel and Schram have studied the $\text{VCl}_4/\text{NMe}_3$ system (147) and have isolated $\text{Me}_3\text{N}^+\text{HCl}^-$ as one of the oxidation products. This is generally accepted to arise from the reaction of NMe_3 with the dimethylmethyleneammonium cation ($\text{Me}_2\text{N}=\text{CH}_2^+$), which has been proposed as the initial oxidation product (147). Although not isolated, evidence for the dimethylmethyleneammonium cation exists in the IR spectrum of the crude products, where a band in the $1678\text{--}1690\text{ cm}^{-1}$ region was identified as a $\nu(\text{C}=\text{N})$ stretching mode. It has also been suggested that in addition to giving $\text{Me}_3\text{NH}^+\text{Cl}^-$, reaction of $\text{Me}_2\text{NCH}_2^+\text{Cl}^-$ with NMe_3 provides $\text{Me}_2\text{NCH}_2\text{NMe}_3^+\text{Cl}^-$ and $(\text{Me}_2\text{NCH})_n$ as secondary products, although there appears to be some controversy over the existence of the former.

We have studied the reactions of NMe_3 with a number of metal halides and oxyhalides. Reduction was found to occur in several cases and the complex $(\text{MoCl}_2.2\text{NMe}_3)_x$ provided a possible example of a low coordination number. Substitution reactions of some $\text{MCl}_4.2\text{NMe}_3$ species were studied briefly; octahedral adducts were found to be useful albeit limited intermediates in complex synthesis.

2.2 Reactions of HfX_4 ($\text{X} = \text{Br}, \text{I}$) and ZrCl_4 with NMe_3

Extraction of HfX_4 ($\text{X} = \text{Br}, \text{I}$) with liquid NMe_3 using the double ampoule technique yielded crystals of white $\text{HfBr}_4.2\text{NMe}_3$, and of orange/yellow $\text{HfI}_4.2\text{NMe}_3$ respectively. It should be noted that commercial samples of the tetrahalides were found to be unsuitable, the products obtained being either insoluble in NMe_3 , or in the case of HfI_4 , badly contaminated with iodine. Attempts to produce analogous MeCN , pyridine or THF adducts either by direct reaction with HfI_4 or via ligand substitution with $\text{HfI}_4.2\text{NMe}_3$ resulted in the elimination of molecular iodine and the formation of non-stoichiometric products. Similarly, HfBr_4 produced poorly defined adducts with all ligands except NMe_3 . Little is known of the complex chemistry of HfBr_4 and HfI_4 where, somewhat surprisingly, the trimethylamine adducts remain the sole

examples of 6 coordinate bromo and iodo species respectively.

The IR spectra of the complexes in the $4000\text{--}400\text{ cm}^{-1}$ region were similar with bands at $1220\text{--}1230\text{ cm}^{-1}$, $\nu_{\text{as}}(\text{CN})$; $970\text{--}980\text{ cm}^{-1}$, $\rho(\text{CH}_3)$; $800\text{--}805\text{ cm}^{-1}$, $\nu_{\text{s}}(\text{CN})$ and $520\text{--}530\text{ cm}^{-1}$, $\delta_{\text{as}}(\text{CN})$ confirming the presence of coordinated NMe_3 (68). Single intense bands in the low IR at 307 cm^{-1} (HfBr) and 165 cm^{-1} (HfI) correlate with a trans ($\text{D}_{4\text{h}}$) arrangement of ligands (149). Both complexes were found to be either insoluble or rapidly decompose in most common solvents. Sufficient stability however, was found in MeNO_2 solutions to observe single resonances in the ^1H NMR spectra (90 MHz) due to equivalent NMe_3 groups ($\delta = 2.70$, $\text{X} = \text{Br}$, $\delta = 2.80$, $\text{X} = \text{I}$) before decomposition set in (~ 4 mins). A general feature of the MX_4 ($\text{M} = \text{Zr}, \text{Hf}$, $\text{X} = \text{Cl}, \text{Br}$)/ NMe_3 reactions was the production of varying amounts of a white amine-insoluble product (143). The IR spectra of these solids in the $4000\text{--}400\text{ cm}^{-1}$ region differed only slightly from those of the crystalline amine-soluble fractions, but the metal-halogen stretching region showed a more complex situation than that found for the bis adducts, with poorly defined broad M-X bands. A polymeric model, in which only partial solvolysis of the M-X bridges occurs is proposed. The slightly high halide analyses obtained for these products would tend to support this view, (admittedly the inclusion of unreacted metal tetrahalide as part of the products would give a similar result). The fact that ZrI_4 and HfI_4 leave no such residues may be a reflection of weaker iodine bridging in the MI_4 lattice.

The observation that the reaction of ZrCl_4 and gaseous NMe_3 gave another product in addition to $\text{ZrCl}_4 \cdot 2\text{NMe}_3$, prompted an examination of some $\text{MX}_4(\text{s}) + \text{NMe}_3(\text{g})$ systems. One possibility was that such an approach would lead to the elusive M(III) species. Whereas exposure of HfX_4

(X = Cl, Br, I) to $\text{NMe}_3(\text{g})$ at room temperature merely gave mixtures of $\text{HfX}_4 \cdot 2\text{NMe}_3$ and unreacted metal halide, the reaction with ZrCl_4 was highly exothermic, giving $\text{ZrCl}_4 \cdot 2\text{NMe}_3$ as the major NMe_3 soluble product, ($\sim 60\%$), and a dark brown C_6H_6 insoluble residue. Characterisation of this residue proved difficult, but low IR evidence suggested that the product was $\text{ZrCl}_4 \cdot \text{NMe}_3$ (138), apparently formed by the thermal degradation of $\text{ZrCl}_4 \cdot 2\text{NMe}_3$ rather than any reduced species.

2.3 Reactions of NMe_3 with Cp_2MCl_2 (M = Ti, Zr, Hf)

Cp_2TiCl_2 dissolves in liquid NMe_3 to give bright green crystals of $(\text{Cp}_2\text{Ti}(\text{II})\text{Cl})_2$ over a period of several months. Under the same conditions Cp_2ZrCl_2 and Cp_2HfCl_2 dissolved without reaction. This situation resembles the reaction of NMe_3 with the corresponding tetrahalides, where TiCl_4 readily gives $\text{TiCl}_3 \cdot 2\text{NMe}_3$ (65, 67), but ZrCl_4 (141) and HfCl_4 (144) only the M(IV) bis adducts.

No trace of coordinated NMe_3 was found in any of the $\text{Cp}_2\text{MCl}_2/\text{NMe}_3$ systems studied. Reaction of Cp_2MCl_2 (M = Ti, Zr) with MeCN , Et_3N , py , THF and Et_2O likewise failed to give any evidence for adduct formation. For the Cp_2MCl_2 series, lack of acceptor behaviour can be interpreted in terms of the vacant coordination sites on the metal being shielded by the large cyclopentadienyl groups. The isolation of adducts of Cp_2TiCl with several amines and phosphines (i.e. $\text{Cp}_2\text{TiCl} \cdot \text{L}$, L = NH_3 , RNH_2 , py , Me_2PPh , MePPh_2 (150)) weakens this argument for the $\text{Cp}_2\text{Ti}(\text{III})$ species, and it has been suggested that the reticence of secondary and tertiary amines in general to give such complexes is a reflection of the electronic dictates of the metal rather than steric factors (150). Previous preparative routes to $(\text{Cp}_2\text{TiCl})_2$ have often featured Zn as the reducing species (e.g. $\text{Zn}/\text{Me}_2\text{CO}$, Zn/THF , Zn (metal) (151)). Addition of Zn dust to the $\text{Cp}_2\text{TiCl}_2/\text{NMe}_3$ system notably accelerated the rate of formation of

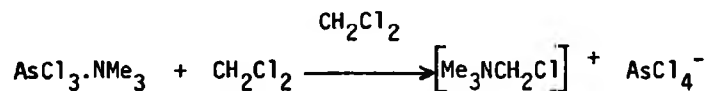
$(\text{Cp}_2\text{TiCl})_2$ giving crystals of the product as the sole amine soluble fraction within a week. The exact role of the Zn metal, i.e. either as the primary reducing species, or as a catalyst (cf. the $\text{CrCl}_3/\text{NMe}_3$ (68) and $\text{ZrCl}_4/\text{NMe}_3$ (141) systems) could not be established. The ZnCl_2 bridged dimer $(\text{Cp}_2\text{Ti(III)Cl})_2\text{ZnCl}_2$ (151) constitutes a major fraction of the products from the Zn reduction of Cp_2TiCl_2 in non-polar solvents such as benzene (151). Although its absence was confirmed in the product, contamination from residual Zn prevented the establishment of $(\text{Cp}_2\text{TiCl})_2\text{ZnCl}_2$ or a similar species as a component of the amine-insoluble fraction.

2.4 Reactions of NMe_3 with some Group VB Halides

Reaction of MX_3 ($\text{M} = \text{As, Sb, X} = \text{Br, Cl}$) and trimethylamine at 273 K in C_6H_6 solution gives two series of products: the white $\text{MX}_3.\text{NMe}_3$ ($\text{M} = \text{As, Sb, X} = \text{Cl, Br}$) and the pale yellow $\text{SbX}_3.2\text{NMe}_3$ ($\text{X} = \text{Cl, Br}$) adducts. All are air-moisture sensitive, ranging in extent from $\text{AsCl}_3.\text{NMe}_3$ which fumes immediately in air to $\text{SbBr}_3.2\text{NMe}_3$ which decolourises only after a few hours exposure. Thermal stability was of the order $\text{Sb} > \text{As}$ and $\text{Br} > \text{Cl}$, decomposition occurring at the melting point to give brown solids. Pyrolysis of $\text{SbCl}_3.2\text{NMe}_3$ in vacuo at 359 K gave $\text{SbCl}_3.\text{NMe}_3$ in low yield ($\sim 10\%$), but no such reaction was observed for the bromo analogue. No evidence could be found for the bis adducts $\text{AsX}_3.2\text{NMe}_3$ ($\text{X} = \text{Cl, Br}$). The existence of $\text{PCl}_3.2\text{NMe}_3$ only at very low temperatures (125) suggests a general thermal instability of these bis adducts. Attempts to prepare $\text{AsCl}_3.\text{NMe}_3$ by direct reaction of AsCl_3 and NMe_3 in the absence of a solvent proved to be far from satisfactory, yielding a hard mass, whose ^1H NMR spectrum (C_6D_6 solution) showed > 20 resonances in the NMe region. $\text{AsCl}_3.\text{NMe}_3$ is evidently present as a component of this mixture. (Somewhat surprisingly this method has been used to prepare samples of $\text{AsCl}_3.\text{NMe}_3$ for single crystal X-ray analysis (126)). A reaction of this type could

also account for an early report of the non-stoichiometric complexes $\text{AsCl}_3(\text{NMe}_3)_{0.82}$ and $\text{SbCl}_3(\text{NMe}_3)_{1.1}$ (153).

The products are soluble to varying extents in coordinating solvents (THF, MeCN), usually with some ligand exchange, although no pure substitution products were isolated. Decomposition occurred in chlorinated solvents after ~ 25 minutes to give white insoluble solids. Similar products to these were obtained during the preparation of the adducts in CH_2Cl_2 solution. Solvent attack on the amine to give initially a quaternary ammonium salt in a Menshutkin-type reaction is proposed (154).



Evidence for a formulation of this type comes from the low IR spectrum, where bands at 345, 340, 330, 304 and 275 cm^{-1} correlate well with those found for the AsCl_4^- ion in $(\text{Et}_4\text{N})^+ \text{AsCl}_4^-$ (155) (i.e. 352, 343, 329 and 302 cm^{-1}).

Proton and ^{13}C spectra (CDCl_3 or CH_2Cl_2 solns., rel. TMS) (Table 2.4.1) show one sharp singlet in all cases, confirming the equivalence of the NMe_3 groups in solution. There is no obvious trend in chemical shifts for either the ^1H or ^{13}C spectra.

Complex	^1H δ (ppm)	^{13}C δ (ppm)
$\text{AsCl}_3 \cdot \text{NMe}_3$	2.42	46.21
$\text{AsBr}_3 \cdot \text{NMe}_3$	2.51	47.18
$\text{SbCl}_3 \cdot \text{NMe}_3$	2.47	46.73
$\text{SbBr}_3 \cdot \text{NMe}_3$	2.50	-
$\text{SbCl}_3 \cdot 2\text{NMe}_3$	2.49	46.53
$\text{SbBr}_3 \cdot 2\text{NMe}_3$	2.51	47.83

Table 2.4.1 NMR Data for $\text{MX}_3 \cdot \text{NMe}_3$ and $\text{MX}_3 \cdot 2\text{NMe}_3$

Strong bands in IR spectra at $1247\text{--}1259\text{ cm}^{-1}$ $\nu_{\text{as}}(\text{CN})$; $998\text{--}1004\text{ cm}^{-1}$ $\rho(\text{CH}_3)$; $794\text{--}803\text{ cm}^{-1}$ $\nu_{\text{s}}(\text{CN})$ and $456\text{--}474\text{ cm}^{-1}$ $\delta(\text{NMe}_3)$ are associated with coordinated amine (68). In the low IR region, intense bands at $387, 356\text{ cm}^{-1}$ ($\text{AsCl}_3\cdot\text{NMe}_3$); $285, 205\text{ cm}^{-1}$ ($\text{AsBr}_3\cdot\text{NMe}_3$); 185 cm^{-1} ($\text{SbCl}_3\cdot\text{NMe}_3$); 180 cm^{-1} ($\text{SbBr}_3\cdot\text{NMe}_3$); 195 cm^{-1} ($\text{SbCl}_3\cdot 2\text{NMe}_3$) and 176 cm^{-1} ($\text{SbBr}_3\cdot 2\text{NMe}_3$) are tentatively assigned to metal-halogen stretching modes. Structural assignment via the low IR spectra is complicated in the case of Group VB adducts by the variety of geometries the complex can assume; these may or may not include a stereoactive lone pair.

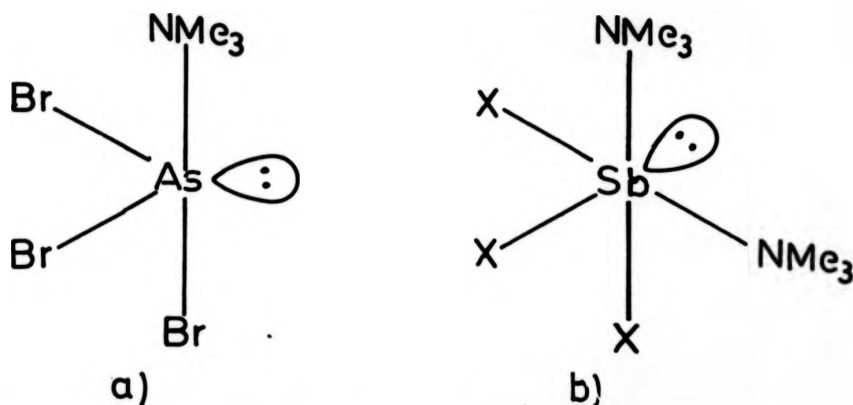


Fig. 2.4.1 Proposed Geometries of $\text{AsBr}_3\cdot\text{NMe}_3$ and $\text{SbX}_3\cdot 2\text{NMe}_3$
($\text{X} = \text{Cl}, \text{Br}$).

Single crystal X-ray studies of $\text{AsCl}_3\cdot\text{NMe}_3$ (126) and $\text{SbCl}_3\cdot\text{PhNH}_2$ (127) and vibrational analyses of $\text{PX}_3\cdot\text{NMe}_3$ ($\text{X} = \text{Br}, \text{Cl}$) (125) have been interpreted in terms of a pseudo-trigonal bipyramidal structure (Fig. 2.4.1a) in which the lone pair is active, and occupies an equatorial site. A similar situation is proposed for $\text{AsBr}_3\cdot\text{NMe}_3$. By analogy with $\text{SbCl}_3\cdot 2\text{PhNH}_2$ (128), $\text{SbCl}_3\cdot 2\text{Ph}_3\text{AsO}$ (115) and $\text{SbCl}_3\cdot 2\text{NH}_3$ (156), a pseudo-octahedral configuration (Fig. 2.4.1b) is proposed for the bis adducts $\text{SbX}_3\cdot 2\text{NMe}_3$ ($\text{X} = \text{Cl}, \text{Br}$), although a structure similar to that found for $\text{AsCl}_3\cdot\text{bipy}$ (where the lone pair is inactive and octahedral coordination is achieved by halogen bridging) (130) cannot be excluded.

In the case of $\text{SbX}_3 \cdot \text{NMe}_3$ ($\text{X} = \text{Cl}, \text{Br}$), the close similarity in terms of the low IR spectra with the corresponding bis SbX_3 adducts suggests a structure other than Fig. 2.4.1b. A pseudo square-based pyramidal structure (Fig. 2.4.2) is proposed, in which the SbX_3 unit is re-aligned to give a long range $\text{Sb} \cdots \text{X}$ interaction leading to weak halogen bridging.

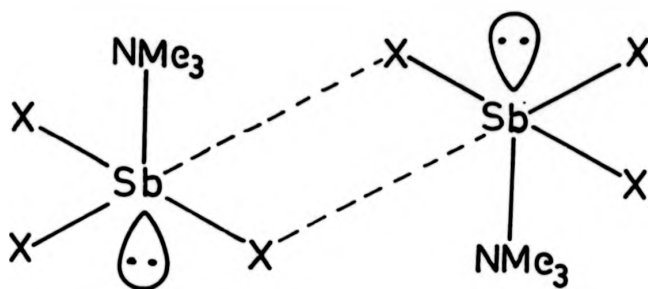


Fig. 2.4.2 Proposed Structure of $\text{SbX}_3 \cdot \text{NMe}_3$ ($\text{X} = \text{Cl}, \text{Br}$)

This type of secondary bonding to give loosely bonded dimeric molecules has been established for $\text{MX}_3 \cdot \text{dimit}$ in the solid phase. ($\text{M} = \text{As}, \text{Sb}$; $\text{X} = \text{Cl}, \text{Br}$; $\text{dimit} = 1,3$ dimethyl-2(3H)imidazolethione (157, 158)). An electron impact (70 eV) mass spectrum of $\text{AsCl}_3 \cdot \text{NMe}_3$ gave a molecular ion at $m/e = 239$, confirming the mononuclear nature of the complex in the gas phase. Other prominent ions were found at $m/e = 180$ (AsCl_3^+) and $m/e = 145$ (AsCl_2^+).

2.5 NMe_3 Complexes of some Halides and Oxyhalides of Molybdenum

2.5.1 Reactions of NMe_3 with MoCl_3 and MoCl_4

Extraction of a MoCl_3/Zn dust mixture with NMe_3 over a period of seven months gave $\text{MoCl}_2 \cdot 2\text{NMe}_3$ as bright purple crystals. Preparations in which the Zn dust was omitted failed to give any reaction even after several months, the MoCl_3 being recovered unchanged. Fowles and coworkers

found a similar situation with the $\text{MoBr}_3/\text{NMe}_3$ system (159) where no reaction was observed even after a year. MoCl_4 also proved to be totally unreactive towards NMe_3 over extended periods, both with and without the use of a Zn catalyst. $\text{MoCl}_4 \cdot 2\text{PrCN}$ has successfully been employed as a precursor to several MoCl_4 complexes via ligand exchange reactions (160). When $\text{MoCl}_4 \cdot 2\text{MeCN}$ was treated with excess NMe_3 , however, no such reaction was observed, and workup of the products revealed only unchanged starting materials.

The complex $\text{MoCl}_2 \cdot 2\text{NMe}_3$ proved to be highly air/moisture sensitive, decomposition to a green solid occurring almost immediately on exposure to moist air. Deep purple solutions were initially formed in a variety of donor and non-donor solvents, e.g. MeCN , CHCl_3 , C_6H_6 , but in all cases decomposition to brown/black solids eventually occurred (~ 1 s MeCN , THF CHCl_3 , C_6H_6 , ~ 2 weeks NMe_3). Strong bands in the IR spectrum at 1236 $\nu_{\text{as}}(\text{CN})$, 986 $\rho(\text{CH}_3)$, 819 $\nu_{\text{s}}(\text{CN})$, 520 $\delta_{\text{as}}(\text{CN})$ and 445 cm^{-1} $\delta_{\text{s}}(\text{CN})$ are diagnostic of coordinated trimethylamine (68). Low IR bands at 332 and 297 cm^{-1} are tentatively assigned as $\nu(\text{Mo-Cl})$ stretching modes.

Examples of discrete Mo(II) halo complexes are rare, the 6 coordinate $\text{MoX}_2(\text{diars})_2$ ($\text{X} = \text{Cl}, \text{Br}, \text{I}$) adducts being the sole examples (161, 162). Interestingly, a $\text{MoCl}_2/\text{NMe}_3$ species has already been isolated (163), but here the chemistry was based on a $\text{Mo}_6\text{Cl}_{12}$ metal cluster ($\text{Mo}_6\text{Cl}_{12} \cdot 2\text{NMe}_3$), the amine groups occupying the two vacant axial sites on the central Mo_6 octahedral core.

Two possible structures for the novel $\text{MoCl}_2 \cdot 2\text{NMe}_3$ complex are presented in Fig. 2.5.1. A structure such as (a), where the central metal atom is maintained in an octahedral environment by two dimensional

halide bridging has already been established for several $\text{CrX}_2 \cdot 2\text{L}$ species ($\text{L} = \text{py}, \text{DMSO}$) (92). The problem with a structure of this type, however,

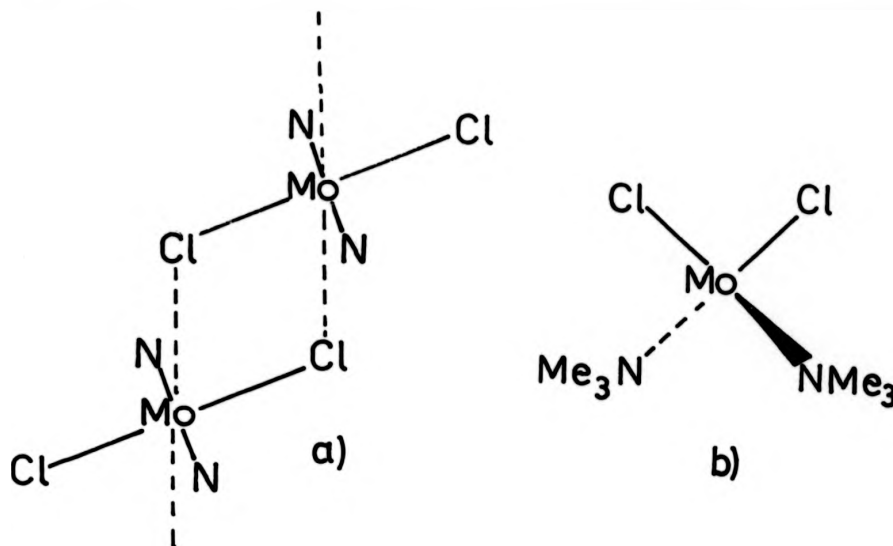


Fig. 2.5.1 Possible Structures for $\text{MoCl}_2 \cdot 2\text{NMe}_3$

is that $\text{MoCl}_2 \cdot 2\text{NMe}_3$ retains its distinctive purple colouration in NMe_3 solution, a phenomenon which would be highly unusual for a polymeric lattice, as in (a). Alternatively, a tetrahedral geometry as in (b) which is well known for the later transition metals (1) and has been proposed for $\text{CrX}_2 \cdot 2\text{Ph}_3\text{PO}$ ($\text{X} = \text{Br}, \text{I}$) (64) is possible. Two $\nu(\text{Mo}-\text{Cl})$ bands in the far IR region at $332, 297 \text{ cm}^{-1}$ ($A_1 + B_1$) tend to support this assignment.

2.5.2 Reactions of MoOCl_3 and MoOCl_4 with NMe_3

MoOCl_3 and neat NMe_3 reacted in a double ampoule bomb to initially give a deep green solution and a pale brown solid. The green solution was decanted, but over a period of several hours was observed to deposit a chocolate brown precipitate. Total extraction of the amine soluble products resulted in a mixture of deep green crystals, and a chocolate brown solid, which defied all attempts at separation. A single extraction

of MoOCl_3 , however, afforded a small amount of uncontaminated green crystals analysing as $\text{MoOCl}_3 \cdot 2\text{NMe}_3$.

The product was highly air sensitive, and dissolved with decomposition in a range of donor solvents, chlorocarbons and hydrocarbons to give deep brown solutions. Coordinated trimethylamine was shown to be present in $\text{MoOCl}_3 \cdot 2\text{NMe}_3$ by strong bands in the IR spectrum at $1234 \nu_{\text{as}}(\text{CN})$, $976 \rho(\text{CH}_3)$, $816 \nu_{\text{s}}(\text{CN})$, $534 \delta_{\text{as}}(\text{CN})$ and $433 \delta_{\text{s}}(\text{CN}) \text{ cm}^{-1}$ (68). A strong band at 955 cm^{-1} , assigned to a $\nu(\text{Mo}=\text{O})$ stretching mode falls well within the range of values found for analogous compounds, i.e. 950 cm^{-1} ($\text{MoOCl}_3 \cdot \text{PPh}_3$), 967 cm^{-1} ($\text{MoOCl}_3 \cdot 2\text{Ph}_3\text{PO}$) (164). The low IR spectrum shows bands at 345, 324 and 255 cm^{-1} which are tentatively assigned as octahedral Mo-Cl modes. Octahedral adducts of MoOCl_3 can realistically exist in three isomeric forms, the structures of which are depicted in Fig. 2.5.2.

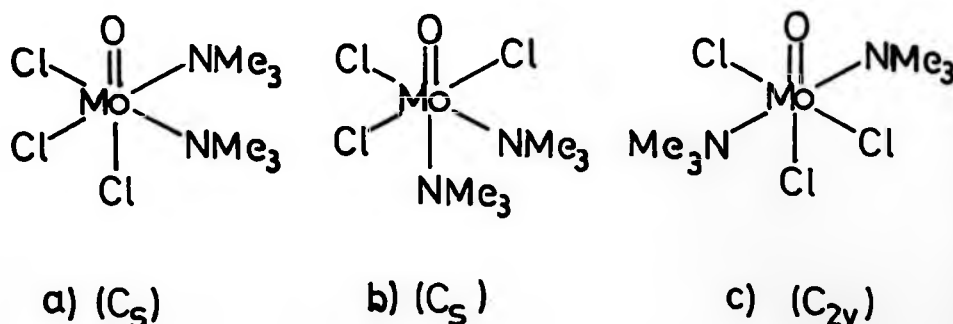


Fig. 2.5.2 Possible Structures of $\text{MoOCl}_3 \cdot 2\text{NMe}_3$

A simple group theoretical analysis of the possible structures shows that in each case three fundamental Mo-Cl stretching modes are expected (i.e. (a) (C_s), $2A' + A''$; (b) (C_s), $A' + 2A''$; (c) (C_{2v}), $A_1 + 2B_1$) making structural assignment on the basis of low IR data alone impossible. Evidence for a (b) type structure in the case of $\text{MoOCl}_3 \cdot 2\text{HMPA}$ comes from

a single crystal X-ray study where a distorted mer geometry was found (165). It seems reasonable to assume that a similar situation exists with $\text{MoOCl}_3 \cdot 2\text{NMe}_3$.

A pure sample of the chocolate brown precipitate was obtained by careful re-extraction of the amine soluble products with NMe_3 . Microanalysis showed the solid to have the same composition as the green crystals ($\text{MoOCl}_3 \cdot 2\text{NMe}_3$), but although coordinated trimethylamine was again shown to be present ($1234 \text{ cm}^{-1} \nu_{\text{as}}(\text{CN})$, $821 \text{ cm}^{-1} \nu_{\text{s}}(\text{CN})$, $526 \text{ cm}^{-1} \delta_{\text{as}}(\text{CN})$ (68), the $950\text{--}990 \text{ cm}^{-1}$ region of the spectrum revealed the complexity of the product with four separate bands ($\rho(\text{CH}_3) + 3 \times \nu(\text{Mo}=\text{O})$). In addition bands found at 675 and 656 cm^{-1} respectively which are absent in the spectrum of the parent green $\text{MoOCl}_3 \cdot 2\text{NMe}_3$ are suggestive of $\nu(\text{Mo-O-Mo})$ asymmetric stretching modes, and thus a polymeric formulation (166, 167).

The amine insoluble product shows similar trends both in multiple bands in the $970\text{--}990 \text{ cm}^{-1}$ region, and a weak band at 656 cm^{-1} . High analytical values, both for NMe_3 and Cl however, are more in line with an ionic structure. Unfortunately, a general insolubility in all suitable solvents precluded the measurement of confirmatory conductivity data.

Reaction of MoOCl_4 with NMe_3 was both slow and low yielding, providing only about 3% of orange-brown product after thirty extractions with NMe_3 . Elemental microanalysis gave an empirical formula for the solid approximating to $\text{MoOCl} \cdot \text{NMe}_3$, viz reduction $\text{Mo(VI)} \rightarrow \text{Mo(III)}$. Redox under these conditions is perhaps not too surprising considering both the reducing properties of NMe_3 and the oxidising properties of MoOCl_4 towards organic molecules (3, 4). Coordinated amine was again demonstrated to be

present by IR bands at 822 cm^{-1} $\nu_s(\text{CN})$, 522 cm^{-1} $\delta_{as}(\text{CN})$ and 403 cm^{-1} $\delta_s(\text{CN})$. As with the polymeric brown MoOCl_3 adducts, multiple bands were found in the $950\text{--}990\text{ cm}^{-1}$ region. These are tentatively assigned as 978 cm^{-1} $\rho(\text{CH}_3)$ and $989, 968, 951\text{ cm}^{-1}$ $\nu(\text{Mo}=\text{O})$ modes. Additional support for a polymeric structure lies with strong bands at $754, 655$ and 450 cm^{-1} , which are again in line with an O bridged formulation (166, 167).

2.6 Reaction of NMe_3 with Zirconium Trihalides

ZrCl_3 and ZrBr_3 initially reacted with liquid NMe_3 to give a pale yellow solution and a dark brown solid in each case. Decanting the solution and back-distillation of NMe_3 resulted in the formation of pale yellow solids which, on recrystallisation from C_6H_6 , yielded colourless crystals of trans $\text{ZrCl}_4 \cdot 2\text{NMe}_3$ and trans $\text{ZrBr}_4 \cdot 2\text{NMe}_3$, respectively, as a minor product (yield $\sim 5\%$). Microanalytical data obtained for several different samples of the amine insoluble residues, revealed the non-stoichiometric nature of the products with between 1.6 and 1.9 NMe_3 molecules coordinated per ZrX_3 unit. The addition of a small amount of Zn dust had no observable effect on the reaction.

Bands in the IR spectra of $\text{ZrX}_3(\text{NMe}_3)_{1.6\text{--}1.9}$ at $1265\text{--}1270\text{ cm}^{-1}$ $\nu_{as}(\text{CN})$, $982\text{--}985\text{ cm}^{-1}$ $\rho(\text{CH}_3)$, $803\text{--}804\text{ cm}^{-1}$ $\nu_s(\text{CN})$ and $503\text{--}505\text{ cm}^{-1}$ $\delta_{as}(\text{CN})$ were taken as being diagnostic of coordinated trimethylamine (68). For the ZrCl_3 adduct, a broad band in the $250\text{--}350\text{ cm}^{-1}$ region was assigned to $\text{Zr}\text{--}\text{Cl}$ stretching modes. A number of ZrX_3 adducts with nitrogen donors have been isolated (168–172). In the majority of cases, these were found to be non-stoichiometric (e.g. $\text{ZrCl}_3(2,4\text{-lutidine})_{1.2\text{--}1.3}$) (168) or of an unusual stoichiometry (e.g. $\text{ZrCl}_3 \cdot 2(3,5\text{-lutidine})$ (168), $\text{ZrX}_3 \cdot 2\text{py}$, $\text{ZrX}_3 \cdot 2.5\text{MeCN}$, $\text{ZrX}_3 \cdot 1.5\text{bipy}$ ($\text{X} = \text{Cl, Br, I}$) (169, 170)). During the final stages of this work, a report by Daake and Corbett indicated the non-stoichiometric nature of the

parent ZrX_3 halides [15]. A situation is proposed here in which incomplete solvolysis of the non-stoichiometric ZrX_3 lattice takes place, to create polymeric $(ZrX_3)_x(\text{ligand})_y$ units of varying composition. Those adducts which appear to have well defined proportions (e.g. $ZrX_3 \cdot 2L$) can be considered as a similar mixture of $(ZrX_3)_x(\text{ligand})_y$ units which statistically averages as the experimentally found stoichiometry. Low values for the room temperature magnetic moment of the py, MeCN, bipy [169, 170] and lutidine [168] adducts were seen in terms of a strong Zr-Zr interactions. Such a result could be interpreted as being due to the residual Zr-Zr metal-metal bonding implicit in the proposed formulation.

The presence of $ZrX_4 \cdot 2NMe_3$ as part of the reaction products remains somewhat of a mystery. A simple explanation is that the ZrX_3 starting materials were contaminated with unreacted tetrahalide. Rigorous attempts to remove such a contaminant by sublimation met with little success, however, and elemental analysis failed to show the presence of any Zr (IV) species. An alternative is the generation of ZrX_4 by disproportionation within the reaction mixture. Larson and Henzler [169] obtained a similar result with the $ZrCl_3/3,5$ -lutidine and 2,4-lutidine systems, $ZrCl_4 \cdot 2L$ being identified by their X-ray powder photographs. As with the $ZrCl_3$ /lutidine systems, no evidence was found for any reduced species.

2.7 Reaction of NMe_3 with $AuCl_3$

$AuCl_3$ (Au_2Cl_6) initially dissolved in liquid NMe_3 to give a pale brown solution. Precipitation of a pale yellow solid occurred after a few minutes; this pale yellow solid turning brown over a three week period. The brown solid was identified as a mixture of metallic gold and several organic products which defied all attempts at separation.

Reduction of Au (III) to Au (I) has previously been observed for the $\text{AuCl}_4^-/\text{XPh}_3$ ($\text{X} = \text{P}, \text{As}, \text{Sb}$) systems (173). In the majority of cases where NMe_3 has been found to act as a reducing agent, a radical mechanism has been favoured (99, 145-147). A similar approach is proposed in the present instance (Fig. 2.7.1). One of the features of this mechanism is the 1:1 adduct $\text{AuCl}_3.\text{NMe}_3$. While no physical evidence exists for this species, the isolation of similar square planer $\text{AuX}_3.\text{L}$ adducts with 'hard' donors supports such an intermediate (173). Au (I) is a much softer acid than Au (III) and it is therefore unlikely that any $\text{AuCl}(\text{NMe}_3)_x$ type adducts would be formed. The observation that the yellow solid intermediate and AuCl are identical in colour suggests that the Au (I) species is in fact uncoordinated $(\text{AuCl})_x$.

The mechanism also contains the two electron $\text{Au (III)} \rightarrow \text{Au (I)}$ reduction. Although stable Au (II) complexes have been isolated (173), they invariably feature polydentate sulphur ligands, and the existence of the similar Au (II) species in the present system is, therefore, unlikely.

The composition of the organic oxidation products remains uncertain. IR spectra showed only broad bands in similar positions to the parent NMe_3 , although a small broad band in the $1660\text{--}1700\text{ cm}^{-1}$ region could be assigned as $\nu(\text{C}=\text{N})$ (i.e. from $\text{Me}_2\text{N}=\text{CH}_2^+\text{Cl}^-$) (147).

2.8 Ligand Exchange Reactions of NMe_3 Complexes

2.8.1 Substitution reactions of $\text{MCl}_4.2\text{NMe}_3$ ($\text{M} = \text{Zr}, \text{Hf}$)

Dropwise addition of a two-fold excess of THF to solutions of $\text{MCl}_4.2\text{NMe}_3$ ($\text{M} = \text{Zr}, \text{Hf}$) in C_6H_6 resulted in facile ligand substitution, and the precipitation of the bis THF adducts. For the white solids

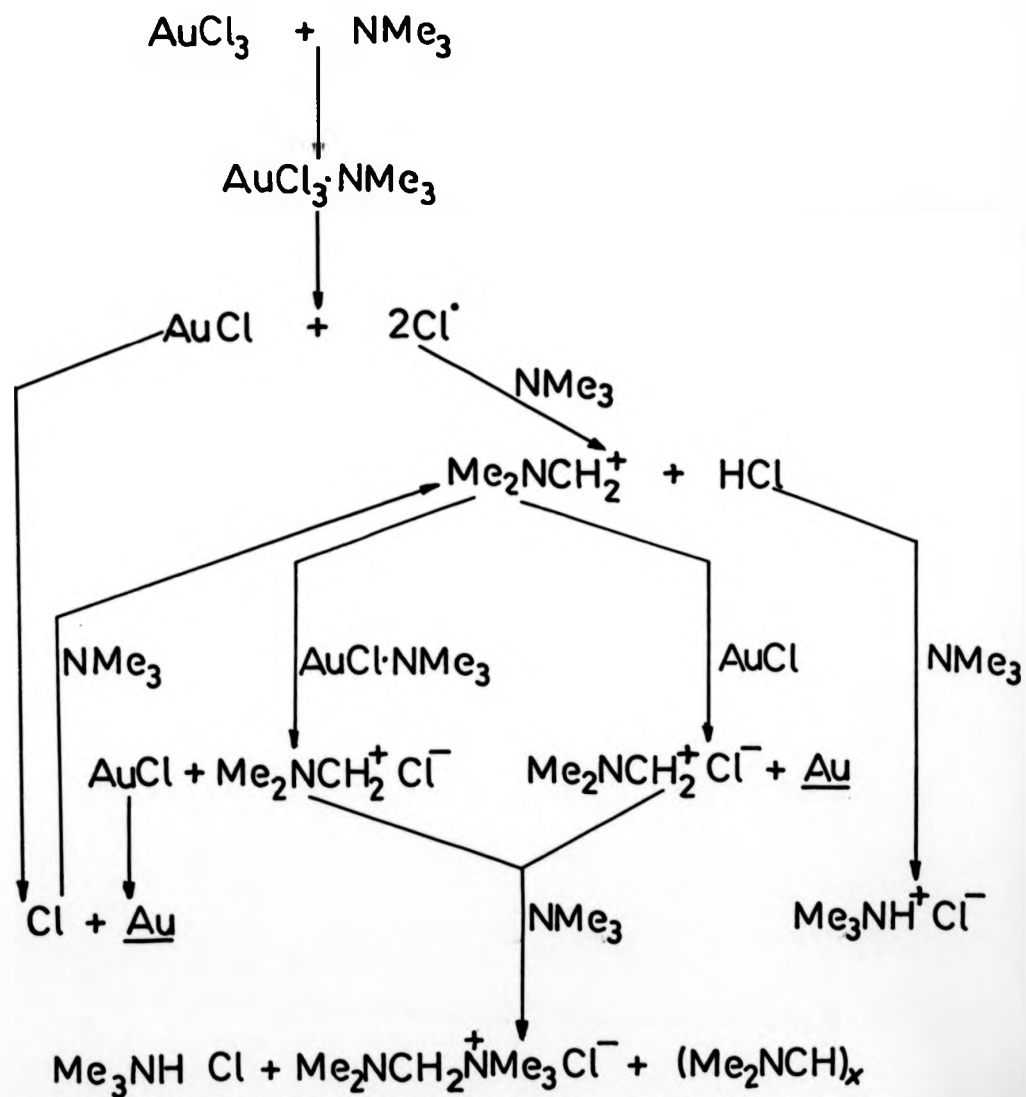


Fig. 2.7.1 Reaction Scheme for $\text{AuCl}_3 + \text{NMe}_3 \rightarrow \text{Au}$

$\text{MCl}_4 \cdot 2\text{THF}$ ($\text{M} = \text{Zr}, \text{Hf}$) (60), coordination of THF is accompanied by a shift to lower energies of the νCOC (asymmetric) stretch ($1045, 1015 \text{ cm}^{-1}$, $\text{M} = \text{Zr}$, $1043, 110 \text{ cm}^{-1}$, $\text{M} = \text{Hf}$) found at 1070 cm^{-1} in the free ligand (174). Single intense bands in the low IR spectra at 301 cm^{-1} ($\text{N} = \text{Zr}$) and 270 cm^{-1} ($\text{M} = \text{Hf}$) confirm a trans (D_4h) configuration of ligands in each case.

Attempts to displace NMe_3 from the bis amine adducts under similar conditions with the sulphur (THT) or bidentate phosphorus (dpm) donors were unsuccessful. With MeCN and phen partial amine substitution occurred, the IR spectra of the products showing bands attributable to both coordinated NMe_3 and ligand. The failure to obtain either THT or dpm complexes can be rationalised in terms of the HSAB principle (Section 1.3.1); the soft sulphur or phosphorus donors being incompatible with the hard Zr or Hf acceptor atoms. Partial substitution by MeCN or phen cannot be due to differences in hard/soft character as both ligands and NMe_3 are hard N donors. Here complex kinetic factors are considered to dominate the substitution process.

2.8.2 Complexes of MCl_4 ($\text{M} = \text{Ti}, \text{Zr}, \text{Hf}$) with tren and Me_6tren

Tris(2-aminoethyl)amine (tren) and tris(2-dimethylaminoethyl)amine (Me_6tren) are tripod shaped ligands with four potential donor atoms. Interest in these ligands with the later t-metals has provided many 5 coordinate complexes (175).

In the majority of cases all four nitrogen atoms are coordinated, often with the exclusion of a halide ion(s) from the coordination sphere, e.g. $\text{MBr}(\text{Me}_6\text{tren}) \text{ Br}$, ($\text{M} = \text{Mn}, \text{Fe}, \text{Co}, \text{Ni}, \text{Cu}, \text{Zn}$) (175). On going to the early t-metals similar behaviour is found with the trigonal

bipyramidal (Cr(II) complexes $\text{Cr}(\text{Me}_6\text{tren})\text{X}^+\text{X}^-$ ($\text{X} = \text{Cl}, \text{Br}, \text{I}$) prepared by Ciampolini (176). With the trivalent metal halides, tren was found to give both a neutral ($\text{MCl}_3\cdot\text{tren}$, $\text{M} = \text{Ti}, \text{Cr}$) and an ionic ($\text{M}(\text{tren})_2^{3+}3\text{Cl}^-$, $\text{M} = \text{Ti}, \text{Cr}$) series depending on the stoichiometry of the reaction (177). In both series of compounds only the terminal (primary) N donor atoms were believed to be coordinated. Me_6tren under the same conditions yielded only the neutral $\text{MCl}_3\cdot\text{Me}_6\text{tren}$ ($\text{M} = \text{Ti}, \text{Cr}$) adducts (178). An octahedral geometry for the metal ion was achieved in this case by donation through the central N atom and two terminal NMe_2 groups, leaving the third 'arm' uncomplexed.

The reactions of Me_6tren with TiCl_4 and $\text{MCl}_4\cdot 2\text{NMe}_3$ ($\text{M} = \text{Zr}, \text{Hf}$) provided the 1:1 adducts $\text{MCl}_4\cdot\text{Me}_6\text{tren}$ as pea-green ($\text{M} = \text{Ti}$) or white ($\text{M} = \text{Zr}, \text{Hf}$) solids. Limited solubility was found in CH_2Cl_2 and MeNO_2 solutions, with decomposition apparent after 2-3 minutes at room temperature. By reducing the temperature to 230 K, however, CH_2Cl_2 solutions of the adducts were sufficiently stable to record their ^1H NMR spectra. A single sharp resonance due to equivalent NMe_2 protons at $\delta 2.60$ ($\text{M} = \text{Ti}$), $\delta 2.68$ ($\text{M} = \text{Zr}$) and $\delta 2.70$ ($\text{M} = \text{Hf}$) reflect a progressive shift to low field ($\delta 2.32$ for NMe_2 groups in free Me_6tren) commensurate with $\text{Me}_2\text{N} \rightarrow \text{N}$ bonding. Additional evidence for equivalent coordinated NMe_2 groups comes from the IR spectra where bands associated with a free NMe_2 group in the $2820\text{--}2760\text{ cm}^{-1}$ region, and in particular the NMe_2 inversion mode at 2806 cm^{-1} (179) are absent. Coordination of the central atom is indicated by the shift to lower energy of the 796 cm^{-1} skeletal CH_2 rocking mode in the ligand and (781 cm^{-1} ($\text{M} = \text{Ti}$), and 786 cm^{-1} ($\text{M} = \text{Zr}$), 785 cm^{-1} ($\text{M} = \text{Hf}$) which occurs on formation of a five membered fused chelate ring (180-182). A five membered ring (all four N atoms coordinated) is favoured over an eight membered ring (only terminal N atoms coordinated) on

thermodynamic grounds (183). The complex multiplets in the ^1H NMR spectra of free Me_6tren at $\delta 2.55$, 2.44 corresponding to the backbone CH_2 protons are observed at lower field in the adduct spectra ($\delta 3.51$, 3.82 ($\text{M} = \text{Ti}$), $\delta 3.51$, 2.92 ($\text{M} = \text{Zr}$), $\delta 3.52$, 2.97 ($\text{M} = \text{Hf}$)) due to strain set up on ring formation. A 6 coordinate structure in which all four N atoms are coordinated is proposed (Fig. 2.8.1).

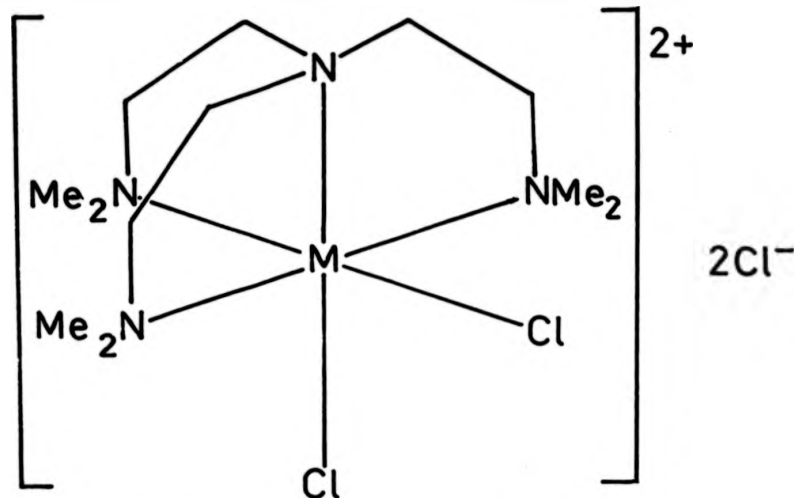


Fig. 2.8.1 Proposed Structure of $\text{MCl}_4 \cdot \text{Me}_6\text{tren}$

Attempts to verify the existence of the chloride counter ions by conductivity or halide precipitation studies were thwarted by the instability of the adducts in solution. Evidence for the remaining covalently bonded Cl atoms was found in the low IR spectra, where two strong M-Cl bands at 387 , 356 ($\text{M} = \text{Ti}$), 372 , 318 ($\text{M} = \text{Zr}$) and 327 , 277 ($\text{M} = \text{Hf}$) cm^{-1} support the proposed octahedral C_{2v} structure.

A similar series of reactions under the same conditions with tren yielded pale brown ($\text{M} = \text{Ti}$) or white ($\text{M} = \text{Zr}, \text{Hf}$) complexes of approximate composition $\text{TiCl}_4 \cdot 4\text{tren}$, and $\text{MCl}_4 \cdot 3\text{tren}$ ($\text{M} = \text{Zr}, \text{Hf}$). The complexity of the products is demonstrated in the $3320\text{--}3000$ cm^{-1} region

of the IR spectra where bands attributable to both free and coordinated NH_2 groups are found. Metal-halide stretching vibrations are absent from the spectra of the adducts, suggesting either an ionic formulation as with the Me_6tren series, or that aminolysis to give M-NH-linkages has taken place. The failure of tren to give a similar series of compounds to $\text{MCl}_4 \cdot \text{Me}_6\text{tren}$ is perhaps due to the increased basicity of primary over tertiary amine donor centres. Here indiscriminate coordination by NH_2 groups could lead to a kinetically controlled precipitation of non-stoichiometric and perhaps polymeric products.

2.9 Experimental

2.9.1 Reaction of HfX_4 ($\text{X} = \text{Br}, \text{I}$) and Cp_2MCl_2 ($\text{M} = \text{Ti}, \text{Zr}, \text{Hf}$) with NMe_3

(a) $\text{HfBr}_4 \cdot 2\text{NMe}_3$. Extraction of ~ 3 g HfBr_4 with NMe_3 (~ 60 ml) gave $\text{HfBr}_4 \cdot 2\text{NMe}_3$ ($\sim 10\%$) as colourless crystals, and a white amine insoluble residue.

Analysis based on $\text{C}_6\text{H}_{18}\text{N}_2\text{HfBr}_4$

Calculated	C(11.7)	H(2.9)	N(4.5)	Br(51.9)	%
Found	C(11.6)	H(3.2)	N(4.3)	Br(52.1)	%

Bands were found in the IR spectrum at:-

3135(vs), 3023(m), 2990(m), 2934(s), 2836(w), 2722(w), 1478(s), 1465(s), 1410(m), 1374(w), 1245(sh), 1228(m), 1103(m), 970(vs), 803(vs), 720(m), 528(s) and 307(s) cm^{-1} , respectively.

The amine insoluble fraction had a bromide content of 53.2%.

(b) $\text{HfI}_4 \cdot 2\text{NMe}_3$. Extraction of HfI_4 with liquid NMe_3 (~ 60 ml) gave $\text{HfI}_4 \cdot 2\text{NMe}_3$ as a yellow powder, or orange crystals as the sole product.

Analysis based on $\text{C}_6\text{H}_{18}\text{N}_2\text{HfI}_4$

Calculated	C(9.0)	H(2.3)	N(3.5)	I(63.1)	%
Found	C(9.0)	H(2.4)	N(3.6)	I(63.3)	%

Bands were found in the IR spectrum at:-

3115(vs), 3010(w), 2970(m), 2940(w), 2910(s), 2893(s), 2845(w),

2721(vs), 1473(vs), 1460(vs), 1446(m), 1410(m), 1402(w), 1247(m), 1215(w), 1096(m), 965(s), 804(vs), 720(m), 527(m), 187(w) and 165(vs) cm^{-1} , respectively.

(c) Reaction of Cp_2TiCl_2 with NMe_3 . Cp_2TiCl_2 (1 g) dissolved in liquid NMe_3 to give over a period of five months green crystals of $(\text{Cp}_2\text{TiCl})_2$ (~ 0.2 g) which gave an IR spectrum identical to an authentic sample.

Analysis calculated for $\text{C}_{10}\text{H}_{10}\text{TiCl}$, Calculated Cl(16.6) %.
Found Cl(16.5) %.

(d) Cp_2TiCl_2 (~ 2 g) was sealed in a double ampoule bomb with NMe_3 (~ 50 ml) and Zn dust (~ 0.1 g). After several hours the solution gradually became green, and extraction with NMe_3 over a four week period yielded $(\text{Cp}_2\text{TiCl})_2$ as the only amine soluble product. The absence of Zn in the product was confirmed by a negative dithizone test.

Analysis calculated for $\text{C}_{10}\text{H}_{10}\text{TiCl}$, Calculated Cl(16.6) %,
Found Cl(16.8) %.

2.9.2 Reactions of NMe_3 with Group VB trihalides

Preparation of complexes

In a typical reaction, gaseous trimethylamine, calculated by volume on a closed section of the vacuum line was distilled onto a frozen solution (77 K) of the appropriate metal halide contained in a single ampoule glass bomb. On warming to 273 K, reaction occurred precipitating the product from solution, which was stirred for several hours before isolation.

(a) $\text{AsCl}_3 \cdot \text{NMe}_3$. AsCl_3 (6.3 g, 34.7 mmol) and NMe_3 (775 ml, 34.6 mmol) gave the white product which was purified by sublimation under high vacuum at room temperature. Yield 3.1 g (37%).

Analysis Calculated for $C_3H_9NAsCl_3$

Calculated	C(15.0)	H(3.7)	N(5.8)	Cl(44.1)	%
Found	C(14.8)	H(3.4)	N(5.6)	Cl(44.0)	%

The IR spectrum contained bands at:-

3023(w), 2975(m), 2959(m), 2920(w), 2895(w), 2870(w,sh), 2850(m), 2820(w), 2785(w), 2710(s,br), 2515(m), 2460(m), 1473(sh), 1464(s), 1446(sh), 1436(sh), 1406(m), 1248(s), 1150(w), 1093(m), 1052(w), 1002(m), 994(w), 982(s), 803(s), 750(s), 720(w), 546(s), 464(s), 387(s), 377(m), 356(s), 332(s), 302(w), 260(w), 207(s), 182(s) and 135(w) cm^{-1} , respectively.

A repeat experiment using a three-fold excess of NMe_3 yielded an identical product.

(b) $AsBr_3 \cdot NMe_3$. $AsBr_3$ (4.3 g, 13.6 mmol) and NMe_3 (30 ml, 13.6 mmol) gave $AsBr_3 \cdot NMe_3$ as a white product. Small amounts of pure product could be obtained by sublimation in high vacuum. Yield 1.1 g (22%). M.p. (uncorr., decomp.) 360-361 K.

Analysis calculated for $C_3H_9NAsBr_3$

Calculated	C(9.6)	H(2.4)	N(3.7)	Br(64.1)	%
Found	C(9.7)	H(2.3)	N(3.6)	Br(64.1)	%

The IR spectrum showed bands at:-

3005(m), 2980(m), 2910(w), 2895(w,sh), 2865(m), 2830(w), 2795(w), 2730(s), 2503(m), 2456(m), 1473(sh), 1463(s), 1447(sh), 1434(sh), 1401(m), 1265(w), 1250(s), 1145(w), 1095(m), 1000(s), 993(vw), 980(w), 795(s), 735(s), 725(w), 460(s), 387(w), 295(w), 285(m), 265(m), 225(m), 205(s), 175(m), 130(m) and 86(w) cm^{-1} , respectively.

Again, a repeat experiment with a three-fold excess of NMe_3 yielded an identical product.

(c) SbCl₃.NMe₃. SbCl₃ (7.6 g, 33.3 mmol) and NMe₃ (745 ml, 33.3 mmol) gave white SbCl₃.NMe₃, which was purified by washing with benzene in vacuum, followed by pumping for several hours. Yield 41 g (42%). M.p. 466-468 K.

Analysis based on C₃H₉NSbCl₃

Calculated	C(12.5)	H(3.5)	N(5.0)	Cl(37.1)	%
Found	C(12.5)	H(3.7)	N(5.1)	Cl(37.1)	%

Bands were found in the IR spectrum at:-

3030(s), 3005(m), 2955(w), 2920(w), 2895(w), 2870(vw), 2845(w), 2750(s,br), 2505(w), 2460(m), 1475(sh), 1466(s), 1448(sh), 1432(sh), 1405(m), 1259(s), 1155(vw), 1097(s), 1063(vw), 1004(s), 977(w), 801(s), 719(s), 458(s), 335(m), 316(m), 260(w), 232(m), 185(vs) and 110(w) cm⁻¹, respectively.

(d) SbBr₃.NMe₃. SbBr₃ (8.2 g, 22.7 mmol) and NMe₃ (508 ml, 22.7 mmol) gave white SbBr₃.NMe₃ which was purified by washing with benzene in vacuum, then pumping dry. Yield 4.6 g (48%). M.p. (decomp.) 477-480 K.

Analysis calculated for C₃H₉SbBr₃

Calculated	C(8.5)	H(2.1)	N(3.3)	Br(56.9)	%
Found	C(8.7)	H(2.1)	N(3.5)	Br(56.9)	%

Bands were found in the IR spectrum at :-

3030(s), 3006(m), 2954(m), 2910(w,sh), 2890(m), 2870(w,sh), 2840(m), 2755(s), 2490(w), 2445(m), 1473(sh), 1464(s), 1445(w), 1435(sh), 1405(m), 1247(s), 1095(m), 1053(w), 1002(m), 996(w), 977(s), 800(s), 705(s), 673(w), 474(s), 290(m), 275(w), 258(m), 234(m), 180(s), 147(w) and 118(w) cm⁻¹, respectively.

(e) SbCl₃.2NMe₃. SbCl₃ (6.0 g, 26.3 mmol) and NMe₃ (1310 ml, 58.5 mmol) gave pale yellow SbCl₃.2NMe₃ which was washed and dried as above. Yield 8.2 g, (93%). M.p. (decomp.) 359 K.

Analysis based on $C_6H_{18}N_2SbCl_3$

Calculated	C(20.8)	H(5.2)	N(8.0)	Cl(30.7)	%
Found	C(20.4)	H(5.1)	N(7.9)	Cl(30.6)	%

The IR spectrum showed bands at:-

3035(m), 3010(m), 2990(w,sh), 2965(m), 2921(sh), 2905(s), 2880(sh), 2850(m), 2780(m), 2755(m), 1476(sh), 1467(s), 1456(sh), 1452 (sh), 1436(sh), 1413(sh), 1406(m), 1402(sh), 1249(s), 1096(s), 1003(s), 966(s), 803(s), 721(s), 673(sh), 668(w), 456(s), 388(w), 298(m), 245(w), 195(s), 143(w) and 121(w) cm^{-1} , respectively.

(f) $SbBr_3 \cdot 2NMe_3$. $SbBr_3$ (5.9 g, 16.3 mmol) and NMe_3 (764 ml, 34.1 mmol) gave pale yellow $SbBr_3 \cdot 2NMe_3$, which was washed and dried as above.

Yield 6.9 g (88.3%). M.p. (decomp.) 380 K.

Analysis based on $C_6H_{18}N_2SbBr_3$

Calculated	C(15.0)	H(3.8)	N(5.8)	Br(50.0)	%
Found	C(14.7)	H(3.6)	N(5.9)	Br(50.0)	%

Bands were found in the IR spectrum at:-

3035(m), 3010(m), 2960(m), 2920(sh), 2900(s), 2878(sh), 2850(m), 2780(m), 2760(m), 1477(sh), 1470(s), 1460(sh), 1450(sh), 1440(sh), 1415(sh), 1410(m), 1406(sh), 1250(s), 1097(s), 998(s), 956(s), 794(s), 705(s), 686(sh), 670(w), 467(s), 395(w), 255(w), 235(w), 176(s), 128(w) and 115(w) cm^{-1} , respectively.

2.9.3 Complexes of Mo halides and oxyhalides with NMe_3

(a) $MoCl_2 \cdot 2NMe_3$ $MoCl_3$ (~4 g) and Zn dust (~0.5 g) were sealed in a double ampoule bomb with NMe_3 (~40 ml). After a few hours, a pale pink colour developed. Filtration of the solution through the sinter, and back distillation of amine resulted in a small amount of a bright purple solid. Two such bombs over a seven month period (about 50 extractions each) yielded about 1 g of crude product, which was purified

by re-extraction with NMe_3 (to free it from the black decomposition product) giving ~ 0.5 g of $\text{MoCl}_2 \cdot 2\text{NMe}_3$ as bright purple crystals. The absence of Zn in the product was confirmed by a negative dithizone test.

Analysis based on $\text{C}_6\text{H}_{18}\text{N}_2\text{MoCl}_2$

Calculated	C(25.3)	H(6.4)	N(9.8)	Cl(24.8)	%
------------	---------	--------	--------	----------	---

Found	C(25.7)	H(6.4)	N(9.7)	Cl(25.5)	%
-------	---------	--------	--------	----------	---

Bands were found in the IR spectrum at:-

3038(m,br), 3002(m), 2977(w), 2927(w), 2898(m), 2870(w), 2848(m),
2818(w), 2786(w), 1484(s), 1465(s), 1439(w), 1402(m), 1254(w),
1236(w), 1106(w), 1098(w), 1003(w), 986(s), 895(w), 819(s),
724(m), 520(m), 507(vw), 445(w, br), 332(s), 297(w,sh), 280(m)
and $230(\text{w}) \text{ cm}^{-1}$, respectively.

(b) Reaction of MoOCl_3 with NMe_3 . MoOCl_3 (~ 2 g) and NMe_3 (~ 50 ml) were sealed in a double ampoule bomb at 77 K. On warming to room temperature, the NMe_3 solution almost immediately became dark green. A single extraction afforded $\text{MoOCl}_3 \cdot 2\text{NMe}_3$ as dark green crystals.

Analysis based on $\text{C}_6\text{H}_{18}\text{N}_2\text{MoOCl}_3$

Calculated	C(21.4)	H(5.4)	N(8.3)	Cl(31.6)	%
------------	---------	--------	--------	----------	---

Found	C(21.6)	H(5.3)	N(8.4)	Cl(31.4)	%
-------	---------	--------	--------	----------	---

Bands were found in the IR spectrum at:-

3020(m), 2985(s), 2930(sh), 2910(sh), 2880(sh), 2854(w), 2798(m)
1474(sh), 1457(s), 1408(s), 1234(m), 1113(m), 976(s), 955(s),
816(s), 725(m), 534(s), 433(w), 345(s) and $324(\text{s}) \text{ cm}^{-1}$, respectively.

(c) On standing for several days, the green solution as obtained in (b) gave a light brown precipitate. Careful re-extraction of this solid with NMe_3 gave the light brown powdery product, a Nujol mull of which showed IR bands at:-

1409(s), 1243(w,br), 1108(w), 984(sh), 980(s), 970(s), 952(m), 821(s), 752(w,sh), 733(m), 675(m), 656(m), 526(m), 334(w) and 310(s) cm^{-1} , respectively.

Analysis found C(21.83, 22.02), H(5.63, 5.67), N(8.75, 8.67), Cl(28.18, 28.28) %.

(d) Total extraction of all NMe_3 soluble products, i.e. (b) and (c), left a light red/brown residue, which showed IR bands at:-

3085(m), 3028(w), 2962(w), 2927(m), 2903(m), 2850(w), 2795(w), 1487(s), 1467(m), 1418(w), 1374(w), 1270(w), 1158(w,br), 1103(w,br), 1073(w,br), 986(s), 980(w,sh), 970(w,sh), 820(s), 723(m), (656(w), 522(m) and 313(s,br) cm^{-1} , respectively.

Analysis found C(26.71, 27.18), H(6.96, 7.08), N(9.15, 8.83), Cl(31.94, 32.80) %.

(e) Addition of a small amount of Zn dust to reaction (a) did not affect the products, but noticeably speeded up the formation of the brown solid (c). Attempts to prepare samples of $\text{MoOCl}_3 \cdot 2\text{NMe}_3$ in the presence of Zn always resulted in contamination with (c).

(f) Reaction of MoOCl_4 with NMe_3 . Extraction of ~ 3 g MoOCl_4 with 40 ml of NMe_3 over a four month period gave ~ 0.2 g of an orange brown amine soluble solid. Use of a piece of Zn wire as a catalyst had no effect; the wire remained unconsumed at the end of the reaction. The IR spectrum of the product showed bands at:-

3060(m), 2983(m), 2947(m), 2912(sh), 2860(w), 2842(w), 2787(w), 1480(s), 1460(s), 1448(sh), 1406(w), 1238(w), 1106(m), 989(s), 978(s), 968(s), 951(s), 822(s), 754(s), 723(m), 655(vs), 522(s), 450(s), 430(w), 404(s), 350(w), 333(s), 308(s) and 273(w) cm^{-1} , respectively.

Microanalysis found C(19.6, 19.5), H(4.8, 4.8), N(8.0, 8.0), Cl(18.9, 19.2) %.

2.9.4 Reaction of NMe_3 with AuCl_3 . Red platelets of AuCl_3 (~ 1 g) were placed in a double ampoule bomb and NMe_3 distilled on at 77 K. On warming to room temperature, the AuCl_3 dissolved to give a pale brown solution which, after a few minutes, began to precipitate a pale yellow solid. After 30 mins. precipitation was complete leaving the NMe_3 solution colourless. A further slow reaction of the yellow precipitate was observed over a three week period to give a dark brown solid and a colourless solution. There were no amine soluble products.

Extraction of the brown material with CHCl_3 or MeOH gave a dark brown solid, identified as metallic gold by a featureless IR spectrum and its high electrical conductivity. Concentration of the MeOH or CHCl_3 washings produced a mixture of organic products analysing overall as $\text{C}_3\text{H}_9\text{NCl}$. Separation of the organic compounds was not achieved.

Analysis of organic mixture based on $\text{C}_9\text{H}_{27}\text{N}_3\text{Cl}_3\text{Au}$

Calculated	C(22.5)	H(5.6)	N(8.8)	Cl(22.1)	%
Found	C(22.3)	H(5.6)	N(10.0)	Cl(21.7)	%

2.9.5 Reaction of $\text{MCl}_4 \cdot 2\text{NMe}_3$ ($\text{M} = \text{Zr, Hf}$) with THF

Addition of 2.1 fold excess of THF to solutions of $\text{MCl}_4 \cdot 2\text{NMe}_3$ ($\text{M} = \text{Zr, Hf}$) in C_6H_6 gave white precipitates of the bis THF adducts. Displaced trimethylamine was trapped out at 77 K and identified by its IR spectrum. The complexes were washed well with n-Hexane to remove excess ligand before being punped dry in vacuo.

(a) $\text{ZrCl}_4 \cdot 2\text{THF}$. THF (0.5 ml, 6.0 mmol) was added dropwise to a solution of $\text{ZrCl}_4 \cdot 2\text{NMe}_3$ (1.1 g, 2.4 mmol) in C_6H_6 to give $\text{ZrCl}_4 \cdot 2\text{THF}$,

(1.03 g, 87%).

Analysis based on $C_2H_{16}O_2ZrCl_4$

Calculated C(25.5) H(4.3) Cl(37.4) %

Found C(25.3) H(4.5) Cl(37.3) %

Bands were found in the IR spectrum at:-

3158(s), 3028(m), 2950(m), 2920(m), 2900(w), 2848(m), 1480(m),
1465(m), 1451(sh), 1415(w), 1380(w), 1368(w), 1344(w), 1251(w),
1200(w), 1145(m), 1124(s), 1064(w), 1045(w), 1015(m), 982(s),
948(w), 925(w), 860(m), 817(w), 765(w), 738(sh), 725(w), 678(m)
and 301(vs) cm^{-1} , respectively.

(b) $HfCl_4 \cdot 2THF$. Similarly, $HfCl_4 \cdot 2NMe_3$ (1.3 g, 3.0 mmol) and THF (0.5 ml, 6.2 mmol) gave $HfCl_4 \cdot 2THF$ (1.23 g, 89%).

Analysis based on $C_6H_{16}O_2HfCl_4$

Calculated C(20.0) H(3.4) Cl(30.5) %

Found C(19.3) H(3.6) Cl(30.0) %

Bands were found in the IR spectrum at:-

3160(s), 3030(w), 2955(m), 2030(m), 2856(m), 2737(w), 1483(m),
1467(m), 1454(m), 1417(w), 1276(w), 1251(w), 1194(vw), 1141(s),
1115(s), 1060(s), 1041(s), 1019(sh), 1009(m), 977(s), 910(w),
855(sh), 841(m), 812(w), 717(w) and 270(vs) cm^{-1} , respectively.

2.9.6 Preparation of $MCl_4 \cdot Me_6tren$ (M = Ti, Zr, Hf)

Addition of Me_6tren to either $TiCl_4$ or $MCl_4 \cdot 2NMe_3$ (M = Zr, Hf) in benzene solutions gave immediate reaction, with precipitation of the respective mono-adduct $MCl_4 \cdot Me_6tren$. For M = Zr, Hf, displaced NMe_3 was trapped out at 77 K and identified by its IR spectrum. The adducts were purified by washing with both benzene and n-Hexane.

(a) $TiCl_4 \cdot Me_6tren$. Dropwise addition of Me_6tren (4.6 g, 20.0 mmol)

to TiCl_4 (1.17 g, 9.0 mmol) gave pale green $\text{TiCl}_4 \cdot \text{Me}_6\text{tren}$ (3.3 g, 88%)

Analysis based on $\text{C}_{12}\text{H}_{30}\text{N}_4\text{Cl}_4\text{Ti}$

Calculated C(34.3) H(7.2) N(13.3) Cl(33.7) %

Found C(34.4) H(7.1) N(13.0) Cl(33.3) %

Bands were found in the IR spectrum at:-

3018(w), 2950(s), 2925(s), 2828(m), 2808(w), 1474(w), 1461(s),
1439(w), 1436(w), 1400(w), 1375(w), 1300(w), 1279(m), 1259(m),
1237(w), 1208(w), 1166(w), 1112(w), 1063(w), 1052(w), 1040(m),
1020(m), 1004(m), 980(m), 894(s), 803(m), 781(s), 765(w), 746(m),
724(m), 387(s), 356(s) and 187(m) cm^{-1} , respectively.

^1H NMR (90 MHz , CD_2Cl_2 solution, rel. TMS) showed resonances at
 δ 2.60, δ 2.82 (multiplet) and δ 3.51 (multiplet).

(b) $\text{ZrCl}_4 \cdot \text{Me}_6\text{tren}$. Similarly, addition of Me_6tren (2.2 g, 11.0 mmol)
to $\text{ZrCl}_4 \cdot 2\text{NMe}_3$ (1.6 g, 4.7 mmol) gave white $\text{ZrCl}_4 \cdot \text{Me}_6\text{tren}$ (1.8 g, 84%)
with release of trimethylamine.

Analysis based on $\text{C}_{12}\text{H}_{30}\text{N}_4\text{Cl}_4\text{Zr}$

Calculated C(31.1) H(6.5) N(12.0) Cl(30.6) %

Found C(30.8) H(6.8) N(11.8) Cl(29.9) %

Bands were found in the IR spectrum at:-

3020(m), 2952(s), 2930(s), 2845(m), 2820(w), 1475(w), 1470(s),
1458(w), 1435(w), 1403(m), 1288(m), 1259(w), 1209(w), 1166(w),
1125(w), 1108(w), 1076(w), 1063(w), 1041(s), 1000(w), 990(s),
910(w), 801(m), 786(s), 764(s), 735(w), 719(m), 683(s), 372(s),
318(s) and 168(m) cm^{-1} , respectively.

^1H NMR (CD_2Cl_2 , rel. TMS) δ 2.68, δ 2.92, (multiplet), δ 3.51
(multiplet).

(c) $\text{HfCl}_4 \cdot \text{Me}_6\text{tren}$. Similarly, addition of Me_6tren (1.3 g, 5.5 mmol)
to $\text{HfCl}_4 \cdot 2\text{NMe}_3$ (1.1 g, 2.5 mmol) gave white $\text{HfCl}_4 \cdot \text{Me}_6\text{tren}$ (1.2 g, 88%) with

release of trimethylamine.

Analysis based on $C_{12}H_{30}N_4Cl_4Hf$

Calculated	C(26.1)	H(5.5)	N(10.1)	Cl(25.8)	%
Found	C(25.8)	H(5.7)	N(9.8)	Cl(25.3)	%

Bands were found in the IR spectrum at:-

3130(w), 3020(w), 2955(s), 2940(s), 2855(m), 2820(w), 1480(w),
1470(s), 1463(w), 1445(w), 1412(w), 1378(w), 1308(w), 1295(w),
1265(m), 1230(w), 1213(w), 1156(w), 1100(w), 1085(m), 1053(w),
1037(m), 1005(s), 937(s), 915(w), 815(w), 785(s), 763(m), 725(m),
680(w), 327(s), 277(s) and 143(m) cm^{-1} , respectively.

1H NMR (CD_2Cl_2 , rel. TMS) δ 2.70, δ 2.97 (multiplet) δ 3.52
(multiplet).

CHAPTER 3

COMPLEX CHEMISTRY OF DIMETHYLAMINO SUBSTITUTED PHOSPHINE CHALCONIDES

CHAPTER 3

3.1 INTRODUCTIONStructure and Bonding in $(\text{Me}_2\text{N})_3\text{PY}$ ($\text{Y} = \text{O}, \text{S}, \text{Se}$) Systems

Critical to an understanding of the nature of phosphine chalcogenide complexes, is an explanation of the phosphorus chalcogen bond, and considerable effort has been expended in this direction. Bond dissociation energies (184), short bond lengths (185), bond moment (186) and IR data (187) all point to multiple bond character in the P-Y bond, caused principally by $\text{P}(\text{d}\pi) - \text{Y}(\text{p}\pi)$ overlap. Dorshner and Kaufmann have performed molecular orbital calculations on $(\text{H}_2\text{N})_3\text{PY}$ (188) and $(\text{Me}_2\text{N})_3\text{PY}$ (189), ($\text{Y} = \text{O}, \text{S}$) to examine this on a theoretical basis. For $(\text{Me}_2\text{N})_3\text{PO}$ (HMPA) the P-O bond was calculated to consist of 30% σ character (principally due to $\text{O}(2\text{pz}) \times \text{P}(3\text{pz})$, $\text{O}(2\text{pz}) \times \text{P}(3\text{s})$ and $\text{O}(2\text{pz}) \times \text{P}(\text{dz}^2)$ overlap) and 70% π character, this mainly from $\text{O}(2\text{px}, \text{y}) \rightarrow \text{P}(3\text{p}, 3\text{d})$ donation. The sulphur analogue $(\text{Me}_2\text{N})_3\text{PS}$, (HMPTA) shows considerably less π character in the P-Y bond (55%), with σ character accounting for the remainder (45%) of the P-S overlap population. This is mostly due to a large reduction in $\text{S} \rightarrow \text{P}(3\text{d}) \pi$ back bonding.

A reduction in P-Y π bonding, therefore, leaves the P(d) orbitals more open to N(p) - P(d) bonding, which should increase in the order $\text{O} < \text{S} < \text{Se}$. This can be seen in the X-ray crystal structures of $(\text{H}_2\text{N})_3\text{PO}$ (190) and $(\text{Me}_2\text{N})_3\text{PSe}$ (191) (Fig. 3.1.1). $(\text{H}_2\text{N})_3\text{PO}$ has an almost $\text{C}_{3\text{v}}$ geometry, with small variations in the P-N bond lengths being caused by different H bonded environments for the three nitrogen atoms.

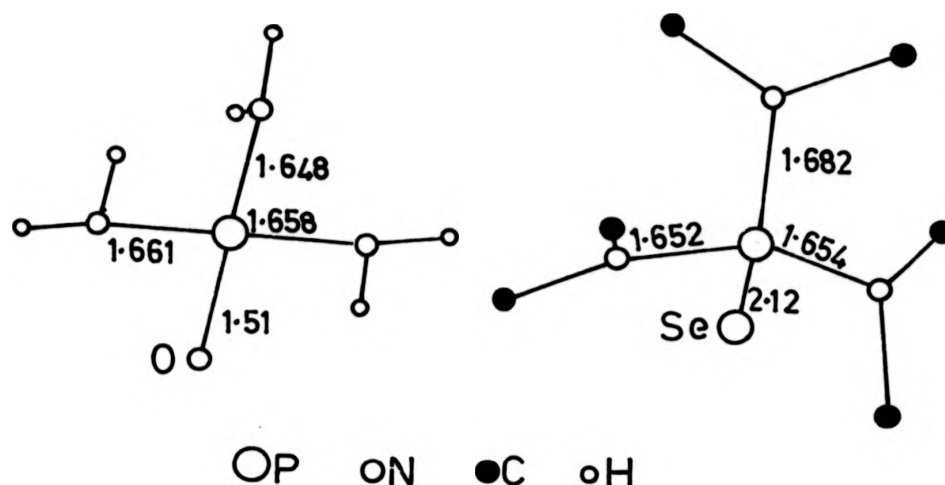


Fig. 3.1.1 X-ray Crystal Structures of $(\text{H}_2\text{N})_3\text{PO}$ and $(\text{Me}_2\text{N})_3\text{PSe}$

Substantial deviations from C_{3v} symmetry are found for $(\text{Me}_2\text{N})_3\text{PS}$ however, with two different sets of P-N bond lengths, and nitrogen geometries, suggesting two sp_2 and one sp_3 NMe_2 groups (190). The P-Y bond in both cases was considered to be long (190, 191) compared to similar systems in which little or no π bonding between the P atom and the various substituents takes place. Elongation of the P-Se bond was particularly large, and was interpreted in terms of dipolar $\text{P}^{\delta+} - \text{Se}^{\delta-}$ character in the P-Se bond. This view would seem to be supported by earlier ^{77}Se NMR shift data for similar PSe containing molecules (192).

Coordination site

The complex chemistry of the Phosphine chalconides has been widely studied, and reviewed (193, 194). One point that emerges is that for virtually all the complexes studied O or S have been proposed as the donor site, apparently the sole exception being the tris(dimethoxyphosphato)-M (III), (M = Ti, V, Cr) series where bidentate behaviour was observed (195).

Single crystal X-ray studies have confirmed either O (83, 87, 165, 196-201) or S (202) donation for a number of species. The lack of any N donor complexes with amino substituted ligands can be explained by a combination of electronic and steric factors. Vilesov *et al* (203) and Lux *et al* (204) have studied the gas phase photoelectron spectra of $(\text{NMe}_2)_x\text{Cl}_{3-x}\text{PS}$ and $(\text{NMe}_2)_x\text{Cl}_{3-x}\text{PO}$ respectively, and determined the first ionisation energies (Table 3.1.1). This generally corresponds to the lone pair on the most basic donor atom (189).

Compound	1st I.E. (eV)	Compound	1st I.E. (eV)	2nd I.E. (eV)	3rd I.E. (eV)	4th I.E. (eV)
$(\text{NMe}_2)_3\text{PS}$	8.05(S)	$(\text{NMe}_2)_3\text{PO}$	8.25(N)	8.73(N)	9.17(N)	10.44(O)
$(\text{NMe}_2)_2\text{ClPS}$	8.75(S)	$(\text{NMe}_2)_2\text{ClPO}$	9.19(N)	9.43(N)	10.90(O)	-
$(\text{NMe}_2)\text{Cl}_2\text{PS}$	9.35(S)	$(\text{NMe}_2)\text{Cl}_2\text{PO}$	9.87(N)	11.28(N)	-	-
Cl_3PS	10.15(S)	Cl_3PO	11.91(O)	-	-	-

Table 3.1.1 Vertical Ionisation Energies for $(\text{NMe}_2)_x\text{Cl}_{3-x}\text{PO(S)}$

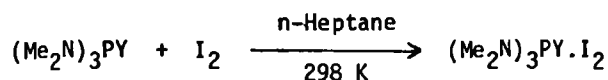
In the $(\text{NMe}_2)_x\text{Cl}_{3-x}\text{PS}$ series, the 1st I.E. is from the S lone pair, and S-bonded systems can be seen simply in terms of the greater basicity of the S atom. For the analogous O series, however, the lowest ionisation energy was found to correspond to the 2p orbitals on the nitrogen atoms, which on this basis, are thus more basic than the oxygen atom. The preference for O rather than N donation in this case can only be explained by a consideration of steric factors, where repulsive forces between adjacent NMe_2 groups are strong enough to prevent inversion of the N lone pair. O donation has also been proposed for the less hindered complexes $\text{MCl}_4.2((\text{NMe}_2)_2\text{ClPO})$ and $\text{MCl}_4.2((\text{NMe}_2)\text{Cl}_2\text{PO})$ ($\text{M} = \text{Sn}, \text{Zr}$ (205)); here presumably NMe_2 -Cl repulsive forces are dominant.

On coordination to a metal, donation of electron density from the O or S atom reduces $\text{Y} \rightarrow \text{P(d)}$ back bonding, therefore, increasing $\text{P(d}\pi) - \text{N(p}\pi)$

bonding and reducing the basicity of the N substituents, although this effect seems to be small in the complexes studies so far (196-201).

Relative donor behaviour of $(\text{Me}_2\text{N})_3\text{PY}$, $\text{Y} = \text{O}, \text{S}$

An examination of Table 3.1.1 shows the ionisation energy of the donor atom lone pair to be 8.05 and 10.44 eV for $(\text{Me}_2\text{N})_3\text{PS}$ and $(\text{Me}_2\text{N})_3\text{PO}$ respectively. The inference from this, that $(\text{Me}_2\text{N})_3\text{PS}$ should act as a better ligand than $(\text{Me}_2\text{N})_3\text{PO}$, is not justified, however, by the known donor chemistry of these ligands. Complexes of $(\text{Me}_2\text{N})_3\text{PO}$ (193, 207-211) are plentiful and well documented, whilst those of $(\text{Me}_2\text{N})_3\text{PS}$ (212-214) are scarce. Factors in addition to straightforward basicity must, therefore, be involved. Teichmann and Hilgetag (194) have rationalised this phenomenon in terms of the HSAB principle (Section 1.3). Thermodynamic data for the reactions of $(\text{Me}_2\text{N})_3\text{PY}$, ($\text{Y} = \text{O}, \text{S}, \text{Se}$) with the soft Lewis acid I_2 is presented in Table 3.1.2 (215).



Ligand	$K(\text{l mol}^{-1})$	$-\Delta G(\text{KJ mol}^{-1})$	$\Delta H(\text{KJ mol}^{-1})$
$(\text{NMe}_2)_3\text{PO}$	284 ± 6	14.03	-30.7 ± 0.4
$(\text{NMe}_2)_3\text{PS}$	829 ± 8	16.72	-34.0 ± 0.8
$(\text{NMe}_2)_3\text{PSe}$	$23,800 \pm 1,200$	25.07	53.8 ± 2.1

Table 3.1.2 Thermodynamic Data for $(\text{Me}_2\text{N})_3\text{PY} + \text{I}_2$

Inspection of the values of K and ΔG shows that the donor properties decrease in the order $\text{Se} > \text{S} > \text{O}$. Conversely, with the hard acid NbCl_5 , Favez and Merbach (216) found that for the ligand exchange reaction,



the exchange rate for $(\text{NMe}_2)_3\text{PS}$ was $>10^{10}$ times faster than for $(\text{NMe}_2)_3\text{PO}$.

This was seen as a reflection of the relative donor capacities of the ligand, and thus $O \gg S$. The preference for O donor complexes with hard acids can also be seen in the Sn (IV) adducts of trimethylthionephosphate, which spontaneously isomerise to give the O bonded trimethylthiolphosphate complexes (217). $(MeO)_3PS + SnCl_4 \rightarrow SnCl_4 \cdot 2((MeO)_3PS) \rightarrow (MeO)_3P^+SR \cdot SnCl_4 \cdot OP(OMe)_2S^- \rightarrow ((MeO)_2(RS)PO)_2 \cdot SnCl_4$.

Phosphorus substituent effects on the donor behaviour of $R_1R_2R_3PY$

To a first approximation, the effect of a particular substituent on the donor ability of the $R_1R_2R_3PY$ molecule can be predicted (193) by a consideration of the phosphoryl σ substituent constants (Table 3.1.3) (218).

Substituent	σ	Substituent	σ
NMe_2	-1.22	H	0.00
Me	-0.96	SMe	0.15
OMe	-0.12	CCl_3	+0.30
$ClCH_2$	-0.05	Cl	+0.93

Table 3.1.3 Selected σ Phosphoryl Substituent Constants.

Substituents with negative σ constants increase the ligand field strength of the $R_1R_2R_3PY$ molecule, while those with a positive value produce a decrease. The effect is additive. The donor properties of the series $(NMe_2)_xCl_{3-x}PO(S)$, again with I_2 as the reference Lewis acid, illustrate this (204). (Table 3.1.4)

Donor	$-\Delta G^0$ KJ mol ⁻¹	$-\Delta H^0$ KJ mol ⁻¹	Donor	$-\Delta G^0$ KJ mol ⁻¹	$-\Delta H^0$ KJ mol ⁻¹
$(NMe_2)_3PO$	10.71	19.95	$PS(NMe_2)_3$	15.75	35.3
$(NMe_2)_2ClPO$	4.49	-	$PSCl(NMe_2)_2$	6.47	23.1
$(NMe_2)Cl_2PO$	-0.55	10.50	$PSCl_2(NMe_2)$	1.60	12.2
Cl_3PO	-3.99	6.3	$PSCl_3$	-5.71	10.5

Table 3.1.4 Thermodynamic Data for the Reaction
 $(NMe_2)_xCl_{3-x}PO(S) + I_2 \xrightleftharpoons{CCl_4} (NMe_2)_xCl_{3-x}PO(S) \cdot I_2$

Donor properties (i.e. $-\Delta G^0$) decrease in the order $(\text{Me}_2\text{N})_3\text{PY} > (\text{Me}_2\text{N})_2\text{ClPY} > (\text{Me}_2\text{N})\text{Cl}_2\text{PY} > \text{Cl}_3\text{PY}$. It is of interest that Cl_3PS , freed from the inductive and π bonding effects of the NMe_2 group, becomes a poorer donor than POCl_3 , even towards class B acids. Hence, complexes of Cl_3PO are numerous (115), whilst those of Cl_3PS (219) are rare and/or thermally unstable.

Stereochemical considerations

$(\text{Me}_2\text{N})_3\text{PO}$ and $(\text{Me}_2\text{N})_3\text{PS}$ are examples of 'bulky' ligands and can often induce low coordination in metal complexes. An example of this is found in HMPA adducts of the lanthanide trichlorides where the 6-coordinate $\text{MCl}_3 \cdot 3\text{HMPA}$ (209) rather than the expected $\text{MCl}_3 \cdot 4\text{HMPA}$ ($\text{M} = \text{La-Lu}$) complexes were formed. (N.B. The lanthanide tribromides (210) do give compounds of the latter stoichiometry). Another effect due to ligand size is seen in the $\text{MX}_4 \cdot 2\text{HMPA}$ adducts (165, 197-201), which tend to be trans, in contrast to the cis geometry adopted by $\text{MCl}_4 \cdot 2\text{Cl}_3\text{PO}$ ($\text{M} = \text{Ti}$ (83), Sn (196)) adducts. The latter is favoured on the grounds of stabilising interatomic attractions between the donor atoms (118, 220). Le Coz and Guerchais (205) in their study of $\text{MCl}_4 \cdot 2(\text{NMe}_2)_x\text{Cl}_{3-x}\text{PO}$, ($\text{M} = \text{Sn, Zr}$, $x = 0, 1, 2, 3$) also found a crossover in geometry on going from trans $\text{MCl}_4 \cdot 2\text{HMPA}$ to cis $\text{MCl}_4 \cdot 2(\text{NMe}_2)_2\text{ClPO}$ in which the ligand is only slightly less hindered. Phosphine sulphides have also been observed in a bridging mode as in $(\text{WCl}_4 \cdot \text{Ph}_3\text{PS})_2$, where the S atom in Ph_3PS bridges between the two WCl_4 units (221).

We have studied the coordination chemistry of $(\text{NMe}_2)_3\text{PO}$ and the series $(\text{NMe}_2)_x\text{Cl}_{3-x}\text{PS}$ ($x = 1, 2, 3$) with hard Lewis acids with four basic points in view.

(a) To try to form complexes involving the nitrogen as a donor atom, either by using high metal halide:ligand ratios, or by the use of

less hindered ligands such as $(\text{NMe}_2)\text{Cl}_2\text{PS}$.

(b) A study of the sparsely investigated chemistry of $(\text{NMe}_2)_x\text{Cl}_{3-x}\text{PS}$ complexes with hard acids, where successive replacement of NMe_2 groups by Cl should produce large differences in donor ability.

(c) To investigate the possibility of producing reduced coordination using the bulky ligands $(\text{NMe}_2)_3\text{PS}$ and $(\text{NMe}_2)_3\text{PO}$, especially with the MCl_3 halides ($\text{M} = \text{Ti}, \text{V}, \text{Cr}$), as found for $\text{MCl}_3 \cdot 2\text{NMe}_3$. The $(\text{NMe}_2)_x\text{Cl}_{3-x}\text{PS}$ series could also give geometry changes in their complexes as x is reduced.

(d) An evaluation of the electronic changes in the ligand on coordination, using changes in ν_{PS} in the IR spectrum and ^{31}P shifts as probes.

3.2.1 Adducts of $(\text{NMe}_2)_3\text{PO}$, (HMPA) with MCl_4 ($\text{M} = \text{Ti}, \text{Sn}, \text{Zr}$ and Hf and SnI_4)

Dropwise addition of a two-fold excess of HMPA to solutions of TiCl_4 , ZrCl_4 , HfCl_4 , SnCl_4 and SnI_4 in MeNO_2 gave $\text{MX}_4 \cdot 2\text{HMPA}$ as colourless ($\text{M} = \text{Sn}, \text{Zr}, \text{Hf}, \text{X} = \text{Cl}$) (208), or dark red-brown ($\text{M} = \text{Sn}, \text{X} = \text{I}$) crystals. $\text{MCl}_4 \cdot 2\text{HMPA}$ ($\text{M} = \text{Sn}, \text{Ti}, \text{Zr}, \text{Hf}$) were recrystallised from either MeNO_2 or CH_2Cl_2 solutions. A repeat experiment using a three-fold excess of either TiCl_4 or SnCl_4 yielded $2\text{TiCl}_4 \cdot \text{HMPA}$ and $\text{SnCl}_4 \cdot \text{HMPA}$ respectively. No evidence was found for any higher Sn (IV) adduct. $\text{TiCl}_4 \cdot \text{HMPA}$ was isolated from CH_2Cl_2 solution as bright orange cubic crystals by interaction of stoichiometric quantities of TiCl_4 and HMPA. Considerable heat of formation was noted for all the above reactions.

Stability towards moist air varied greatly between the adducts, with $2\text{TiCl}_4 \cdot \text{HMPA}$ rivaling the reactivity of the parent TiCl_4 , while

$\text{SnCl}_4 \cdot 2\text{HMPA}$ appeared stable towards aqueous hydrolysis. $2\text{TiCl}_4 \cdot \text{HMPA}$ and $\text{TiCl}_4 \cdot \text{HMPA}$ dissolved in coordinating solvents (MeCN, THF, DMSO, py) to give bright yellow solutions, apparently with formation of mixed adducts. Evidence was also found for ligand exchange when $\text{SnCl}_4 \cdot \text{HMPA}$ was dissolved in similar solvents. Values obtained for the molar conductivity between 0.18 and $0.23 \text{ ohm}^{-1} \text{ cm}^2 \text{ mol}^{-1}$ (10^{-3} M , CH_2Cl_2 solution) were well within the range expected for non-conducting species (222).

The IR spectra of the adducts are given in Tables 3.2.1 and 3.2.2. Assignments are made after Kottgen *et al* (223), and De Bolster and Groeneveld (207). The fact that only minor differences exist between the IR spectra of HMPA and its complexes in the $4000\text{--}400 \text{ cm}^{-1}$ region strongly indicates O-donor behaviour. This formulation is supported by a decrease in the PO stretching frequency of between $18\text{--}28 \text{ cm}^{-1}$, i.e. Oxygen \rightarrow metal electron donation gives a consequent reduction in $\text{O} \rightarrow \text{P}$ back bonding, and loss of P-O bond order. The failure of HMPA to act as anything other than a monodentate O-donor even in the higher complexes $2\text{TiCl}_4 \cdot \text{HMPA}$ and $\text{TiCl}_4 \cdot \text{HMPA}$ is ascribed to steric crowding between the three NMe_2 groups preventing inversion of the nitrogen lone pair. Reduction in the PO bond order is accompanied by an increase in $\text{N}(\text{p}\pi)\text{--P}(\text{d}\pi)$ bonding, which causes an increase in the ν_{PN} bands due to asymmetry in the ligand. For example, the 744 cm^{-1} band in the free HMPA is found as a triplet ($768, 758$ and 725 cm^{-1}) in $\text{TiCl}_4 \cdot 2\text{HMPA}$. The fact that no splitting of C-N or C-H stretching modes occurs suggests that the differences in the P-N bond order are small enough not to effect the state (sp_3 vs sp_2) of the $\text{N}(\text{CH}_3)_2$ groups. This argument is supported by the X-ray crystal structures of several HMPA adducts (196-201), where only small deviations in C-N bond lengths were found.

HMPA	TiCl ₄ .2HMPA	ZrCl ₄ .2HMPA	HfCl ₄ .2HMPA	SnCl ₄ .2HMPA	SnI ₄ .2HMPA	Assignment
2933(s)	3000(s)	2995(m)	3003(m)	3000(m)	2987(m)	ν(CH ₃)
2920(vs)	2940(s)	2948(sh)	2945(s)	2945(sh)	2920(s)	
2875(vs)	2911(sh)	2925(s)	2915(sh)	2925(s)	2890(m)	
2840(vs)	2858(m)	2857(m)	2864(m)	2856(m)	2846(m)	
2798(vs)	2810(s)	2823(m)	2825(m)	2820(m)	2801(m)	
	2805(w)	2813(w)	2815(w)	2812(w)		
1481(s)	1488(w,sh)	1495(w,sh)	1494(w,sh)	1492(w,sh)	-	δ(CH ₃)
1457(s)	1481(m)	1482(m)	1485(m)	1482(m)	1476(m)	
1435(sh)	1463(sh)	1463(s)	1462(m)	1462(s)	1452(m)	
1405(w)	1456(s)	1453(m)	1456(m)	1455(m)	1477(m)	
	1417(w)	1415(w)	1415(w)	1413(w)	1410(w)	
1306(vs)	1302(s)	1301(s)	1300(vs)	1300(vs)	1295(vs)	ρ _s (CH ₃)
1210(s)	1187(s)	1185(s)	1182(s)	1185(s)	1180(s)	ν(P = O)
1166(m)	1170(m)	1175(sh)	1169(w,sh)	1167(s)	1150(m)	ρ _{as} (CH ₃)
1150(w)	-	-	-	1150(vw)	1143(sh)	
1001(s)	1035(s)	1048(vs)	1068(vs)	1100(vs)	1096(vs)	ν _{as} (NC ₂)
982(s)	995(s)	994(vs)	996(s)	989(vs)	980(vs)	ν _s (NC ₂)
745(s)	768(s)	769(s)	768(s)	760(s)	752(s)	ν _{as} (PN)
	758(m)	760(m)	760(s)	755(m)	-	
	725(m)	726(m)	735(sh)	725(w,sh)	721(sh)	
634(m)	665(m)	662(m)	660(w)	654(vw)	-	ν _s (PN)
484(s)	540(m)	530(m)	525(m)	518(w)	510(w)	PNC ₂
	475	480(s)	479(s)	475(vs)	475(s)	
380(m)	390(s)	387(s)	388(s)	385(s)	382(s)	δ(O = PN ₃)
-	354(vs)	308(vs)	287(vs)	310(s)	212(vs)	ν(M-Cl)

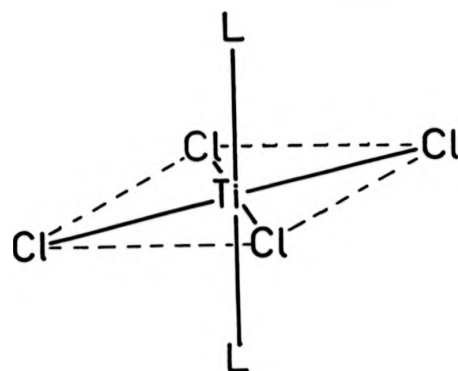
Table 3.2.1
(Continued)

TiCl ₄ .HMPA	2TiCl ₄ .HMPA	SnCl ₄ .HMPA	Assignment
3006(w)	3005(m)	3005(m)	ν(CH ₃)
2943(s)	2928(s)	2940(s)	
2910(s)	2910(m)	2910(sh)	
2862(m)	2860(m)	2859(m)	
2825(m)	2825(w)	2819(m)	
2815(w)			
1485(s)	1483(m)	1485(m)	δ(CH ₃)
1463(m)	1463(m)	1461(m)	
1450(s)	1451(m)	1451(m)	
1420(w)	1412(w)	1415(w)	
1312(vs)	1310(s)	1305(s)	ρ _s (CH ₃)
1185(m)	1182(s)	1192(s)	ν(P = O)
1178(m)	1170(sh)	1171(s)	ρ _{as} (CH ₃)
1145(w)	1147(m)	1143(sh)	
1040(s)	1067(vs)	1097(vs)	ν _{as} (NC ₂)
1005(vs)	1008(s)	993(vs)	ν _s (NC ₂)
777(m)	774(m)	767(m)	ν _{as} (PN)
770(m)	760(m)	756(m)	
730(w)	-	723(w)	
677(m)	677(m)	675(vw)	ν _s (PN)
535(m)	550(m)	520(w)	PNC ₂
475(s)	462(m)	470(w)	
404(m, sh)	416(vs)	375(s)	ν(M-Cl)
381(m)	379(s)	340(m)	
354(vs)	268(m)	315(m)	
320(m)	230(m)	172(m)	
287			

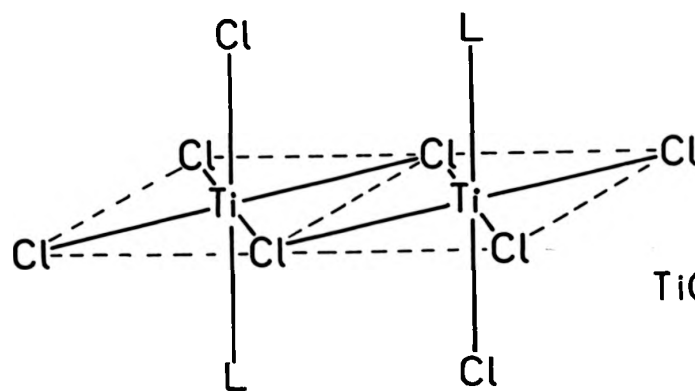
Table 3.2.1 IR Spectra of M(IV)HMPA Adducts

The low IR spectra ($400\text{--}200\text{ cm}^{-1}$) of $\text{MCl}_4 \cdot 2\text{HMPA}$ ($\text{M} = \text{Ti, Zr, Hf}$ and Sn) and $\text{SnI}_4 \cdot 2\text{HMPA}$ show single strong absorptions in accordance with an octahedral trans (D_{4h}) symmetry (149) (Fig. 3.2.1). Adoption of a trans geometry is in contrast to the corresponding Cl_3PO complexes, where cis arrangement of ligands was found (83, 196). This change in coordination geometry is probably due to the increased bulk of HMPA, cf. Cl_3PO . The structure of $\text{TiCl}_4 \cdot \text{HMPA}$ is interpreted in terms of a halogen bridged dimer with a trans (C_{2h}) arrangement of ligands (Fig. 3.2.1). This geometry has been confirmed for other 1:1 adducts of Ti (IV) viz. $(\text{TiCl}_4 \cdot \text{POCl}_3)_2$ (87), $(\text{TiCl}_4 \cdot \text{MeNO}_2)_2$ (88) and $(\text{TiCl}_4 \cdot \text{EtOAc})_2$ (89). Bands in the low IR spectrum due to Ti-Cl stretching modes are assigned as 404 cm^{-1} (terminal, A_g), 381 cm^{-1} (terminal, B_g), 354 cm^{-1} (terminal, A_g), 320 cm^{-1} (bridging, A_g) and 287 cm^{-1} (bridging, B_g). Assignments are after the vibrational analysis of $(\text{TiCl}_4 \cdot \text{Cl}_3\text{PO})_2$ performed by Kawano and coworkers (224).

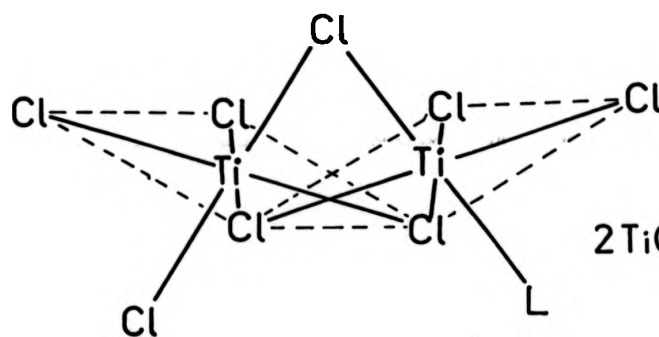
Adducts of the type $2\text{TiCl}_4 \cdot \text{L}$ ($\text{L} = \text{RCOOR}'$ (225), Ph_3PS (226)) have been reported in the literature, but have remained without characterisation. Crystallographic studies of $\text{PCl}_4 \cdot \text{Ti}_2\text{Cl}_9$ (227) have shown the $\text{Ti}_2\text{Cl}_9^{2-}$ unit to possess a confacial bioctahedral structure; we proposed that $2\text{TiCl}_4 \cdot \text{HMPA}$ being isoelectronic with $\text{Ti}_2\text{Cl}_9^{2-}$, is also isostructural (Fig. 3.2.1). The metal halide bands in the low IR spectrum are assigned as $416, 379\text{ cm}^{-1}$ (Ti-Cl terminal) and $268, 230\text{ cm}^{-1}$ (Ti-Cl bridging) modes. It is not possible to determine the position of the ligand in the structure of $2\text{TiCl}_4 \cdot \text{HMPA}$ from IR evidence alone. Templeton and coworkers found that for the confacial bioctahedral tetrahydrothiophene (THT) complexes $\text{Ta}_2\text{X}_6(\text{THT})_3$ ($\text{X} = \text{Cl}$ (228), Br (228, 229)) and $\text{Nb}_2\text{Br}_6(\text{THT})_3$ (228, 229), the extra drain of electron density from bridging THT molecules resulted in a larger downfield ^1H NMR shift than that of a terminal placed ligand. The similarity between the ^1H , ^{13}C and ^{31}P chemical shift



$\text{TiCl}_4 \cdot 2\text{HMPA}$



$\text{TiCl}_4 \cdot \text{HMPA}$



$2\text{TiCl}_4 \cdot \text{HMPA}$

Fig. 3.2.1 Proposed Structures of $\text{TiCl}_4 \cdot 2\text{HMPA}$, $\text{TiCl}_4 \cdot \text{HMPA}$
and $2\text{TiCl}_4 \cdot \text{HMPA}$

in the NMR spectra of $2\text{TiCl}_4\cdot\text{HMPA}$ and $\text{TiCl}_4\cdot 2\text{HMPA}$ strongly suggests that the HMPA molecule is not present in a bridging capacity. The proposed isomer of $2\text{TiCl}_4\cdot\text{HMPA}$ (Fig. 3.2.1) in which the ligand is placed trans to the bridgehead Cl atom rather than cis, is based on a comparison with $(\text{TiCl}_4\cdot\text{HMPA})_2$ in which a trans geometry has also been proposed.

The elucidation of the solid state structure of $\text{SnCl}_4\cdot\text{HMPA}$ via its low IR spectrum is complicated by the existence of two possible geometries, Fig. 3.3.2, both of which can be used to interpret the four bands found in the $400\text{--}150\text{ cm}^{-1}$ region.

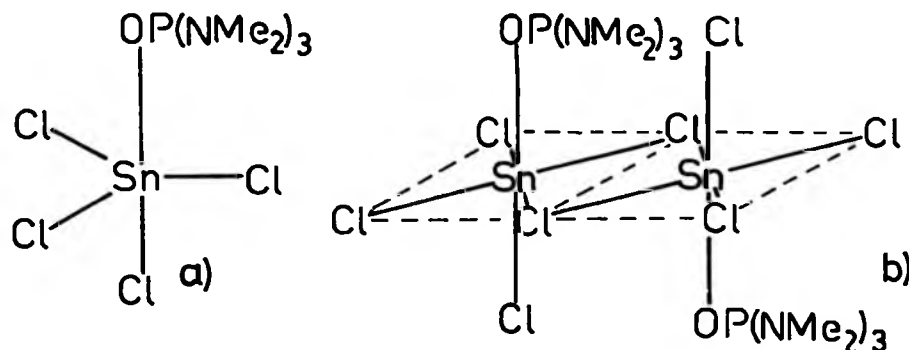


Fig. 3.2.2 Possible Structures for $\text{SnCl}_4\cdot\text{HMPA}$

Examples of structures (a) (C_{3v}) and (b) (C_{2v}) are $\text{SnCl}_4\cdot\text{NMe}_3$ (73) and $(\text{PCl}_4)_2(\text{Sn}_2\text{Cl}_{10})$ (230, 231) respectively. Low IR data for $\text{SnCl}_4\cdot\text{HMPA}$, $\text{SnCl}_4\cdot\text{NMe}_3$ and $\text{Sn}_2\text{Cl}_{10}^{2-}$ is presented with appropriate assignments in Table 3.2.2.

$\text{SnCl}_4\cdot\text{HMPA}$	$\text{SnCl}_4\cdot\text{NMe}_3$	$\text{Sn}_2\text{Cl}_{10}^{2-}$
375	370 (ν_{as})	347(E')
340	338 (ν_s)	333(A_2'')
315	307 (ν_s)	318(A_2'')
172	-	167(A_2''), 150(E')

Table 3.2.2 Low IR Spectra of some Sn (IV) Species

No band comparable to that at 172 cm^{-1} for $\text{SnCl}_4\cdot\text{HMPA}$ exists in the spectrum of $\text{SnCl}_4\cdot\text{NMe}_3$. For $\text{SnCl}_4\cdot\text{HMPA}$ to be isostructural with $\text{SnCl}_4\cdot\text{NMe}_3$, the 172 cm^{-1} band must therefore, originate with a vibration other than a Sn-Cl mode. An asymmetric PN (223), or SnO bend are two possibilities (the Sn-O stretching mode is probably masked by the strong 375 cm^{-1} Sn-Cl band). Considering the large number of 1:1 complexes of SiX_4 and GeX_4 (113, 232) for which no dimeric form has been found, it seems here preferable to designate an (a)-type structure to $\text{SnCl}_4\cdot\text{HMPA}$.

NMR data (^1H (90 MHz), ^{13}C and ^{31}P (proton decoupled)) for HMPA and M (IV) HMPA adducts appears in Table 3.2.3.

Complex	^1H (60 MHz)	^{13}C	^{31}P
$\text{TiCl}_4\cdot 2\text{HMPA}$	2.91	37.45	25.18
$\text{TiCl}_4\cdot\text{HMPA}$	2.87	-	-
$2\text{TiCl}_4\cdot\text{HMPA}$	2.96	37.19	28.06
$\text{ZrCl}_4\cdot 2\text{HMPA}$	2.93	37.24	24.38
$\text{HfCl}_4\cdot 2\text{HMPA}$	2.91	37.16	25.34
$\text{SnCl}_4\cdot 2\text{HMPA}$	2.86	37.31	19.42
$\text{SnCl}_4\cdot\text{HMPA}$	2.67	36.88	19.66
$\text{SnI}_4\cdot\text{HMPA}$	2.76	37.47	18.73
HMPA	2.65	36.84	22.49

Table 3.2.3 NMR Data for M (IV) HMPA

Spectra appeared as sharp doublets (^1H , $^3\text{J}(\text{P-H}) = 9\text{--}10\text{ Hz}$; ^{13}C , $^2\text{J}(\text{P-C}) = 3.7\text{--}5.1\text{ Hz}$) or in the case of ^{31}P , singlets. Evidence for inequivalent NMe_2 groups (as found in the solid state by IR) was absent in solution. It can only be concluded here that rapid change between the various forms of the PN bond presents an averaged spectrum. Little change was found

in the P-H and C-P coupling constants on complex formation. Shifts to low field of between 0.04 and 0.63 ppm occurred in the ^{13}C resonance on complexation but there was no obvious trend in terms of chemical shifts.

^{31}P NMR has been shown to be a useful and sensitive probe in the investigation of phosphoryl complexes (233-235), and proved to be so again when applied to the $\text{MX}_4\cdot\text{HMPA}$ system. The complexes here fell into two distinct categories, with the complexes of the Group IV (A) metals (Ti, Zr and Hf) giving downfield shifts relative to free HMPA (1.89-5.57 ppm), while the Sn based complexes gave upfield shifts (2.83-3.07 ppm). Also of note was the magnitude of their shifts, which were small compared to comparable phosphoryl complexes, e.g. $\text{TiCl}_4\cdot 2\text{Cl}_3\text{PO}$, $\Delta\delta = 16.6$ ppm (233).

Formation of a M-O coordinate bond weakens $\text{O} \rightarrow \text{P}$ back bonding and thus reduces the P-O bond order. The electron density on the phosphorus is, therefore, reduced resulting in a downfield ^{31}P shift. For dimethylamino substituted ligands such as HMPA, this can be compensated by a combination of $\text{N} \rightarrow \text{P}$ electron donation due to inductive effects, and P electron density gained by the partial delocalisation of the N lone pair into the N-P π bond. If the gain of P electron density from the NMe_2 groups outweighs the loss of density from the reduction of P-O bond order, the nett result is an upfield ^{31}P shift, as seen for $\text{SnCl}_4\cdot 2\text{HMPA}$, $\text{SnCl}_4\cdot\text{HMPA}$ and $\text{SnI}_4\cdot 2\text{HMPA}$. The M (IV), (M = Ti, Zr, Hf) complexes also show greater downfield shifts (0.22-0.31 ppm) in their ^1H NMR spectra than do the corresponding Sn (IV) adducts (0.02-0.21 ppm). A greater loss of electron density in the M (IV), (M = Ti, Zr, Hf) adducts from both the NMe_2 groups and the P atom suggests that the metal atom here acts as an electron 'sink' and the M-O bond is stronger in the M (IV), (M = Ti, Zr, Hf) complexes than in those of Sn (IV). This is not perhaps

unexpected, as M (IV), M = Ti, Zr, Hf) possessing low lying d orbitals, should be more capable of accepting electron density than Sn (IV). Single crystal X-ray studies of trans $\text{UCl}_4 \cdot 2\text{HMPA}$ (198) have already established strong M-O bonds.

No line broadening due to ligand exchange was observed in any of the spectra. Favez and Merbach (216) found for the $\text{NbCl}_5 \cdot \text{HMPA}$ system that ligand exchange was too slow to measure even at 393 K, and similar considerations would seem to apply to the Group IV complexes. The differences in the ^1H NMR spectra $\text{SnCl}_4 \cdot 2\text{HMPA}$ and $\text{SnCl}_4 \cdot \text{HMPA}$ are noteworthy. Several authors have observed disproportionation reactions of the type,



in solution (74, 236). The well-defined $\text{SnCl}_4 \cdot \text{HMPA}$ spectra obtained suggests that the assumed equilibrium in this case lies well to the left hand side. Although not directly observable, evidence for such an equilibrium exists in the behaviour of $\text{SnCl}_4 \cdot \text{HMPA}$ towards aqueous hydrolysis. Solutions of $\text{SnCl}_4 \cdot \text{HMPA}$ in wet CH_2Cl_2 gave on extraction, drying and removal of solvent, colourless crystals of trans $\text{SnCl}_4 \cdot 2\text{HMPA}$. The insoluble white residue, although not identified, was presumably SnO_2 .



It is hard to envisage a situation in which initial attack of H_2O on the $\text{SnCl}_4 \cdot \text{HMPA}$ molecule produces anything except total hydrolysis of the complex. A mechanism such as that proposed above avoids this by producing water stable $\text{SnCl}_4 \cdot 2\text{HMPA}$ in the initial step.



3.2.2 $\text{MCl}_3 \cdot 3\text{HMPA}$ complexes (M = Ti, V, Cr)

THF solutions of $\text{TiCl}_3 \cdot 3\text{THF}$ or $\text{VCl}_3 \cdot 3\text{THF}$ when treated with a three-fold

excess of HMPA underwent rapid ligand exchange reactions to give $MCl_3 \cdot 3HMPA$ ($M = Ti, V$). Removal of solvent gave the complexes as pale blue ($M = Ti$) or pink ($M = V$) microcrystalline solids. $CrCl_3 \cdot 3THF$ under the same conditions gave no noticeable reaction, even after several weeks. Addition of a small amount of Zn dust to a $CrCl_3 \cdot 3THF/HMPA$ solution, however, gave precipitation of green crystals of $CrCl_3 \cdot 3HMPA$ after four weeks at 313 K. Direct reaction of HMPA with $CrCl_3$, again with a zinc dust catalyst gave green $CrCl_3 \cdot 3HMPA$ after ~ 24 hours. Reaction of $CrCl_3 \cdot 2NMe_3$ with a three-fold excess of HMPA in C_6H_6 solution and subsequent removal of solvent and excess ligand gave a pale mauve solid analysing as $CrCl_3 \cdot 3HMPA$.

All the complexes were soluble in polar and chlorinated solvents, and show air moisture sensitivity, $TiCl_3 \cdot 3HMPA$ being particularly susceptible to aqueous hydrolysis. Values for molar conductivities between 0.1 and $1.4 \Omega^{-1} cm^2 mol^{-1}$ (taken as $10^{-3} M$ solutions in CH_2Cl_2 , 298 K) are well within the range expected for a non-ionic formulation (222). The trends found in the IR spectra of the quadrivalent complexes were continued in the trivalent derivatives (Table 3.2.4). Bands corresponding to ν_{CH} ($1490-1400 cm^{-1}$) vibrations were again found to be virtually unchanged on complexation, indicating equivalent uncoordinated NMe_2 groups and thus implying 0 coordination. A reduction in the phosphoryl stretching frequency from that found in the free ligand ($\Delta\nu_{PO} = 15 cm^{-1}$ ($M = Ti$), $15 cm^{-1}$ ($M = V$), $14 cm^{-1}$ ($M = Cr$ (purple)), $20 cm^{-1}$ ($M = Cr$ (green))) supports this view. A weaker M-O interaction for the M (III) derivatives, over that found in the comparable M (IV) complexes, was suggested from IR data, e.g. $TiCl_3 \cdot 3HMPA$ $\Delta\nu(P-O) = 15 cm^{-1}$, $TiCl_4 \cdot 2HMPA$ $\Delta\nu(P-O) = 23 cm^{-1}$. Splitting of the $\nu_{as} PN$ mode ($745 cm^{-1}$ HMPA) as a consequence of the increased ligand $P(d\pi) - N(p\pi)$ bonding was observed for the complexes (i.e. $TiCl_3 \cdot 3HMPA$ 766, 756, $727 cm^{-1}$).

HMPA	<u>fac</u> $\text{TiCl}_3 \cdot 3\text{HMPA}$	<u>fac</u> $\text{VCl}_3 \cdot 3\text{HMPA}$	<u>fac</u> $\text{CrCl}_3 \cdot 3\text{HMPA}$	<u>mer</u> $\text{CrCl}_3 \cdot 3\text{HMPA}$	Assmt.
2993(s)	2995(m)	2993(m)	2995(m)	2999(m)	νCH_3
2920(vs)	2915(s)	2920(s)	2910(s)	2905(s)	
2875(vs)	2899(vs)	2895(vs)	2887(s)	2895(vs)	
2840(vs)	2855(m)	2848(m)	2848(m)	2850(m)	
2798(vs)	2810(s)	2806(s)	2806(s)	2805(vs)	
1481(s)	1480(m)	1480(m)	1482(m)	1482(m)	δCH_3
1457(s)	1461(m)	1463(m)	1463(m)	1463(m)	
1435(sh)	1453(m)	1457(m)	1453(m)	1452(m)	
1405(m)	1412(vw)	1415(vs)	1410(w)	1410(w)	
1306(s)	1308(vs)	1303(vs)	1304(vs)	1308(vs)	ρNCH_3
1210(s)	1195(s)	1195(s)	1196(s)	1190(s)	$\nu\text{P}=\text{O}$
1166(m)	1164(sh)	1168(sh)	1165(sh)	1165(m)	ρNCH_3
1106(w)	1115(s)	1110(s)	1150(s)	1135(s)	
1067(m)	1085(m)	1070(s)	1075(s)	1075(s)	$\nu_{\text{as}}\text{NC}_2$
1001(m,sh)	1002(w,sh)	1010(w,sh)	1005(w,sh)	1010(w,sh)	$\nu_{\text{as}}\text{NC}_2$
982(vs)	990(s)	980(vs)	990(s)	980(s)	$\nu_{\text{s}}\text{NC}_2$
745(vs)	766(sh)	761(sh)	757(s)	756(s)	$\nu_{\text{as}}\text{PN}_3$
	756(s)	750(s)	749(sh)	752(sh)	
	727(sh)	725(w,sh)	725(sh)	729(sh)	
634(m)	657(w)	650(w)	650(w)	650(w)	$\nu_{\text{s}}\text{PN}_3$
484(vs)	532(w)	523(m)	530(w)	510(m)	PNC_2
	476(s)	478(s)	477(m)	480(s)	
380(m)	380(sh)	-	-	394(w)	$\delta\text{O}=\text{PN}_3$
355(m)	345(sh)	350(w,sh)	350(w,sh)	345(sh)	$\delta_{\text{s}}\text{PN}_3$
	365(s)	380(br)	398(br)	374(m)	M-Cl
	303(s)	300(s)	324(s)	324(s)	
				287(s)	

Table 3.2.4 IR Spectra of M(III)HMPA Adducts

In the far IR region the two strong bands ($365, 303, \text{cm}^{-1}$ ($M = \text{Ti}$), $380, 300 \text{ cm}^{-1}$ ($M = \text{V}$), $398, 324 \text{ cm}^{-1}$ ($M = \text{Cr}$ (purple)) were assigned as Metal-chlorine stretching vibrations consistent with a fac (C_{3v}) octahedral configuration (149). The green $\text{CrCl}_3 \cdot 3\text{HMPA}$ shows three such bands at $374, 324$ and 287 cm^{-1} in agreement with a mer (C_{2v}) octahedral arrangement of ligands (Fig. 3.2.3). It is unlikely that the broad band at $\sim 380 \text{ cm}^{-1}$ is a pure M-Cl mode, and coupling with M-O and internal ligand modes is probable.

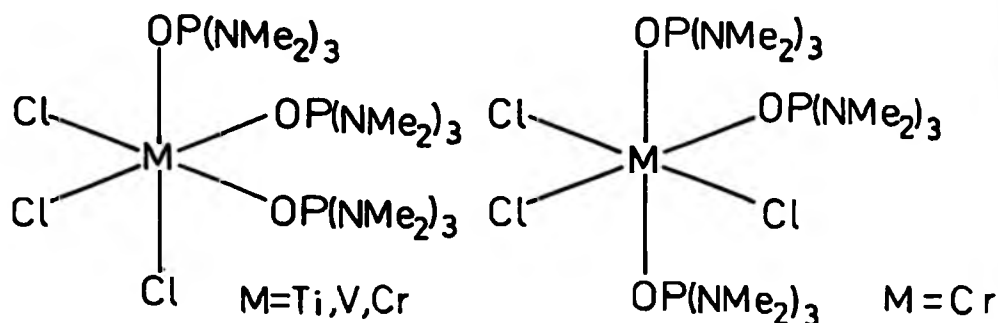


Fig. 3.2.3 Proposed Structures of $\text{MCl}_3 \cdot 3\text{HMPA}$

Band maxima and extinction coefficients characterising the electronic spectra of the complexes are as follows:-

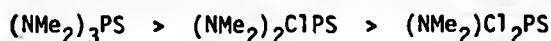
fac $\text{TiCl}_3 \cdot 3\text{HMPA}$ (ν_1) $16,310 \text{ cm}^{-1}$ ($\epsilon_{\text{max}} 4$) ${}^2E_g + {}^2T_{2g}$, fac $\text{VCl}_3 \cdot 3\text{HMPA}$ (ν_1) $13,240 \text{ cm}^{-1}$ ($\epsilon_{\text{max}} 17$) ${}^3T_{2g}(\text{F}) + {}^3T_{1g}(\text{F})$, (ν_2) $19,880 \text{ cm}^{-1}$ ($\epsilon_{\text{max}} 20$) ${}^3T_{1g}(\text{P}) + {}^3T_{1g}(\text{F})$, fac $\text{CrCl}_3 \cdot 3\text{HMPA}$ (ν_1) $13,260$ ($\epsilon_{\text{max}} 40$) ${}^4T_{2g}(\text{F}) + {}^4A_{2g}(\text{F})$, (ν_2) $18,860 \text{ cm}^{-1}$ ($\epsilon_{\text{max}} 50$) ${}^4T_{1g}(\text{F}) + {}^4A_{2g}(\text{F})$, mer $\text{CrCl}_3 \cdot 3\text{HMPA}$ (ν_1) $15,150 \text{ cm}^{-1}$ ($\epsilon_{\text{max}} 16.4$) ${}^4T_{2g}(\text{F}) + {}^4A_{2g}(\text{F})$, (ν_2) $23,255 \text{ cm}^{-1}$ ($\epsilon_{\text{max}} 19$) ${}^4T_{1g}(\text{F}) + {}^4A_{2g}(\text{F})$. ν_3 in $\text{CrCl}_3 \cdot 3\text{HMPA}$ (fac and mer) is masked by an intense HMPA charge transfer band.

Isomerisation of fac $\text{CrCl}_3 \cdot 3\text{HMPA}$ to mer $\text{CrCl}_3 \cdot 3\text{HMPA}$ was achieved by addition of a small piece of Zn wire to a THF solution of the former, the reaction proceeding to completion within 24 hours. Attempts to

isomerise $\text{TiCl}_3 \cdot 3\text{HMPA}$ and $\text{VCl}_3 \cdot 3\text{HMPA}$ in a similar manner yielded dark brown oils. A complex of the type $\text{CrX}_3 \cdot 3\text{L}$ can theoretically exist as both fac and mer isomers. In practice, however, only one isomer can usually be isolated, e.g. mer $\text{CrCl}_3 \cdot 3\text{THF}$ (149, 237). In a few cases, notably with the use of large 'bulky' ligands, examples of both stereochemistries have been achieved, i.e. $\text{CrCl}_3 \cdot 3\text{NH}_3$ (93), $\text{CrCl}_3 \cdot 3\text{THT}$ (94) and $\text{CrCl}_3 \cdot \text{dien}$ (95). For $\text{CrCl}_3 \cdot 3\text{HMPA}$, the fac-isomer evidently results from conditions under kinetic control, with formation of the less strained mer isomer as the thermodynamic preference. Ease of isomerisation can be related to the 'bulk' of the ligand and to the nature of the metal atom-donor bond. Whereas mer $\text{CrCl}_3 \cdot 3\text{THT}$ is spontaneously precipitated from benzene solutions of fac $\text{CrCl}_3 \cdot 3\text{THT}$ (94), conversion of blue fac $\text{CrCl}_3 \cdot 3\text{NH}_3$ to green mer $\text{CrCl}_3 \cdot 3\text{NH}_3$ is only complete after three days at 426 K (93). HMPA which is relatively bulky, but is an O donor (and should, therefore, form strong Cr-O bonds) could be expected to give complexes which isomerise at a rate intermediate to $\text{CrCl}_3 \cdot 3\text{THT}$ and $\text{CrCl}_3 \cdot 3\text{NH}_3$. Attempts to induce thermal isomerisation (fac \rightarrow mer) in solid $\text{CrCl}_3 \cdot 3\text{HMPA}$ proved unsuccessful, with no observable isomerisation below 411 K (the M.p. of fac $\text{CrCl}_3 \cdot 3\text{HMPA}$), and decomposition occurring above 411 K to give free HMPA.

3.3.1 Complexes and reactions of $(\text{NMe}_2)_x\text{Cl}_{3-x}\text{PS}$ ($x = 1, 2, 3$) with metal chlorides

The donor chemistry of the thiophosphoramides $(\text{NMe}_2)_x\text{Cl}_{3-x}\text{PS}$ ($x = 1, 2, 3$) with the metal and metalloid chlorides Ti (IV), Zr (IV), Hf (IV), Sn (IV), Ge (IV), As (III), Sb (III), Sb (V), Al (III), Au (III) and B (III) was investigated. As predicted from consideration of ionisation potentials and thermodynamic data (203, 204), the reactivity sequence



was observed.

$(\text{NMe}_2)_3\text{PS}$ and $(\text{NMe}_2)_2\text{ClPS}$ gave well defined adducts with SnCl_4 , ZrCl_4 , SbCl_5 and HfCl_4 , while complexes of $(\text{NMe}_2)\text{Cl}_2\text{PS}$ could only be formed with the strong acceptor SbCl_5 . TiCl_4 gave red/brown oils with both $(\text{NMe}_2)_3\text{PS}$ and $(\text{NMe}_2)_2\text{ClPS}$ in MeNO_2 solution; these gave dark red solids on careful addition of C_6H_6 . Spectroscopic analysis showed no simple compounds, however, with varying amounts of coordinated nitromethane present, and this line of research was not pursued further. Solution of AuCl_3 in $(\text{NMe}_2)\text{Cl}_2\text{PS}$ gave a deep orange solution, from which a crop of orange/yellow crystals was obtained. The product was found to contain uncoordinated ligand (which could not be removed by standard techniques), the amount varying from sample to sample. Low values for %Cl in the analytical data suggested reduction $\text{Au (III)} \rightarrow \text{Au (I)}$ as a major component of the reaction. The oxidation product is proposed as $(\text{Me}_2\text{N})\text{Cl}_2\text{PSSPCl}_2(\text{Me}_2\text{N})^{2+}$ by analogy with the reported $\text{Cu (II)}/(\text{NMe}_2)_3\text{PS}$ system (238).

No analogues to the known HMPA complexes of GeCl_4 , SbCl_3 or AlCl_3 (207) were found with any of the $(\text{NMe}_2)_x\text{Cl}_{3-x}\text{PS}$ series. Lack of donor behaviour is here attributed to differences in hard/soft characteristics of the metal chloride and S donor atom rather than low basicity of the ligands. Attempts to provide adducts of Ti, V and Cr trichlorides by ligand exchange reactions were also unsuccessful, $\text{TiCl}_3 \cdot 3\text{THF}$, $\text{VCl}_3 \cdot 3\text{MeCN}$ and $\text{CrCl}_3 \cdot 3\text{THF}$ failing to react with either $(\text{NMe}_2)_3\text{PS}$ or $(\text{NMe}_2)_2\text{ClPS}$. $\text{CrCl}_3 \cdot 2\text{NMe}_3$ gave the decomposition product $\text{Cr}_2\text{Cl}_6(\text{NMe}_3)_3$ when reacted with either ligand in C_6H_6 solution. Again, incompatibility in the hard/soft natures of the ligand and acceptor is proposed as the principal factor influencing reactivity.

3.3.2 Complexes with SnCl_4 , ZrCl_4 , HfCl_4 and SbCl_5

MeNO_2 solutions of SnCl_4 , ZrCl_4 and HfCl_4 with a two-fold excess of

$(\text{NMe}_2)_3\text{PS}$ and $(\text{NMe}_2)_2\text{ClPS}$ as ligand gave, on standing, colourless crystals of the appropriate 1:2 adduct. Reaction of $(\text{NMe}_2)_3\text{PS}$ with excess SnCl_4 under similar conditions gave crystals of the 1:1 adduct. $\text{SbCl}_5(\text{NMe}_2)_3\text{PS}$, $\text{SbCl}_5(\text{NMe}_2)_2\text{ClPS}$ and $\text{SbCl}_5(\text{NMe}_2)\text{Cl}_2\text{PS}$ were prepared by direct interaction of SbCl_5 and the appropriate ligand in CCl_4 . All the reactions were exothermic, but noticeably less so than with the formation of the analogous $(\text{NMe}_2)_3\text{PO}$ adducts, suggesting on an empirical basis that $(\text{NMe}_2)_3\text{PS}$ is less strongly bound to be metal halide than $(\text{NMe}_2)_3\text{PO}$.

Decomposition in moist air was a constant feature for all the adducts, those of $(\text{NMe}_2)_2\text{ClPS}$ and $(\text{NMe}_2)\text{Cl}_2\text{PS}$ being particularly susceptible to hydrolysis. Aqueous hydrolysis of $\text{SnCl}_4(\text{NMe}_2)_3\text{PS}$ with subsequent extraction of the products by CH_2Cl_2 did not yield the 1:2 adduct as did $\text{SnCl}_4(\text{NMe}_2)_3\text{PO}$. Evidence for ligand replacement was found in solutions of the complexes in coordinating solvents. Solubility in MeNO_2 was sufficient in most cases to facilitate some solution studies, the exception being $\text{SbCl}_5(\text{NMe}_2)\text{Cl}_2\text{PS}$, where almost instantaneous decomposition was found. The IR spectral data for $\text{MCl}_4 \cdot 2(\text{NMe}_2)_3\text{PS}$, ($\text{M} = \text{Sn}, \text{Zr}, \text{Hf}$), $\text{SnCl}_4(\text{NMe}_2)_3\text{PS}$ and $\text{SbCl}_5(\text{NMe}_2)_3\text{PS}$ are summarised in Table 3.3.1. Assignments are made after Kottgen *et al* (223) and Kincaid (239) and coworkers. Of particular interest are the changes in $\text{P}=\text{S}$ stretching frequency on complexation. Factors influencing $\nu(\text{P}=\text{S})$ are complex. Donation of electron density ($\text{NMe}_2 \rightarrow \text{P}$) which increases the $\text{P}-\text{S}$ bond order is offset by $\text{P}(\text{d}\pi) - \text{N}(\text{p}\pi)$ back donation, which decreases the $\text{P}-\text{S}$ bond order. A lowering in $\nu(\text{P}=\text{S})$ on substituting NMe_2 for Cl in the series $(\text{NMe}_2)_x\text{Cl}_{3-x}\text{PS}$ ($752 \text{ cm}^{-1}(\text{PSCl}_3)$, $677 \text{ cm}^{-1}(\text{NMe}_2)\text{Cl}_2\text{PS}$, $612 \text{ cm}^{-1}(\text{NMe}_2)_2\text{ClPS}$, $565 \text{ cm}^{-1}(\text{NMe}_2)_3\text{PS}$) (223) shows, as expected, the latter effect to be dominant. Complexation to a metal ion should, therefore, remove s-electron density, and providing

(NMe ₂) ₃ PS	ZrCl ₄ ·2L	HfCl ₄ ·2L	SnCl ₄ ·2L	SnCl ₄ ·L	SbCl ₅ ·L	Assignment
3000(m)	3038(s)	3040(s)	3020(w)	3010(w)	3010(sh)	νCH ₃
2930(s)	3017(s)	3015(s)	3005(m)	2950(m)	2958(m)	
2890(s)	2960(s)	2958(s)	2941(w)	2931(m)	2934(m)	
2841(m)	2931(s)	2925(sh)	2930(s)	2858(w)	2918(m)	
2798(m)	2860(w)	2853(w)	2900(s)	2820(w)	2870(w)	
	2820(w)	2820(w)	2830(m)	2730(vw)	2830(w)	
	2733(w)	2731(w)	2818(w)			
	2624(w)	2626(w)	2808(w)			
1477(s)	1487(sh)	1486(w)	1480(s)	1481(s)	1486(m)	δCH ₃
1455(s)	1468(s)	1466(w)	1455(s)	1459(s)	1464(m)	
1409(w)	1457(m)	1456(s)	1414(w)	1445(sh)	1450(sh)	
	1431(w)	1432(w)	1409(w)	1413(w)	1415(w,br)	
	1412(w)	1413(w)	1386(vw)	1365(w,br)	1365(vw)	
	1402(w)	1401(w)				
	1377(w)	1376(w)				
	1366(w)	1366(w)				
1285(s)	1301(m)	1301(m)	1299(m)	1298(s,br)	1305(s,br)	ρ _s NCH ₃
1270(s)	1283(m)	1282(m)	1290(m)			
			1262(w)			
1189(s)	1173(m)	1174(m)	1174(m)	1182(sh)	1165(s,br)	ρ _{as} NC ₂
1151(sh)	1159(m)	1159(m)	1150(w,sh)	1170(s)		
	1144(m)	1144(m)	1147(w)	1145(sh)		
	1115(m)	1115(m,br)	1108(w)	1115(vw)		
1061(s)	1061(m)	1061(m)	1067(m)	1064(m)	1053(m)	ν _{as} NC ₂
982(s)	1001(s)	1001(s)	995(m)	995(vs,br)	1003(s)	ν _s NC ₂
963(sh)	975(s)	974(s)	981(s)		988(m)	
739(s)	866(w)	867(w)	865(w)	867(w)	748(m)	ν _{as} PN ₃ + ν _{as} PN ₃
722(s)	860(m)	861(m)	804(m,br)	773(m)	723(m)	
	768(s)	769(s)	775(w)	758(m)	654(m)	
	749(m)	748(m)	741(m)	747(m)		
	725(m)	723(m)	723(w)	724(w)		
	658(vw)	615(s)	681(s)	673(s)		
	612(s)					

Table 3.3.1 (Continued)

$(\text{NMe}_2)_3\text{PS}$	$\text{ZrCl}_4 \cdot 2\text{L}$	$\text{HfCl}_4 \cdot 2\text{L}$	$\text{SnCl}_4 \cdot 2\text{L}$	$\text{SnCl}_4 \cdot \text{L}$	$\text{SbCl}_5 \cdot \text{L}$	Assignment
565(m)	550(m)	548(m)	546(s)	537(m)	515(m)	$\nu\text{P}=\text{S}$
503					443(w)	
458(m)	473(w)	474(w)	450(m)	443(w)		δPCN_2
431(sh)	432(w)	432(w)				
378(w)	376(vw)		380(w)			$\delta_{\text{as}}\text{NC}_2$
	360(vw)					
	302(vs)	283(vs)	313(vs)	353(s)	345(vs)	M-Cl
				324(vs)		

Table 3.3.1 IR Spectral Data of $(\text{NMe}_2)_3\text{PS}$ Complexes

$\text{M}(\text{d}\pi) \rightarrow \text{S}(\text{p}, \text{d}\pi)$ back bonding is small, will lower the P-S bond order and $\nu(\text{P}=\text{S})$, and increase $\text{N}(\text{p}\pi) - \text{P}(\text{d}\pi)$ bonding. With Zr, Hf (d^0) or Sn, Sb (d^{10}), M-S back bonding is limited by the absence of available electron density on the metal atoms, and the complexes show a low energy shift of $\nu(\text{P}=\text{S})$, e.g. 15 cm^{-1} $\text{ZrCl}_4 \cdot 2(\text{NMe}_2)_3\text{PS}$ and 50 cm^{-1} $\text{SbCl}_5 \cdot (\text{NMe}_2)_3\text{PS}$ in accordance with S donation. No evidence could be found for bands at 622 and 630 cm^{-1} in the spectra of $\text{SnCl}_4 \cdot 2(\text{NMe}_2)_3\text{PS}$ and $\text{ZrCl}_4 \cdot 2(\text{NMe}_2)_3\text{PS}$ respectively, described by Le Coz and Guerchais (205) as $\nu(\text{P}=\text{S})$ modes. It is possible that the band quoted at 630 cm^{-1} for $\text{ZrCl}_4 \cdot 2(\text{NMe}_2)_3\text{PS}$ is the band found at 612 cm^{-1} in this work, which has been assigned as a P-N stretch.

Increase in $\text{P}(\text{d}\pi) - \text{N}(\text{p}\pi)$ bonding produces asymmetry in the ligand and results in multiple splitting of the P-N stretching frequencies. The strong P-N bands in the spectrum of $(\text{NMe}_2)_3\text{PS}$ at 739 cm^{-1} ($\nu_{\text{S}}\text{PN}_3$) are found in the complexes as a series of bands in the $867\text{--}612\text{ cm}^{-1}$ range. Variations in acceptor behaviour of the metals cause the P-N bands to split to different extents, making correlation between individual bands

difficult. Consequently, no attempt has been made to specifically assign each band. Splitting was also found for the CH and $\rho_{as}NCH_3$ bands. In addition to the splitting caused by inequivalence of the NMe_2 groups (i.e. sp_2 vs. sp_3), differences in site symmetry may also play a part. Another possible contribution to ρNCH_3 multiplicity is the weak band at 1105 cm^{-1} , which only appears in the Raman spectrum of $(NMe_2)_3PS$ (N.B. this could become IR active in the spectra of the complexes with the lowering of ligand symmetry).

Strong metal halide stretching vibrations at 302 cm^{-1} ($ZrCl_4 \cdot 2(NMe_2)_3PS$), 283 cm^{-1} ($HfCl_4 \cdot 2(NMe_2)_3PS$), 313 cm^{-1} ($SnCl_4 \cdot 2(NMe_2)_3PS$) are in accordance with an octahedral trans (D_{4h}) arrangement of ligands. This geometry is not unexpected considering the bulky nature of the ligand (the analogous $(NMe_2)_3PO$ complexes also have a trans configuration (213)). An octahedral (C_{4v}) geometry is proposed for $SbCl_5 \cdot (NMe_2)_3PS$ on the basis of previous structural work, although only one (345 cm^{-1}) of the three ($a_1 + 2e$) expected M-Cl bands could be seen in the low IR spectrum. It is possible that two or more bands are coincidentally isoenergetic, or that the remaining two bands appear below 200 cm^{-1} . The structure of $SnCl_4 \cdot (NMe_2)_3PS$ is less well defined by the pattern of M-Cl bands than those of the other complexes. Only two strong bands at 353 and 324 cm^{-1} are found in the low IR as opposed to the three bands seen in the spectrum of $SnCl_4 \cdot (NMe_2)_3PO$. Rather than invoke a halide bridged dimeric structure (which is common for $TiCl_4 \cdot L$ (87-89) but not for $SnCl_4 \cdot L$ (230)) it seems preferable to assign a trigonal bipyramidal (C_{3v}) structure to $SnCl_4 \cdot (NMe_2)_3PS$ and assume that two of the SnCl bands are isoenergetic.

The IR spectra of the $(NMe_2)_2ClPS$ (Table 3.3.2) and $(NMe_2)Cl_2PS$ complexes show similar trends to those found with $(NMe_2)_3PS$ shifts to

$(\text{NMe}_2)_2\text{CIPS}$	$\text{ZrCl}_4 \cdot 2\text{L}$	$\text{HfCl}_4 \cdot 2\text{L}$	$\text{SnCl}_4 \cdot 2\text{L}$	$\text{SbCl}_5 \cdot \text{L}$	Assignment
3006(w)	3038(w)		3031(w)	2970(sh)	νCH_3
2952(m)	2960(w)		3010(w)	2943(s,br)	
2922(sh)	2941(s,br)		2955(w)	2860(w)	
2893(sh)	2721(w)		2930(s)	2828(w)	
2848(w)	2635(w)		2858(w)		
2806(w)			2827(w)		
			2811(w)		
1471(sh)	1483(sh)		1475(m)	1478(m)	δCH_3
1450(m)	1456(s)		1458(s)	1451(s,br)	
1409(w)	1424(m)		1450(sh)	1418(w)	
	1405(w)		1412(m)	1391(w)	
	1397(w)		1397(w)		
	1376(w)		1318(w)		
1290(m)	1330(w)	1313(m)	1302(s,br)	1304(s,br)	$\rho_s\text{NCH}_3$
1270(sh)	1297(s)	1301(m)			
1186(m)	1215(w)	1245(w)	1177(m)	1156(s,br)	$\rho_{as}\text{NCH}_3$
1156(m)	1165(s)	1230(w)	1164(m)		
1101(vw)	1155(sh)	1176(m)	1152(m)		
	1128(m)	1112(w)	1121(m)		
	1120(w)				
	1111(w)				
1061(m)	1060(s)	1068(s)	1062(s)	1057(s)	$\nu_{as}\text{NC}_2$
		1048(s)			
989(s,br)	1004(vs)	1012(s)	998(s,br)	1022(w)	$\nu_s\text{NC}_2$
964(s)	988(m)	998(w)	963(sh)	1010(m)	
				992(s)	
756(s,br)	856(s)	884(s)	810(w)	868(s)	$\nu_{as}\text{PN}_2$ $+\nu_s\text{PN}_2$
737(sh)	780(s)	811(s)	778(w)	805(w)	
	724(w)	760(s)	763(w)	787(w)	
	698(m)	726(m)	755(w)	776(w)	
			730(s)	719(w)	
			695(w)	704(w)	
			654(w)	614(m)	

Table 3.3.2 (continued)

$(\text{NMe}_2)_2\text{ClPS}$	$\text{ZrCl}_4 \cdot 2\text{L}$	$\text{HfCl}_4 \cdot 2\text{L}$	$\text{SnCl}_4 \cdot 2\text{L}$	$\text{SbCl}_5 \cdot \text{L}$	Assignment
612(s)	577(s)	575(m)	574(s)	580(m)	$\nu_{\text{P}=\text{S}}$
489(m)	509(s)	495(m)	498(m)	490(m)	$\nu_{\text{S}}\text{PCl}$
435(vw)	432(w)	440(w)	455(vw)		δ_{PNC_2}
413(vw)	415(w)	389(w)	426(w)		
354(w)	356(w)				$\delta_{\text{S}}\text{PN}_2$
	305(vs,br)	285(vs,br)	316(vs,br)	346(vs,br)	$\nu_{\text{M}-\text{Cl}}$

Table 3.3.2 IR Spectral Data of $(\text{NMe}_2)_2\text{ClPS}$ Complexes

lower energy of between 32 and 38 cm^{-1} were found for the $\nu(\text{P}=\text{S})$ band in the complexes, in accordance with S donation. Kincaid *et al* (239) have suggested that $\Delta\nu(\text{P}=\text{S})$ on complexation will be larger for those ligands possessing the greatest amount of PS multiple bonding. An example of this was found with the complexes of $(\text{NMe}_2)_2\text{ClPS}$ and $(\text{NMe}_2)_3\text{PS}$ with Sn (IV), Zr (IV) and Hf (IV), where $\Delta\nu(\text{P}=\text{S})$ was greater for the $(\text{NMe}_2)_2\text{ClPS}$ complexes than the corresponding $(\text{NMe}_2)_3\text{PS}$ adducts. The $\nu(\text{P}=\text{S})$ shift in $\text{SbCl}_5 \cdot (\text{NMe}_2)_2\text{ClPS}$, however, presents an intriguing problem. According to the hypothesis of Kincaid *et al* (239), the $\nu(\text{P}=\text{S})$ shift of $\text{SbCl}_5 \cdot (\text{NMe}_2)_2\text{ClPS}$ should lie somewhere between the 50 cm^{-1} shift for $\text{SbCl}_5 \cdot (\text{NMe}_2)_3\text{PS}$ and the 108 cm^{-1} shift found for $\text{SbCl}_5 \cdot \text{Cl}_3\text{PS}$ (219). The observed shift was found to be only 32 cm^{-1} . Misassignment of the $\text{P}=\text{S}$ stretching bands in both $\text{SbCl}_5 \cdot (\text{NMe}_2)_2\text{ClPS}$ and $\text{SbCl}_5 \cdot (\text{NMe}_2)_3\text{PS}$ is unlikely, as in both cases, all bands to lower energy can be assigned unambiguously, as either P-Cl or $\delta(\text{PNC})$ modes. Unfortunately, no data is available for $\nu(\text{P}=\text{S})$ from the spectrum of $\text{SbCl}_5 \cdot (\text{NMe}_2)\text{Cl}_2\text{PS}$, as splitting of $\nu\text{P-N}$ creates a multitude of bands in the 784-610 cm^{-1} region, making an accurate assignment of $\nu(\text{P}=\text{S})$, impossible. It does, however, seem reasonable that the band at 572 cm^{-1} in $\text{SbCl}_5 \cdot (\text{NMe}_2)\text{Cl}_2\text{PS}$ corresponds to the unassigned 569 cm^{-1} band in the free ligand ($\nu\text{P-Cl?}$) and that $\Delta\nu(\text{P}=\text{S})$ is, therefore, <67 cm^{-1} , the 610 cm^{-1} band being the lowest energy candidate for $\nu(\text{P}=\text{S})$. An explanation of the $\nu(\text{P}=\text{S})$ shifts in the SbCl_5 complexes on the basis of the simple Kincaid model probably fails in this case because substituent resonance effects are ignored. Molecular orbital calculations and/or extensive crystallographic studies would seem to be the only way of resolving this problem.

As with the $(\text{NMe}_2)_3\text{PS}$ complexes, extensive splitting of the P-N and C-N bands results from the reduction in ligand symmetry on complex formation. In contrast, $\nu\text{P-Cl}$ modes are found as single bands throughout

the spectra of the complexes. For the $(\text{NMe}_2)_2\text{ClPS}$ adducts, the observed $\nu\text{P-Cl}$ shift $< 20 \text{ cm}^{-1}$. It has been established by ^{35}Cl NQR experiments that P-Cl π bonding in phosphoryl-type molecules is present, but very weak (240, 241). The increase in availability of P(d) orbitals for π bonding which causes splitting of the $\nu\text{P-N}$ and $\nu\text{C-N}$ modes has little effect on the P-Cl bonding and the $\nu\text{P-Cl}$ stretch remains invariant.

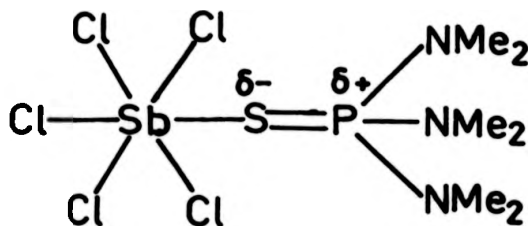
An octahedral trans (D_{4h}) symmetry was proposed for $\text{MCl}_4 \cdot 2(\text{NMe}_2)_2\text{ClPS}$ ($\text{M} = \text{Zr}, \text{Hf}, \text{Sn}$) on the basis of strong metal halide vibrations at 305, 285 and 316 cm^{-1} respectively. In this respect the complexes differ from their $(\text{NMe}_2)_2\text{ClPO}$ analogues which have been assigned as cis (C_{2v}) (205). Two possible factors influencing the change in geometry on going from an oxygen to sulphur donor are differences in $\text{O}\cdots\text{O}$ and $\text{S}\cdots\text{S}$ attractive forces (which stabilise the cis form)(118), and the fact that $(\text{NMe}_2)_2\text{ClPS}$ being asymmetric will be slightly more bulky than $(\text{NMe}_2)_2\text{ClPO}$, and, therefore, favour a trans structure. $\text{SbCl}_5 \cdot (\text{NMe}_2)_2\text{ClPS}$ and $\text{SbCl}_5 \cdot (\text{NMe}_2)\text{Cl}_2\text{PS}$ are interpreted as being of octahedral (C_{4v}) geometry by similar reasoning to that used to establish the structure of $\text{SbCl}_5 \cdot (\text{NMe}_2)_3\text{PS}$.

Complex	L = $(\text{NMe}_2)_3\text{PS}$		L = $(\text{NMe}_2)_2\text{ClPS}$	
	^1H	^{31}P	^1H	^{31}P
L	2.65	81.15	2.73	91.4
$\text{SnCl}_4 \cdot 2\text{L}$	2.80	79.84	2.77	86.87
$\text{SnCl}_4 \cdot \text{L}$	2.91	-	-	-
$\text{ZrCl}_4 \cdot 2\text{L}$	2.85	84.67	3.04	-
$\text{HfCl}_4 \cdot 2\text{L}$	3.03	88.67	3.02	-
$\text{SbCl}_5 \cdot \text{L}$	3.04	60.23	3.38	-

Table 3.3.3 ^1H and ^{31}P Spectra of the $(\text{NMe}_2)_3\text{PS}$ and $(\text{NMe}_2)_2\text{ClPS}$ Complexes. (MeNO_2 soln., $T = 298 \text{ K}$)

The available ^1H and ^{31}P NMR data for the $(\text{NMe}_2)_3\text{PS}$ and $(\text{NMe}_2)_2\text{ClPS}$ complexes

is summarised in Table 3.3.3. Parallels to the behaviour found for the HMPA complexes exist in the spectra of the thiophosphoryl compounds. No significant change in the value of the P-H coupling constants ($J(\text{P-H})$ $(\text{NMe}_2)_3\text{PS} = 10\text{-}12$ Hz, $J(\text{P-H})$ $(\text{NMe}_2)_2\text{ClPS} = 14\text{-}16$ Hz) occurred on complexation. The spectra of the $\text{MCl}_4 \cdot 2(\text{NMe}_2)_3\text{PS}$ ($\text{M} = \text{Zr}, \text{Hf}$) complexes show a reduction in both phosphorus and hydrogen electron density as evidenced by the downfield shift of both resonances. A strong metal-sulphur bond is thus implied. The ^{31}P spectra of $\text{SnCl}_4 \cdot 2(\text{NMe}_2)_3\text{PS}$ and $\text{SnCl}_4 \cdot 2(\text{NMe}_2)_2\text{ClPS}$ present the converse situation. In the case of Sn (IV) $\text{N} \rightarrow \text{P}$ electron donation slightly exceeds the loss in P density caused by the reduction of the $\text{P}=\text{S}$ bond order, resulting in a small upfield ^{31}P shift ($\Delta\delta$ $\text{SnCl}_4 \cdot 2(\text{NMe}_2)_3\text{PS} = 1.31$ ppm, $\text{SnCl}_4 \cdot (\text{NMe}_2)_2\text{ClPS} = 4.53$ ppm). This, coupled with the very small downfield shifts found in the corresponding ^1H spectra, suggests a weaker metal-sulphur bond than that found in the Zr and Hf complexes. A large increase in phosphorus electron density ($\Delta\delta$ $^{31}\text{P} = 21\text{-}82$ ppm), and a large decrease in both proton electron density ($\Delta\delta = +0.25$ ppm), and PS bond order ($\Delta\nu$ $\text{PS} = -50$ cm^{-1}) in the spectra (^{31}P , ^1H and IR) of $\text{SbCl}_5 \cdot (\text{NMe}_2)_3\text{PS}$ are taken as evidence of dipolar character in the $\text{P}=\text{S}$ bond, i.e.



$(\text{NMe}_2)_3\text{PSe}$ provides an example where the dipolar nature of the phosphorus chalcogen bond has already been established (191, 192).

Temperature dependent line broadening was found to be a feature of the spectra (^1H and ^{31}P) of $\text{SnCl}_4 \cdot (\text{NMe}_2)_3\text{PS}$, $\text{SnCl}_4 \cdot 2(\text{NMe}_2)_3\text{PS}$ and

$\text{SbCl}_5 \cdot (\text{NMe}_2)_3\text{PS}$, indicating some sort of dynamic behaviour in solution.

Two possible sources of such broadening are:-

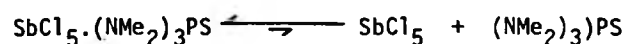
- (a) Non-equivalence between NMe_2 groups within the coordinated ligand
- and (b) Ligand exchange.

Splitting of the P-N stretching modes in the IR spectra of the adducts was attributed to inequivalent NMe_2 groups in the solid state. If this behaviour was carried over into solution, it could account for the broadened resonances in the ^1H NMR spectra. The P nucleus, however, is presented with an averaged view of all three NMe_2 groups and should give sharp resonances irrespective of the state of the NMe_2 substituents. Broadening of the ^{31}P resonances, therefore, suggests that the NMe_2 groups are either equivalent in solution, or 'exchange' sufficiently fast to remain unobserved by NMR.

To investigate the second possibility (ligand exchange) the $\text{SbCl}_5/(\text{NMe}_2)_3\text{PS}$ system was studied in some detail. Evidence that an exchange process exists comes from the ^1H NMR spectra obtained for a mixture of equimolar solutions of $\text{SbCl}_5 \cdot (\text{NMe}_2)_3\text{PS}$ and free $\text{SbCl}_5(\text{NMe}_2)_3\text{PS}$ (Fig. 3.3.1). The spectrum at 313 K represents the fast exchange limit, the shift (δ 2.82) being intermediate between that of the free ligand (δ 2.65) and that of the complex (δ 3.04). Lowering the temperature induces broadening via a slowing down of the exchange process until at 283 K, P-H coupling could no longer be resolved. At temperatures between 263 K and 253 K, the single resonance splits into two, corresponding to $\text{SbCl}_5(\text{NMe}_2)_3\text{PS}$ and free $(\text{NMe}_2)_3\text{PS}$. At 233 K (M.p. $\text{CD}_3\text{NO}_2 = 238$ K), ligand exchange between free and bound $(\text{NMe}_2)_3\text{PS}$ is sufficiently slow to enable the P-H coupling to be resolved in each resonance.

Having established that for the $\text{SbCl}_5/(\text{NMe}_2)_3\text{PS}$ system ligand

exchange lies somewhere between the slow and fast exchange limits in the 313 K - 233 K range; this knowledge can now be applied to the original ^1H spectra for $\text{SbCl}_5 \cdot (\text{NMe}_2)_3\text{PS}$ (Fig. 3.3.2). One immediate difference is that the resonances are broadened to a much smaller extent than when a molar excess of ligand was used, i.e. $\text{SbCl}_5 \cdot (\text{NMe}_2)_3\text{PS} + (\text{NMe}_2)_3\text{PS}$ as above. An equilibrium of the type:-



is proposed. The extent to which dissociation occurs is not known, but needs only be in the order of 1 - 2% to account for the observed broadening phenomenon. Spectra measured for $\text{SbCl}_5 \cdot (\text{NMe}_2)_3\text{PS}$ (Fig. 3.3.2) do not represent the true chemical shift of the complex but appear as weighted intermediate values between the unobservable true shift of $\text{SbCl}_5 \cdot (\text{NMe}_2)_3\text{PS}$ and that of free $(\text{NMe}_2)_3\text{PS}$. The weighting is dependant upon the unknown degree of dissociation. The free and bound $(\text{NMe}_2)_3\text{PS}$ resonances broaden each other by ligand exchange. Since the amount of broadening observed is proportional to the concentration of the species producing the broadening, the $\text{SbCl}_5 \cdot (\text{NMe}_2)_3\text{PS}$ resonance suffers only a small linewidth change (i.e. only a small amount of free ligand). The free $(\text{NMe}_2)_3\text{PS}$ resonance, however, is affected by $\text{SbCl}_5 \cdot (\text{NMe}_2)_3\text{PS}$ which is in large excess, and is consequently broadened so much that it becomes unobservable.

Ligand exchange undoubtedly also occurs in the $\text{SnCl}_4/(\text{NMe}_2)_3\text{PS}$ systems, but here the situation is complicated by the presence of two stable interrelated species ($\text{SnCl}_4 \cdot 2(\text{NMe}_2)_3\text{PS}$ and $\text{SnCl}_4 \cdot (\text{NMe}_2)_3\text{PS}$) which are likely to have different ligand exchange rates. The small temperature dependant chemical shifts seen in the ^1H spectra of $\text{SnCl}_4 \cdot (\text{NMe}_2)_3\text{PS}$ in addition to line broadening are a further indication of the complexity

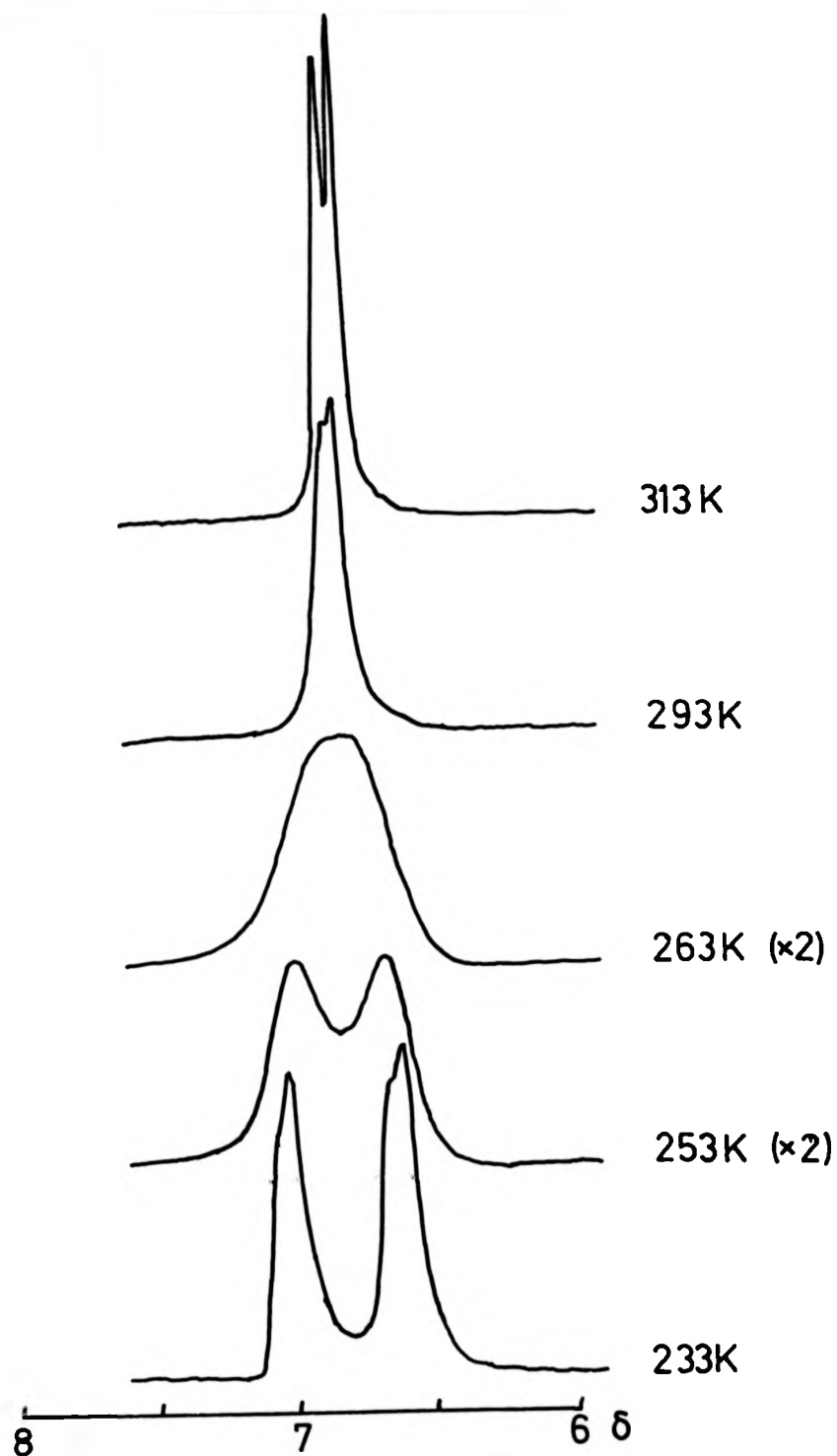


Fig. 3.3.1 ^1H NMR Spectra (220 MHz, CD_3NO_2 soln., rel. TMS) for $\text{SbCl}_5 \cdot (\text{NMe}_2)_3\text{PS} + (\text{NMe}_2)_3\text{PS}$ (1:1).

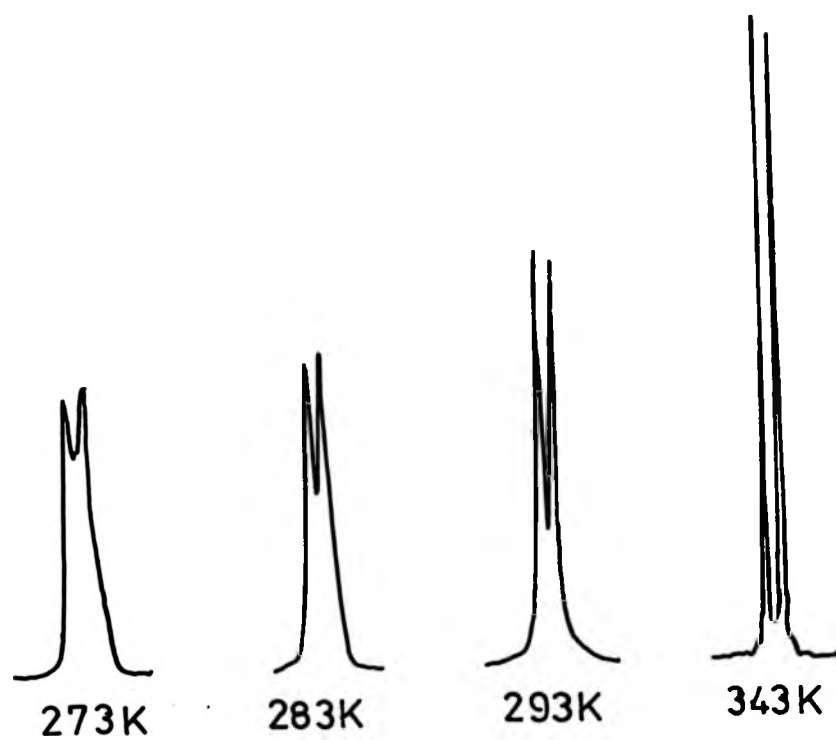


Fig. 3.3.2 ^1H NMR Spectra (220 MHz) of $\text{SbCl}_5 \cdot (\text{NMe}_2)_3\text{PS}$, CD_3NO_2 soln.,
rel. TMS.

of the system.

3.3.3 Reaction of $(\text{NMe}_2)_2\text{ClPS}$ with BCl_3

Reaction of BCl_3 with a three fold excess of $(\text{NMe}_2)_2\text{ClPS}$ (CH_2Cl_2 soln., 298 K) gave no isolable coordination compound. Instead, over a four month period, large colourless crystals of $(\text{BCl}_2\text{NMe}_2)_2$ were deposited from solution. The product was identified by microanalysis, and by its ^1H NMR spectrum (Fig. 3.3.3). The single septet seen in the ^1H NMR spectrum (242) results from long range coupling to two equivalent ^{11}B nuclei (243).

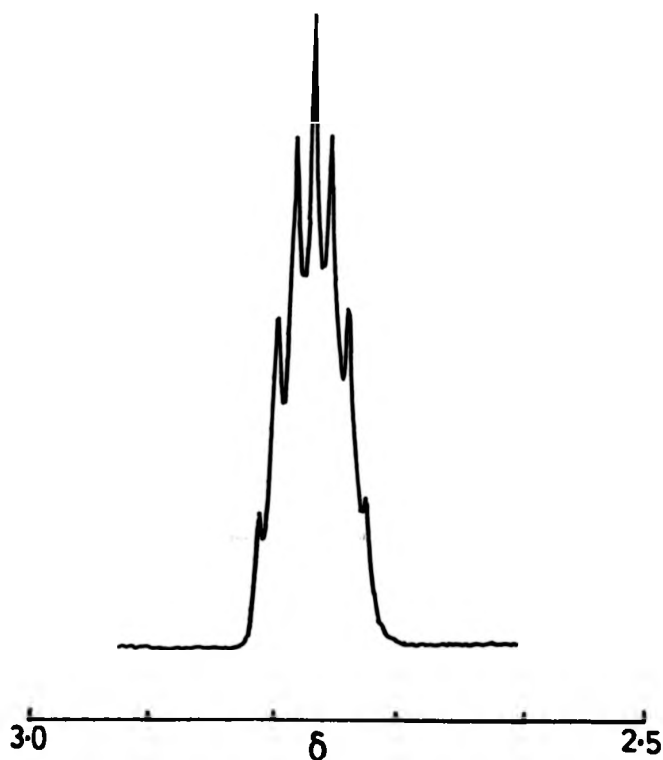
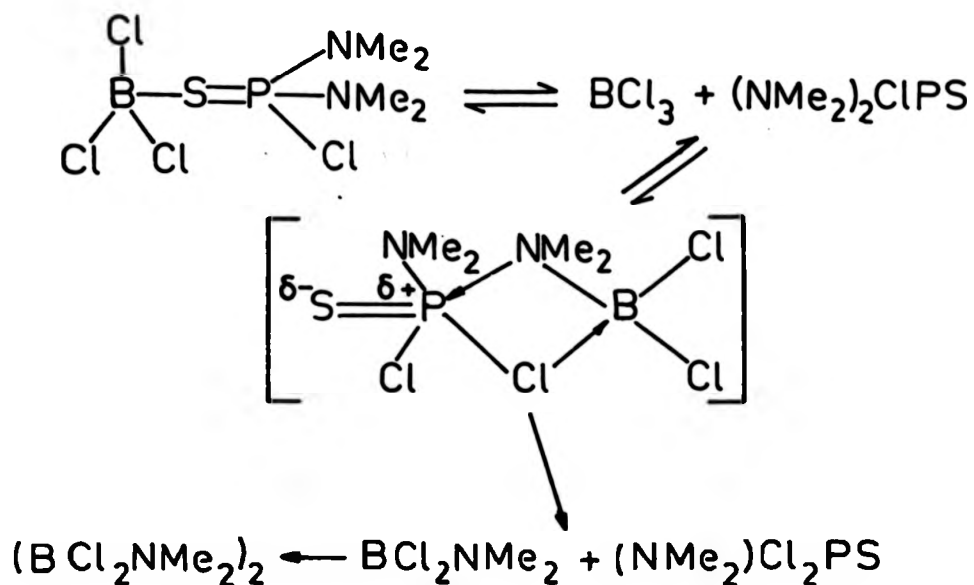


Fig. 3.3.3 ^1H NMR Spectrum of $(\text{BCl}_2\text{NMe}_2)_2$, (CDCl_3 , 220 MHz)

The other reaction product, although not identified was taken to be



Exchange between dialkylamino and halo substituents has previously been noted for phosphoramidate and thiophosphoramidate compounds with certain organosilicon compounds (244), and in the $\text{Cl}_3\text{PY}/\text{B}(\text{NR}_2)_3$ ($\text{Y} = \text{O}, \text{S}$, $\text{R} = \text{Me}, \text{Et}$) systems (245). The mechanism of the reaction raises an interesting point. A sulphur coordinated $\text{BCl}_3 \cdot (\text{NMe}_2)_2\text{ClPS}$ complex as a possible reaction intermediate is hampered by the large distance between the phosphorus and boron reaction centres. A mechanism involving the elusive coordination through a NMe_2 group, however, enables the reaction to be explained in terms of a simple 'four centre' transition state, i.e.

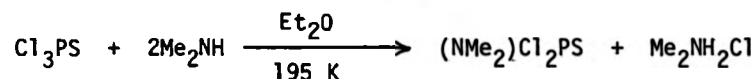


Dimerisation of the liquid $\text{BCl}_2(\text{NMe}_2)$ to the crystalline solid $(\text{BCl}_2\text{NMe}_2)_2$ proposed as the terminal step of the reaction scheme, has been found to be slow both as a pure liquid, and in solution ($t^{1/2} = 35 \text{ hr.}$, 1.7 M in C_6H_6 , 298 K)(246).

3.4 Experimental

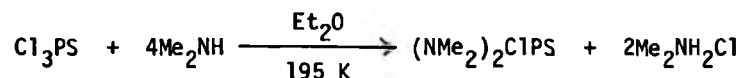
3.4.1 Preparation of ligands

(a) $(\text{NMe}_2)\text{Cl}_2\text{PS}$. Dimethylamine (250 ml, 3.77 mmol) was added dropwise from a cooled (195 K) dropping funnel to a solution of Cl_3PS (192 mls, 1.89 mol) in dry Et_2O (1 litre), also cooled to 195 K. An immediate reaction occurred producing a voluminous precipitate of $\text{Me}_2\text{NH}_2^+\text{Cl}^-$ according to the reaction:-



On completion of addition, the reaction mixture was allowed to warm to room temperature. The precipitate was removed by filtration, and washed with 2 x 500 ml portions of dry Et_2O . Combining the filtrate and washings and removal of the Et_2O on a rotary evaporator gave the crude product, which was distilled in vacuo (B.p. 313 K/0.6 mm) to give $(\text{NMe}_2)\text{Cl}_2\text{PS}$ as a colourless mobile liquid (283 g, 84.3%).

(b) $(\text{NMe}_2)_2\text{ClPS}$. Under the same reaction conditions as above, Cl_3PS (95.4 mls, 0.94 mol) reacted with Me_2NH (250 mls, 3.77 mol) to give $(\text{NMe}_2)_2\text{ClPS}$ as a



colourless low melting point solid (136g, 77.52%) (B.p. 328 K/0.4 mm)

(c) $(\text{NMe}_2)_3\text{PS}$. Me_2NH (~100 ml, 1.5 mol) was distilled in vacuo into a single ampoule glass bomb containing $(\text{NMe}_2)_2\text{ClPS}$ (58 g, 0.31 mol) at 77 K. On warming to room temperature, a strongly exothermic reaction occurred which was moderated by placing the bomb in an ice bath. After opening, the bomb was purged with dry N_2 to remove excess Me_2NH , and the product extracted with 5 x 100 ml portions Et_2O . Removal of solvent and distillation in vacuo (330 K/0.15 mm) yielded $(\text{NMe}_2)_3\text{PS}$ as a colourless

crystalline solid (57.6 g, 95.2%).

3.4.2 Preparation of HMPA complexes

(a) $\text{MCl}_4 \cdot 2\text{HMPA}$ ($\text{M} = \text{Ti, Zr, Hf, Sn}$). The complexes $\text{MCl}_4 \cdot 2\text{HMPA}$ ($\text{M} = \text{Ti, Zr, Hf, Sn}$) were prepared by the addition of a two-fold excess of HMPA to a solution or suspension of the metal tetrachloride in MeNO_2 solution according to the method of Sadie and Dupreez (208).

Recrystallisation was achieved from either CH_2Cl_2 , MeNO_2 , or in the case of $\text{TiCl}_4 \cdot 2\text{HMPA}$, C_6H_6 .

(b) $\text{SnI}_4 \cdot 2\text{HMPA}$. Direct addition of HMPA (1.3 g, 6.9 mmol) to SnI_4 (2.1 g, 3.3 mmol) in CH_2Cl_2 solution gave the dark brown crystalline product, purified as described above. Yield (3.1 g, 95%) M.p. 419-421 K (uncorr.).

Analysis based on $\text{C}_{12}\text{H}_{36}\text{N}_6\text{P}_2\text{O}_2\text{SnI}_4$

Calculated	C(14.6)	H(3.7)	N(8.5)	P(6.3)	I(51.5)	%
Found	C(15.0)	H(3.9)	N(8.9)	P(5.6)	I(51.2)	%

(c) $\text{TiCl}_4 \cdot \text{HMPA}$. TiCl_4 (1 ml, 9.1 mmol) was carefully added to a solution of HMPA (1.63 g, 9.1 mmol) in CH_2Cl_2 (5 mls) to give a bright orange solution, which on standing gave bright orange cubic crystals of $\text{TiCl}_4 \cdot \text{HMPA}$. The product was recrystallised from CH_2Cl_2 . Yield 2.8 g, 83%.

Analysis based on $\text{C}_6\text{H}_{18}\text{N}_3\text{PTiCl}_4$

Calculated	C(19.5)	H(4.9)	N(11.4)	Cl(38.4)	%
Found	C(19.5)	H(5.1)	N(11.4)	Cl(38.5)	%

$\Lambda_M = 1.53 \Omega^{-1}\text{cm}^2\text{mol}^{-1}$ at $1 \times 10^3 \text{M}$ concentration, (CH_2Cl_2 , 298 K).

(d) $2\text{TiCl}_4 \cdot \text{HMPA}$. Slow addition of HMPA (1.0 g, 5.7 mmol) to TiCl_4 (2.3 g, 12.0 mmol) each dissolved in ~5 mls MeNO_2 produced an initial dark

red oil, which solidified after standing for several days. The solid was carefully washed with n-hexane to give the dark red product (2.6 g, 81%). M.p. 400-402 K (uncorr.).

Analysis based on $C_6H_{18}N_3POTi_2Cl_2$

Calculated C(12.9) H(3.2) N(7.5) P(5.5) Cl(50.8) %

Found C(12.6) H(3.2) N(7.6) P(5.6) Cl(50.9) %

$\Lambda_M = 0.18 \Omega^{-1}cm^2mol^{-1}$ at $1 \times 10^{-3}M$ concentration (CH_2Cl_2 , 298 K).

(e) $SnCl_4$.HMPA. Direct addition of HMPA (1.0 g, 5.7 mmol) to $SnCl_4$ (3.1 g, 12.0 mmol) each dissolved in ~5 ml $MeNO_2$ gave the white crystalline product which was well washed with n-hexane, and thoroughly pumped dry to remove excess $SnCl_4$. Yield 3.3 g, (62%). M.p. 361-362 K (uncorr.).

Analysis based on $C_6H_{18}N_3POSnCl_4$

Calculated C(16.4) H(4.1) N(9.5) Cl(32.5) %

Found C(15.8) H(4.0) N(9.1) Cl(32.9) %

$\Lambda_M = 0.23 \Omega^{-1}cm^2mol^{-1}$ at $1 \times 10^{-3}M$ concentration (CH_2Cl_2 , 298 K).

(f) $TiCl_3$.3HMPA. $TiCl_3$ (1.6 g, 10.3 mmol) was extracted into 200 ml dry THF, and HMPA (5.5 g, 31 mmol) was added to the resulting purple solution. The pale blue product which precipitated on partial removal of solvent in vacuo was collected, washed with n-hexane and pumped in vacuo for several hours. Yield 6.8 g (95%). M.p. 381-383 K (uncorr.).

Analysis based on $C_{18}H_{54}N_9P_3O_3TiCl_3$

Calculated C(31.2) H(7.9) N(18.2) P(13.4) Cl(15.4) %

Found C(31.1) H(7.9) N(18.4) P(13.2) Cl(15.4) %

$\Lambda_M = 0.10 \Omega^{-1}cm^2mol^{-1}$ at $1 \times 10^{-3}M$ concentration (CH_2Cl_2 , 298 K).

(g) VCl_3 .3HMPA. VCl_3 (2.6 g, 16.5 mmol) and HMPA (8.9 g, 50 mmol) reacted as for $TiCl_3$.3HMPA to give the product as a pink solid (10.5 g, 91%).

M.p. 401-403 K (uncorr.).

Analysis based on $C_{18}H_{54}N_9P_3O_3VCl_3$

Calculated C(31.1) H(7.8) N(18.1) P(13.4) Cl(15.3) %

Found C(31.3) H(7.9) N(18.2) P(13.7) Cl(15.3) %

$\Lambda_M = 0.12 \Omega^{-1}cm^2mol^{-1}$ at $1 \times 10^{-3}M$ concentration (CH_2Cl_2 , 298 K).

(h) fac $CrCl_3 \cdot 3HMPA$. Extraction of $CrCl_3 \cdot 2NMe_3$ (2.7 g, 9.6 mmol) with dry benzene into a solution of HMPA (5.2 g, 29 mmol) also in benzene, gave the product as a purple solid on partial removal of solvent. Yield 6.4 g (96%). M.p. 411-412 K.

Analysis based on $C_{18}H_{54}N_9P_3O_3CrCl_3$

Calculated C(31.0) H(7.8) N(18.1) P(13.3) Cl(15.3) %

Found C(31.2) H(8.0) N(18.3) P(13.3) Cl(15.3) %

$\Lambda_M = 1.1 \Omega^{-1}cm^2mol^{-1}$ at $1 \times 10^{-3}M$ concentration (CH_2Cl_2 , 298 K).

(i) mer $CrCl_3 \cdot 3HMPA$. A mixture of $CrCl_3$ (1.5 g, 9.2 mmol) and Zn dust (0.2 g) was sealed in a glass ampoule with HMPA (5.0 g, 28.1 mmol) and dry THF (200 cm^3). The resultant green solution was filtered, and slow removal of solvent gave the product as dark green crystals. M.p. 359-360 K.

Analysis based on $C_{18}H_{54}N_9P_3O_3CrCl_3$

Calculated C(31.0) H(7.8) N(18.1) P(13.3) Cl(15.3) %

Found C(31.3) H(7.8) N(18.2) P(13.1) Cl(15.2) %

$\Lambda_M = 1.4 \Omega^{-1}cm^2mol^{-1}$ at $1 \times 10^{-3}M$ concentration (CH_2Cl_2 , 298 K).

3.4.3 Complexes of $(NMe_2)_xCl_{3-x}PS$

$SnCl_4 \cdot 2(NMe_2)_3PS$ and $ZrCl_4 \cdot 2(NMe_2)_3PS$ were prepared by addition of a two fold excess of ligand to a solution of the appropriate metal halide in $MeNO_2$ according to the method of LeCoz and Guerschais (205). Both complexes were recrystallised from warm $MeNO_2$.

(a) $\text{SnCl}_4 \cdot (\text{NMe}_2)_3\text{PS}$. Dropwise addition of $(\text{NMe}_2)_3\text{PS}$ (1.6 g, 8.2 mmol) in MeNO_2 (5 ml) to SnCl_4 (1 ml, 2.226 g, 8.5 mmol) also in MeNO_2 (5 mls) gave on cooling, colourless crystals of $\text{SnCl}_4 \cdot (\text{NMe}_2)_3\text{PS}$.

Analysis based on $\text{C}_6\text{H}_{18}\text{N}_3\text{PSSnCl}_4$

Calculated C(15.8) H(3.9) N(9.2) Cl(31.1) %

Found C(15.9) H(3.9) N(9.0) Cl(30.8) %

(b) $\text{SnCl}_4 \cdot 2(\text{NMe}_2)_2\text{ClPS}$. SnCl_4 (1 ml, 8.5 mmol) and $(\text{NMe}_2)_2\text{ClPS}$ (3.5 g, 18.7 mmol) reacted as above gave off-white crystals, which on recrystallisation from warm MeNO_2 afforded $\text{SnCl}_4 \cdot 2(\text{NMe}_2)_2\text{ClPS}$ as a white crystalline solid. Yield 1.89 g (35.1%).

Analysis based on $\text{C}_8\text{H}_{24}\text{N}_4\text{P}_2\text{S}_2\text{SnCl}_6$

Calculated C(15.16) H(3.8) N(8.9) P(9.7) S(10.1) Cl(33.5) %

Found C(15.3) H(3.9) N(9.0) P(9.5) S(10.3) Cl(33.3) %

$\Lambda_M = 1.5 \Omega^{-1}\text{cm}^2\text{mol}^{-1}$ at $1 \times 10^{-3}\text{M}$ concentration (CH_2Cl_2 , 298 K).

(c) $\text{ZrCl}_4 \cdot 2(\text{NMe}_2)_2\text{ClPS}$. $(\text{NMe}_2)_2\text{ClPS}$ (9.2 g, 24.6 mmol) in MeNO_2 (10 mls) was carefully added to a suspension of ZrCl_4 (2.6 g, 11.2 mmol) in MeNO_2 (10 mls) the rate of addition being controlled as to keep the reaction mixture in slight excess of room temperature. The pale yellow solution thus formed gave colourless crystals of $\text{ZrCl}_4 \cdot 2(\text{NMe}_2)_2\text{ClPS}$ on standing. Yield 4.2 g, (61.9%). Increasing the reaction temperature resulted in extensive decomposition of the complex which reduced yield dramatically.

Analysis based on $\text{C}_8\text{H}_{24}\text{N}_4\text{P}_2\text{S}_2\text{ZrCl}_6$

Calculated C(15.8) H(4.0) N(9.2) Cl(35.1) %

Found C(15.5) H(4.0) N(9.1) Cl(35.2) %

(d) $\text{HfCl}_4 \cdot 2(\text{NMe}_2)_3\text{PS}$. $(\text{NMe}_2)_3\text{PS}$ (1.33 g, 6.8 mmol) and HfCl_4 (0.92 g, 2.9 mmol) reacted in MeNO_2 (7 mls) as above to give $\text{HfCl}_4 \cdot 2(\text{NMe}_2)_3\text{PS}$, which

was recrystallised from warm MeNO_2 as a white microcrystalline solid.

Yield 1.6 g (66.2%).

Analysis based on $\text{C}_{12}\text{H}_{36}\text{N}_6\text{P}_2\text{S}_2\text{HfCl}_4$

Calculated C(20.3) H(5.1) N(11.8) Cl(19.9) %

Found C(20.0) H(5.0) N(11.8) Cl(20.1) %

$\Lambda_M = 1.5 \Omega^{-1}\text{cm}^2\text{mol}^{-1}$ at $1 \times 10^{-3}\text{M}$ concentration (CH_2Cl_2 , 298 K)

(e) $\text{HfCl}_4 \cdot 2(\text{NMe}_2)_2\text{ClPS}$. $(\text{NMe}_2)_2\text{ClPS}$ (1.5 g, 8.0 mmol) and HfCl_4 (0.92 g, 2.9 mmol) reacted as for $\text{ZrCl}_4 \cdot 2(\text{NMe}_2)_2\text{ClPS}$ to give the product as colourless microcrystals. Yield 1.7 g (84.5%).

Analysis based on $\text{C}_8\text{H}_{24}\text{N}_4\text{P}_2\text{S}_2\text{HfCl}_6$

Calculated C(13.8) H(3.5) N(8.0) Cl(30.07) %

Found C(13.5) H(3.9) N(7.7) Cl(31.0) %

(f) $\text{SbCl}_5 \cdot (\text{NMe}_2)_3\text{PS}$. $(\text{NMe}_2)_3\text{PS}$ (1.6 g, 8.2 mmol) in dry CCl_4 (150 mls) was added dropwise to a solution of SbCl_5 (1.0 ml, 2.34 g, 7.8 mmol) in CCl_4 (200 mls) over a 2 hour period. On continued stirring of the pale yellow solution thus formed, $\text{SbCl}_5 \cdot (\text{NMe}_2)_3\text{PS}$ precipitated from solution as a pale yellow solid. It was collected, and washed in vacuo with CCl_4 . Yield 2.3 g (59.7%). The complex was also obtained as bright yellow needles by recrystallisation from MeNO_2 (Yield ~10%).

Analysis based on $\text{C}_6\text{H}_{18}\text{N}_3\text{PSSbCl}_5$

Calculated C(14.6) H(3.7) N(8.5) Cl(35.8) %

Found C(14.4) H(3.9) N(8.8) Cl(35.8) %

$\Lambda_M = 1.5 \Omega^{-1}\text{cm}^2\text{mol}^{-1}$ at $1 \times 10^{-3}\text{M}$ concentration (CH_2Cl_2 , 298 K).

(g) $\text{SbCl}_5 \cdot (\text{NMe}_2)_2\text{ClPS}$. Reaction of $(\text{NMe}_2)_2\text{ClPS}$ (1.12 g, 6.0 mmol) and SbCl_5 (0.7 mls, 5.4 mmol) as above gave the product as a white solid. Yield 2.0 g (76.3%).

Analysis based $C_4H_{12}N_2PSSbCl_6$

Calculated	C(10.0)	H(2.5)	N(5.8)	Cl(43.8)	%
Found	C(10.1)	H(2.6)	N(5.8)	Cl(43.6)	%

(h) $SbCl_5 \cdot (NMe_2)Cl_2PS$. $(NMe_2)_2ClPS$ (1.39 g, 7.8 mmol) and $SbCl_5$ (0.9 ml, 7.0 mmol) when reacted as for $SbCl_5 \cdot (NMe_2)_3PS$ gave the product as a white solid. Yield 1.9 g (56.8%).

Analysis based on $C_2H_6NPSSbCl_7$

Calculated	C(5.0)	H(1.3)	N(2.9)	Cl(52.0)	%
Found	C(5.1)	H(1.5)	N(2.9)	Cl(51.2)	%

Bands were observed in the IR spectrum at:-

3005(w), 2955(s), 2936(sh), 2870(w), 1470(w), 1460(s), 1425(w)
1410(w), 1298(s,br), 1150(m), 1148(sh), 1049(m,br), 1007(s,br),
971(w), 784(s), 721(sh), 741(sh), 730(sh), 723(m), 665(m), 646(m),
610(s), 572(s,br), 479(m), 483(m) and 343(vs,br) cm^{-1} respectively.

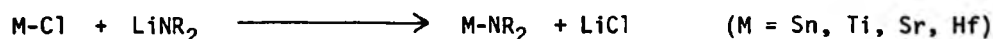
CHAPTER 4

COMPLEXATION AND EXCHANGE REACTIONS OF SOME
DIMETHYLAMINO SUBSTITUTED GROUP (IV) COMPOUNDS

CHAPTER 4

4.1 INTRODUCTION

The Group (IVA) amides and Group (IVB) amines exhibit a wide range of chemical behaviour due to the presence of a direct metal-nitrogen linkage. These compounds can be prepared either by aminolysis, or litho-aminolysis of the metal-halogen bond,



The products are usually liquids, or low melting point molecular solids, which can be conveniently purified by either distillation or sublimation in vacuo. The M-N bond is essentially covalent in character giving well defined M-N stretches in both IR and Raman spectra (247-250). Despite the high reactivity of these compounds it is not due to a weak M-N bond (e.g. $\bar{D}(\text{Ti-N})$ in $\text{Ti}(\text{NEt}_2)_4 = \sim 306 \text{ KJmol}^{-1}$) (251).

The chemistry of M-NR_2 species has attracted much interest, and review of $\text{M} = \text{Si}$ (252), Ge (253), Sn (253), Pb (253,254), Ti (255-257), Zr and Hf (256, 257) have appeared.

Nature of the M-N bond

A common feature for all of the M-NR_2 systems is the possibility of $\text{N}(\text{p}\pi) \rightarrow \text{M}(\text{d}\pi)$ bonding. The two extreme cases are presented in Fig. 4.1.1. The first of these (a) is typified by aliphatic amines where carbon, having no d-orbitals, is unable to engage in any $\text{N}(\text{p}\pi) \rightarrow \text{M}(\text{d}\pi)$ bonding.

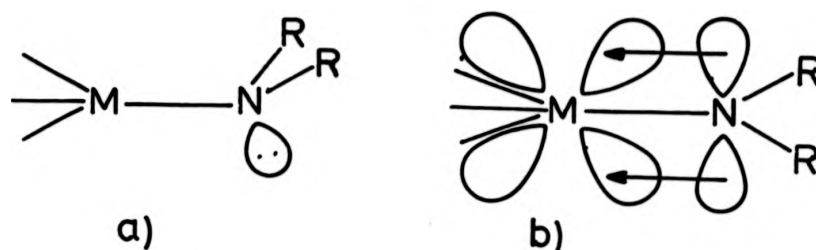
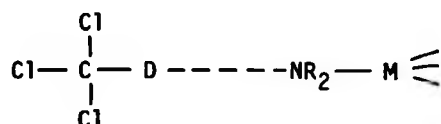


Fig. 4.1.1 Bonding Schemes for $M-NR_2$ Species

The carbon-nitrogen bond is, therefore, long in comparison and the nitrogen atom assumes a tetrahedral geometry with a formal lone pair. Systems of this type might be expected to be highly basic. In bonding scheme (b), the lone pair on the nitrogen atoms is partially delocalised into the $N(p\pi) \rightarrow M(d\pi)$ bond producing a reduction of the M-N bond length, and forcing the N atom into an sp_2 configuration. Loss of electron density from the nitrogen atom must seriously affect the basicity of the NR_2 group. The M-N bond length, the N atom configuration, and the basicity of the N atom can all, therefore, be employed as convenient probes in evaluating $N(p\pi) \rightarrow M(d\pi)$ bonding. X-ray data give a direct evaluation of the first two.

One of the simplest ways of obtaining a relative scale of Lewis basicity is to study the donor capacity towards a reference Lewis acid. The shift of the $\nu(C-H)$ band in the IR spectrum of $CHCl_3$ on H bonding to a Lewis base has been found to be suitable in this respect. In practice, $CDCl_3$ is used as the $\nu(C-D)$ band is in a 'clearer' area of the IR spectrum.



Some typical values are presented in Table 4.1.1 (258, 259).

Amine	$\Delta\nu(\text{C-D})$	Ratio Unshifted; Shifted Peak Area	Amine	$\Delta\nu(\text{C-D})$	Ratio
Me_3CNHET	89	1:100	$(\text{Me}_3\text{Si})_2\text{NH}$	30	1:1
Me_3CNMe_2	96	-	$(\text{Me}_3\text{Si})_2\text{NMe}$	39	2:1
Me_3SiNHET	52	1:10	$(\text{Me}_3\text{Si})_3\text{N}$	No observed shift	
$\text{Me}_3\text{SiNH}(\text{n-C}_4\text{H}_9)$	51	1:6	$\text{Me}_3\text{GeNMe}_2$	76	
$\text{Me}_3\text{SiNMe}_2$	62	1:12	$\text{Si}(\text{NMe}_2)_4$	10	-
$\text{Me}_3\text{SiNEt}_2$	64	1:8	$\text{Ge}(\text{NMe}_2)_4$	60	-
$\text{Me}_3\text{SiN}(\text{n-C}_4\text{H}_9)_2$	64	1:1			

Table 4.1.1 IR Shifts of the $\nu(\text{C-D})$ Band for some CDCl_3 Amine Mixtures

An examination of the data reveals the Si and Ge species to be much poorer bases than their C counterparts. For the aminosilanes in particular, a small increase in basicity is evident on substitution at the N atom. Addition of further SiMe_3 groupings, however, drastically reduces the N atom basicity. Thus whereas NMe_3 is a powerful donor, $\text{N}(\text{SiMe}_3)_3$ contains a trigonal planar N atom and shows no donor activity at all (252). The ratio of the peak area $\nu(\text{C-D})_{\text{unshifted}}:\nu(\text{C-D})_{\text{shifted}}$ gives an indication of the steric accessibility of the N lone pair for donation (258), and is roughly proportional to the bulk of the N atom substituents.

A similar but more quantitative picture is given by the heats of mixing with chloroform (260).

Amine	Heat of Mixing Jmol^{-1}	Amine	Heat of Mixing Jmol^{-1}
$\text{n-C}_4\text{H}_9\text{NH}_2$	2984	Me_3SiNHMe	1484
$(\text{n-C}_4\text{H}_9)_2\text{NH}$	3386	$\text{Me}_3\text{SiNMe}_2$	1500
$(\text{C}_2\text{H}_5)_2\text{NH}$	3620	Et_3SiNH_2	1137
$(\text{C}_2\text{H}_5)_3\text{N}$	3636	$(\text{Me}_3\text{Si})_2\text{NH}$	117

Table 4.1.2 Heats of Mixing for some CHCl_3 /Amine Systems

As with the IR data the relative order of basicity is found to be



and



Methods involving $CHCl_3$ or $CDCl_3$ as the reference Lewis acid suffer from the high reactivity of $CHCl_3$ towards many metal amides, making them unsuitable in most cases. As an alternative approach, Yoder and coworkers (259, 261) examined $N(p\pi) \rightarrow M(d\pi)$ bonding more directly by measuring the ^{13}C -H coupling constants for a number of Si, Ge and Sn dimethylamino substituted compounds (Table 4.1.3).

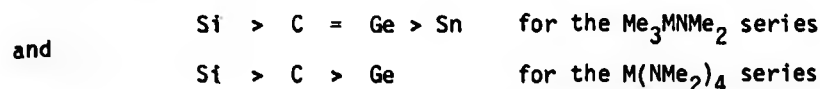
Compound	$J(^{13}C-H)$ (Hz)	Compound	$J(^{13}C-H)$ Hz
$C(NMe_2)_4$	133.4	Me_3GeNMe_2	131.4
$Si(NMe_2)_4$	135.0	Me_3SnNMe_2	130.2
$Ge(NMe_2)_4$	132.4	$Me_2Si(NMe_2)_2$	132.25
Me_3CNMe_2	131.4	$Me_2Si(NMe_2)Cl$	134.1
Me_3SiNMe_2	132.2	$Me_2Ge(NMe_2)Cl$	133.5

Table 4.1.3 ^{13}C -H Coupling Constants for Selected Amines (259,261)

An increase in the effective electronegativity of the N atom will increase the s-character of the C-H bond. As spin information is largely carried through s-orbitals the magnitude of the ^{13}C -H coupling constant should increase. The electronegativity of the N atom depends on the electronegativity of the Si, Ge or Sn atom substituent and the amount of $N(p\pi) \rightarrow M(d\pi)$ bonding present. The result is a small but measurable change in the ^{13}C -H coupling constant. In the absence of $N(p\pi) \rightarrow M(p\pi)$ bonding, the relative order should be based solely on electronegativity, i.e.



the observed order



indicates substantial $N(p\pi) - M(d\pi)$ bonding in the Si species, less in the Ge series and little or none at all in the Sn species. Also worthy of note is that $\text{Me}_2\text{SiCl}(\text{NMe}_2)$ is considerably less basic than $\text{Me}_2\text{Si}(\text{NMe}_2)_2$.

The data from these and other studies (262, 263) can to a certain extent be rationalised in terms of the diffuseness of the d orbitals, e.g. $N(p\pi) \rightarrow M(d\pi)$ overlap should be greatest in those elements possessing compact d-orbitals. Si-N should thus be more highly $N(p\pi) - M(d\pi)$ bonded than Ge-N or Sn-N, an argument which fits well with the experimental data. Even so, there is a substantial amount of $N(p\pi) - M(d\pi)$ bonding even in Sn-N systems, e.g. the planar (sp_2) NMe_2 groups in the structure of $\text{Sn}(\text{NMe}_2)_4$ (264).

Although there is little or no comparable basicity data for the early t-metal amides, structural data is often available. Several structures have been determined using single crystal techniques. The NR_2 groups in $\text{W}(\text{NMe}_2)_6$ (265), $\text{Nb}(\text{NMe}_2)_5$ (266), $\text{Mo}(\text{NMe}_2)_4$ (267), $\text{TiCl}_3\text{NET}_2$ (268) (Fig. 4.1.2) and $\text{Cr}(\text{N}(\text{i-C}_3\text{H}_7)_2)_3$ (269), all exhibit small or negligible deviations from a trigonal planar (sp_2) configuration associated with delocalisation of the N lone pair into the M-N bond.

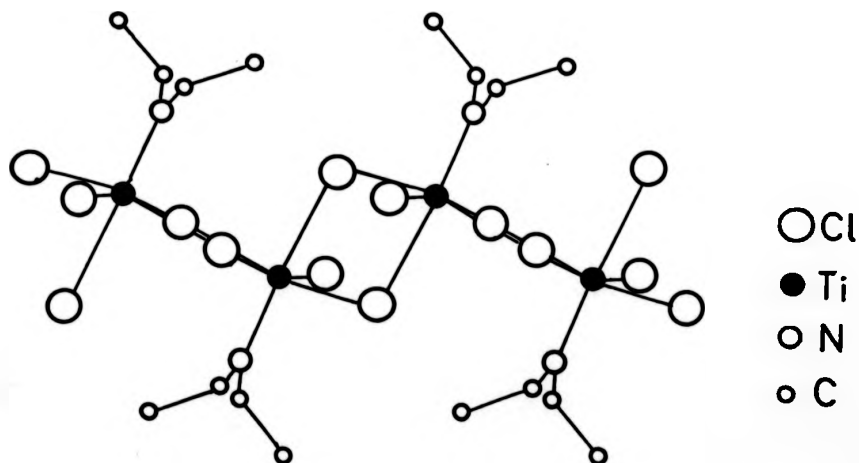
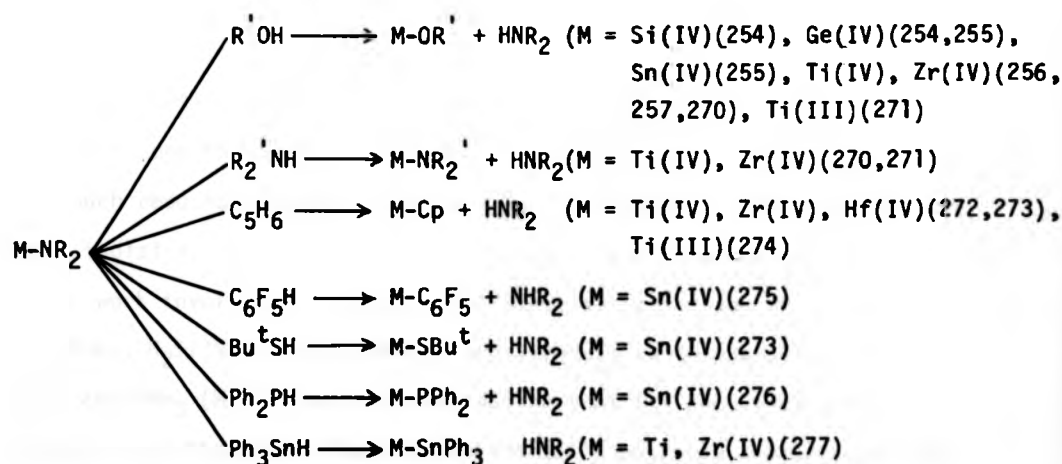


Fig. 4.1.2 Crystal Structure of $\text{TiCl}_3(\text{NEt}_2)$ (268)

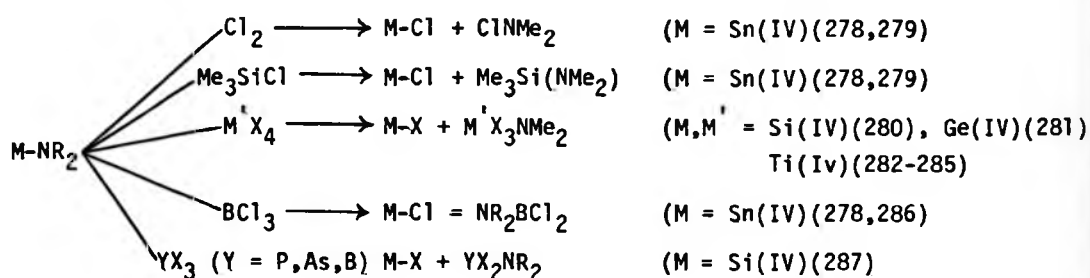
An estimation of the extent of $N(p\pi) - M(d\pi)$ bonding in the systems via changes in bond length is complicated in most cases by the lack of data on singly bonded species. For $(TiCl_3(NEt_2))_x$, however, a Ti-N bond length of 1.85 Å was found to be significantly shorter than 1.96 Å calculated for a hypothetical single Ti-N bond (268). Bridging via chlorine atoms rather than the NEt_2 groups is an additional indication of the low basicity of this system. The structure of $Cr(N(i-C_3H_7)_2)_3$ (269) also shows shortened M-N bonds (1.87 Å) compared to a Cr-N distance of 2.08 - 2.11 Å in $CrCl_3 \cdot dien$, for example. An interesting feature of the square based pyramidal $Nb(NMe_2)_5$ is the one short (axial, 1.977 Å) and four long (basal, 2.042 Å) Nb-N bonds (266). It was suggested that the longer Nb-N bonds may result from a delocalised π system involving the four basal N atoms and only two metal d-orbitals (266).

Reactions involving M-NR₂ bond cleavage (M = Si, Ge, Sn, Pb, Ti, Zr, Hf)

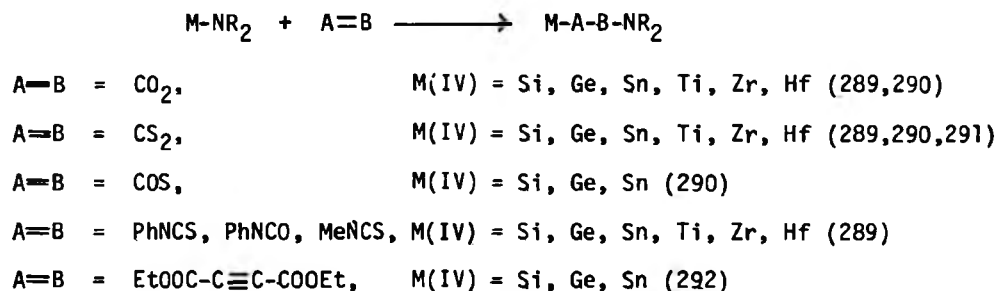
The metal-nitrogen bond in the Group (IVB) amines and (IVA) amides is particularly reactive and facile bond cleavage takes place with both protic reagents, and activated hydrocarbons, e.g.



Many exchange reactions involve the regeneration of the original M-X bond, e.g.



Group redistribution of this type is often known as 'scrambling' and has been reviewed for $\text{M} = \text{Si}, \text{Ge}, \text{Sn}$ and Pb (288). An extensive area of chemistry covers the insertion of small unsaturated dipolar molecules into the M-N bond, e.g.



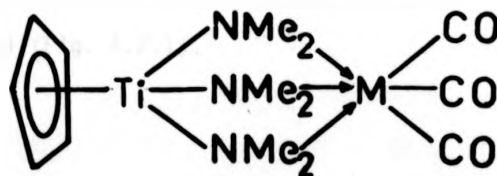
Insertion reactions up to 1967 have been reviewed by Lappert and Prokai (293).

Donor properties of M-NR_2 systems ($\text{M} = \text{Si, Ge, Sn, Ti, Zr, Hf}$)

Although the basicities of the Group (IVB) amines and Group (IVA) amides are much reduced compared to the alkylamines, several donor adducts have been isolated. The majority of this work concentrates on the aminosilanes. Early work involving the methylamino substituted silanes $(\text{H}_3\text{Si})_3\text{N}$, $(\text{H}_3\text{Si})_2\text{NMe}$, H_3SiNMe_2 , $\text{H}_2\text{Si(NMe}_2)_2$, $\text{HSi(NMe}_2)_3$ and $\text{Si(NMe}_2)_4$ with the soft Lewis acids B_2H_6 and MMe_3 ($\text{M} = \text{B, Al, Ga}$) provided several 1:1 complexes (294-296); in each case these were found to be thermally unstable and/or completely dissociated at room temperature. Methyl substitution of the Si atom appears to increase the thermal stability of such complexes, enabling

Ebsworth and Emeleus to isolate $\text{MeH}_2\text{SiNMe}_2 \cdot \text{BMe}_3$ and $\text{Me}_3\text{SiNMe}_2 \cdot \text{BMe}_3$ as white solids (297). Lappert and Srivastava have reported stable adducts between $\text{Me}_x\text{Si}(\text{NMe}_2)_{4-x}$ ($x = 1, 2$) and $(\text{Me}_3\text{Si})_2\text{NH}$ with the hard acids MCl_4 ($\text{M} = \text{Sn, Ti, Zr}$) and VOCl_3 although detailed information is lacking. The cyclosilazanes $(\text{Me}_2\text{SiNH})_x$ ($x = 3, 4$) provided a series of both 1:1 $(\text{Me}_2\text{SiNH})_3 \cdot \text{SnCl}_4$ (298), $(\text{Me}_2\text{SiNH})_3 \cdot \text{MCl}_3$ ($\text{M} = \text{Ti, V}$) (299) and 2:1 $((\text{Me}_2\text{SiNH})_3(\text{TiCl}_4)_2, (\text{Me}_2\text{SiNH})_4(\text{TiCl}_4)_2, (\text{Me}_2\text{SiNH})_4 \cdot \text{MCl}_3 \cdot \text{L}_2$ ($\text{M} = \text{Ti, V}$, $\text{L} = \text{THF}$, $\text{M} = \text{Cr}$, $\text{L} = \text{NMe}_3$) (300) complexes. These adducts are further discussed in Chapter 5.

The donor properties of the metal amides are not well established. Molecular weight measurements and low temperature ^1H NMR spectra have confirmed the dimeric nature of $\text{M}(\text{NR}_2)_4$ ($\text{M} = \text{Zr, Hf}$) in solution at low temperatures (301). Internuclear bridging via the NMe_2 groups was here proposed. 1:1 complexes between $\text{M}(\text{NMe}_2)_4$ ($\text{M} = \text{Sn, Ti}$) and SnCl_4 have been reported (298), but again no details have been published. Reaction of $\text{Sn}(\text{NR}_2)_2$ with an excess of BF_3 in C_6H_6 solution has recently led to the isolation of the 3:1 complexes $\text{Sn}(\text{NR}_2)_2 \cdot 3\text{BF}_3$ ($\text{R} = \text{Me, Et}$) (302). The proposed structures for these complexes includes a BF_3 molecule coordinated to each NR_2 group and to the Sn (II) atom via the Sn (II) lone pair. Perhaps the best characterised metal amide complexes are the $\text{CpTi}(\text{NMe}_2)_3 \cdot \text{M}(\text{CO})_3$ ($\text{M} = \text{Cr, Mo, W}$) adducts prepared by Bradley and Kasenally via photolysis of a mixture of $\text{CpTi}(\text{NMe}_2)_3$ and the appropriate metal hexacarbonyl in cyclohexane solution (303). A monomeric structure of the type



was proposed based on the IR spectra. The ^1H NMR spectra, however, showed different magnetic environments for the NMe_2 groups.

4.2 Complexes of $(\text{Me}_2\text{N})_2\text{CH}_2$ with MCl_4 ($\text{M} = \text{Ti}, \text{Sn}$), VCl_3 and $\text{CrCl}_3 \cdot 2\text{NMe}_3$

Dropwise addition of $(\text{Me}_2\text{N})_2\text{CH}_2$ (bis(dimethylamino)methane) to equimolar amounts of either TiCl_4 or SnCl_4 in C_6H_6 solution gave precipitates of the bright yellow ($\text{M} = \text{Ti}$) or white ($\text{M} = \text{Sn}$) 1:1 adducts in almost quantitative yield. A repeat experiment with a two-fold excess of ligand gave an identical product when SnCl_4 was used. Both 1:1 adducts were extremely susceptible to hydrolysis, as evidenced by the analytical data, which in the hands of a professional analyst repeatedly gave low values for halogen %. Solubility was limited generally to coordinating solvents.

The IR spectra of the complexes show several interesting features. Bands at 1058 and 868 cm^{-1} in the free ligand assigned as νNC_2 (asymmetric) and νNC_2 (symmetric) modes (148), appear to lower energies in the adducts ($1041, 991, 952\text{ cm}^{-1}$ (νNC_2 (asymmetric)), $860, 813\text{ cm}^{-1}$ (νNC_2 (symmetric))), $\text{M} = \text{Ti}$; $1045, 1002, 948\text{ cm}^{-1}$ (νNC_2 (asymmetric)), $862, 830\text{ cm}^{-1}$ (νNC_2 (symmetric))), $\text{M} = \text{Sn}$), suggesting both NMe_2 groups to be coordinated. The distinctive 1383 cm^{-1} CH_2 deformational mode in $(\text{Me}_2\text{N})_2\text{CH}_2$ (148) is absent from the spectra of the complexes, apparently masked by strong $\delta(\text{CH}_3)$ bands in the $1500\text{--}1450\text{ cm}^{-1}$ region. Such a shift is in line with the formation of a four-membered aliphatic ring which is produced on chelation (148). In the low IR strong metal-chlorine vibrations at $397, 379, 356$ and 332 cm^{-1} ($\text{M} = \text{Ti}$), and $337, 319\text{ cm}^{-1}$ ($\text{M} = \text{Sn}$) support a cis chelated model (Fig. 4.2.1).

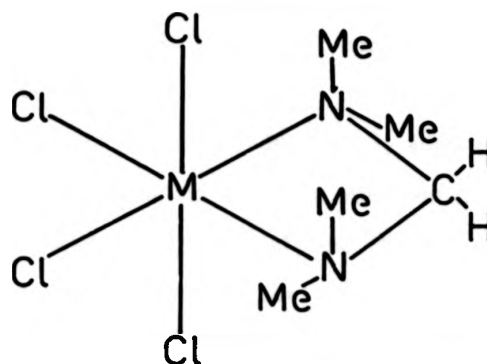


Fig. 4.2.1 Proposed Structure of $\text{MCl}_4 \cdot (\text{Me}_2\text{N})_2\text{CH}_2$ ($\text{M} = \text{Ti}, \text{Sn}$)

A ^1H NMR spectrum of $\text{SnCl}_4 \cdot (\text{Me}_2\text{N})_2\text{CH}_2$ recorded in CDCl_3 solution (220 MHz) at maximum sensitivity showed a single NMe_2 resonance at $\delta 2.80$ ($\delta 2.10$ in free ligand) due to equivalent coordinated NMe_2 groups. The CH_2 resonance, which should be only one-sixth of the intensity of the NMe_2 resonance, could not be resolved from the background noise.

The $\text{TiCl}_4/(\text{Me}_2\text{N})_2\text{CH}_2$ system has already attracted some attention (304). Rather surprisingly, under similar conditions to those employed above, a series of dark yellow to green adducts of varying composition were obtained. In many respects $\text{CH}_2(\text{NMe}_2)_2$ resembles NMe_3 , a molecule whose reducing properties towards Ti (IV) have been firmly established (65, 67). One possibility is that reduction $\text{Ti}(\text{IV}) \rightarrow \text{Ti}(\text{III})$ occurred in these earlier compounds, giving rise to the unusual observed properties and stoichiometries.

Turning to the +3 state, VCl_3 gave an insoluble chocolate brown solid of approximate composition $\text{VCl}_3 \cdot 0.5(\text{Me}_2\text{N})_2\text{CH}_2$. Kiesel and Schram have isolated the 1:1 adduct $\text{VCl}_3 \cdot (\text{Me}_2\text{N})_2\text{CH}_2$ indirectly from the reduction of VCl_4 with $\text{B}_2(\text{NMe}_2)_4$ (148), the complex being interpreted in terms of a monomeric 5 coordinate metal, with the ligand active in a bidentate capacity.

The situation with $\text{VCl}_3 \cdot 0.5(\text{Me}_2\text{N})_2\text{CH}_2$ appears to be more complicated, with IR bands associated with the presence of both bidentate (1040, 1024, 998, 974, 963 cm^{-1}) and unidentate (1368, 1063, 1045 cm^{-1}) ligand. $(\text{Me}_2\text{N})_2\text{CH}_2$ has previously been found to act as a monodentate, and bridging bidentate ligand in $\text{Me}_3\text{M} \cdot (\text{Me}_2\text{N})_2\text{CH}_2$ ($\text{M} = \text{B}, \text{Al}$) and $(\text{Me}_3\text{Al})_2 \cdot (\text{Me}_2\text{N})_2\text{CH}_2$, respectively (305). As a possible structure for $\text{VCl}_3 \cdot 0.5(\text{Me}_2\text{N})_2\text{CH}_2$, a polymeric model with the ligand randomly coordinated to the VCl_3 lattice and the remainder of the V coordination sphere taken up by bridging Cl atoms seems the most appropriate. The pattern of V-Cl bands at 387, 350, 315 and 277 cm^{-1} shows a distinct resemblance to that of the recently isolated chocolate brown $\text{VCl}_3 \cdot \text{NMe}_3$ (145) (νVCl at 386, 358, 317 and 286 cm^{-1}), and the adducts may, therefore, have similar structures. Total displacement of ligand is achieved by dissolving $\text{VCl}_3 \cdot 0.5(\text{Me}_2\text{N})_2\text{CH}_2$ in pyridine to give mauve $\text{VCl}_3 \cdot 3\text{py}$.

Attempts to prepare $(\text{Me}_2\text{N})_2\text{CH}_2$ complexes via ligand exchange reactions gave only intractable oils with $\text{VCl}_3 \cdot 3\text{THF}$, $\text{VCl}_3 \cdot 3\text{MeCN}$ and $\text{CrCl}_3 \cdot 3\text{MeCN}$. With $\text{CrCl}_3 \cdot 2\text{NMe}_3$ in C_6H_6 solution, partial ligand exchange occurred to give the mixed adduct $\text{CrCl}_3 \cdot \text{NMe}_3 \cdot (\text{Me}_2\text{N})_2\text{CH}_2$. Although the IR spectrum showed bands attributable to both coordinated NMe_3 and $(\text{Me}_2\text{N})_2\text{CH}_2$, vibrations diagnostic of the denticity of the latter were, in each case, masked by strong NMe_3 bands, making detailed structural assignments impossible.

4.3 Reaction of bis(diphenylphosphino)methane (dpm) with TiCl_4

Addition of a solution of TiCl_4 in benzene to an equimolar amount of bis(diphenylphosphino)methane (dpm) in benzene gave $\text{TiCl}_4 \cdot \text{dpm}$ as a bright orange solid. The complex proved to be highly air sensitive, decomposing in moist air in less than a minute. $\text{TiCl}_4 \cdot \text{dpm}$ was soluble in a range of

polar solvents such as MeCN, THF, MeNO₂ and CH₂Cl₂, but was generally insoluble in nonpolar solvents. Solution in pyridine and DMSO was accompanied by an immediate colour change (orange to pale yellow) indicating solvolysis had taken place. In the case of DMSO, this was confirmed by the ¹H NMR spectrum of TiCl₄.dpm in DMSO which only showed resonances due to uncomplexed dpm.

The IR spectra of TiCl₄.dpm in the 4000 to 400 cm⁻¹ showed a close similarity with that of the free ligand, most bands differing by only a few wavenumbers, between the free and bound ligand. This suggests that the ligand has approximately the same symmetry in the free and bound states. A single band at 1434 cm⁻¹ in dpm, assigned as a ν(P-Ph) (306) mode also appears as a singlet in the complex (1434 cm⁻¹). As monodentate behaviour on the part of dpm would result in different P environments, and splitting of the ν(P-Ph) bands, this result was interpreted in terms of bidentate coordination. In the low IR spectrum bands attributable to ν(Ti-Cl) stretching modes at 388, 380, 345 and 320 cm⁻¹ are in accordance with an octahedral cis (C_{2v}) geometry, and thus chelated dpm (Fig. 4.3.1).

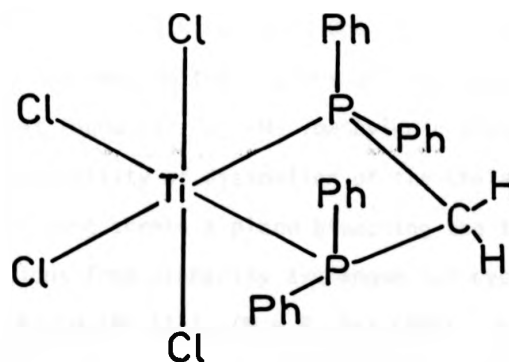


Fig. 4.3.1 Proposed Structure of TiCl₄.dpm

Bands at 469 and 416 cm^{-1} are provisionally assigned as $\nu(\text{Ti-P})$ modes cf. 453, 414 cm^{-1} for $\text{TiCl}_4 \cdot (\text{Ph}_2\text{P})\text{C}_2\text{H}_4$ (307).

The ^1H NMR spectra (220 MHz, CD_3NO_2) of dpm and $\text{TiCl}_4 \cdot \text{dpm}$ are shown in Fig 4.3.2. Considering first the uncoordinated ligand, complex multiple resonances in the aromatic region centred on $\delta 7.41$ (meta) and $\delta 7.21$ (ortho and para) correspond to the P-Ph protons. For the methylenic protons, values as both the chemical shift ($\delta 2.85$) and P-H coupling constant ($^2J(\text{P-H})$ 2.0Hz) agree well with published data (308).

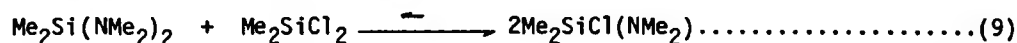
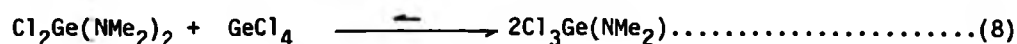
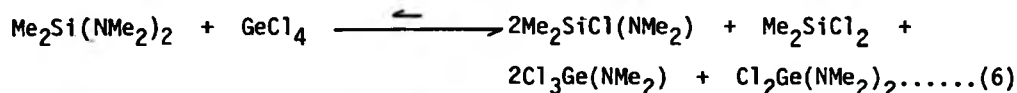
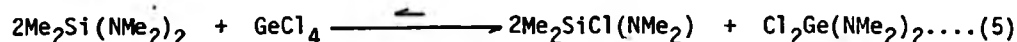
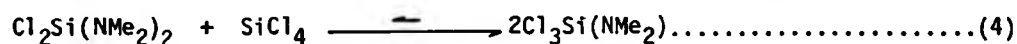
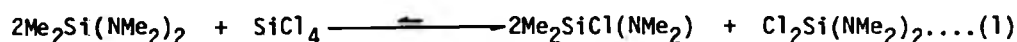
On complexation the methylene resonance moves appreciably downfield to $\delta 3.73$ due to the strain caused by the formation of a four-membered chelate ring. The value of the P-H coupling constant increases in the adduct to 6.6 Hz. There are two possible contributions. Firstly, the loss of electron density from the P atom that occurs on coordination should increase the amount of s character in the P-C bond, and thus increase $^2J(\text{P-H})$. Secondly, complexation eliminates rotation about the P- CH_2 bond, which again maximises $^2J(\text{P-H})$. The phenyl resonances for $\text{TiCl}_4 \cdot \text{dpm}$ are markedly different from that of the free ligand, with a single complex multiplet in the $\delta 3.2 - 3.6$ region. One factor instrumental in this change is probably an increase in the various $J(\text{P-Ph})$ coupling constants, paralleling that found for $^2J(\text{P-H})$ (methylenic protons). In addition, there is the possibility of distortion of the chelate ring, i.e. 'folding' of the Ti-P-P-C ring across a plane bisecting the two P atoms (Fig. 4.3.2). Similar deviations from planarity are known for cyclobutane and $(\text{CO})_2\text{Cl}_2(\text{Ph}_2\text{M})_2\text{CH}_2\text{Mo}$ (II), ($\text{M} = \text{P}, \text{As}$) (309). Assuming a structure of this type, the phenyl groups become magnetically inequivalent, and thus give rise to slightly different ^1H resonances.

Reaction of TiCl_4 with two mol equivalents of dpm did not result in the

formation of an 8 coordinate complex. Where coordination number 8 has been established, Clark and Chatt have examined the factors that tend to produce 8 coordination (Section 1.3), and have determined that while the choice of donor atom is not critical (i.e. As or P), the choice of donor atom substituents is. The bulk, and electron withdrawing properties of the phenyl group substituents in dpm make the ligand less likely to give 8 coordinate complexes.

4.4.1 Exchange reactions between $\text{Me}_2\text{Si}(\text{NMe}_2)_2$ and MCl_4 ($\text{M} = \text{Si}, \text{Ge}$)

Mixing of $\text{Me}_2\text{Si}(\text{NMe}_2)_2$ and MCl_4 ($\text{M} = \text{Si}, \text{Ge}$) in various mol ratios, either as C_6D_6 solutions or as neat liquids, gave rise to reactions 1-3 and 5-7. Exchange between $\text{Cl}_2\text{M}(\text{NMe}_2)_2$ and MCl_4 ($\text{M} = \text{Si}, \text{Ge}$) was also studied in C_6D_6 solution (equations 4 and 8).



The products in each case remained unchanged after thermostating the solutions at 313 K for 24 hours. Common features to all of these reactions were fuming and evolution of considerable heat, to eventually give a clear colourless liquid. Products were identified by ^1H NMR (2% solutions in C_6D_6 , re. TMS). Sharp, well resolved resonances were observed in all cases.

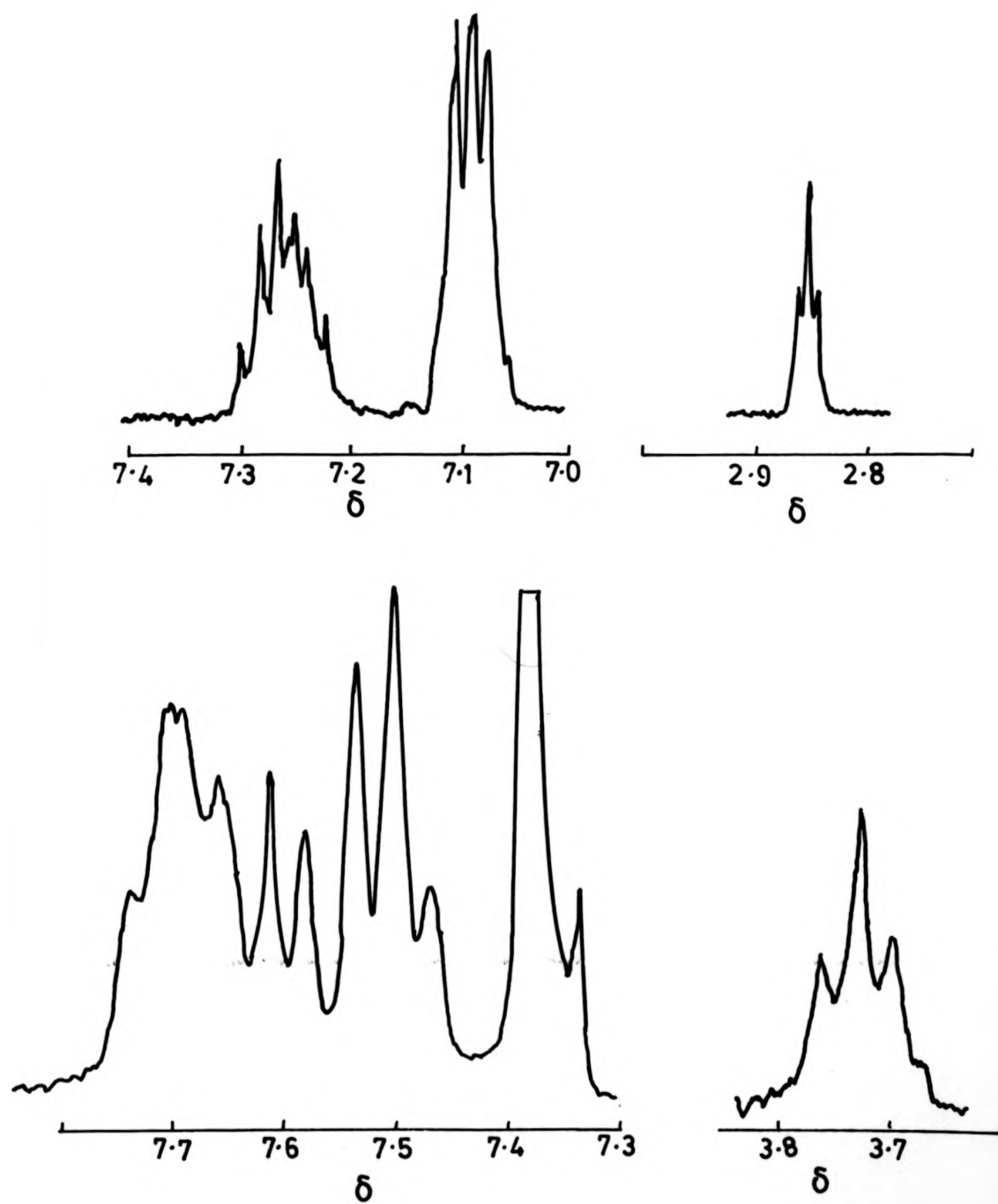


Fig. 4.3.2 ^1H NMR Spectra (CD_3NO_2 , 220 Mhz) of dpm and $\text{TiCl}_4\cdot\text{dpm}$

There was no evidence for line broadening as found in some germanium systems (281). In general, for most of the silanes and germanes studied, considerable differences were found between the value of the chemical shift in C_6D_6 , and literature values for chlorocarbons (310, 311), or neat liquids (312). Table 4.4.1 contains 1H chemical shift data for the various silanes and germanes studied, synthesised by routes independent of equations 1 to 8.

Compound	$\delta(N-Me)$	$\delta(Si-Me)$
$Me_2Si(NMe_2)_2$	2.48	0.1
$Me_2SiCl(NMe_2)$	2.35	0.33
Me_2SiCl_2	-	0.40
$Cl_3Ge(NMe_2)$	2.18	-
$Cl_2Si(NMe_2)_2$	2.42	-
$Cl_3Ge(NMe_2)$	2.23	-
$Cl_2Ge(NMe_2)_2$	2.42	-

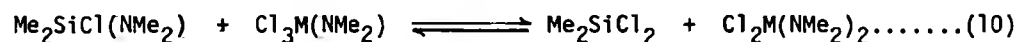
Table 4.4.1 220 MHz 1H NMR Chemical Shift Data for Various Silanes, Aminosilanes and Aminogermanes (2%, C_6D_6)

N.B. Since scrambling reactions involving rupture of the Si-C bond are known, the reactivity of the Si-Me bond in $Me_2Si(NMe_2)_2$ and of TMS itself falls into question. As these scrambling reactions involve either high temperatures (313, 314), or the use of a suitable Lewis acid catalyst (such as $AlCl_3$) (315), the Si-Me linkages under the mild reaction conditions used in the present study, can be considered inert, and TMS therefore, remains a valid NMR standard.

Substituent exchanges on silicon have been studied widely (280, 316). Møedritzer and Van Wazer have found that the extent of the back reaction varies considerably with different substituents on the central silicon atom.

In the $\text{Si}(\text{OMe})_4/\text{Si}(\text{OEt})_4$ system (312), once equilibrium had been attained, the proportions of the various mixed products $\text{Si}(\text{OMe})_n(\text{OEt})_{4-n}$, $n = 0-4$ could be explained by a simple random exchange approach. For the Cl/NMe_2 exchange systems (312, 316), the back reaction accounts for only a few percent of the total Si content at any given ratio of reactants. The systems studied in reactions 1-9 show no observable back reaction at all, suggesting that a large enthalpy of reaction, forces the equilibrium totally towards products. The discontinuities in dielectric constant vs. mol ratio curves observed for these systems by Scharschmidt (317), supports this argument.

An interesting aspect of equilibria 2 and 6 is that while a 1:1 mixture of SiCl_4 and $\text{Me}_2\text{Si}(\text{NMe}_2)_2$ results in total exchange of NMe_2 groups (equilibrium 2), GeCl_4 and $\text{Me}_2\text{Si}(\text{NMe}_2)_2$ in the same proportions (equilibrium 6) give a mixture of products arising from the 1:2 (equilibrium 5) and 2:1 (equilibrium 7) reactions. A consideration of the reaction

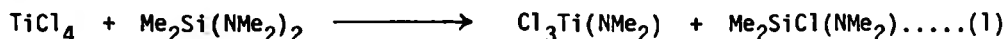


provides a possible explanation. Since $\text{Me}_2\text{SiCl}(\text{NMe}_2)$ and $\text{Cl}_3\text{Ge}(\text{NMe}_2)$ have been identified as components of the $\text{Me}_2\text{Si}(\text{NMe}_2)_2/\text{GeCl}_4$ equilibrium, (6), it is not unreasonable to assume that the analogous silanes ($\text{Me}_2\text{SiCl}(\text{NMe}_2)$ and $\text{Cl}_3\text{Si}(\text{NMe}_2)$) are intermediates in the reaction between $\text{Me}_2\text{Si}(\text{NMe}_2)_2$ and SiCl_4 (equilibrium 1). Should equilibrium 10 lie to the right hand for ($\text{M} = \text{Si}$) and to the left hand for ($\text{M} = \text{Ge}$) respectively, a good fit would be obtained with the observed data. To test this hypothesis the $\text{Me}_2\text{SiCl}(\text{NMe}_2)/\text{Cl}_3\text{M}(\text{NMe}_2)$ ($\text{M} = \text{Si}, \text{Ge}$) equilibria were investigated. Somewhat surprisingly for both $\text{M} = \text{Si}$ and $\text{M} = \text{Ge}$, Me_2SiCl_2 and $\text{Cl}_2\text{M}(\text{NMe}_2)_2$ ($\text{M} = \text{Si}, \text{Ge}$) were the sole observable products, i.e. equilibrium 10 lies well to the R.H.S. for both $\text{M} = \text{Si}$ and $\text{M} = \text{Ge}$. The fact that $\text{Me}_2\text{SiCl}(\text{NMe}_2)$

and $\text{Cl}_3\text{Ge}(\text{NMe}_2)$ react in isolation, but not within the context of equilibrium 6 suggests the $\text{Me}_2\text{Si}(\text{NMe}_2)_2/\text{GeCl}_4$ system is far more complex than that indicated by the simple stoichiometry of reaction 6.

4.4.2 Exchange reactions between $\text{Me}_2\text{Si}(\text{NMe}_2)_2$ and TiCl_4

TiCl_4 reacted in C_6H_6 with an equimolar amount of $\text{Me}_2\text{Si}(\text{NMe}_2)_2$ to initially give a pale yellow precipitate of $\text{TiCl}_4 \cdot \text{Me}_2\text{Si}(\text{NMe}_2)_2$ (Section 4.5). On standing at 323 K for a few hours the yellow solid rapidly turned green, and subsequent work up yielded $\text{Cl}_3\text{Ti}(\text{NMe}_2)$ as dark green crystals, which were identified by their IR spectrum (318). The solvent on distillation (380K/760 mm) gave a colourless, fuming liquid which was identified from its ^1H NMR spectrum to be $\text{Me}_2\text{SiCl}(\text{NMe}_2)$ (Table 4.4.1), i.e.



Reaction also occurred in the solid phase. Solid samples of yellow $\text{TiCl}_4 \cdot \text{Me}_2\text{Si}(\text{NMe}_2)_2$ stored in glass ampoules under a nitrogen atmosphere decomposed over a period of several weeks to give identical products. Pyrolysis of $\text{TiCl}_4 \cdot \text{Me}_2\text{Si}(\text{NMe}_2)_2$ at 423 K in high vacuum gave a small amount of $\text{Cl}_3\text{Ti}(\text{NMe}_2)$ as the only isolable product. This type of halogen/amide exchange has been observed for TiX_4 with a number of metal and metalloid amides, including B (318), Si (319, 283, 225) and Ti (282).

With a two-fold excess of $\text{Me}_2\text{Si}(\text{NMe}_2)_2$, $\text{Me}_2\text{SiCl}(\text{NMe}_2)$ was again isolated as the sole silane product. Isolation of the Ti containing product gave a chocolate brown solid, approximating to $\text{Cl}_2\text{Ti}(\text{NMe}_2)_2$ on the basis of a halogen analysis. The ^1H NMR spectrum showed a complicated NMe_2 region including a very intense broad resonance at $\delta 3.5$ which is possibly due to paramagnetic Ti (III) species. Quite possibly, this is the same non-stoichiometric product found by Bürger *et al* (319) as a product of the

reaction of TiCl_4 and $\text{Me}_3\text{Si}(\text{NMe}_2)$. $\text{Cl}_2\text{Ti}(\text{NMe}_2)_2$ has successfully been isolated as brown crystals by disproportionation of TiCl_4 and $\text{Ti}(\text{NMe}_2)_4$. In both the $\text{TiCl}_4/\text{Me}_2\text{Si}(\text{NMe}_2)_2$ and $\text{TiCl}_4/2\text{Me}_2\text{Si}(\text{NMe}_2)_2$ systems, $\text{Me}_2\text{SiCl}(\text{NMe}_2)$ fails to react further with the Ti containing product, and this may be a reflection of the reduced basicity of $\text{Me}_2\text{SiCl}(\text{NMe}_2)$ with respect to $\text{Me}_2\text{Si}(\text{NMe}_2)_2$.

4.4.3 Mechanism of Si-N bond cleavage

Considerable interest has been shown in the mechanism of Si-N/M-Cl exchange (280, 288, 320). Proposed mechanisms fall into two categories, the four-centre type mechanism (Fig. 4.4.1a) and the termolecular approach of Sommer *et al* (320) (Fig. 4.4.1b). A common feature of all these mechanisms involves nitrogen coordination to the appropriate Lewis acid, and a similar first step is put forward here for two reasons. Firstly, the use of non-polar solvents argues strongly against any free ions, making a bimolecular intermediate essential. Secondly, on coordination it is not unreasonable to assume that, to a certain extent, electron density will flow out of the $\text{N}(\text{p}\pi) - \text{Si}(\text{d}\pi)$ bond reducing the Si-N bond order and therefore, facilitating Si-N bond cleavage. Evidence for such a phenomenon is found in the IR spectra of the $\text{Me}_2\text{Si}(\text{NMe}_2)_2.\text{MX}_4$ adducts described in Section 4.5. The isolation of the intermediate $\text{TiCl}_4.\text{Me}_2\text{Si}(\text{NMe}_2)_2$ adduct from the $\text{TiCl}_4/\text{Me}_2\text{Si}(\text{NMe}_2)_2$ exchange system argues strongly for an intermediate complex.

Exchange in a four-centre mechanism (Fig. 4.4.1a) is simply by simultaneous cleavage of the Si-N and Ti-Cl bonds in the intermediate, followed by expulsion of $\text{Me}_2\text{SiCl}(\text{NMe}_2)$, which has been rendered a weaker donor due to inductive effects from the Cl atom. In the case of $\text{Me}_2\text{Si}(\text{NMe}_2)_2$ another intermediate is possible (Fig. 4.4.2). Here it can

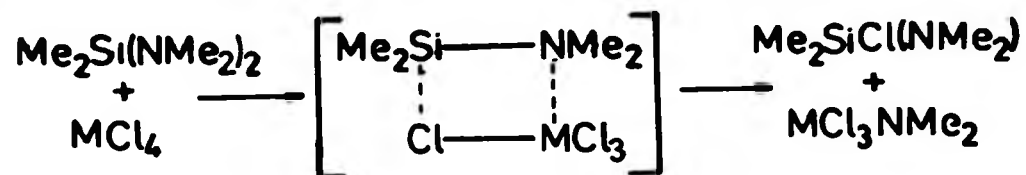


Fig. 4.4.1a '4-Centre Mechanism

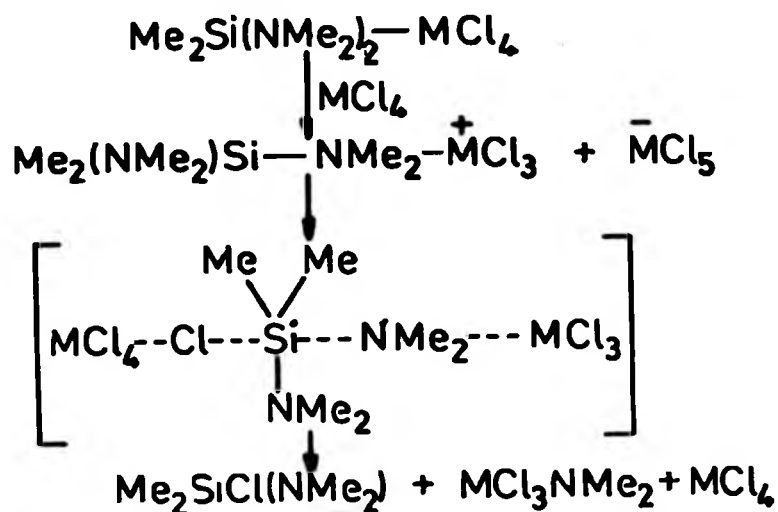


Fig. 4.4.1b 'Sommer'-Type Mechanism

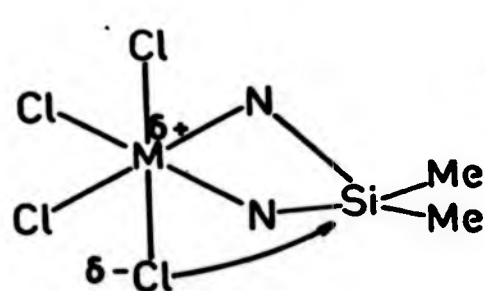


Fig. 4.4.2 6 Coordinate Intermediate

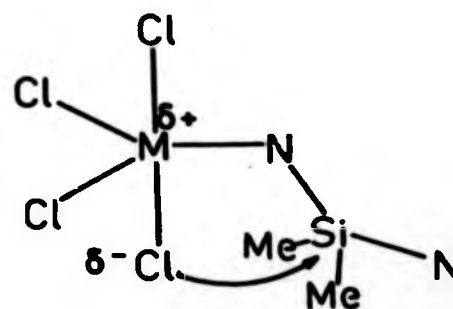
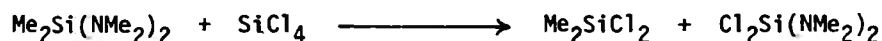


Fig. 4.4.2 5 Coordinate Intermediate

be postulated that distortion in the MN_2Si plane (as found for $SnCl_4 \cdot Me_2Si(NMe_2)$ (Section 4.5)) force the Me_2Si moiety closer to one of the axial Cl atoms than would be expected for a planar system, increasing the probability of exchange. An approach of this type explains that



is multi-step, as only one Cl atom is available for exchange at any one time.

Sommer et al (320) have shown, with a series of chiral aminosilanes, that inversion about the silicon atom occurred in greater than 50% yield for nine out of the ten aminosilane/metal halide exchange reactions studied. As a four-centre reaction pathway with an intermediate such as (Fig. 4.4.2) would produce a silyl halide with retention of the original stereochemistry, an alternative pathway is needed. By adopting a 5 coordinate intermediate (Fig. 4.4.3) produced by cleavage of a metal nitrogen coordinate bond, the simple four-centre mechanism need not be abandoned. Although 5 coordination for Ti (IV) is rare, it is common for both Si (IV) and Ge (IV) (113). In such an intermediate, the reduction of bond order in the Si-N bond adjacent to the metal atom, enables free rotation to occur, giving greater exposure of the rear face of the Si atom, and thus inversion on Cl attack.

The alternative mechanism of Sommer (320) is immediately less attractive for MCl_4 ($M = Ti, Si, Ge$) than for BX_3 (the Lewis acid for which the route was originally proposed), because of the use of a second MX_4 molecule. Whereas this is quite reasonable for $SiCl_4$ and $GeCl_4$, it is almost impossible for the solid phase decomposition of $TiCl_4 \cdot Me_2Si(NMe_2)_2$. Additionally, although BX_4^- is well characterised, MX_5^- ($M = Ti, Ge, Si$) species are not, and therefore, this mechanism must be considered as a minor,

or impossible pathway for the MCl_4 species.

4.5 Complexes of $\text{Me}_2\text{Si}(\text{NMe}_2)_2$ with MX_4 ($\text{M} = \text{Ti, Zr, Hf, X} = \text{Cl, M} = \text{Sn, X} = \text{Cl, Br}$)

Dropwise addition of solutions of $\text{Me}_2\text{Si}(\text{NMe}_2)_2$ to an equimolar quantity of MX_4 in benzene ($\text{M} = \text{Zr, Hf, X} = \text{Cl, M} = \text{Sn, X} = \text{Cl, Br}$) solution or suspension gave immediate white precipitates of $\text{MX}_4 \cdot \text{Me}_2\text{Si}(\text{NMe}_2)_2$ ($\text{M} = \text{Zr, Hf, X} = \text{Cl, M} = \text{Sn, X} = \text{Cl, Br}$). The precipitates were washed with C_6H_6 and dried in vacuo. Reaction between equimolar quantities of TiCl_4 and $\text{Me}_2\text{Si}(\text{NMe}_2)_2$ in C_6H_6 gave a pale yellow precipitate which rapidly decomposed to $\text{Cl}_3\text{Ti}(\text{NMe}_2)$ and $\text{Me}_2\text{SiCl}(\text{NMe}_2)$ (Section 4.4). However, by simply changing the reaction medium to the less polar n-hexane, a pale yellow precipitate of $\text{TiCl}_4 \cdot \text{Me}_2\text{Si}(\text{NMe}_2)_2$ and a pale brown solution were obtained. Concentration of the pale brown solution followed, and sublimation of the green solid, thus produced, gave a small amount ($\sim 1\%$) of $\text{Cl}_3\text{Ti}(\text{NMe}_2)$. All attempts to isolate $\text{TiCl}_4 \cdot \text{Me}_2\text{Si}(\text{NMe}_2)_2$ from C_6H_6 solution resulted in the desired product being contaminated with $\text{Cl}_3\text{Ti}(\text{NMe}_2)$. A series of repeat experiments using a two-fold excess of ligand gave identical products to those above, in all cases.

Attempts to obtain adducts with tervalent metals proved less successful. $\text{Me}_2\text{Si}(\text{NMe}_2)_2$ readily displaced MeCN from $\text{VCl}_3 \cdot 3\text{MeCN}$, but samples of the dark mauve solid produced were found to contain varying amounts of MeCN. Using a three-fold excess of ligand a dark brown solid was produced, which again was found to be non-stoichiometric. Towards $\text{CrCl}_3 \cdot 2\text{NMe}_3$, $\text{Me}_2\text{Si}(\text{NMe}_2)_2$ proved an insufficiently strong Lewis base to displace coordinated trimethylamine and $\text{Cr}_2\text{Cl}_6(\text{NMe}_3)_3$ (produced from the decomposition of $\text{CrCl}_3 \cdot 2\text{NMe}_3$ (142)) was the only isolated product.

All the $\text{MCl}_4 \cdot (\text{Me}_2\text{Si}(\text{NMe}_2))_2$ adducts were air sensitive, decomposing instantly in water to give the appropriate metal oxide. A general insolubility in common solvents was observed, the one exception being the SnCl_4 adduct, which was slightly soluble in C_6H_6 , CHCl_3 and CH_2Cl_2 (recrystallisation in low yields from hot CH_2Cl_2 was possible). Evidence for ligand displacement by MeCN (but not by pyridine or DMSO) was found in the ^1H NMR spectra, although no pure products could be isolated. $\text{TiCl}_4 \cdot \text{Me}_2\text{Si}(\text{NMe}_2)_2$ decomposed in all common solvents (Section 4.4), except CCl_4 and n-hexane in which it was insoluble. Thermal stability of the adducts varied considerably. $\text{SnCl}_4 \cdot \text{Me}_2\text{Si}(\text{NMe}_2)_2$ sublimed at 403 - 413 K in vacuo without change, whereas $\text{ZrCl}_4 \cdot (\text{Me}_2\text{Si}(\text{NMe}_2))_2$ and $\text{HfCl}_4 \cdot (\text{Me}_2\text{Si}(\text{NMe}_2))_2$ decomposed at 423 and 428 K respectively. $\text{TiCl}_4 \cdot \text{Me}_2\text{Si}(\text{NMe}_2)$ decomposed at 423 K to give a sublimate of dark green $\text{Cl}_3\text{Ti}(\text{NMe}_2)$ in low yield (Section 4.4).

The low IR spectra of the adducts showed strong metal halide bands at 340, 328, 320 and 260 cm^{-1} (Sn-Cl), 417, 405, 365 and 322 cm^{-1} (Ti-Cl), 344 and 311 cm^{-1} (Zr-Cl) and 342, 313 cm^{-1} (Hf-Cl), associated with an octahedral cis (C_{2v}) geometry (149). A strong band at 214 cm^{-1} in the spectrum of $\text{SnBr}_4 \cdot \text{Me}_2\text{Si}(\text{NMe}_2)_2$ is assigned as an Sn-Br stretching mode. A C_{2v} geometry immediately suggests that the ligand is chelated (i.e. bidentate) (Fig. 4.5.1).

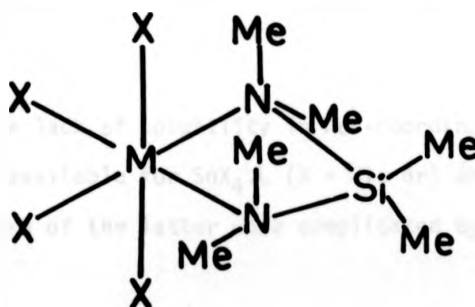


Fig. 4.5.1 Proposed Structure of $\text{MX}_4 \cdot \text{Me}_2\text{Si}(\text{NMe}_2)_2$

Alternatively, a binuclear complex of the type $\text{MCl}_4 \cdot (\text{NMe}_2)\text{SiMe}_2(\text{NMe}_2)_2\text{MCl}_4$ where the ligand is active in a bridging mode, is possible, but here adduct formation would be hindered by the presence of an eight-membered ring which is unfavourable on thermodynamic grounds. Cyclosilazanes have already been observed in a chelating capacity in the case of $(\text{Me}_2\text{SiNH})_3 \cdot \text{MCl}_3$ ($\text{M} = \text{Ti}, \text{V}$) (299), although the tetrameric ring appears not to form chelate complexes, but instead gives dimeric halogen bridged species (300).

Aminosilanes are strongly $\text{N}(\text{p}\pi) \rightarrow \text{Si}(\text{d}\pi)$ bonded. The removal of N electron density that occurs on adduct formation could well be expected to result in a reduction in $\text{N}(\text{p}\pi) \rightarrow \text{Si}(\text{d}\pi)$ electron donation and thus a lowering of the Si-N bond order. This was reflected in the IR spectra of the adducts, which were virtually identical in the $4000\text{--}500\text{ cm}^{-1}$ region (the range for each band being only a few wavenumbers), but varied considerably from free $\text{Me}_2\text{Si}(\text{NMe}_2)_2$ (250). The differences between the spectra of the free and bound ligand were particularly noticeable in the $800\text{--}500\text{ cm}^{-1}$ region, due to a shift in the Si-N stretching modes. Assignments for bands which should be relatively unaffected by any change in Si-N bonding, i.e. $3036\text{--}3780\text{ cm}^{-1}$, $\nu(\text{CH})$; $1474\text{--}1302\text{ cm}^{-1}$, $\delta(\text{CH})$; $1262\text{--}1265\text{ cm}^{-1}$, $\delta_{\text{as}}(\text{NMe})$; $1229\text{--}1234\text{ cm}^{-1}$, $\delta_{\text{s}}(\text{SiCH}_3)$; $1002\text{--}1009\text{ cm}^{-1}$, $\nu_{\text{s}}(\text{NC}_2)$; and $874\text{--}849\text{ cm}^{-1}$, $\rho(\text{SiMe})$ are made on a tentative basis. In view of the changes observed in the spectra it is unlikely that the $716\text{--}719\text{ cm}^{-1}$ band in $\text{MX}_4 \cdot \text{Me}_2\text{Si}(\text{NMe}_2)_2$ corresponds to the Si-N stretch in $\text{Me}_2\text{Si}(\text{NMe}_2)_2$ at 698 cm^{-1} (250).

Due to the lack of solubility in non-coordinating solvents ^1H NMR data was only available for $\text{SnX}_4 \cdot \text{L}$ ($\text{X} = \text{Cl}, \text{Br}$) and $\text{ZrCl}_4 \cdot \text{L}$ (Table 4.5.1), although spectra of the latter were complicated by decomposition products.

Compound	δSiMe	δNMe
$\text{Me}_2\text{Si}(\text{NMe}_2)_2$	0.1 (6)	2.45 (12)
$\text{SnCl}_4 \cdot \text{Me}_2\text{Si}(\text{NMe}_2)_2$	0.36 (6)	2.17 (6)
		2.19 (6)
$\text{SnBr}_4 \cdot \text{Me}_2\text{Si}(\text{NMe}_2)_2$	-	2.12 (6)
		2.14 (6)
$\text{ZrCl}_4 \cdot \text{Me}_2\text{Si}(\text{NMe}_2)_2$	0.37 (6)	2.09 (6)
		2.15 (6)

Table 4.5.1 ^1H NMR Spectra of $\text{MX}_4 \cdot \text{L}$ (220 MHz in C_6D_6) (Relative Intensities given in brackets)

In each case a sharp doublet was found in the $\delta 2.09 - 2.19$ region corresponding to coordinated NMe_2 groups. The ^1H NMR spectra of $\text{SnX}_4 \cdot \text{Me}_2\text{Si}(\text{NMe}_2)_2$ ($\text{X} = \text{Cl}, \text{Br}$) were also found to be temperature dependent, the doublet decaying to a broad single resonance on raising the temperature to 373 K. Two possible models for the structure in solution are shown in Fig. 4.5.2.

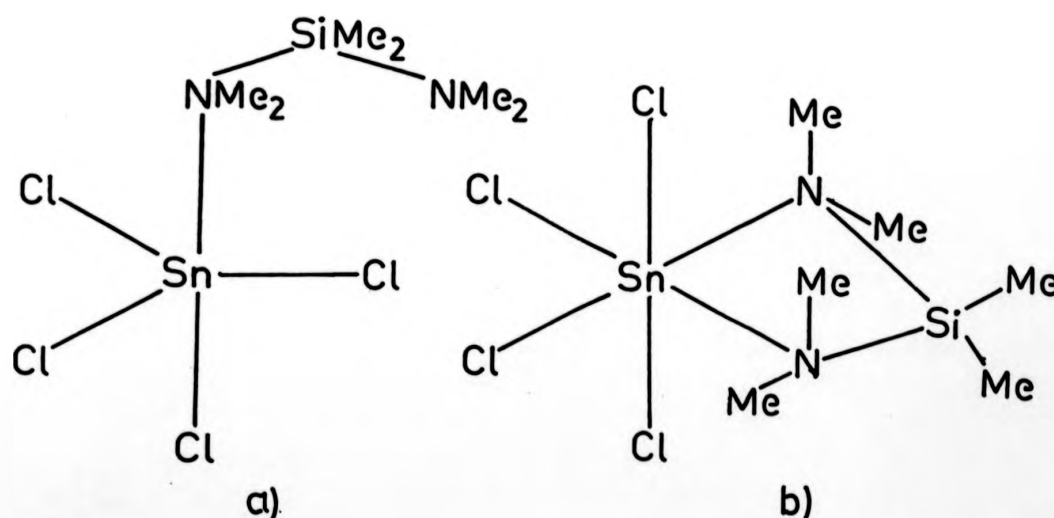


Fig. 4.5.2 Possible Structures for $\text{MX}_4 \cdot \text{Me}_2\text{Si}(\text{NMe}_2)_2$

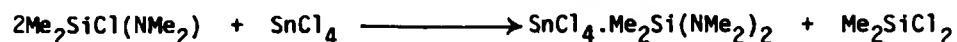
In the first of these structures (Fig. 4.5.2a) the metal assumes a 5 coordinate geometry, and the NMe_2 groups give different resonances corresponding to free and bound N donor centres. Raising the temperature increases the exchange rate between free and bound NMe_2 groups until the fast exchange limit is reached and a single resonance is seen. While such a structure is attractive for $\text{M} = \text{Sn}$, where 5 coordination is well established, it is much less so for $\text{M} = \text{Zr}$, where there are no verified examples of the pentacoordinate state. A solution structure such as that in Fig. 4.5.2b, may therefore, be preferable. Here the ligand is again bidentate, and the metal retains its solid state 6 coordinate geometry. Deviations from planarity of the four membered MN_2Si ring (see Section 4.3) produce inequivalent magnetic environments for the NMe_2 groups, and thus gives rise to a doublet in the ^1H NMR spectra. Rapid inversion of the chelate ring at higher temperatures averages out the different magnetic environments causing the NMe doublet to collapse to a single resonance.

The shift of the SiMe protons from $\delta 0.1$ to $\delta 0.36-0.37$ on adduct formation (Table 4.5.1) is possibly due to the combination of two separate phenomena. Lowering of the Si-N bond order can cause changes in the electron density around the Si atom, thus affecting the chemical shift of any substituents. Strain imposed in the MN_2Si ring should also cause a Me shift, as in $\text{TiCl}_4\cdot\text{dpm}$ (Section 4.3). The magnitude of the strain-imposed shift should be much less than that found in $\text{TiCl}_4\cdot\text{dpm}$, as the protons are one bond further removed from the central strained ring.

4.6 Reaction of $\text{Me}_2\text{SiCl}(\text{NMe}_2)$ with MCl_4 ($\text{M} = \text{Sn}, \text{Ti}$)

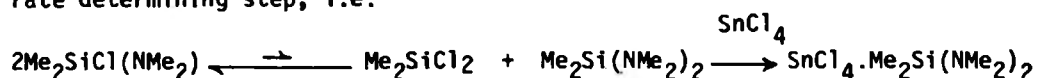
Dropwise addition of a two-fold excess of $\text{Me}_2\text{SiCl}(\text{NMe}_2)$ to a solution of SnCl_4 in C_6H_6 gave (3 days) colourless crystals of $\text{SnCl}_4\cdot\text{Me}_2\text{Si}(\text{NMe}_2)_2$.

Distillation of the remaining solution yielded Me_2SiCl_2 as the sole volatile product, which was identified by its ^1H NMR spectrum, i.e.

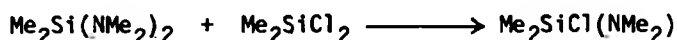


Addition of equimolar quantities of $\text{Me}_2\text{SiCl}(\text{NMe}_2)$ to solutions of TiCl_4 in either hexane or C_6H_6 gave an immediate reaction to give a brown solution, which on standing for 24 hours deposited green crystals of $\text{Cl}_3\text{TiNMe}_2$. Me_2SiCl_2 was again recovered from the residual solution. A repeat reaction with a two-fold excess of $\text{Me}_2\text{SiCl}(\text{NMe}_2)$ yielded identical products.

For the $\text{Me}_2\text{SiCl}(\text{NMe}_2)/\text{SnCl}_4$ system, disproportionation of $\text{Me}_2\text{SiCl}(\text{NMe}_2)$ to $\text{Me}_2\text{Si}(\text{NMe}_2)_2$ and Me_2SiCl_2 is proposed as the initial rate determining step, i.e.



The disproportionation equilibrium evidently lies well to the left hand side as the reaction

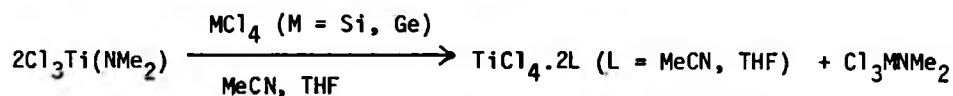


proved to be exothermic, and the product could be isolated in quantitative yield by vacuum distillation. No evidence was found for the analogous $\text{TiCl}_4 \cdot \text{Me}_2\text{Si}(\text{NMe}_2)_2$ in either hexane or C_6H_6 solution. The original preparation of $\text{TiCl}_4 \cdot \text{Me}_2\text{Si}(\text{NMe}_2)_2$ involved precipitation of the complex from hexane solution under conditions of kinetic control, and even here some adduct decomposition took place. The slow disproportionation of $\text{Me}_2\text{SiCl}(\text{NMe}_2)$ ensures that even if $\text{TiCl}_4 \cdot \text{Me}_2\text{Si}(\text{NMe}_2)_2$ is produced as an intermediate, decomposition is sufficiently fast as to render it undetectable. No isolable donor complexes between $\text{Me}_2\text{SiCl}(\text{NMe}_2)$ and MCl_4 ($\text{M} = \text{Sn}, \text{Ti}$) were found in any of the systems studied. The low basicity of $\text{Me}_2\text{SiCl}(\text{NMe}_2)$ compared to that of $\text{Me}_2\text{Si}(\text{NMe}_2)_2$ has been indicated (Section 4.1), and both

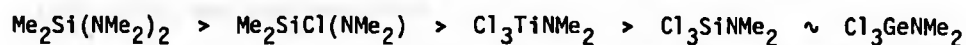
the lack of donor activity, and the reluctance of $\text{Me}_2\text{SiCl}(\text{NMe}_2)$ to further react with $\text{Cl}_3\text{Ti}(\text{NMe}_2)$, cf. $\text{Me}_2\text{Si}(\text{NMe}_2)_2$ (Section 4.4), would seem to support this view.

4.7 Reaction of $\text{Cl}_3\text{Ti}(\text{NMe}_2)$ with MCl_4 ($\text{M} = \text{Si, Ge, Sn, Ti}$) and Donor Solvents

Deep green $\text{Cl}_3\text{Ti}(\text{NMe}_2)$ is a chloride bridged polymer in the solid phase (282), and is, therefore, likely to be only weakly basic unless the monomeric form is easily released in solution. A slight solubility was found in C_6D_6 to give a pale brown solution, the ^1H NMR of which, showed a single broad resonance at $\delta 3.42$. Line broadening is possibly due to intermolecular association in solution via either Cl or NMe_2 bridging. No reaction was found between $\text{Cl}_3\text{TiNMe}_2$ and either TiCl_4 or SnCl_4 , again indicating the weakly basic nature of the NMe_2 group. In THF and MeCN, however, deep green solutions were formed, which on addition of equimolar amounts of MCl_4 ($\text{M} = \text{Si, Ge}$) gave pale yellow solutions of the appropriate bis TiCl_4 complexes, i.e.

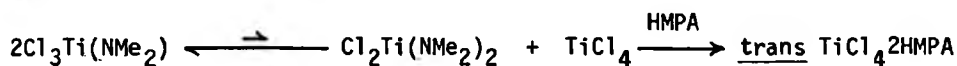


The silyl and germyl species were not isolated. At first sight such behaviour seems a little odd, as $\text{Cl}_3\text{TiNMe}_2$ is itself formed by the rupture of a Si-N bond. Scharschmidt (317) has pointed out that the silyl substituents greatly affect the reactivity of the Si-N bond. The order of reactivity of the M-N bond on the basis of the various reactions studied in this section is,



$\text{Cl}_3\text{TiNMe}_2$ is coordinatively unsaturated, and should in theory be able to function as a Lewis acid. Addition of excess MeCN or THF to $\text{Cl}_3\text{TiNMe}_2$

resulted in deep green solutions compared to the brown solutions formed in non-coordinating solvents. On removal of solvent, deep green, tarry products were formed which although showing IR bands indicative of coordinated solvent, resisted all attempts at purification. With a two-fold excess of HMPA in C_6H_6 solution, reaction occurred over a two-week period to give a deep brown solution, and pale yellow crystals of trans $TiCl_4 \cdot 2HMPA$ (Section 3.2.1). As with the $Me_2SiCl(NMe_2)/SnCl_4$ systems (Section 4.6), slow disproportionation is proposed as the initial step, i.e.



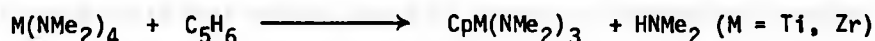
The stoichiometry of the brown $Cl_2Ti(NMe_2)_2$ was not established.

4.8 Exchange Reactions between $CpTi(NMe_2)_3$ and $Cp_2Zr(NMe_2)_2$ with some Covalent Metal Tetrahalides

4.8.1 Reaction of Cp_2TiCl_2 with Me_2NLi

Cp_2TiCl_2 reacted with 3 mol equivalents of Me_2NLi in n-hexane/toluene to give a deep brown solution. Removal of solvent and distillation in vacuo gave $CpTi(NMe_2)_3$ as a deep red crystalline solid in 36% yield.

Interestingly, with the same reactants under similar conditions Chandra and Lappert (273) obtained a low yield of $Cp_2Ti(NMe_2)_2$. Evidently, factors such as reaction time/temperature and exact solvent composition are critical in determining the products of this reaction. Although displacement of $C_5H_5^-$ by strongly basic oxo anions (e.g. β -diketonates) has already been recorded (151), this appears to be the first example where NR_2^- acts in a similar capacity. The reverse of this reaction, i.e. displacement of $HNMe_2$ by C_5H_6 has been studied by Lappert and coworkers (272, 273), who concluded that



Addition of excess C_5H_6 resulted in the displacement of a second mol of HNR_2

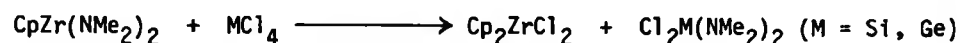
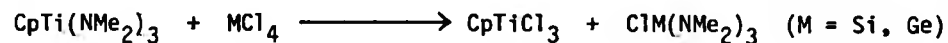
for $M = \text{Zr}$, but not for $M = \text{Ti}$ (273). Steric crowding between bulky Cp groups on the small Ti (cf. Zr) was here suggested as a possible explanation (273), and in a similar vein, reduction of steric compression may be the driving force for the displacement of C_5H_5^- in the currently studied reaction.

4.8.2 Reaction of $\text{CpTi}(\text{NMe}_2)_3$ and $\text{Cp}_2\text{Zr}(\text{NMe}_2)_2$ with MCl_4 ($M = \text{Si, Ge, Sn, Ti, Zr, Hf}$)

Dropwise addition of MCl_4 ($M = \text{Si, Ge, Sn, Ti}$) in C_6H_6 to an equimolar amount of $\text{CpTi}(\text{NMe}_2)_3$, also in C_6H_6 , resulted in an immediate colour change (red/brown \rightarrow yellow, $M = \text{Si, Ge}$; red/brown \rightarrow light brown, $M = \text{Sn, Ti}$). Workup of the reaction in each case gave CpTiCl_3 as one of the products. Similarly, $\text{CpTi}(\text{NMe}_2)_3$ when added to a suspension of MCl_4 ($M = \text{Zr, Hf}$) in C_6H_6 (1:1) gave a dark brown solid and a light brown solution, which on removal of solvent and extraction with n-hexane, likewise yielded CpTiCl_3 . The identity of the tarry Zr- or Hf-containing product could not be established. Reaction between bright yellow benzene solutions of $\text{Cp}_2\text{Zr}(\text{NMe}_2)_2$ and MCl_4 ($M = \text{Si, Ge, Sn, Ti}$) gave Cp_2ZrCl_2 as the Zr-containing product in each case. With the $\text{TiCl}_4/\text{Me}_2\text{Si}(\text{NMe}_2)_2$ system, use of non-polar solvents such as n-hexane led to the isolation of 1:1 adducts. When n-hexane was used as the solvent for the reaction between $\text{Cp}_2\text{Zr}(\text{NMe}_2)_2$ and SnX_4 ($X = \text{Cl, Br}$), exchange was still the dominant reaction, and Cp_2ZrX_2 ($X = \text{Cl, Br}$) was isolated from the reaction products.

The general theme of these reactions is then one of group exchange. No evidence was found for stable donor complexes in any of the systems studied, certainly in concrete terms of isolable material(s), although it is conceivable that adducts could be formed as intermediate species in the exchange process.

Identification of the dimethylamino-bearing exchange product proved more difficult. For the $\text{CpTi}(\text{NMe}_2)_3/\text{MCl}_4$ ($\text{M} = \text{Si}, \text{Ge}$) and $\text{Cp}_2\text{Zr}(\text{NMe}_2)_2/\text{MCl}_4$ ($\text{M} = \text{Si}, \text{Ge}$) systems, removal of the volatile products in vacuo, followed by distillation in vacuo, gave $\text{ClM}(\text{NMe}_2)_3$ ($\text{M} = \text{Si}, \text{Ge}$) and $\text{Cl}_2\text{M}(\text{NMe}_2)_2$ respectively, which were identified by their ^1H NMR and IR ($\text{M} = \text{Si}$) spectra, i.e.



On treatment with a large excess of MCl_4 ($\text{M} = \text{Si}, \text{Ge}$), CpTiCl_3 and Cp_2ZrCl_2 were again produced, but redistribution of the silyl or germyl species occurred to give $\text{Cl}_3\text{M}(\text{NMe}_2)$ ($\text{M} = \text{Si}, \text{Ge}$).

From the 1:1 reaction of $\text{Cp}_2\text{Zr}(\text{NMe}_2)_2$ and TiCl_4 a brown solid was produced which yielded a chocolate brown sublimate, identified as the non-stoichiometric form of " $\text{Cl}_2\text{Ti}(\text{NMe}_2)_2$ " (319). With $\text{CpTi}(\text{NMe}_2)_3$ a dark brown solid was again formed. A ^1H NMR spectrum revealed a sharp resonance at $\delta 3.21$ and a series of low intensity resonances in the $\delta 2.0$ to $\delta 3.7$ region, again suggesting a mixture of Ti-NMe₂ species. To clarify the situation, the reactions between $\text{CpTi}(\text{NMe}_2)_3$ or $\text{Cp}_2\text{Zr}(\text{NMe}_2)_2$ with a three-fold ($\text{M} = \text{Ti}$) or two-fold ($\text{M} = \text{Zr}$) excess of TiCl_4 were investigated. In both cases, deep green crystals of $\text{Cl}_3\text{TiNMe}_2$ were isolated, i.e.



Formation of the non-stoichiometric " $\text{Cl}_2\text{Ti}(\text{NMe}_2)_2$ " in the 1:1 reactions is paralleled by the exchange reactions with Sn-NMe_2 , but not Ti-NMe_2 , where well defined crystalline products were obtained.

The dimethylamino-bearing products from the reactions of $\text{CpTi}(\text{NMe}_2)_3$ and $\text{Cp}_2\text{Zr}(\text{NMe}_2)_2$ with SnX_4 ($\text{X} = \text{Cl}, \text{Br}$) were only poorly defined. Extraction of the crude reaction mixtures with Et_2O gave CpTiCl_3 or Cp_2ZrX_2 ($\text{X} = \text{Cl}, \text{Br}$) and a pale brown involatile solid in each case. The ^1H NMR spectra of these latter compounds (C_6D_6 , 220 MHz) showed several resonances in the $\delta 2.0 - 3.0$ region (presumably due to Sn-NMe_2 protons) indicating a complex mixture of products. The fact that the simple aminochlorostannanes have yet to be characterised is perhaps a reflection of the difficulty in obtaining these species as pure compounds.

4.9 Experimental

4.9.1 Reactions of $\text{Me}_2\text{NCH}_2\text{NMe}_2$ with MX_4 ($\text{M} = \text{Ti}, \text{Sn}$), VCl_3 and $\text{CrCl}_3 \cdot 2\text{NMe}_3$

(a) $\text{TiCl}_4 \cdot (\text{Me}_2\text{N})_2\text{CH}_2$. Dropwise addition of TiCl_4 (1 ml, 9.1 mmol) to a stirred C_6H_6 solution of $(\text{Me}_2\text{N})_2\text{CH}_2$ (1.2 mls, 9.1 mmol) gave an immediate yellow precipitate and a lime green solution. The solution was decanted in vacuo, and the solid $\text{TiCl}_4 \cdot (\text{Me}_2\text{N})_2\text{CH}_2$ washed well in n-hexane before pumping in vacuo for several hours. Yield 2.5 g (94%).

Analysis based on $\text{C}_5\text{H}_{14}\text{N}_2\text{TiCl}_4$

Calculated	C(20.6)	H(4.8)	N(9.6)	Cl(48.6)	%
Found	C(17.0)	H(4.0)	N(7.7)	Cl(46.6)	%

Bands were found in the IR spectrum at:-

3178(s), 3125(m), 3038(m), 2296(m), 2936(s), 2831(w), 2799(w), 1500(w), 1477(w), 1456(s), 1447(w), 1430(w), 1409(w), 1233(w), 1213(m), 1190(vw), 1168(m), 1098(w), 1045(s), 1002(s), 948(s), 862(s), 830(s), 725(m), 676(w), 560(w), 510(w), 427(m), 397(s), 379(s), 356(s), 332(m) and 265 cm^{-1} respectively.

(b) $\text{SnCl}_4 \cdot (\text{Me}_2\text{N})_2\text{CH}_2$. Reaction of SnCl_4 (1 ml, 8.5 mmol) and $(\text{Me}_2\text{N})_2\text{CH}_2$ (1.2 ml, 8.5 mmol) in C_6H_6 solution as above gave white $\text{SnCl}_4 \cdot (\text{Me}_2\text{N})_2\text{CH}_2$. Yield 2.8 g (91%).

Analysis based on $C_5H_{14}N_2SnCl_4$

Calculated	C(16.6)	H(3.9)	N(7.7)	Cl(39.1) %
Found	C(17.7)	H(5.2)	N(9.0)	Cl(38.5) %

The IR spectrum showed bands at:-

3170(br), 3036(w), 3018(w), 3001(m), 2946(s), 2855(sh), 2806(w), 1494(w,sh), 1479(w), 1467(s), 1462(sh), 1449(w), 1239(w), 1220(s), 1166(w), 1101(w), 1041(s), 991(s), 952(s), 860(s), 813(w), 722(m), 561(w), 461(w), 392(m), 337(sh) and 319(vs) cm^{-1} respectively.

(c) $VCl_3 \cdot 0.5(Me_2N)_2CH_2$. VCl_3 (~1 g) was stirred overnight in excess liquid $(Me_2N)_2CH_2$ to give insoluble chocolate brown $VCl_3 \cdot 0.5(Me_2N)_2CH_2$ in quantitative yield.

Analysis based on $C_5H_{14}N_2V_2Cl_6$

Calculated	C(14.4)	H(3.4)	N(6.7)	Cl(51.0) %
Found	C(11.7)	H(2.7)	N(4.5)	Cl(38.6) %

Bands were found in the IR spectrum at:-

3144(s), 3030(m), 2996(m), 2975(w), 2940(m), 2790(w), 2737(w), 1697(w), 1654(s), 1498(w), 1470(w,sh), 1462(s), 1404(w), 1436(w), 1410(w), 1368(s), 1261(w), 1245(m), 1234(w), 1227(w), 1171(w), 1122(m), 1063(w), 1045(w), 1040(w), 1024(m), 998(m), 974(w), 963(m), 920(w), 865(s), 835(w), 723(m), 695(m), 556(w), 475(w), 428(w), 413(w), 387(w), 350(s), 315(s,br) and 227(s) cm^{-1} respectively.

(d) $CrCl_3 \cdot NMe_3 \cdot (Me_2N)_2CH_2$. A solution of $CrCl_3 \cdot 2NMe_3$ (1.1g, 4.0 mmol) in 40 ml C_6H_6 was added in vacuo to $(Me_2N)_2CH_2$ (1.6 ml, 12.1 mmol). An immediate colour change (mauve \rightarrow purple) occurred, and on further stirring a pale lavender solid precipitated from solution. The solid was washed with n-hexane and dried in vacuo to give $CrCl_3 \cdot NMe_3 \cdot (NMe_2)_2CH_2$. Yield 0.9 g (70%).

Analysis based on $C_8H_{23}N_3CrCl_3$

Calculated	C(30.1)	H(7.2)	N(13.1)	Cl(33.3)	%
Found	C(32.5)	H(7.0)	N(12.4)	Cl(32.7)	%

The IR spectrum showed bands at:-

3040(m), 2995(m), 2930(s), 2855(sh), 2760(w), 1645(m,br), 1485(m),
1463(m), 1461(m), 1445(w), 1408(w), 1368(w), 1265(w), 1245(w),
1237(w), 1226(w), 1200(w), 1176(w), 1124(m), 1105(m), 1040(m),
1006(m), 997(m), 960(m), 817(s), 821(s), 717(m), 530(w), 400(m),
362(m), 350(w) and 347(m) cm^{-1} respectively.

4.9.2 Reaction of $TiCl_4$ with $Ph_2PCH_2PPh_2$ (dpm)

(a) $TiCl_4$ (0.5 ml, 4.5 mmol) in C_6H_6 was added dropwise to a solution of dpm (1.76 g, 4.5 mmol) in C_6H_6 (120 ml). The pale yellow solution formed immediately upon addition, soon gave way to a flocculent orange precipitate. Decanting the supernatant liquid and careful washing of the solid in vacuo with C_6H_6 gave $TiCl_4 \cdot dpm$, as a bright orange solid. Yield 2.91 g (91%).

Analysis based on $TiCl_4 \cdot C_{25}H_{22}P_2$

Calculated	C(52.3)	H(3.9)	P(10.8)	Cl(24.7)	%
Found	C(53.9)	H(4.4)	P(10.6)	Cl(24.3)	%

The IR spectrum showed bands at:-

3085(w,sh), 3070(w,sh), 3050(w), 3037(m), 2954(s), 2933(sh), 2900(sh),
2870(sh), 1484(s), 1470(w,sh), 1461(vw), 1449(vs), 1366(m), 1357(m),
1347(m), 1308(m), 1278(w), 1262(w), 1189(m), 1160(w), 1114(s), 1098(vs),
1072(w), 1038(m), 1029(m), 1003(vs), 977(w), 888(w), 796(m), 770(w),
757(w), 750(m), 744(w), 736(s), 726(s), 696(vs), 678(s), 614(w),
525(m), 506(s), 484(w), 469(s), 447(w), (416(s), 388(s), 380(s),
364(sh), 345(m), 333(m) and 320(sh) cm^{-1} respectively.

(b) A repeat experiment used a two-fold excess of dpm under the same reaction conditions yielded an identical product to (a).

4.9.3 Exchange reactions between $\text{Me}_2\text{Si}(\text{NMe}_2)_2$ and MCl_4 ($\text{M} = \text{Si}, \text{Ge}, \text{Ti}$)

(a) Reactions between $\text{Me}_2\text{Si}(\text{NMe}_2)_2$ and MCl_4 , $\text{M} = \text{Si}, \text{Ge}$. Reactions between $\text{Me}_2\text{Si}(\text{NMe}_2)_2$ and MCl_4 were carried out on a small scale as neat liquids or as C_6D_6 solutions, e.g. GeCl_4 (0.5 ml, 4.3 mmol), was added dropwise to $\text{Me}_2\text{Si}(\text{NMe}_2)_2$ (0.78 ml, 4.3 mmol), and after the solution had cooled the products were investigated by ^1H NMR (2% C_6D_6 solutions, rel. TMS 220 MHz). $\text{Cl}_2\text{Si}(\text{NMe}_2)_2$ was also detected by strong Si-N bonds at 741 and 686 cm^{-1} in the IR spectra of the products (liquid film).

(b) Reaction of $\text{Me}_2\text{Si}(\text{NMe}_2)_2$ and TiCl_4 (1:1). TiCl_4 (1 ml, 9.1 mmol) in C_6H_6 (30 ml) was added dropwise into a single ampoule bomb containing a C_6H_6 solution (30 ml) of $\text{Me}_2\text{Si}(\text{NMe}_2)_2$ (1.07 ml, 9.1 mmol). Initially, a yellow precipitate and a brown solution was formed, but started to turn green after only a few minutes. The bomb was degassed, sealed and placed in a water bath thermostated at 323 K. After 2 hours no trace of the original yellow precipitate remained. The solution was decanted, and distilled in vacuo (318-319 K/0.5 mm) to give a fuming, colourless liquid identified as $\text{Me}_2\text{SiCl}(\text{NMe}_2)$ by ^1H NMR.

The solid was washed in benzene (3 x 50 ml portions), dried and sublimed in vacuo (353 K) to give dark green needles of $\text{Cl}_3\text{Ti}(\text{NMe}_2)$, identified by its IR spectrum. A small amount of unreacted yellow solid remaining after sublimation was found to be $\text{TiCl}_4 \cdot \text{Me}_2\text{Si}(\text{NMe}_2)_2$ by comparison with an authentic sample.

(c) Reaction of $\text{Me}_2\text{Si}(\text{NMe}_2)_2$ with TiCl_4 (2:1). TiCl_4 (1 ml, 9.1 mmol) in C_6H_5 (35 ml) was reacted with $\text{Me}_2\text{Si}(\text{NMe}_2)_2$ (2.1 ml, 18.2 mmol) as for (b).

The initially formed yellow precipitate turned green, then brown, reaction being complete after 24 hours at 323 K. The solution was decanted and distilled in vacuo to give $\text{Me}_2\text{SiCl}(\text{NMe}_2)$ (B.p. 318-320 K/0.5 mm). The residual solid was washed with n-hexane and sublimed in vacuo (363-373 K) to give a dark brown solid approximating to $\text{Cl}_2\text{Ti}(\text{NMe}_2)_2$.

% Cl Calculated (34.3) Found (32.5).

4.9.4 Complexes of $\text{Me}_2\text{Si}(\text{NMe}_2)_2$ with MCl_4 (M = Ti, Zr, Hf, Sn) and SnBr_4

(a) $\text{TiCl}_4 \cdot \text{Me}_2\text{Si}(\text{NMe}_2)_2$. TiCl_4 (1 ml, 9.1 mmol) in hexane (100 ml) was added dropwise over 20 minutes to a solution of $\text{Me}_2\text{Si}(\text{NMe}_2)_2$ (1.07 mls, 9.1 mmol) in hexane (200 ml) give a pale yellow precipitate and a light brown solution. The solution was decanted, and the solvent removed in vacuo to give a small amount of gree/brown solid (~ 0.1 g), vacuum sublimation of which gave $\text{Cl}_3\text{Ti}(\text{NMe}_2)$, identified from its IR spectrum. Repeated washing of the yellow solid until the washings were colourless (4 x 200 ml hexane) gave $\text{TiCl}_4 \cdot \text{Me}_2\text{Si}(\text{NMe}_2)_2$ as a pale yellow solid (2.9 g, 95%).
M.p. (decomp.) ~ 423 K.

Analysis based on $\text{TiCl}_4\text{C}_6\text{H}_{18}\text{N}_2\text{Si}$

Calculated	C(21.5)	H(5.4)	N(8.3)	Cl(42.2)	%
Found	C(21.7)	H(5.5)	N(8.5)	Cl(42.1)	%

The IR spectrum showed bands at:-

3140(br), 3040(w), 2975(m), 2940(m), 2855(m), 2804(w), 1469(s), 1458(w), 1450(w), 1440(w), 1413(m), 1305(m), 1264(s), 1233(m), 1176(w), 1110(s), 1100(w), 1009(s), 1005(m), 900(vs), 847(s), 816(s), 810(s), 719(s), 637(m), 589(s), 491(m), 417(s), 405(m), 365(vs) and 322(m) cm^{-1} respectively.

(b) A repeat experiment of (a) using a two-fold excess of $\text{Me}_2\text{Si}(\text{NMe}_2)_2$ gave an identical product.

(c) $\text{SnCl}_4 \cdot \text{Me}_2\text{Si}(\text{NMe}_2)_2$. SnCl_4 (1 ml, 8.5 mmol) in C_6H_6 (100 ml) when added dropwise to $\text{Me}_2\text{Si}(\text{NMe}_2)_2$ (1.54 mls, 8.5 mmol) in C_6D_6 (200 ml) gave a white precipitate of $\text{SnCl}_4 \cdot \text{Me}_2\text{Si}(\text{NMe}_2)_2$, which was washed with 4 x 150 ml portions of C_6H_6 . Yield 3.1 g (91%). Further purification could be achieved by either sublimation in high vacuum (403–413 K) or recrystallisation from hot CH_2Cl_2 .

Analysis based on $\text{SnCl}_4\text{C}_6\text{H}_{18}\text{N}_2\text{Si}$

Calculated	C(17.7)	H(4.4)	N(6.9)	Cl(34.9)	%
------------	---------	--------	--------	----------	---

Found	C(17.6)	H(4.5)	N(6.9)	Cl(34.9)	%
-------	---------	--------	--------	----------	---

IR bands were observed at:-

3210(br), 3036(m), 2990(w), 2980(m), 2948(s), 2910(w), 2855(w), 2820(w), 2862(w), 2780(w), 1474(w), 1464(s), 1450(sh), 1436(w), 1413(m), 1407(vw), 1397(w), 1302(w), 1265(s), 1234(m), 1168(w), 1114(s), 1102(w), 1009(vs), 890(vs), 849(vs), 818(vs), 716(s), 610(m), 588(s), 484(s), 393(w), 378(w), 340(m), 328(sh), 320(vs) and 260(m) cm^{-1} respectively.

(d) A repeat experiment of (c) using a two-fold excess yielded an identical product.

(e) $\text{ZrCl}_4 \cdot \text{Me}_2\text{Si}(\text{NMe}_2)_2$. $\text{Me}_2\text{Si}(\text{NMe}_2)_2$ (1.3 ml, 7.25 mmol) in C_6H_6 (50 ml) was added dropwise to a vigorously stirred suspension of ZrCl_4 (1.7 g, 7.25 mmol) in C_6H_6 (200 ml). After addition was complete, stirring was continued for 24 hours. Removal of the solvent, and washing with C_6H_6 gave $\text{ZrCl}_4 \cdot \text{Me}_2\text{Si}(\text{NMe}_2)_2$ as a slightly off-white solid. Yield 2.6 g (96%). M.p. (decomp.) 423 K.

Analysis based on $\text{ZrCl}_4\text{C}_6\text{H}_{18}\text{N}_2\text{Si}$

Calculated	C(19.0)	H(4.8)	N(7.4)	Cl(38.2)	%
------------	---------	--------	--------	----------	---

Found	C(19.2)	H(4.9)	N(7.4)	Cl(37.5)	%
-------	---------	--------	--------	----------	---

The IR spectrum showed bands at:-

3030(m), 2970(s), 2905(w), 2858(w), 2810(w), 1468(s), 1460(sh), 1448(w), 1415(m), 1305(s), 1266(s), 1230(s), 1164(m), 1169(s), 1101(m), 1071(m), 1005(vs), 890(s), 848(s), 816(sh), 809(s), 717(s), 677(w), 619(m), 582(s), 486(s), 392(w), 380(m), 344(vs), and 311(m) cm^{-1} respectively.

(f) A repeat experiment of (e) with a two-fold excess of ligand gave an identical product.

(g) $\text{HfCl}_4 \cdot \text{Me}_2\text{Si}(\text{NMe}_2)_2$. $\text{Me}_2\text{Si}(\text{NMe}_2)_2$ (0.7 ml, 3.9 mmol) and HfCl_4 (1.24 g, 3.9 mmol) reacted as in (e) to give $\text{HfCl}_4 \cdot \text{Me}_2\text{Si}(\text{NMe}_2)_2$ (1.60 g), 89% as an off-white solid. M.p. (decomp.) 428 K.

Analysis based on $\text{HfCl}_4\text{C}_6\text{H}_{18}\text{N}_2\text{Si}$

Calculated	C(15.4)	H(3.9)	N(6.0)	Cl(30.4)	%
Found	C(15.2)	H(3.7)	N(5.7)	Cl(30.1)	%

The IR spectrum showed bands at:-

3031(br), 2969(s), 2948(m), 2900(w), 2856(m), 2820(w), 2800(w), 1465(s), 1458(sh), 1438(m), 1416(m), 1305(m), 1262(s), 1229(m), 1164(w), 1110(m), 1100(w), 1002(s), 888(s), 849(s), 810(vs), 718(s), 625(m), 585(m), 492(m), 398(w), 378(w), 342(m) and 313(vs) cm^{-1} respectively.

(h) $\text{SnBr}_4 \cdot \text{Me}_2\text{Si}(\text{NMe}_2)_2$. SnBr_4 (2.9 g, 6.8 mmol) in C_6H_6 (150 mls) was added dropwise to $\text{Me}_2\text{Si}(\text{NMe}_2)_2$ (1.2 mls, 6.8 mmol) in C_6H_6 (200 ml). An immediate reaction occurred to give a white precipitate of $\text{SnBr}_4 \cdot \text{Me}_2\text{Si}(\text{NMe}_2)_2$, which was washed with C_6H_6 and n-hexane, and dried in vacuo. Yield 3.7 g (94%).

Analysis based on $\text{SnBr}_4\text{C}_6\text{H}_{18}\text{N}_2\text{Si}$

Calculated	C(12.3)	H(3.1)	N(4.8)	Br(54.7)	%
Found	C(12.4)	H(3.1)	N(4.7)	Br(54.8)	%

Bands were found in the IR spectrum at:-

3195(w), 3038(w), 2972(m), 2931(s), 2897(m), 2855(m), 2805(w),
1467(s), 1458(m), 1440(w), 1415(m), 1274(s), 1234(m), 1172(w),
1162(w), 1117(m), 1106(s), 1016(s), 983(s), 852(s), 827(s),
821(s), 723(s), 618(m), 588(m), 484(m), 395(w), 378(w) and 214 (vs) cm^{-1}
respectively.

(i) A repeat experiment of (h) using a two-fold excess of $\text{Me}_2\text{Si}(\text{NMe}_2)_2$ yielded an identical product.

4.9.5 Reaction of $\text{Me}_2\text{SiCl}(\text{NMe}_2)$ with MCl_4 ($\text{M} = \text{Sn}, \text{Ti}$)

(a) SnCl_4 (1.4 ml, 12.3 mmol) in C_6H_6 (~30 ml) was added dropwise to a single ampoule bomb containing $\text{Me}_2\text{SiCl}(\text{NMe}_2)$ (3.4 g, 24.6 mmol) in C_6H_6 (~30 ml). The bomb was degassed, sealed and placed in a thermostat bath at 313 K. After 3 days, colourless crystals began to appear, which were collected, washed with n-hexane and dried in vacuo. An IR spectrum identified the product as $\text{SnCl}_4 \cdot \text{Me}_2\text{Si}(\text{NMe}_2)_2$. Yield 2.6 g (67.1%). Distillation of the remaining liquid fraction gave a colourless liquid, identified as Me_2SiCl_2 by its ^1H NMR spectrum. B.p. 342 K/760 mm, lit. 343 K/760 mm.

(b) A repeat experiment of (a) using a four-fold excess of $\text{Me}_2\text{SiCl}(\text{NMe}_2)$ yielded an identical product.

(c) TiCl_4 (1.3 ml, 11.8 mmol) in C_6H_6 (~10 ml) was added dropwise to a single ampoule bomb containing $\text{Me}_2\text{SiCl}(\text{NMe}_2)$ (1.6 g, 11.8 mmol) in C_6H_6 (~60 ml), to give a dark brown solution. The bomb was degassed,

sealed and placed in a thermostated bath at 313 K. After 24 hours, green needles were deposited. These were collected, washed with n-hexane, dried in vacuo and sublimed in vacuo (363 k) to give $\text{Cl}_3\text{Ti}(\text{NMe}_2)$ in almost quantitative yield. There were no other solid products. Distillation of the remaining solution gave Me_2SiCl_2 in low yield (~15 %). B.p. 340 K/760 mm, lit. 343 K/760 mm.

(d) A repeat experiment to (c) using identical proportions of reactants, but n-hexane as the solvent gave the same products, but precipitation of $\text{Cl}_3\text{Ti}(\text{NMe}_2)$ appeared to be complete after only 2 hours.

1

(e) A repeat experiment to (c) using a two-fold excess of $\text{Me}_2\text{SiCl}(\text{NMe}_2)$ also gave $\text{Cl}_3\text{Ti}(\text{NMe}_2)$ as the sole solid product.

4.9.6 Reaction of $\text{Cl}_3\text{Ti}(\text{NMe}_2)$ with MCl_4 (M = Si, Ge) and HMPA

(a) Samples of re-sublimed $\text{Cl}_3\text{Ti}(\text{NMe}_2)$ (~1 g) were dissolved in either MeCN or THF (~60 ml) to give deep green solutions. Dropwise addition of equimolar amounts of either SiCl_4 or GeCl_4 in C_6H_6 (~10 ml) to these solutions gave an immediate colour change (green → pale yellow). The THF solutions were reduced to ~5 ml by removal of solvent and volatile reaction products in vacuo, whereupon, yellow crystals of $\text{TiCl}_4 \cdot 2\text{THF}$ appeared on cooling. An IR spectrum of the product proved to be identical to that of an authentic sample of $\text{TiCl}_4 \cdot 2\text{THF}$. MeCN solutions were worked up as follows:- removal of all volatile products gave a pale yellow solid, which on vacuum sublimation (33 K) gave pale yellow crystals of $\text{TiCl}_4 \cdot 2\text{MeCN}$, identified by comparison to an authentic sample.

(b) HMPA (3.5 ml, 20.0 mmol) was added to a single ampoule bomb containing $\text{Cl}_3\text{Ti}(\text{NMe}_2)$ (0.9 g, 4.5 mmol) in C_6H_6 (~60 ml), giving a

dark brown solution. After 2 weeks, a small amount of pale yellow crystals had formed, which were collected, carefully washed with C_6H_6 and n-hexane and dried in vacuo. An IR spectrum identified the product as trans $TiCl_4 \cdot 2HMPA$ (0.5 g, 20.3%). The Ti/NMe_2 species was not isolated.

4.9.7 Exchange reactions between $CpTi(NMe_2)_3$ and $Cp_2Zr(NMe_2)_2$ and covalent metal halides

(a) Reaction between Cp_2TiCl_2 and $LiNMe_2$. A suspension of Me_2NLi was prepared by admitting gaseous Me_2NH (18.0 g, 0.4 mol) to a stirred, cooled (195 K) solution of $BuLi$ (19.6 g, 0.31 mol) in n-hexane (600 ml), the whole operation being carried out in vacuo. After allowing the reactants to warm to room temperature, butane and excess Me_2NH were pumped off to give a white Me_2NLi /n-hexane slurry. The slurry was cooled to 273 K and a solution/suspension of Cp_2TiCl_2 (38 g, 0.15 mol) in toluene (600 ml) was carefully added under a N_2 atmosphere. As the reaction proceeded, the colour changed from yellow + brown, eventually giving an almost black solution after 24 hours. The reaction mixture was refluxed for 6 hours, and on cooling, the $LiCl$ formed was removed by filtration under an N_2 atmosphere. Removal of the solvent in vacuo gave a dark red/brown liquid, which on distillation (371 K, 1.5 mmHg) gave 13.6 g of $CpTi(NMe_2)_3$ as a dark red low melting point crystalline solid (36.0%).

Analysis based on $C_{11}H_{23}N_3Ti$

% Ti Calculated (19.53 Found (19.40)

The 1H NMR spectrum (10%/ C_6D_6 /220 MHz) showed sharp, single resonances at δ 3.14 (18 protons) and δ 5.97 (5 protons).

The IR spectrum (liquid film) showed bands at:-

3100(w), 2978(m), 2957(m), 2890(w), 2844(s), 2806(s), 2760(s), 2695(w), 2644(w), 2230(w), 2144(w), 2080(w), 1790(w), 1690(w), 1661(vw), 1625(w).

1590(w), 1447(s), 1415(s), 1395(w), 1373(w), 1365(w), 1238(s), 1140(s), 1118(w), 1098(m), 1075(w), 1048(m), 1018(m), 965(w), 950(vs), 795(s), 570(s), 401(sh) and 380(m) cm^{-1} respectively.

(b) Preparation of $\text{Cp}_2\text{Zr}(\text{NMe}_2)_2$. $\text{Cp}_2\text{Zr}(\text{NMe}_2)_2$ was prepared from Cp_2ZrCl_2 and Me_2NLi by the method of Jenkins *et al* (275).

Bands were found in the IR spectrum at:-

3090(w), 2960(m), 2855(m), 2810(s), 2760(s), 1650(w), 1635(w), 1610(w), 1565(m), 1445(m), 1425(w), 1365(w), 1236(s), 1132(s), 1124(sh), 1056(m), 1028(m), 1016(m), 952(s), 943(s), 849(w), 795(vs), 616(s), 668(w), 645(w), 537(m) and 350(m) cm^{-1} respectively.

The ^1H NMR spectrum (C_6D_6 rel. TMS, 220 MHz) showed single, sharp resonances at δ 2.86 (12 protons) and δ 5.33 (10 protons) corresponding to the NMe_2 and Cp groups respectively.

(c) Reaction between $\text{CpTi}(\text{NMe}_2)_3$ and SiCl_4 . $\text{CpTi}(\text{NMe}_2)_3$ (2.04 g, 8.3 mmol) was dissolved in C_6H_6 (~50 ml) and SiCl_4 (1.41 g, 8.3 mmol) was condensed onto the frozen solution at 77 K. On warming to room temperature a dark brown solid was formed, and a pale yellow solution. The solvent and volatile products were removed in vacuo to leave a dark brown solid, which on sublimation in vacuo (333 K) gave CpTiCl_3 as an orange/yellow crystalline sublimate. Yield 0.899 (48.8%).

Analysis based on $\text{C}_5\text{H}_5\text{TiCl}_3$

% Cl Calculated (48.5) Found (48.5)

Distillation of the volatile products in vacuo gave a colourless, fuming liquid, identified as $\text{ClSi}(\text{NMe}_2)_3$ by its ^1H NMR spectrum which was found to be identical to an authentic sample.

(d) Reaction between $\text{CpTi}(\text{NMe}_2)_3$ and GeCl_4 . $\text{CpTi}(\text{NMe}_2)_3$ (0.98 g, 4.0 mmol) and GeCl_4 (0.86 g, 4.0 mmol) when reacted together in C_6H_6 solution

as for (a) gave CpTiCl_3 (0.46 g, 52.5%). $\text{ClGe(NMe}_2)_3$ was identified as the germyl reaction product by its ^1H NMR spectrum, which was identical to that of an authentic sample.

(e) Reaction between $\text{CpTi(NMe}_2)_3$ and SnCl_4 . $\text{CpTi(NMe}_2)_3$ (1.6 g, 6.5 mmol) was dissolved in C_6H_6 (~60 ml) to give a dark red solution. To this was added SnCl_4 (0.76 ml, 6.5 mmol) in C_6H_6 (~20 ml) which gave a deep brown solution and a brown oil. The solution was decanted in vacuo, and on removal of the solvent gave a red/brown tarry product. Extraction of this solid with dry Et_2O gave a pale red solution and a light brown solid. Removal of Et_2O from the red solution gave an orange solid which on sublimation in vacuo gave CpTiCl_3 (0.21g, 15%). The light brown solid showed bands in the IR spectrum at:-

3215(s), 3025(w), 3005(w), 2996(w), 2848(w), 2832(m), 1463(s),
1450(w), 1433(m), 1410(w), 1398(m), 1278(m), 1230(w), 1123(s),
1078(s), 1026(s), 866(s), 816(m,br), 727(w), 555(w,br), 485(m,br),
445(m,br) and 323(vs,br) cm^{-1} respectively.

(f) Reaction between $\text{CpTi(NMe}_2)_3$ and TiCl_4 (1:1). $\text{CpTi(NMe}_2)_3$ (0.8 g, 3.0 mmol) and TiCl_4 (0.33 ml, 3.0 mmol) when reacted as in (e) gave a dark brown solution. Removal of the solvent in vacuo and washing with n-hexane gave a dark brown product, analysing as $\text{C}_{11}\text{H}_{23}\text{N}_3\text{Ti}_2\text{Cl}_4$. A ^1H NMR spectrum (C_6D_6) of the solid revealed the presence of CpTiCl_3 as the sole cyclopentadienyl-containing species.

(g) A repeat experiment to (f) using a three-fold excess of TiCl_4 gave a dark brown solid, which on careful sublimation, gave traces of both CpTiCl_3 and $\text{Cl}_3\text{Ti(NMe}_2)_2$, identified by their IR spectra.

(h) Reaction of $\text{CpTi}(\text{NMe}_2)_3$ with MCl_4 ($\text{M} = \text{Zr, Hf}$). $\text{CpTi}(\text{NMe}_2)_3$ was added to an equimolar amount of either ZrCl_4 or HfCl_4 in C_6H_6 to give a dark brown solution and a dark brown oil, in each case. Removal of solvent and extraction of the resultant tarry brown solids with n-hexane, gave pale yellow solutions which, on concentration, gave traces of CpTiCl_3 . In neither case could the brown, tarry residue be identified.

(i) Reaction of $\text{Cp}_2\text{Zr}(\text{NMe}_2)_2$ with SiCl_4 (1:1). A single ampoule bomb containing $\text{Cp}_2\text{Zr}(\text{NMe}_2)_2$ (0.34 g, 1.1 mmol) was connected to the vacuum line, and C_6H_6 (~50 ml) distilled on at 77 K. SiCl_4 (0.2 g, 1.1 mmol) was then distilled onto the frozen benzene solution at 77 K as for (c). On warming to room temperature, the pale yellow colour of $\text{Cp}_2\text{Zr}(\text{NMe}_2)_2$ was discharged to give a colourless solution. Removal of solvent and volatile products in vacuo gave a white solid, identified as Cp_2ZrCl_2 by its IR spectrum in quantitative yield. Distillation of the volatile products gave a small amount of $\text{Cl}_2\text{Si}(\text{NMe}_2)_2$ identified by its ^1H NMR spectrum (C_6H_6).

(j) A repeat experiment to (i) using a two-fold excess of SiCl_4 gave Cp_2ZrCl_2 and a fuming liquid identified as $\text{Cl}_3\text{Si}(\text{NMe}_2)$ by its ^1H NMR spectrum (C_6H_6).

(k) Reaction of $\text{Cp}_2\text{Zr}(\text{NMe}_2)_2$ with GeCl_4 . $\text{Cp}_2\text{Zr}(\text{NMe}_2)_2$ (0.55 g, 1.76 mmol) and GeCl_4 (0.38 g, 1.8 mmol) reacted as in (i) to give Cp_2ZrCl_2 in quantitative yield and a fuming liquid identified as $\text{Cl}_2\text{Ge}(\text{NMe}_2)_2$ by comparison of its ^1H NMR spectrum (C_6H_6) with an authentic sample.

(l) A repeat experiment to (k) with a two-fold excess of GeCl_4 again gave Cp_2ZrCl_2 , and a colourless fuming liquid identified as $\text{Cl}_3\text{Ge}(\text{NMe}_2)$ by its ^1H NMR spectrum (C_6H_6).

(m) Reaction of $\text{Cp}_2\text{Zr}(\text{NMe}_2)_2$ with SnCl_4 . SnCl_4 (0.64 ml, 5.5 mmol) in C_6H_6 (~150 ml) was added dropwise to a well stirred solution of $\text{Cp}_2\text{Zr}(\text{NMe}_2)_2$ (1.7 g, 5.5 mmol) in C_6H_6 (200 ml) to give a pale brown solid and a pale brown solution. The solvent was removed in vacuo, and the resultant pale brown solid extracted with dry Et_2O to leave a pale brown insoluble solid. Removal of the Et_2O solvent gave an off-white solid which, on sublimation in vacuo (423 K) gave Cp_2ZrCl_2 , identified by its IR spectrum.

(n) A repeat experiment to (m) using similar quantities of reagents but with n-hexane, led to the immediate precipitation of a white solid. An IR spectrum of the crude products showed Cp_2ZrCl_2 to be a major constituent of the reaction products. The ^1H NMR spectrum (C_6D_6) contained a single resonance in the Cp region of the spectrum corresponding to Cp_2ZrCl_2 .

(o) Reaction of $\text{Cp}_2\text{Zr}(\text{NMe}_2)_2$ with SnBr_4 . SnBr_4 (0.85 g, 1.9 mmol) in n-hexane (150 ml) was added dropwise to $\text{Cp}_2\text{Zr}(\text{NMe}_2)_2$ (0.6 g, 1.9 mmol) also in n-hexane (200 ml) giving an immediate precipitate of a white solid. An IR spectrum of the crude products revealed Cp_2ZrBr_2 to be a major constituent of the reaction products. The ^1H NMR spectrum (C_6D_6) contained a single Cp resonance corresponding to Cp_2ZrBr_2 .

(p) Reaction of $\text{Cp}_2\text{Zr}(\text{NMe}_2)_2$ with TiCl_4 . TiCl_4 (1.4 ml, 1.3 mmol) in C_6H_6 (10 ml) was added to $\text{Cp}_2\text{Zr}(\text{NMe}_2)_2$ (0.4 g, 1.3 mmol) also in C_6H_6 (50 ml) to give a pale brown solution. The solvent was removed in vacuo to give a dark brown solid which, on sublimation (363 K), gave a chocolate brown solid analysing approximately as $\text{Cl}_2\text{Ti}(\text{NMe}_2)_2$. A ^1H NMR spectrum (C_6D_6)

of the residues obtained after sublimation revealed Cp_2ZrCl_2 as the sole Cp containing product.

(q) A repeat experiment of (p) with a two-fold excess of TiCl_4 gave a dark brown solution, which on removal of the C_6H_6 solvent produced a dark green solid. Fractional sublimation of this solid gave two products corresponding to $\text{Cl}_3\text{Ti}(\text{NMe}_2)$ ($T = 363 \text{ K}$) and Cp_2ZrCl_2 ($T = 423 \text{ K}$).

CHAPTER 5

SOME COMPLEX CHEMISTRY OF INORGANIC HETEROCYCLES

CHAPTER 5

5.1 INTRODUCTION5.1.1 Bonding in inorganic heterocycles

The chemistry of heterocycles containing alternating heteroatoms described by Haiduc (321, 322) as 'alternation heterocycles' has long been a subject of interest. In 1834, Liebig and Wohler synthesised their 'phosphonitrilic chloride' ($(\text{Cl}_2\text{PNH})_x$), the forerunners of such species. This discovery was quickly followed by that of $(\text{SN})_4$ in 1835, and later by $(\text{Ph}_2\text{SiO})_3$ (1905) and borazine $(\text{HBNH})_3$ (1926). Since then a large number of alternation heterocycles containing most combinations of p-block elements, and with a wide variety of substituents have been synthesised. This extensive field has been comprehensively reviewed by Haiduc (321, 322).

Much of the interest in alternation heterocycles has focused on the bonding in these systems. In molecules such as sym-trioxan ($(\text{CH}_2\text{O})_3$) or sym-trithiane ($(\text{CH}_2\text{S})_3$) the 4 coordinate sp_3 carbon atoms have no low-energy p- or d-orbitals suitable for further π -bonding to the O or S atoms, and the rings function as simple cyclic polyethers and polythioethers respectively. When atoms with readily available p- (e.g. B, N, O) or d- (e.g. P, S, As, Sb, Se, Si, Ge) orbitals are included as heteroatoms, however, delocalisation of electron density can occur in the ring giving rise to a conjugated π -systems.

The borazines provide an example where such a π -system is made up solely of p-orbitals. The parent borazine molecule $(\text{HBNH})_3$ or cyclo-1,3,5-tribora-2,4,6-triazane is a colourless volatile liquid which is isoelectronic with benzene.

Electron diffraction studies reveal a planar (D_{3h}) symmetry, with six equal B-N bond lengths (321, 322). Both B and N atoms are sp_2 hybridised, and overlap of the filled N(p)-orbital (the N lone pair) and the vacant B(p)-orbital results in the formation of a cyclic 6π -electron system. 1H NMR studies have established that a ring current exists in the borazines, and that they therefore, contain aromatic character (323). The borazines are not as fully delocalised as benzene, however, as differences in the electronegativities of the B and N heteroatoms causes a certain amount of $(B \rightarrow N)\sigma$ -donation which weakens the π -system. Armstrong and Clark (324) have calculated both the $\pi(N \rightarrow B)$ and $\sigma(B \rightarrow N)$ contributions to the π -system in borazine, Fig. 5.1.1. The overall picture for the borazines can, therefore, be summarised as having a totally delocalised but weak π -system.

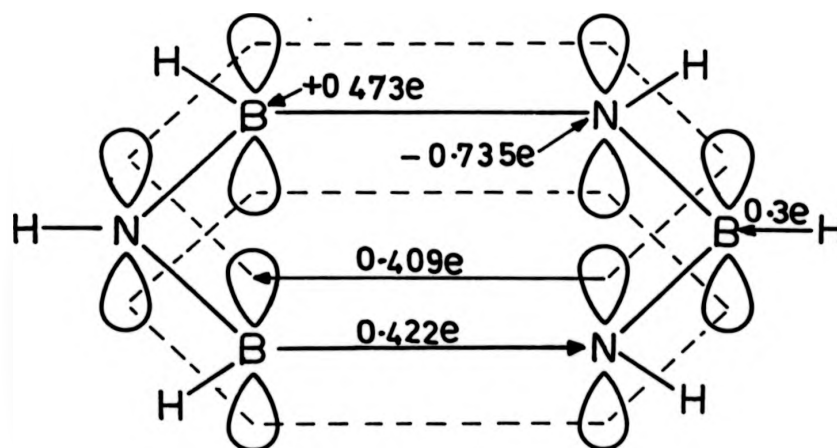


Fig. 5.1.1 Schematic Diagram of Borazine Showing $B \rightarrow N$ σ -Donation, $N \rightarrow B$ π -Donation and Overall Charges on B and N

The boroxines $(RBO)_x$ and borathianes $(RBS)_x$ appear to be delocalised to a

much smaller extent (321).

When second and third row elements (i.e. Si, Ge, P, As, S, Se) are present as ring heteroatoms, the π -system may be augmented by a contribution from (p-d) π -bonding. The most widely studied series of this type in terms of bonding are the phosphazenes. After setting up a simple σ -framework, one electron is left on P(V), and three on N. It is generally accepted that two of the three N electrons are localised in a lone pair (sp_2) orbital, leaving one electron on both P and N free to participate in π -bonding (325). The π -bonding in the phosphazenes can, to a first approximation, be described by a combination of $N(p_z)$, $P(d_{xz})$ and $P(d_{yz})$ orbital overlap. There is no significant interaction between $N(p_z)$ and $P(d_{xy}, d_{x^2-y^2}$ or $d_{z^2})$ orbitals, as the latter are of the wrong symmetry. By taking different combinations of $N(p_z)$ and $P(d_{yz})$ orbitals, two different bonding schemes are possible. If only the $N(p_z)$ and $P(d_{xz})$ orbitals participate in π -bonding a broadly delocalised pseudoaromatic π -orbital would be formed, Fig. 5.1.2a.

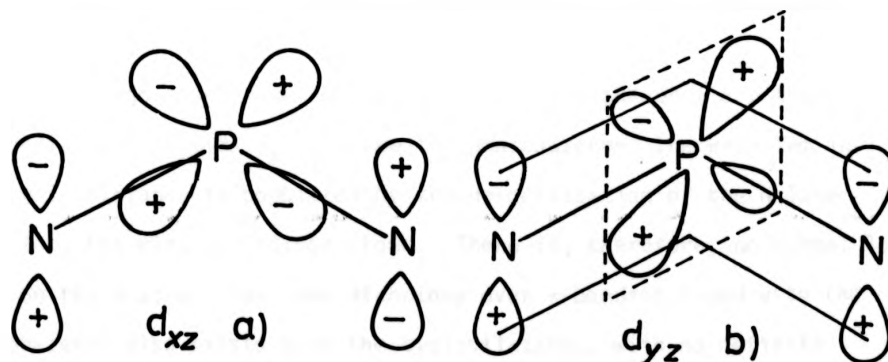


Fig. 5.1.2 Formation of Skeletal $d\pi$ - $p\pi$ Bonds

If overlap is only achieved between $N(p_z)$ and $P(d_{yz})$ a delocalised system would again be formed, similar in character to the $p\pi$ - $p\pi$ aromatic system found in the borazines (325). Involvement of both $P(d_{xz})$ and $P(d_{yz})$

gives a totally different π -system in which the π -orbitals separate out into "islands" of π -character interrupted by the P atoms (326) (Fig. 5.1.3).

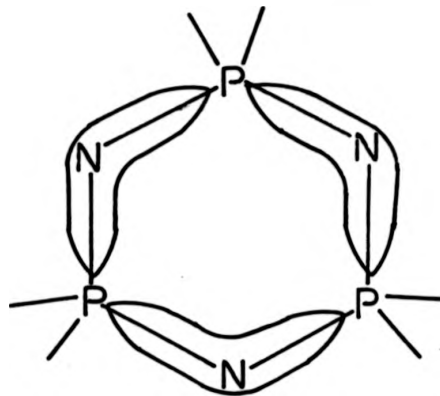


Fig. 5.1.3 "Island" Model for Cyclophosphazenes $(R_2PN)_3$

Craig and Mitchell (326) have calculated that for equal participation of $P(d_{xz})$ and $P(d_{yz})$ orbitals, the three-centre "island" type bonding, accounts for 85-95% of the delocalisation energy, the remaining 5-15% being due to delocalisation over the whole ring. The π -bonding in these molecules is complex, and at present there is no unambiguous experimental evidence which favours one model over the other.

An analogous series of compounds to the phosphazenes are the cyclosilazanes $(R_2SiNR')_x$. Unlike the phosphazenes, the π -system in the cyclosilazanes is populated by the delocalisation of the N lone pair into the ring π -electron cloud. There is, therefore, no formal lone pair on the N atom. The same dichotomy over π -bonding found with the phosphazenes also exists with the cyclosilazanes, with no definite preferred bonding scheme. However, 1H NMR studies have established both a lack of ring current (327), (i.e. aromaticity) and the lack of transmission effects through the Si-N-Si linkages (262). These observations, coupled with the known donor chemistry of the cyclosilazanes

(see Section 5.1.2) suggest an "island" description of the π -bonding to be the most appropriate. For the cyclosiloxanes, short Si-O bond lengths (e.g. 1.614 Å in $(\text{Me}_2\text{SiO})_3$) were again interpreted in terms of a $p\pi-d\pi$ interaction, although the resonance energy in this case appears to be very small. The type of bonding is uncertain, but LCAO-MO calculations favour the "island" bonding scheme. Of note are the low bond angles in $(\text{Me}_2\text{SiO})_3$, i.e. $\text{Si}\hat{\text{O}}\text{Si}$ (136°) and OSiO (104°) cf. $\text{Si}\hat{\text{O}}\text{Si}$ (142.5°), OSiO (109°) in $(\text{Me}_2\text{SiO})_4$ (321). The greater basicity of the trimeric ring was attributed to ring strain (321).

5.1.2 Donor chemistry of alternation heterocycles

The donor chemistry of the alternation heterocycles must, to some extent, reflect the electronic structure of the ring and can, therefore, be used as a probe into the internal ring bonding. Two different sorts of complexes are possible, depending on whether the ring electron density is localised on a donor atom, or spread out over the entire π -system.

The first of these possibilities is illustrated in the complexes of sym-trithiane ($(\text{CH}_2\text{S})_3$) (328-333) and tetrahydrotriazine (334) $(\text{CH}_2\text{NR})_3$. These molecules act purely as σ -donors towards metal halides (328-331) and carbonyls (332-33), there being no evidence for any sort of π -interaction. The borazines on the other hand present a quite different picture. Photolysis of $(\text{RBNR}')_3/\text{M}(\text{CO})_6$ solutions, or displacement of coordinated solvent molecules from $\text{M}(\text{CO})_3 \cdot 3\text{L}$ ($\text{L} = \text{MeCN}$, THF, dioxan) by the appropriate borazine both give neutral octahedral complexes of the type $\text{M}(\text{CO})_3 \cdot (\text{RBNR}')_3$ (335). In each case, the borazine ring was believed to be coordinated to the $\text{M}(\text{CO})_3$ moiety via the ring π -system as in $\text{Cr}(\text{CO})_3(\text{Me}_6\text{C}_6)$. For $\text{Cr}(\text{CO})_3(\text{EtNBt})_3$, this structural assignment has been confirmed by a single

crystal X-ray study (336) (Fig. 5.1.4).

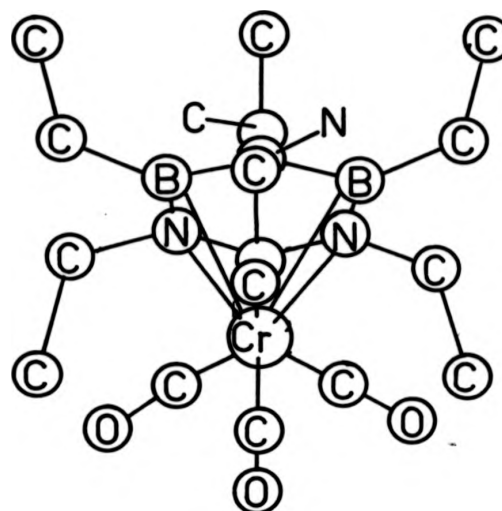


Fig. 5.1.4 Crystal Structure of $\text{Cr}(\text{CO})_3(\text{EtNBt})_3$

Slight puckering of the $(\text{EtNBt})_3$ ring was observed in the complex, the Cr-N bond (2.22 Å) being marginally shorter than Cr-B (2.31 Å). It was suggested that this may be a result of localisation of electron density on the N atoms (337). Since the difference between the Cr-N and Cr-B bond lengths corresponds to the difference in covalent radii of B and N, however, it was not possible to decide between localised and delocalised bonding models (338). The borazines can also act as σ -donors. Reactions of $(\text{MeNBH})_3$ with excess HCl gives the trihydrochloride salt $(\text{MeNBH})_3 \cdot 3\text{HCl}$, in which it is believed that the three ring N atoms are protonated (337). The donor chemistry of the borazines has been reviewed (335).

The uncertainty surrounding the π -bonding in phosphazenes is carried over into their donor chemistry. A number of crystal structures have

appeared, with both metal halides (339, 340), and metal carbonyls (338, 341) as the acceptor species. The structures of $\text{CuCl}_2(\text{Me}_2\text{PN})_4$ (339) and $(\text{N}_6\text{P}_6(\text{NMe}_2)_{12})\text{CuCl}^+\text{CuCl}_2^-$ (340) both show the metal atom coordinated to a N centre in a σ sense via a N lone pair. $(\text{N}_4\text{P}_4(\text{NMe}_2)_8)\text{W}(\text{CO})_4$ presents a rather unusual example (341), with both cyclic and exocyclic N atoms coordinated to W. Cotton and coworkers found a somewhat different mode of coordination with $(\text{Me}_2\text{PN})_4\text{M}(\text{CO})_3$ (338). The crystal structure was here found to bear a distinct overall resemblance to $\text{Mo}(\text{CO})_3$ (cyclooctatetrene), although poor crystal data prevented a detailed bonding analysis. The proposed structure for the bright yellow $(\text{Cl}_2\text{P-N})_3\cdot\text{Cr}(\text{CO})_3$ isolated by Hota and Harris included a ring acting as an arene-type π -donor (342).

The mode of bonding in cyclosilazane complexes appears to be more straightforward. Willey found no evidence for any π -donor activity for $(\text{Me}_2\text{SiNH})_3$ towards $\text{M}(\text{CO})_6$ ($\text{M} = \text{Cr}, \text{Mo}, \text{W}$) (299), which is in accordance with the "island" type model (Section 5.1.1). Instead, well defined octahedral adducts were obtained with covalent metal trihalides, i.e. $(\text{Me}_2\text{SiNH})_3\cdot\text{MCl}_3$ ($\text{M} = \text{Ti}, \text{V}$) (299). A structure of the type

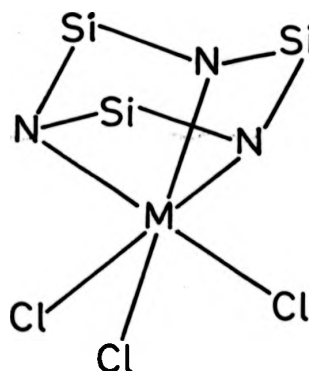


Fig. 5.1.5 Proposed Structure of $(\text{Me}_2\text{SiNH})_3\text{MCl}_3$, ($\text{M} = \text{Ti}, \text{V}$)

was proposed, in which only the N atoms were coordinated to the metal ion (299).

Further studies with both the trimeric and tetrameric rings $((\text{Me}_2\text{SiNH})_{3,4})$ provided complexes with MCl_4 ($\text{M} = \text{Ti}, \text{Sn}$) (298, 300) and MCl_3 ($\text{M} = \text{Ti}, \text{V}$) (300). $(\text{Ph}_2\text{SiPPh})_3$ is also believed to act as a terdentate donor in $(\text{Ph}_2\text{SiPh})_3.\text{Mo}(\text{CO})_3$ (343). Localisation of the donor atom lone pair is apparent in complexes of (S_4N_4) . The crystal structures of $\text{S}_4\text{N}_4.\text{SbCl}_5$ (344) and $\text{S}_4\text{N}_4.\text{BF}_3$ (345) show the ring to be coordinated through only one of the four ring N atoms.

5.2.1 Reactions of $(\text{CH}_2\text{O})_3$ with MCl_4 ($\text{M} = \text{Ti}, \text{Sn}$) and $\text{ZrCl}_4.2\text{NMe}_3$

MCl_4 ($\text{M} = \text{Ti}, \text{Sn}$) reacted with $(\text{CH}_2\text{O})_3$ in C_6H_6 solution (1:2) to give glutinous off-white precipitates. Work up of the reaction products gave off-white powdery solids of indefinite composition. The IR spectra of these products was similar, with only broad bands of little diagnostic value, and a featureless metal halide region. This, coupled with a general insolubility in all common solvents, strongly suggests a polymeric formulation. This result does not set a precedent. Polymerisation involving $(\text{CH}_2\text{O})_3$ has previously been observed with metal halide catalysts, although under somewhat forcing conditions (346). Ring degradation to give the parent formaldehyde (CH_2O) was found with ZnCl_2 and FeCl_3 (347). A mechanism in which ring opening of the trimeric ring occurs as an initial step followed by polymerisation via $\text{M} + (-\text{CH}_2\text{O}-\text{CH}_2\text{O}-\text{CH}_2\text{O}-)$ coordination is proposed. ZnCl_2 and FeCl_3 by virtue of their low Lewis acidities and relatively unreactive M-Cl bonds, are less likely to be able to initiate the second polymerisation step than MCl_4 ($\text{M} = \text{Ti}, \text{Sn}$). The isolation of $\text{SnCl}_4.2\text{CH}_2(\text{OMe})_2$ (348) as a stable adduct is in keeping with the proposed intermediate complex.

s-Trioxan displaced coordinated NMe_3 from solutions of $\text{ZrCl}_4.2\text{NMe}_3$ in C_6H_6 to give a powdery white solid of approximate composition

$\text{ZrCl}_4 \cdot 2(\text{CH}_2\text{O})_3$. The IR spectrum, however, bore little resemblance to that of the free ligand (349), indicating ring opening as the most likely product. A strong band at 305 cm^{-1} is assigned as a Zr-Cl stretching mode. The isolation of the ring opened complex for $\text{M} = \text{Zr}$ is further evidence for the similar complexes proposed in the polymerisation of $(\text{CH}_2\text{O})_3$ by MCl_4 ($\text{M} = \text{Ti}, \text{Sn}$).

5.2.2 Reaction of $(\text{CH}_2\text{O})_3$ with $\text{MCl}_3 \cdot 2\text{NMe}_3$ ($\text{M} = \text{V}, \text{Cr}$)

Addition of C_6H_6 solutions of $\text{MCl}_3 \cdot 2\text{NMe}_3$ ($\text{M} = \text{V}, \text{Cr}$) to a three-fold excess of $(\text{CH}_2\text{O})_3$ produced no immediate change, but on removal of solvent, pale pink ($\text{M} = \text{V}$) or pale mauve ($\text{M} = \text{Cr}$) solids were obtained. Microanalysis revealed the products to be mixed adducts (i.e. containing both NMe_3 and $(\text{CH}_2\text{O})_3$) of no definite stoichiometry. Bands in the IR spectrum at 1265 cm^{-1} , $\nu_{\text{as}}(\text{CN})$; $995\text{--}997 \text{ cm}^{-1}$, $\rho(\text{CH}_3)$; $820\text{--}827 \text{ cm}^{-1}$, $\nu_{\text{s}}(\text{CN})$; $523\text{--}536 \text{ cm}^{-1}$, $\delta_{\text{as}}(\text{cm})$ and $440\text{--}445 \text{ cm}^{-1}$, $\delta_{\text{s}}(\text{CN})$ are attributable to coordinated trimethylamine (66). Bands at $1730\text{--}1735 \text{ cm}^{-1}$; $1244\text{--}1245 \text{ cm}^{-1}$; $995\text{--}998 \text{ cm}^{-1}$ (a_1 breathing mode) and 510 cm^{-1} (a' ring deformation) indicate the presence of coordinated $(\text{CH}_2\text{O})_3$ (349). Unfortunately, bands diagnostic of the denticity of the coordinated $(\text{CH}_2\text{O})_3$ were in each case masked by intense NMe_3 bands. Strong bands at $330, 310 \text{ cm}^{-1}$ ($\text{M} = \text{V}$) and $387, 380 \text{ cm}^{-1}$ ($\text{M} = \text{Cr}$) are assigned as M-Cl stretching modes. Both compounds were found to be surprisingly soluble in non-polar solvents such as C_6H_6 and n-hexane. Coordinating solvents induced ligand substitution. For the V complex, solution in MeCN was accompanied by a colour change (pink \rightarrow green), and $\text{VCl}_3 \cdot 3\text{MeCN}$ was identified by comparison of the UV spectra of the test solution and an authentic sample.

In conclusion, $(\text{CH}_2\text{O})_3$ was found to act as a weak O donor towards both V (III) and Cr (III). With the more powerful Lewis acids MCl_4 ($\text{M} = \text{Ti}, \text{Zr}, \text{Sn}$) ring opening rather than complexation predominates.

5.3 Complexes of $(\text{CH}_2\text{S})_3$ with Covalent Metal Chlorides

Solutions of MCl_4 ($\text{M} = \text{Ti}, \text{Sn}$), AuCl_3 in CHCl_3 or SbCl_5 in CCl_4 reacted with solutions of s-trithiane in the same solvent to precipitate simple 1:1 ($\text{M} = \text{Au (III)}, \text{Sb (V)}$) or 1:2 ($\text{M} = \text{Ti}, \text{Sn}$) adducts. $(\text{CH}_2\text{S})_3$ reacted with a suspension of ZrCl_4 in CHCl_3 to give an addition compound, but samples were found to be contaminated with unreacted metal halide. Attempts to extract the $\text{ZrCl}_4 \cdot 2(\text{CH}_2\text{S})_3$ with CHCl_3 (which proved a suitable solvent for the Sn (IV) adduct) using a Soxhlet apparatus resulted in small amounts of free $(\text{CH}_2\text{S})_3$. Sym-trithiane reacted with two mole equivalents of TiCl_4 in CH_2Cl_2 to give a pale yellow solid analysing approximately as $2(\text{TiCl}_4) \cdot (\text{CH}_2\text{S})_3$. Similar products were produced by stirring a suspension of $\text{TiCl}_4 \cdot 2(\text{CH}_2\text{S})_3$ with an excess of TiCl_4 in non-coordinating solvents such as CH_2Cl_2 and CCl_4 . The second molecule of TiCl_4 was found to be only weakly bonded, however, and could be removed quite easily by pumping in vacuo, or by continuous washing with n-hexane in vacuo, eventually to give bright orange $\text{TiCl}_4 \cdot 2(\text{CH}_2\text{S})_3$. SbCl_3 when reacted with a two-fold excess of ligand gave only the known 1:1 adduct $\text{SbCl}_3 \cdot (\text{CH}_2\text{S})_3$ (350, 351). In contrast AsCl_3 , AlCl_3 and GeCl_4 gave no isolable reaction products. Ligand substitutions as an alternative synthetic route proved far from satisfactory. $(\text{CH}_2\text{S})_3$ failed to replace the coordinated ligands from $\text{MCl}_3 \cdot 3\text{L}$ ($\text{M} = \text{Ti}, \text{V}$, $\text{L} = \text{MeCN}$, THF), $\text{ZrCl}_4 \cdot 2\text{NMe}_3$ or $\text{Mo(CO)}_3\text{MeCN}$. Reactions with MoCl_5 and VOCl_3 in CCl_4 gave dark brown solids in each case. The IR spectra of these products bore little resemblance to that of the free ligand (329) indicating ring opening rather than complexation as the dominant reaction. MoCl_5 at least is well known for reactions in which O is abstracted from donor molecules (2), and a similar situation would seem to be in force with $(\text{CH}_2\text{S})_3$.

The simple 1:2 Sn (IV) , Ti (IV) and 1:1 Sb (V) complexes proved to be highly air-moisture sensitive, but $\text{AuCl}_3 \cdot (\text{CH}_2\text{S})_3$ could be handled on the

bench without any trace of decomposition. Solution in donor solvents was, in general, accompanied by displacement of the ligand. In particular, $\text{TiCl}_4 \cdot 2(\text{CH}_2\text{S})_3$ proved to be extremely susceptible to solvolysis, decomposition occurring even in weak donor solvents such as Et_2O . Interestingly, reaction of TiBr_4 and $(\text{CH}_2\text{S})_3$ in Et_2O leads to the isolation of the stable 1:2 adduct (328). This is perhaps a reflection of the greater class B character of TiBr_4 cf. TiCl_4 . Adducts of s-trithiane have been prepared, but most have involved soft metals such as Ag (I) (329, 330), Hg (II) (329-331), Cr(0), Mo(0), W(0) (332, 333) and Sb (III) (350, 351). The inability of $(\text{CH}_2\text{S})_3$ to displace coordinated solvent from Ti (III), V (III) and Zr (IV) and the ease of removal from Ti (IV) and Sn (IV) suggests that it acts only as a weak donor towards the hard metal halides.

The IR spectra of the complexes are given in Table 5.3.1. Dalziel and coworkers (330) have interpreted the 26 bands in the IR spectrum of $(\text{CH}_2\text{S})_3$ in terms of 17 fundamentals ($7a_1 + 10_e$) expected for a chair (C_{3v}) configuration. Planar (D_{3h}) and boat (C_s) configuration should give rise to 9 and 30 fundamental bands respectively. An X-ray study has confirmed the chair assignment for $(\text{CH}_2\text{S})_3$ in the solid phase, Fig. 5.3.1 (352).

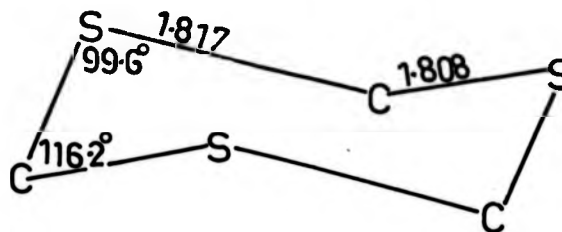


Fig. 5.3.1 Crystal Structure of $(\text{CH}_2\text{S})_3$

$(\text{CH}_2\text{S})_3$	$\text{TiCl}_4 \cdot 2\text{L}$	$\text{SnCl}_4 \cdot 2\text{L}$	$\text{SbCl}_5 \cdot \text{L}$	$\text{AuCl}_3 \cdot \text{L}$	$\text{SbCl}_3 \cdot \text{L}$	Assignment
2959(w)	2995(m) 2964(m)	2983(m) 2972(s)	2985(m) 2950(sh)	2990(s) 2970(m)	2985(m) 2950(sh)	$\nu\text{CH}(\text{e})$
2980(w)	2928(w)	2920(s)	2911(s)	2924(m) 2907(m)	2920(m)	$\nu\text{CH}(\text{a}_1)$
2155(w)	-	-	-	-	-	$3\nu_6$
1380(s)	1388(s) 1374(w) 1320(w)	1386(s) 1375(m) 1375(m)	1388(m) 1367(vw) 1355(m)	1390(s) 1378(s) 1317(w)	1384(sh) 1375(s)	$\text{CH}_2\text{wag}(\text{e})$
1221(m)	1216(m)	1218(m)	1262(w) 1231(vw)	1222(w) 1218(w)	1218(m)	$\text{CH}_2\text{twist}(\text{e})$
907(s)	906(s)	906(s)	917(m) 902(m)	920(vs)	912(s)	$\text{CH}_2\text{rock}(\text{a}_1)$
785(w)	796(w) 764(m)	-	808(w)	810(w)	-	$\nu_2 + \nu_7$
725(s)	749(m) 730(w) 722(m)	743(w) 732(m) 711(m)	738(s) 723(m) 716(w)	745(m) 735(w) 715(m) 705(m)	725(s)	ν_s
660(w)	659(w)	661(w)	665(w)	671(w)	667(m)	ν_6
650(w)	646(w)	636(s)	628(w)	635(s)	-	ν_1
418(w)	-	415(w)	-	-	-	ν_2
390(m) 352(w)	377(w) 367(w)	375(w)	391(w)	-	-	ν_7
326(w) 306(s)	312(w)	296(m)	-	326(m)	-	ν_3
277(m) 254(w)	-	-	287(w)	-	-	ν_8
-	391(vs)	322(vs)	345(vs)	365(vs) 340(m)	306(vs)	M-Cl

Table 5.8.1 IR Spectra of $(\text{CH}_2\text{S})_3$ adducts

The IR spectra of the complexes bear a distinct resemblance to the spectrum of the free ligand, suggesting that the chair configuration of the ligand

persists on complexation. A general lowering of the CS stretching and CH_2 group frequencies from those found in the free ligand was observed, in accordance with S donation (350). Complexation is accompanied by a reduction in the symmetry of the $(\text{CH}_2\text{S})_3$ ring. Consequently, bands associated with CS stretching modes in the free ligand are found as multiplets in the spectra of the adducts, e.g. the strong ring stretch at 725 cm^{-1} in $(\text{CH}_2\text{S})_3$ appears as a triplet in $\text{TiCl}_4 \cdot 2(\text{CH}_2\text{S})_3$ (749 , 730 and 722 cm^{-1}). For complexes which are coordinatively unsaturated, intermolecular association in the solid phase can increase the symmetry of the ligand. This effect is typified in $\text{SbCl}_3 \cdot (\text{CH}_2\text{S})_3$ (Fig. 5.3.2), the crystal structure of which, shows each $(\text{CH}_2\text{S})_3$ molecule to be centrally placed between three different SbCl_3 centres (351).

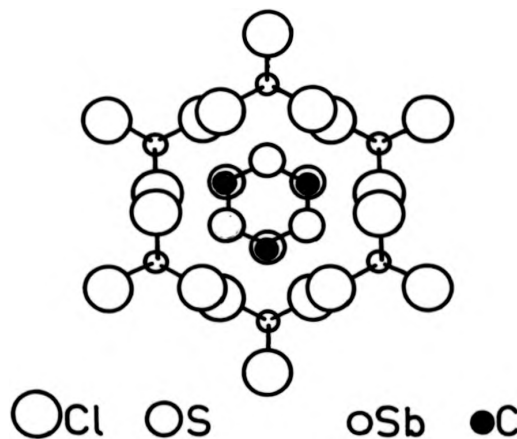


Fig. 5.3.2 Crystal Structure of $\text{SbCl}_3 \cdot (\text{CH}_2\text{S})_3$ (projection on xy plane)

Bands in the IR spectra of the $\text{SbX}_3 \cdot (\text{CH}_2\text{S})_3$ ($\text{X} = \text{Cl}, \text{Br}, \text{I}$) (350) adducts, therefore, show no splitting due to ligand asymmetry.

Single intense bands in the low IR spectra of $\text{MCl}_4 \cdot 2(\text{CH}_2\text{S})_3$ at 391 ($\text{M} = \text{Ti}$)

and $322 \text{ (M = Sn) cm}^{-1}$ are in accordance with an octahedral trans (D_{4h}) arrangement of ligands (Fig. 5.3.3). Bands at 365 and 340 cm^{-1} in the spectrum of $\text{AuCl}_3 \cdot (\text{CH}_2\text{S})_3$ fall well within the range of values found for square planer (C_{2v}) $\text{AuX}_3 \cdot \text{L}$ adducts with substituted pyridine (353), a similar structure is proposed in the present instance (Fig. 5.3.3). An octahedral (C_{4h}) geometry is proposed for $\text{SbCl}_5 \cdot (\text{CH}_2\text{S})_3$ on the basis of a single strong Sb-Cl band at 345 cm^{-1} cf. SbCl_6^- (336 cm^{-1}) (354) (Fig. 5.3.3).

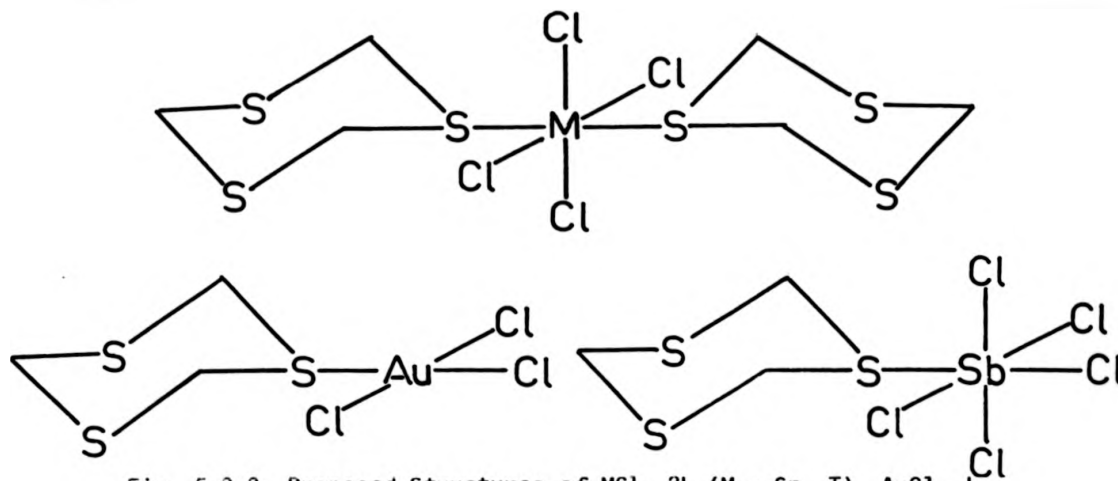


Fig. 5.3.3 Proposed Structures of $\text{MCl}_4 \cdot 2\text{L}$ ($\text{M} = \text{Sn, T}$), $\text{AuCl}_3 \cdot \text{L}$ and $\text{SbCl}_5 \cdot \text{L}$

Samples of brown $\text{AuCl}_3 \cdot (\text{CH}_2\text{S})_3$ sealed in ampoules under an N_2 atmosphere were observed to slowly decompose over a 3 month period to give a pale yellow solid. An IR spectrum showed bands attributable to uncomplexed $(\text{CH}_2\text{S})_3$, and an intense AuCl mode at 333 cm^{-1} . Reduction ($\text{Au (III)} \rightarrow \text{Au (I)}$) is proposed, followed by dissociation of the $\text{Au (I)} \cdot (\text{CH}_2\text{S})_3$ complex. The oxidation product was not identified, but low intensity bands in the IR spectrum not attributable to either $\text{AuCl}_3 \cdot (\text{CH}_2\text{S})_3$ or free $(\text{CH}_2\text{S})_3$, suggest a partially chlorinated $(\text{CH}_2\text{S})_3$ ring as a possible product.

One point emerging from this and previous work is that in all cases

$(\text{CH}_2\text{S})_3$ acts as an essentially monodentate donor. A similar situation was recently found for complexes of 1,4-dithiacycloheptane with SbX_3 ($\text{X} = \text{Cl}, \text{Br}, \text{I}$); the ligand bridging between two SbX_3 units rather than chelating to a single Sb (III) atom (355). Conversely for the 1:1 complexes $\text{TiX}_4 \cdot (\text{C}_4\text{H}_8\text{S}_2)$ ($\text{X} = \text{Cl}, \text{Br}$), bidentate behaviour on the part of the ligand was proposed (328). Factors affecting the coordination behaviour of these polythioethers appear to be complex, but the steric dictates of the SCS moiety must play an important part in deciding the resulting coordination geometry.

Campaigne and coworkers (356) have demonstrated that in solution s-trithiane retains the chair configuration that it adopts in the solid phase (352). The ^1H NMR of s-trithiane at 60 MHz showed only a single sharp resonance due to the rapid interconversion of the axial (a) and equatorial (e) methylinic protons via ring inversion, Fig. 5.3.4.

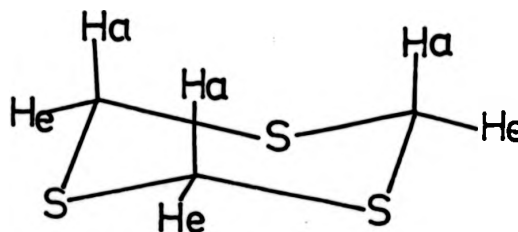


Fig. 5.3.4. s-Trithiane Showing Axial and Equatorial Protons

At higher fields (400 MHz), the single resonance representing the fast exchange limit is seen to broaden on lowering the temperature, due to a reduction in the ring inversion rate (Fig. 5.3.5). Between 263 and 253 K the single resonance splits into two corresponding to the axial (a) and equatorial (e) protons respectively. The spectrum at 238 K is sufficiently well resolved to show geminal coupling between the axial and equatorial protons.

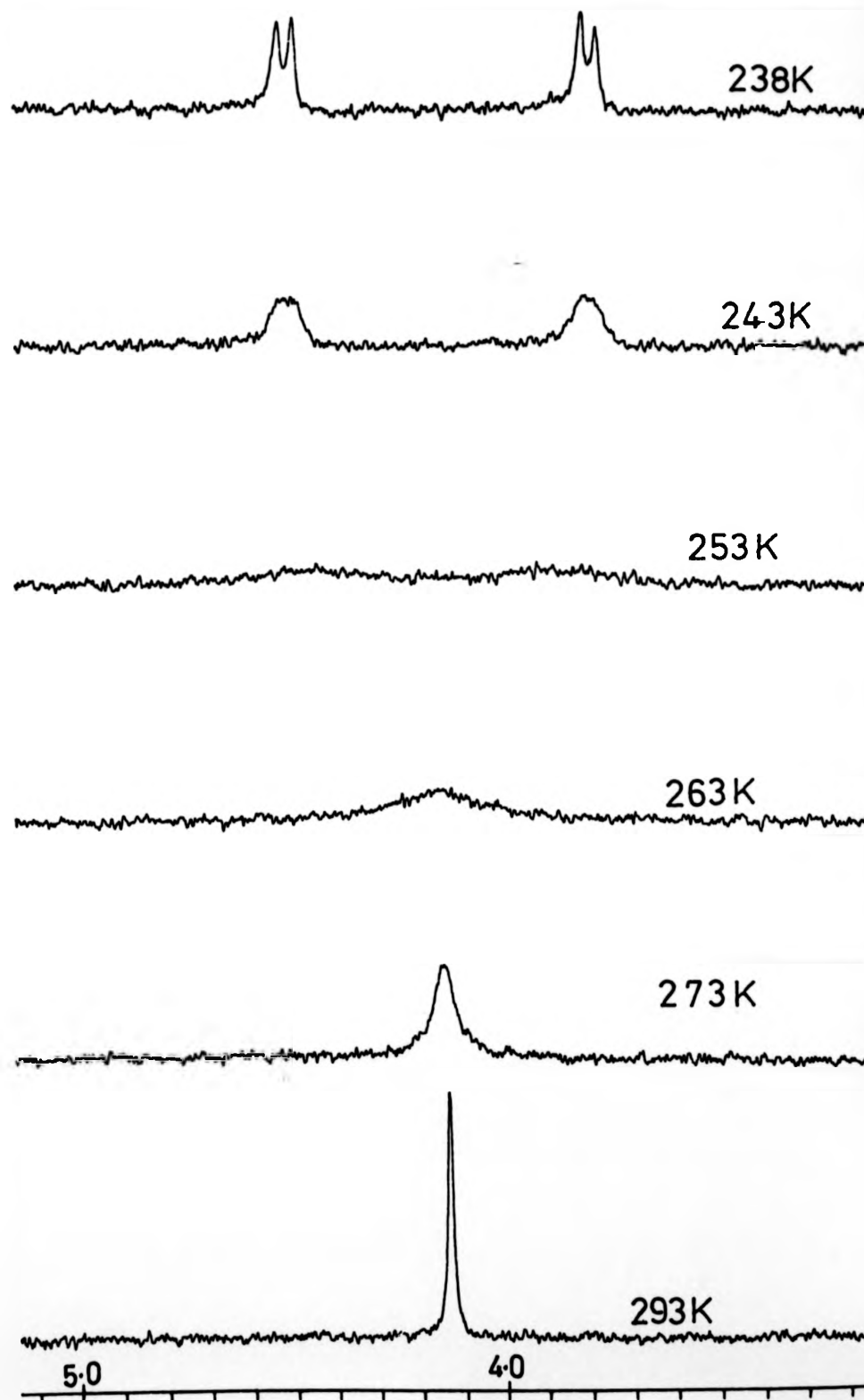


Fig. 5.3.5 Variable Temperature ^1H NMR Spectra of $(\text{CH}_2\text{S})_3$
(400 MHz, CDCl_3)

The variable temperature ^1H NMR spectra of $\text{SnCl}_4 \cdot 2(\text{CH}_2\text{S})_3$ are shown in Fig. 5.3.6. As with the free ligand, dynamic behaviour in the ring is indicated by the broadening of the methylene proton resonance at low temperatures, but here broadening is attributed to a reduction in the rate at which the ligand coordination site interchanges between the three S donor centres (333). The single sharp signals, seen at room temperature, correspond to the fast exchange limit of both the donor site interchange rate and the ring inversion rate. At 243 K the spectrum reveals two resonances due to the methylene protons adjacent to the S donor atom (H_a and H_a') and opposite the S donor atom (H_b and H_b'). No evidence was found for any distinction between the axial (a and b) and equatorial (a' and b') protons (Fig. 5.3.7). The fact that the (220 MHz) spectrum of the free ligand at 233 K (Fig. 5.3.5) is much broader (linewidth at half height = ~ 90 Hz) than that of the coordinated ligand at the same temperature (33 Hz) suggests that the rate of ring inversion is greatly enhanced on complexation

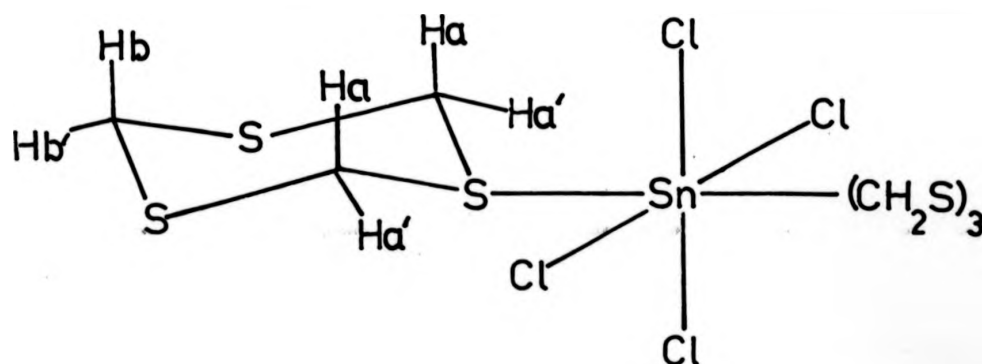


Fig. 5.3.7 $\text{SnCl}_4 \cdot 2(\text{CH}_2\text{S})_3$ Showing Magnetically Inequivalent Protons

A third type of dynamic phenomenon has been observed for the $\text{S}(\text{CH}_2)_5$ ring in trans $\text{PtX}_2(\text{S}(\text{CH}_2)_5)_2$ ($\text{X} = \text{Cl}, \text{Br}, \text{I}$) by Abel and coworkers (357).

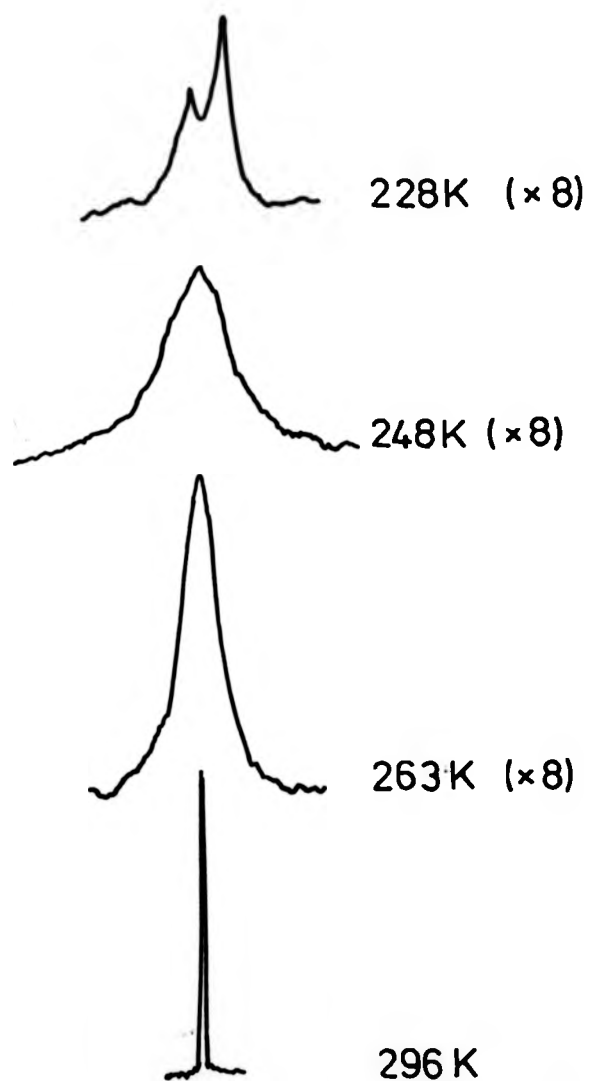


Fig. 5.3.6 Variable Temperature ^1H NMR Spectra of $\text{SnCl}_4 \cdot 2(\text{CH}_2)_3$
(220 MHz, CDCl_3)

The S donor atom can coordinate to the metal atom via either the axial (ax) or equatorial (eq) lone pair. With two such ligands coordinated, there are four possible conformers, namely (ax-ax), (eq-eq) and the degenerate (ax-eq) and (eq-ax). The populations of each of these conformers were established in the trans $\text{PtX}_2\text{2}(\text{S}(\text{CH}_2)_5)$ systems by integration of the ^1H NMR signal observed for each conformation, which were found to have slightly different chemical shifts. There was, however, no indication of similar isomerisation in the trans $\text{SnCl}_4\cdot 2(\text{CH}_2\text{S})_3$ system. For trans $\text{PtX}_2\text{2}(\text{S}(\text{CH}_2)_5)_2$, although the Cl and Br complexes gave a mixture of conformers, the I species was found to reside totally in the eq-eq configuration, and this was attributed to steric interaction between the I atoms and the methylene protons on the ligand. It is not then unreasonable to suggest that the four meridional Cl atoms in trans $\text{SnCl}_4\cdot 2(\text{CH}_2\text{S})_3$ have approximately the same effect as the two I atoms in trans $\text{PtI}_2\cdot 2(\text{S}(\text{CH}_2)_5)$, and that only the eq-eq isomer, Fig. 5.3.7, exists in solution.

Solutions of $\text{SbCl}_3\cdot (\text{CH}_2\text{S})_3$ in CD_3CN also exhibited line broadening in their ^1H NMR spectra, but the spectra obtained were found to closely follow those obtained for the free ligand. The inference from this is that either the rate of donor site interchange is very fast, or the complex is completely dissociated in solution. displacement of the ligand by CD_3CN is unlikely, as spectra of $\text{SbCl}_3\cdot (\text{CH}_2\text{S})_3$ in MeCN solution showed no sign of coordinated MeCN. Considering the weak Sb-S bond found for $\text{SbCl}_3\cdot (\text{CH}_2\text{S})_3$ in the solid state (350), dissociation and fast donor interchange seem equally likely. Unfortunately, the shifts seen on coordination were too small to make any meaningful distinction between the two.

5.4 Reactions of $(\text{Me}_2\text{SiO})_{3,4}$ With Some Covalent Metal Halides

The donor chemistry of the cyclosiloxanes $(\text{Me}_2\text{SiO})_3$ and $(\text{Me}_2\text{SiO})_4$ was investigated with a number of covalent metal halides, but in each case the siloxane ring proved to be insufficiently basic to yield coordination compounds. With $\text{MCl}_3 \cdot 2\text{NMe}_3$ ($\text{M} = \text{Ti}, \text{Cr}$) and $\text{CrCl}_3 \cdot 3\text{MeCN}$, $(\text{Me}_2\text{SiO})_{3,4}$ failed to react, and the ligand was recovered unchanged. Reactions with MCl_4 ($\text{M} = \text{Ti}, \text{Sn}$) although not providing adducts did give some interesting results. Dropwise addition of MCl_4 to a two-fold excess of $(\text{Me}_2\text{SiO})_{3,4}$ in C_6H_6 gave colourless, fuming oils on removal of solvent (10 days). The IR spectra of the products in the $4000\text{--}400\text{ cm}^{-1}$ region were virtually identical. Strong broad bands at $\sim 2964\text{ cm}^{-1}$, $\nu(\text{CH})$; $\sim 1264\text{ cm}^{-1}$, $\delta(\text{CH}_3)$; $\sim 1070\text{ cm}^{-1}$, $\nu(\text{Si-O})$; and 850 cm^{-1} , $\nu(\text{Si-C})$ are typical of those found in a wide range of both linear and cyclic siloxanes (321), and are, therefore, of little diagnostic value. Skeletal ring modes found in the free ligands in the $1000\text{--}300\text{ cm}^{-1}$ region are absent from the spectra of the products however, suggesting a ring opened product. Further evidence for ring opening comes from the ^1H NMR spectra (60 MHz) of the products, which were identical for both the $(\text{Me}_2\text{SiO})_3$ and $(\text{Me}_2\text{SiO})_4$ based products. A series of sharp resonances associated with Si-Me protons were observed at $\delta 0.2\text{--}0.7$; on the basis of each unit in the $(\text{Me}_2\text{SiO})_x$ chain giving a separate resonance, a chain length of at least 12 units is indicated. By analogy with $\text{Cl}(\text{Me}_2\text{SiO})_4\text{TiCl}_3$ (358), a structure of the type $\text{Cl}(\text{Me}_2\text{SiO})_{12}\text{TiCl}_3$ is proposed in the present instance. A strong Ti-Cl mode at 385 cm^{-1} supports this formulation. Polymerisation of the cyclosiloxanes has been achieved using a variety of Lewis acid catalysts, but always employing high temperatures (359). For example, TiCl_4 failed to polymerise $(\text{Me}_2\text{SiO})_4$ at less than 543 K. Reaction times for these experiments were, however, relatively short (~ 6 hours). The present result merely suggests that the

polymerisation is relatively slow.

One point to emerge is that under similar reaction conditions reactions of TiCl_4 with $(\text{Me}_2\text{SiO})_3$ or $(\text{Me}_2\text{SiO})_4$ gave identical products. Although there was no observable reaction between $(\text{Me}_2\text{SiO})_4$ and SnCl_4 , work up of the reaction products of $(\text{Me}_2\text{SiO})_3$ and SnCl_4 found only the tetrameric ring. It would appear that the isomerisation reaction



is promoted by both TiCl_4 and SnCl_4 . Ring expansion and consequently the relief of ring strain has previously been noted for $(\text{Me}_2\text{SiS})_2$, which spontaneously isomerises to $(\text{Me}_2\text{SiS})_2$ at room temperature (321), and for the Lewis acid catalysed expansion of cyclosilazanes (321).

5.5 Complexes of Hexamethylborazine with Covalent Metal Halides

Reaction of hexamethylborazine (HMB) with an equimolar amount of TiCl_4 in C_6H_6 solution led to the isolation of $2\text{TiCl}_4\cdot\text{HMB}$ as an orange solid. No evidence was found for the 1:1 adduct reported by Nöth and coworkers (60). Anderson and Lagowski found no reaction between SnCl_4 and HMB even after 22 hours at 373 K (361). Extended reaction times (1 year) gave a similar result, with HMB being recovered in better than 95% yield. No reaction was observed between HMB and either $\text{VCl}_3\cdot 3\text{MeCN}$ or $\text{TiCl}_3\cdot 3\text{THF}$, while the $\text{CrCl}_3\cdot 2\text{NMe}_3/\text{HMB}$ system yielded only $(\text{CrCl}_3)_2\cdot 2\text{NMe}_3$.

$2\text{TiCl}_4\cdot\text{HMB}$ was found to be highly air-moisture sensitive and insoluble in non-polar solvents (e.g. C_6H_6 , CHCl_3 and CH_2Cl_2). In donor solvents, solution was accompanied by ligand replacement. This was investigated in detail for the $2\text{TiCl}_4\cdot\text{HMB}/\text{MeCN}$ and THF systems.

$2\text{TiCl}_4\cdot\text{HMB}$ dissolved in both MeCN and THF to give pale yellow solutions.

Removal of solvent in vacuo and sublimation of the resultant pale yellow solid in vacuo (363 K) gave a white sublimate of HMB. The yellow sublimation residues were identified as $\text{TiCl}_4 \cdot 2\text{L}$ (L = MeCN, THF), i.e.



In the $1200\text{--}500\text{ cm}^{-1}$ region the IR spectrum of $2\text{TiCl}_4 \cdot \text{HMB}$ closely resembles that of the free ligand (337, 362, 363), strongly suggesting that the HMB ring retains its integrity on complexation. The most marked differences between the spectra of the free and complexed ring occur in the $1450\text{--}1350\text{ cm}^{-1}$ region, where the B-N stretching band at 1415 cm^{-1} in HMB appears as a doublet ($1426, 1350\text{ cm}^{-1}$) in the Ti complex. A shift to lower wavenumbers is consistent with a reduction in the B-N bond order and the localisation of the N lone pair in the formation of a Ti-N σ -coordinate bond (337). The cyclic triborazanes $\text{R}_3\text{B}_3\text{N}_3\text{R}'_3 \cdot 3\text{HX}$ provide an example where the N lone pair is totally localised; the band at $\sim 1260\text{ cm}^{-1}$ being assigned as a B-N single bond (337). Also of notice is the magnitude of low energy $\nu(\text{B-N})$ shift, which is large ($\Delta\nu(\text{B-N}) = 65\text{ cm}^{-1}$) compared to the $\nu(\text{B-N})$ shift found on complexation for the π -complex $\text{HMB} \cdot \text{Cr}(\text{CO})_3$ (363) (41 cm^{-1}), suggesting a stronger M-N bond in the Ti complex. The band found at 1426 cm^{-1} for $2\text{TiCl}_4 \cdot \text{HMB}$ corresponds to a B-N stretching mode where the B-N bond retains the multiple bond character of the free ligand (363). The complexed HMB ring, therefore, contains both coordinated and uncoordinated N donor centres. A dimeric structure is proposed with the HMB ring coordinated through two of the three N atoms in a σ -sense (Fig. 5.4.1). Additional evidence for the proposed structure comes from the low IR spectrum where intense bands at $442, 414, 384\text{ cm}^{-1}$ and 274 cm^{-1} are attributable to terminal and bridging pseudo-octahedral Ti-Cl modes respectively. A similar dimeric structure has been proposed for the TiCl_4 complex of the cyclic silazanes $2\text{TiCl}_4(\text{Me}_2\text{SiNH})_n$ ($n = 3, 4$) (299, 300).

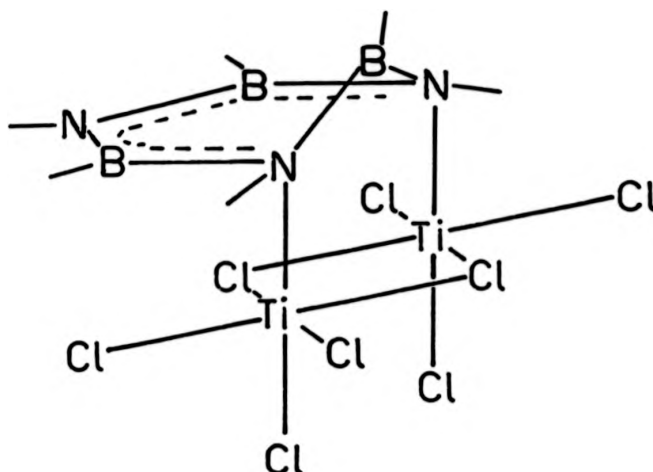


Fig. 5.4.1 Proposed Structure of $2\text{TiCl}_4\cdot\text{HMB}$

One point that emerges from both the HMB and the silazane work concerns the stoichiometry, where reaction of ligand and TiCl_4 in 1:1 ratio led to the isolation of 2:1 adducts. A possible explanation for this behaviour lies with a consideration of the steric dictates of the NBN and NSiN moieties. For both HMB and $(\text{Me}_2\text{SiNH})_3$ formation of a monomeric $\text{TiCl}_4\cdot\text{L}$ complex would involve adjacent N donor sites on the ligand occupying cisoid positions on the Ti atom, (i.e. chelation), thus producing considerable strain in the NBN and NSiN angles. Adoption of the experimentally found 2:1 stoichiometry enables the ligand to act in a bridging rather than in a chelating capacity, and ring strain can therefore, be taken up by distortion of the Ti-Cl-Ti bridges.

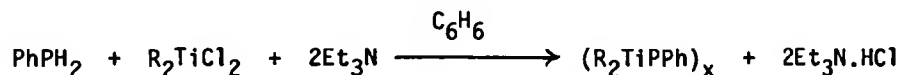
The B-CH_3 stretching mode found at 888 cm^{-1} in HMB is relatively unaffected by coordination, i.e. $\nu_{\text{B-CH}_3}$ in $2\text{TiCl}_4\cdot\text{HMB}$ is found at 879 cm^{-1} ,

with a weak shoulder at 886 cm^{-1} . The N-CH_3 frequencies are more difficult to assign. Adcock and Lagowski (337) observed a small shift to higher wavenumbers for the N-CH_3 rocking mode (1106 cm^{-1} in HMB) in the $\text{Cr(CO)}_3\cdot\text{Me}_3\text{B}_3\text{N}_3\text{MeR}^i\text{R}^{ii}$ systems, and the sharp band at 1118 cm^{-1} in the spectrum $2\text{TiCl}_4\cdot\text{HMB}$ is similarly assigned. The shift to higher frequency was attributed to a combination of electronic and steric effects associated with the puckering of the HMB ring on coordination (337). Considering the distortion of the π -system following ligand coordination in $2\text{TiCl}_4\cdot\text{HMB}$, it is not inconceivable that one or more of the bands in the spectrum of the complex in the $1150\text{--}1350\text{ cm}^{-1}$ region also corresponds to a N-CH_3 mode.

5.6 Comments on the Synthesis of $(\text{R}_2\text{TiPR}^i)_x$

Alternation heterocycles containing a t-metal(s) as a heteroatom(s) have received very little attention. The isolation of $(\text{Cl}_2\text{TiNSiMe}_3)_x$ and the determination of its structure by single crystal X-ray analysis (364) prompted an investigation into the possibility of obtaining an analogous phosphorus heterocycle. The attempted synthesis was approached via three basic routes.

(a) Condensation of a P-H and a Ti-Cl bond, e.g.



With TiCl_4 (i.e. $\text{R} = \text{Cl}$), a black, insoluble, gummy mass was produced. On continued washing with n-hexane this gave a small amount of a white solid identified as $\text{Et}_3\text{N}\cdot\text{HCl}$. The desired condensation reaction then evidently occurred but the nature of the black tarry residue was more in line with a polymeric product than a discrete ring. One possibility here was that the polymeric product may have been formed under conditions of kinetic control. To test this, we carried out a repeat experiment in which dilute

solutions of PhPH_2 and TiCl_4 were simultaneously added to a large volume of the same solvent (i.e. high dilution). The products obtained, however, were virtually identical to those obtained at high concentrations.

An alternative approach, by reducing the number of reactive Ti-Cl bonds on each Ti atom (e.g. $\text{R} = \text{Cp}$), cyclic products, or at least linear polymers, may be formed. When Cp_2TiCl_2 was employed in this capacity, the Ti-Cl bond proved to be resistant towards HCl elimination, and no $\text{Et}_3\text{N} \cdot \text{HCl}$ was recovered from any of the systems studied. One factor deciding reactivity here, may be the ability to form M-PPhH_2 donor complexes as intermediates in the condensation process. The low adduct forming ability of Cp_2TiCl_2 (cf. TiCl_4) has already been established (Section 2.2). Instead of giving condensation products, reaction between equimolar amounts of Cp_2TiCl_2 and PhPH_2 in refluxing THF (6 days) or C_6H_6 (6 weeks) gave deep green solutions, which on work up provided $\text{Cp}_2\text{Ti (III)Cl}$ in each case, i.e. reduction $\text{Ti (IV)} \rightarrow \text{Ti (III)}$. The oxidation products were not isolated, but a P (V) species is likely,



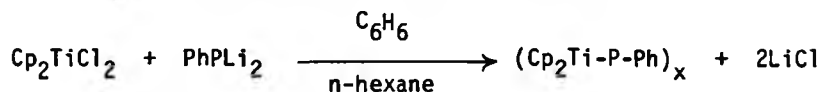
(b) Condensation of $\text{P(SiMe}_3)_3$ and R_2TiCl_2 , e.g.



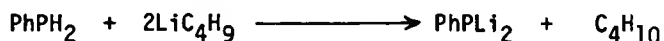
Whereas a reaction scheme of this type led to the isolation of $(\text{Cl}_2\text{TiNSiMe}_3)_x$ (164) from the $\text{TiCl}_4/\text{N(SiMe}_3)_3$ system, reactions involving the analogous P species proved to be far from satisfactory. No reaction was observed between Cp_2TiCl_2 and $\text{P(SiMe}_3)_3$ even after maintaining xylene solutions of the reactants at reflux temperature (~ 393 K) for a week. Addition of TiCl_4 to $\text{P(SiMe}_3)_3$ in C_6H_6 at 273 K did provide a small amount of Me_3SiCl , but on

removal of the solvent in vacuo, a colourless oil was obtained which defied characterisation. The production of poorly defined products compared to the well formed orange crystals of $(\text{Cl}_2\text{TiNMe}_2)_x$ obtained from the $\text{TiCl}_4/\text{N}(\text{SiMe}_3)_3$ system (364) may be a reflection of the increased reactivity of the P-Si bond cf. N-Si.

(c) Litho-phosphinolysis of M-Cl bonds, e.g.



A pale yellow suspension of PhPLi_2 was obtained by reacting PhPH_2 with a two-fold equivalent of $\text{Li n-C}_4\text{H}_9$ in n-hexane, i.e.



Addition of an equimolar amount of Cp_2TiCl_2 in C_6H_6 to the strongly stirred suspension at 273 K gave an immediate colour change (red + deep purple). The solution was decanted and filtered in vacuo. Removal of the solvent in vacuo gave a black crystalline solid which was recrystallised with considerable effort from n-hexane. The ^1H NMR of the solid (200 MHz, C_6D_6 solution) showed a series of phenyl resonances in the $\delta 6.69$ - 6.92 region (20 protons) and Cp resonances at $\delta 4.75$ (singlet, 5 protons) and $\delta 5.06$ (triplet, 5 protons), indicating that the product was not a simple heterocycle. The extreme oxygen sensitivity and intense purple colouration of the sample (cf. dark violet $\text{Cp}_2\text{TiP}_3\text{Ph}_3$ (365)), coupled with the triplet Cp resonance at $\delta 5.06$ (split by $2 \times ^{31}\text{P}$ nuclei) are good indications of the formation of a Ti-P linkage.

In conclusion, none of the synthetic routes attempted led directly to a $(\text{R}_2\text{TiPR})_x$ heterocycle. Evidence was found for the formation of a Ti-P bond via method (c), and variations in the reaction conditions could well lead to the desired product.

5.7 Experimental

5.7.1 Reaction of $(\text{CH}_2\text{O})_3$ with MCl_4 ($\text{M} = \text{Ti}, \text{Sn}$), $\text{ZrCl}_4 \cdot 2\text{NMe}_3$ and $\text{HCl}_3 \cdot 2\text{NMe}_3$ ($\text{M} = \text{V}, \text{Cr}$)

(a) Reaction of $(\text{CH}_2\text{O})_3$ with MCl_4 ($\text{M} = \text{Ti}, \text{Sn}$). Dropwise addition of MCl_4 ($\text{M} = \text{Ti}, \text{Sn}$) to a two-fold excess of $(\text{CH}_2\text{O})_3$ in C_6H_6 gave glutinous, white precipitates of $(\text{CH}_2\text{O})_x$, which were washed with C_6H_6 and dried in vacuo. The metal-containing product was not identified.

(b) Reaction of $(\text{CH}_2\text{O})_3$ with $\text{ZrCl}_4 \cdot 2\text{NMe}_3$. $\text{ZrCl}_4 \cdot 2\text{NMe}_3$ (1.7 g, 4.8 mmol) in C_6H_6 (100 ml) was added in vacuo to $(\text{CH}_2\text{O})_3$ (8 g, 33.3 mmol) in C_6H_6 (150 ml). There was no immediate reaction, but on standing for several hours a small amount of white precipitate formed. The excess solvent was removed by decanting in vacuo, and the product washed in vacuo with C_6H_6 , to give $\text{ZrCl}_4(\text{C}_6\text{O}_6\text{H}_{12})$ as a powdery white solid.

Analysis based on $\text{ZrCl}_4\text{C}_6\text{H}_{12}\text{O}_6$

Calculated Cl(34.3) Found Cl(33.7) %

The IR spectrum showed bands at:-

3155(br), 3090(w), 3030(m), 2960(m), 2932(w), 1730(br), 1409(w), 1479(m), 1442(sh), 1460(sh), 1260(s), 1209(s), 1134(sh), 1180(m), 1035(sh), 1023(m), 984(w), 967(w), 945(w), 960(w), 857(m), 805(m), 758(m), 739(w), 723(w), 701(w), 690(w), 645(w), 678(w), 423(w) and 305(v) cm^{-1} respectively.

(c) Reaction of $(\text{CH}_2\text{O})_3$ with $\text{VCl}_3 \cdot 2\text{NMe}_3$. $\text{VCl}_3 \cdot 2\text{NMe}_3$ (0.8 g, 2.9 mmol) in C_6H_6 (~150 ml) was added in vacuo to $(\text{CH}_2\text{O})_3$ (0.8 g, 8.8 mmol) in C_6H_6 (~200 ml). After stirring for several hours, the solvent was removed in vacuo to give the pale pink solid product, which was purified by washing in vacuo with n-pentane. Microanalysis found:-

C(23.8) H(5.7) N(7.5) Cl(38.5) %

The IR spectrum showed bands at:-

3020(sh), 3012(m), 2986(s), 2962(m), 2931(s), 2907(s), 2880(w), 2856(s), 2878(w), 2795(m), 1485(s), 1480(sh), 1465(s), 1458(sh), 1409(m), 1265(s), 1245(m), 1110(m), 1104(m), 1004(sh), 997(s), 820(s), 725(m), 513(s), 446(s), 411(s), 333(m) and 312(s) cm^{-1} respectively.

(d) Reaction of $(\text{CH}_2\text{O})_3$ with $\text{CrCl}_3 \cdot 2\text{NMe}_3$. $\text{CrCl}_3 \cdot 2\text{NMe}_3$ (1.5 g, 5.4 mmol) and $(\text{CH}_2\text{O})_3$ (1.5 g, 16.4 mmol) reacted in C_6H_6 as for (c) to give a mulberry solid product, which was purified as above. Microanalysis found:-

C(26.7) H(6.6) N(9.1) Cl(32.1) %

Bands were found in the IR spectrum at:-

3040(m), 3021(m), 2989(s), 2960(w), 2932(m), 2915(m), 2880(w), 2857(w), 2803(w), 1483(s), 1465(s), 1422(w), 1405(s), 1340(w), 1265(m), 1245(w), 1238(sh), 1195(s), 1102(s), 995(s), 988(s), 954(m), 856(s), 827(s), 760(m), 726(w), 687(w), 588(m), 536(m), 480(m), 445(m), 422(w), 387(s), 380(s) and 348(s) cm^{-1} respectively.

5.7.2 Complexes at $(\text{CH}_2\text{S})_3$

(a) $\text{TiCl}_4 \cdot 2(\text{CH}_2\text{S})_3$. TiCl_4 (1 ml, 9.1 mmol) in CHCl_3 (150 ml) was added dropwise to a solution of $(\text{CH}_2\text{S})_3$ (2.5 g, 18.2 mmol) in CHCl_3 (300 ml) giving an orange solution and an orange precipitate. The solution was decanted in vacuo, and the resulting orange solid washed in vacuo with benzene and n-hexane before being pumped in vacuo for several hours. The product was $\text{TiCl}_4 \cdot 2(\text{CH}_2\text{S})_3$. Yield 3.8 g (90%).

Analysis based on $\text{TiCl}_4\text{C}_6\text{H}_{12}\text{S}_6$:-

Calculated	C(15.5)	H(2.6)	S(41.3)	Cl(30.4)	%
Found	C(15.2)	H(2.6)	S(41.5)	Cl(30.3)	%

(b) $\text{SnCl}_4 \cdot 2(\text{CH}_2\text{S})_3$. SnCl_4 (1 ml, 8.5 mmol) in CHCl_3 and $(\text{CH}_2\text{S})_3$ (2.4 g, 17.1 mmol) also in CHCl_3 were reacted as in (a) to give $\text{SnCl}_4 \cdot 2(\text{CH}_2\text{S})_3$ as a cream coloured solid. Yield 3.9 g (85%).

Analysis based on $\text{SnCl}_4\text{C}_6\text{H}_{12}\text{S}_6$

Calculated	C(13.4)	H(2.3)	S(35.8)	Cl(26.4)	%
Found	C(13.6)	H(2.3)	S(35.6)	Cl(26.4)	%

(c) $\text{SbCl}_5(\text{CH}_2\text{S})_3$. SbCl_5 (0.5 ml, 3.9 mmol) in CH_2Cl_2 (15 ml) and $(\text{CH}_2\text{S})_3$ (0.6 g, 4.3 mmol) were reacted as in (a) to give $\text{SbCl}_5(\text{CH}_2\text{S})_3$ as a pale yellow solid. Yield 0.8 g (47%).

Analysis based on $\text{SbCl}_5\text{C}_3\text{H}_6\text{S}_3$

Calculated	C(8.2)	H(1.4)	S(22.0)	Cl(40.5)	%
Found	C(9.2)	H(1.7)	S(21.6)	Cl(39.9)	%

(d) $\text{AuCl}_3(\text{CH}_2\text{S})_3$. AuCl_3 (0.74 g, 2.4 mmol) in CH_2Cl_2 and $(\text{CH}_2\text{S})_3$ (0.4 g, 2.7 mmol) also in CH_2Cl_2 were reacted as in (a) to give $\text{AuCl}_3(\text{CH}_2\text{S})_3$ as a chocolate brown solid. Yield 0.98 g (93%).

Analysis based on $\text{AuCl}_3\text{C}_3\text{H}_6\text{S}_3$

Calculated	C(8.2)	H(1.4)	S(21.8)	Cl(24.1)	%
Found	C(8.1)	H(1.3)	S(21.8)	Cl(23.9)	%

Samples of $\text{AuCl}_3(\text{CH}_2\text{S})_3$ sealed in ampoules under an N_2 atmosphere decomposed over a period of three months to give a pale yellow solid. The solid showed bands in the IR spectrum at:-

2987(s), 2975(m), 2970(w), 2910(s), 2902(w), 1400(w), 1386(w), 1380(w), 1365(m), 1245(w), 1220(s), 1186(w), 1170(s), 1100(w), 919(s), 896(m), 842(m), 818(w), 808(w), 744(s), 723(s), 666(s), 353(m) and 334(s) cm^{-1} respectively.

5.7.3 Reaction between $(\text{Me}_2\text{SiO})_{3,4}$ and TiCl_4

(a) Reaction between $(\text{Me}_2\text{SiO})_3$ and TiCl_4 . TiCl_4 (1 ml, 9.1 mmol) was

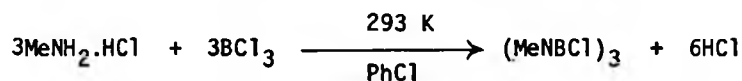
added dropwise to a solution of $(\text{Me}_2\text{SiO})_3$ (2.22 g, 10.0 mmol) in C_6H_6 (60 ml) contained in a single ampoule bomb. The bomb was degassed and sealed in vacuo. After 10 days the bomb was opened, and the solvent removed in vacuo to give a colourless, fuming liquid which showed bands in the IR spectrum at:-

2964(s,br), 1410(m), 1264(s), ~ 1070 (vs,vbr), 945(s,br), 965(w,sh),
925(m,sh), 805(s,br), 705(w,br), 670(m), 475(s,br), 390(sh), 385(s),
375(w) and 349(w) cm^{-1} respectively.

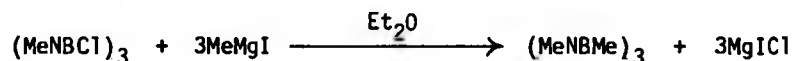
(b) TiCl_4 (1 ml, 9.1 mmol) and $(\text{Me}_2\text{SiO})_4$ (3.0 g, 10.0 mmol) were reacted as in (a) to give an identical product to that obtained in (a).

5.7.4 Reactions of hexamethylborazine with covalent metal halides

(a) Preparation of hexamethylborazine. Hexamethylborazine was prepared by a modified route to that of Turner and Warne (321). The synthesis was carried out in two stages. Firstly, the condensation of $\text{MeNH}_2 \cdot \text{HCl}$ and BCl_3 to give N,N',N'' -trimethylamine- B,B',B'' -trichloroborazine, i.e.



followed by methylation to give the desired product,



MeNH_2 was passed into dilute HCl until the solution was neutral to litmus. The water was removed on a rotary evaporator, and the resultant $\text{MeNH}_2 \cdot \text{HCl}$ recrystallised from EtOH before drying in vacuo at 323 K. Finely ground $\text{MeNH}_2 \cdot \text{HCl}$ (28.7 g, 0.427 mol) was suspended in chlorobenzene (600 ml) and the suspension placed in a litre flask fitted with both water and dry ice condensers. The contents of the flask were cooled to 273 K and BCl_3 (50 g, 0.427 mol) was swiftly added, the whole apparatus being maintained under a slight positive pressure of N_2 . On warming to room temperature,

a slightly exothermic reaction commenced, as evidenced by the slow reflux of BCl_3 on the dry ice cold finger. The temperature was slowly raised until the chlorobenzene solvent started to reflux, and after 6 hours the BCl_3 was totally consumed, and a layer of immiscible, colourless liquid had formed at the bottom of the flask. Reflux was maintained for a further three days, during which time HCl was constantly evolved, and the immiscible layer gradually reduced in volume. After evolution of HCl was complete, the solution was cooled and the solvent removed in vacuo to give crude $(\text{MeNBCl})_3$. Sublimation in vacuo (353 K) gave the product as a white crystalline solid. Yield 25.5 g (79.3%)

A solution of MeMgI in Et_2O (150 ml) was prepared from Mg (10.9 g, 0.48 mol) and MeI (63.7 g, 0.48 mol). Dropwise addition of this solution to $(\text{MeNBCl})_3$ (22.5 g, 0.1 mol) in Et_2O (200 ml) gave an immediate reaction with precipitation of MgICl , the rate of addition being modified to maintain reflux. After addition of the Grignard was complete, the solution was stirred for a further 2 hours. The solution was decanted from the MgICl residues, and the solvent removed in vacuo to give the crude product, which was recrystallised from C_6H_6 and sublimated in vacuo (343 K). Yield 14.5 g (88.0%). Overall yield, 69.8%.

(b) TiCl_4 (hexamethylborazine). TiCl_4 (1 ml, 9.1 mmol) in C_6H_6 (10 ml) was added to a single ampoule bomb containing hexamethylborazine (1.2 g, 9.1 mmol) in C_6H_6 (50 ml). An immediate reaction occurred to give an orange solution, which on cooling gave a pale orange precipitate. The contents of the bomb were degassed, and the bomb was sealed. The bomb was opened after two months and the solvent decanted in vacuo. Washing the orange solid with C_6H_6 and n-hexane (5 x 50 ml portions) gave di- μ -chloro-hexachloro- μ -(hexamethylborazine, N_1,N_2)-dititanium (IV) as a bright orange solid.

Yield 1.49 g (60%).

Analysis based on $\text{Ti}_2\text{Cl}_8\text{C}_6\text{H}_{18}\text{N}_3\text{B}_3$

Calculated	C(13.2)	H(3.3)	N(7.7)	Cl(52.1)	Ti(17.6)	%
------------	---------	--------	--------	----------	----------	---

Found	C(13.8)	H(3.7)	N(7.5)	Cl(52.2)	Ti(17.4)	%
-------	---------	--------	--------	----------	----------	---

Bands were found in the IR spectrum at:-

3210(br), 2970(w,sh), 2958(m), 2927(m), 2912(m), 1470(s), 1426(w),
1350(s,br), 1335(sh), 1282(s), 1237(w), 1223(s), 1200(m), 1191(m),
1163(w), 1118(s), 990(m), 982(w), 886(sh), 879(s), 812(w), 770(w,br),
725(m), 565(s), 509(m), 496(m), 442(s), 427(m), 414(s), 384(s), 335(sh)
and 274(s) cm^{-1} respectively.

CHAPTER 6

COMPLEXES OF SUBSTITUTED OXAMIDES, THIOOXAMIDES AND
MALONAMIDES WITH METAL TETRAHALIDES

CHAPTER 6

6.1 INTRODUCTION

Structural aspects of oxamides, malonamides and related molecules have been the subject of considerable interest (366-371). The crystal structures of oxamide (366) and dithiooxamide (367, 368) are shown in Fig. 6.1.1.

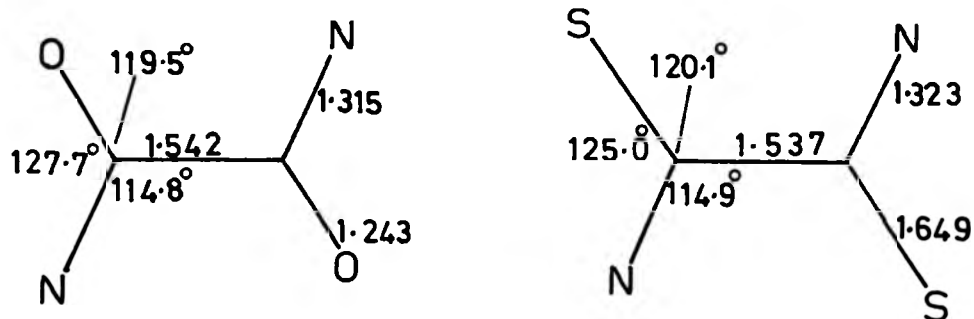


Fig. 6.1.1 X-ray Crystal Structures of $(\text{CONH}_2)_2$ and $(\text{CSNH}_2)_2$

Both molecules are planar in the solid state, held in sheets by hydrogen bonding. Dithiooxamide has two slightly different molecules in the unit cell, and the values given in Fig. 6.1.1 are an average of the two. Values for C-N and C-O(S) bond lengths, intermediate between that expected for formal single and double bonds, were seen as a result of delocalisation of electron density in the NCO(S) moiety. The C-C bond lengths in both cases were found to correspond well to a pure single bond (368), thus no delocalisation between the two NCO(S) units occurs. Although not visible in the structures of oxamide or thiooxamide, well resolved hydrogen atoms were seen in the crystal structure of succinamide (369). Bond angles of $\sim 120^\circ$ round the N atom confirmed the sp_2 type hybridisation required for a

delocalised system.

The effect of N-alkyl substitution on the delocalised system can be seen from the structure of N,N-dimethyldithiooxamide (370), Fig. 6.1.2.

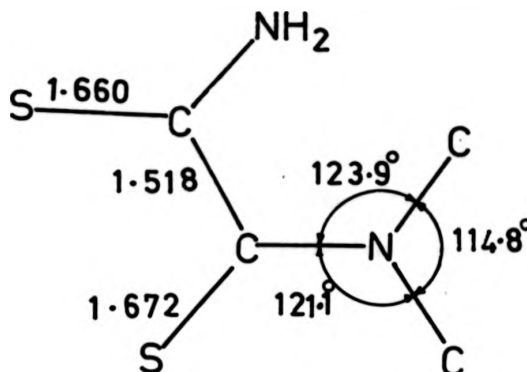


Fig. 6.1.2 Crystal Structure of N,N-dimethyldithiooxamide

As no delocalisation occurs through the central C-C bond the SCN₂ and SCNMe₂ fragments can be considered separately, and from the difference in S-C and C-N bond lengths, it appears that substitution has little effect on the SCN system. Unlike the parent dithiooxamide, N,N-dimethyldithiooxamide is not planar and has a SCCS dihedral angle of 91.8°, presumably due to reduced H-bonding via the NMe₂ groups. In N,N'-bis(trimethylsilyl)-dithiooxamide (371) however, the two NH(SiMe₃) groups are equivalent and the molecule re-assumes a planar centrosymmetric structure comparable to (CSNH₂)₂.

Interest in the coordination chemistry of amides has focused almost entirely on monoamide derivatives. Adducts of formamide (372, 373), N,N-dimethylformamide (372, 373), NMe acetamide (374), N,N,-dimethylacetamide (375) and diacetamide (376), with a number of Lewis acids have been prepared,

and each has been shown to involve donation solely through the O atom. Some early work with monoamide ligands in which N-donation was inferred from IR data (377, 378) was later re-assessed (379, 380) and was also found to be consistent with oxygen donation. The tendency to act as O rather than N donors persists in the diamides, oxamide, malonamide and succinamide which act as bidentate O-bonded chelates towards Group IV metal halides (381).

Complexes of thioamides differ from their oxygen counterparts in two respects. Firstly, unlike the amides, the majority of the work in the literature has centred on dithiodiamides, and secondly, the ligands, themselves, show a diversity in donor behaviour, depending on the Lewis acid involved. Adducts of As, Sb and Bi halides with a wide range of substituted dithiooxamides (382, 383), dithiomalonamides (384) and thiourea (383) have been studied, and have been shown to contain exclusively S-bonded ligands. In contrast to the Group V complexes, a large amount of work on bivalent metal halides and perchlorates (385), and in particular Ni (II) (385-388) and Pd (II) (389-393) found that the active donor atoms in the ligand depended on the conditions under which the complexes were formed. Under neutral conditions, deprotonation of the ligand (HL) occurs to give cationic complexes of the type $(ML_2)^{2+}2X^-$ or ML_2 , the ligand being bonded as either an SS (385-387) or SN donor (388-393). In strong acid media, the neutral adducts $MX_2(HL)$, (389, 390, 392, 393), $M(HL)_2X_2$ (386, 387, 389, 392, 393) and more rarely $M(HL)_3X_2$ (386) are produced. These adducts almost always contain the ligand in a SN-bonded state. The donor behaviour of thiourea (394) and dithiooxamide (381) towards some Group IV halides has also been studied, and donation through the nitrogen atoms has been postulated in both cases.

Our interest in the coordination chemistry of these ligands centred on two considerations:-

(a) Since dithiooxamide appears to give unusual NN-bonded systems with Group IV halides (381), similar substituted dithiooxamides might be expected to adopt an interesting variety of different donor schemes. Although the oxamides were almost certain to give only OO-bonded systems, they would act as useful analogues to their S-bonded counterparts.

(b) If possible, to make a comparison between similar S and O-bonded systems would be useful. Previous work has shown that in some cases, Ti (IV) which is normally classed as a hard (Class A) Lewis acid is a better electron acceptor towards sulphur (Class B) than oxygen (Class A) (60, 62).

To this end, we have examined a series of complexes of some substituted oxamides, malonamides and dithiooxamides with the Group IV halides $TiCl_4$ and $SnCl_4$.

6.2. Complexes of substituted oxamides, thiooxamides and malonamides with MCl_4 ($M = Ti, Sn$)

Dropwise addition of $TiCl_4$ or $SnCl_4$ to an equimolar solution of ligand (B) in $CHCl_3$ gave rise to precipitates of the 1:1 adducts $MCl_4 \cdot B$ ($M = Sn, Ti$, $B = N,N'$ -dimethyloxamide (DMO), $M = Ti$, $B = N,N'$ -diethyloxamide (DEO), $M = Ti, Sn$, $B = N,N'$ -diethylmalonamide (DEM), $M = Ti, Sn$, $B = N,N'$ -dimethyldithiooxamide (DMDTO), $M = Ti, Sn$, $B = N,N'$ -diethyldithiooxamide (DEDTO) in high yield. The adducts were purified by washing with C_6H_6 and pumping in vacuo. Handling in strictly anaerobic conditions proved essential, as all the adducts were extremely air/moisture sensitive, decomposing to the metal oxide within minutes. Decomposition to black or brown solids without melting was observed for the range of complexes on heating in vacuo. A general insolubility was found in non-coordinating solvents, although $MeNO_2$

proved a sufficiently good solvent to permit some solution studies. On an empirical basis, the solubility in MeNO_2 was found to follow the order $\text{Et} > \text{Me}$, $\text{S} > \text{O}$, malonamides $>$ oxamides. Conductivity data in MeNO_2 solution showed, over a range of concentrations, that the complexes were essentially non-conducting.

Principle IR vibrational bands of the ligands and adducts are presented in Table 6.2.1. Assignments are made after Desseyn *et al* (395, 396). It should be noted that, in systems of this type, bands rarely represent pure modes and that any assignments made (apart from $\nu\text{M-Cl}$) are indicative only of the major constituent of a particular band. A series of strong Ti-Cl stretches in the 400 to 250 cm^{-1} range of the spectrum at $368, 303, 276\text{ cm}^{-1}$ ($\text{TiCl}_4\cdot\text{DMO}$), $355, 312, 290\text{ cm}^{-1}$ ($\text{TiCl}_4\cdot\text{DEO}$), $340, 273\text{ cm}^{-1}$ ($\text{TiCl}_4\cdot\text{DEM}$), $370, 342, 305\text{ cm}^{-1}$ ($\text{TiCl}_4\cdot\text{DMDT0}$) and $360, 285\text{ cm}^{-1}$ ($\text{TiCl}_4\cdot\text{DEDT0}$) were in accordance with a *cis* (C_{2v}) symmetry. A similar assignment for the SnCl_4 adducts on the basis of multiple Sn-Cl bands was made ($345, 285\text{ cm}^{-1}$ ($\text{SnCl}_4\cdot\text{DMO}$), $323, 295\text{ cm}^{-1}$ ($\text{SnCl}_4\cdot\text{DEM}$), 315 cm^{-1} ($\text{SnCl}_4\cdot\text{DMT0}$) and $310\text{-}320\text{ cm}^{-1}$ ($\text{SnCl}_4\cdot\text{DEDT0}$)) although not all of the four expected bands were observed.

The active donor atoms in amide and thioamide complexes may be deduced by a consideration of the changes of CO, CS, CN and NH stretching frequencies in the $4000\text{-}700\text{ cm}^{-1}$ region of the IR spectrum on complexation. As electron density is delocalised over the CNO(S) moiety, complexation through O or S donor centres, drains electron density from the S(O) atom, decreasing the C=S bond order, and increasing the C-N bond order. The C=S stretching frequency consequently suffers a shift to lower energy, accompanied by a high energy shift for $\nu(\text{C-N})$ and $\nu(\text{N-H})$ although the magnitude of the latter is expected to be smaller, as the N-H bond is one atom further removed from the donor atom.

Compd. \ Assgn.	$\nu(\text{N-H})$	$\nu(\text{C-N})$	$\nu(\text{C=S})$	$\nu(\text{C=O})$	$\nu(\text{M-Cl})$
DMO	3300(s)	1522(s,br)	-	1655(sbr)	-
$\text{TiCl}_4 \cdot \text{DMO}$	3320(w) 3270(s) 3220(m) 3150(vs)	1578(m)	-	1631(s,br)	368(vs,br) 303(m) 276(w)
$\text{SnCl}_4 \cdot \text{DMO}$	3325(w) 3288(s) 3217(w) 3150(m)	1571(m)	-	1635(s,br)	345(vs,br) 285(m)
DEO	3290(vs)	1518(s)	-	1650(vs)	-
$\text{TiCl}_4 \cdot \text{DEO}$	3310(w) 3260(s) 3202(m) 3135(s)	1572(s)	-	1632(vs,br)	355(vs,br) 312(w) 290(w)
DEM	3292(vs)	1550(s,br)	-	1645(s,br)	-
$\text{TiCl}_4 \cdot \text{DEM}$	3295(vs)	1575(m,br)	-	1630(vs,br)	340(vs,br) 273(m)
$\text{SnCl}_4 \cdot \text{DEM}$	3370(sh) 3340(sh) 3300(vs)	1574(m,br)	-	1628(s,br)	323(vs,br) 295(w)
DMDTO	3169(vs)	1529(s,br)	870(vs)	-	-
$\text{TiCl}_4 \cdot \text{DMDTO}$	3225(vs)	1564(vs,br)	770(s)	-	370(vs,br) 342(w) 305(vs,br)
DEDTO	3186(s)	1518(vs)	842(s)	-	-
$\text{TiCl}_4 \cdot \text{DEDTO}$	3260(s) 3190(s) 3096(m)	1572(vs)	800(m)	-	360(s,br) 285(w)
$\text{SnCl}_4 \cdot \text{DEDTO}$	3210(vs) 3098(s)	1570(vs)	793(s)	-	310-320(vs,br)

Table 6.2.1 Principle IR Bands of $\text{MCl}_4 \cdot \text{B}$ Complexes

Conversely, N-coordination produces a decrease in $\nu(\text{C-N})$ and $\nu(\text{N-H})$ and an increase in $\nu(\text{C=S})$. A situation in which the ligand acts as a mixed donor (NO , or NS) produces splitting of both the C=S(O) and C-N stretching modes corresponding to complexed and uncomplexed functional groups.

An examination of Table 6.2.1 shows that a lowering of $\nu(\text{C=S(O)})$ and raising of $\nu(\text{C-N})$ is observed throughout the spectra of the adducts indicating complexation through the O or S atoms in all cases. The proposed structures of $\text{MX}_4 \cdot \text{B}$ are shown in Figure 6.2.1.

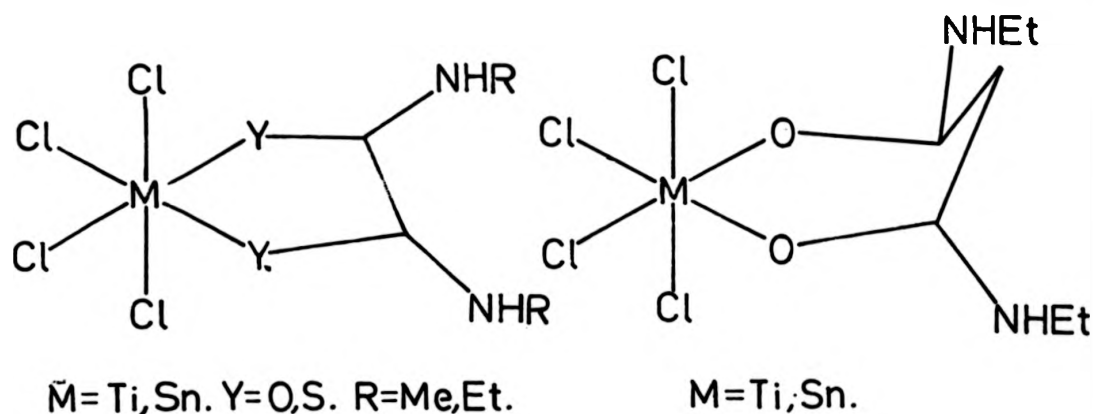


Fig. 6.2.1 Proposed Structures of $\text{MCl}_4 \cdot \text{B}$

The results for the dithiooxamide complexes are in variance with those for the earlier unsubstituted dithiooxamide adducts (381). As the substituted and unsubstituted ligands are expected to have a similar NC(O)S π -system, the difference in donor characteristics is likely to be due to steric effects and changes in basicity of the N atom for the substituted molecules.

Splitting of the N-H stretching frequency is observed for some, but not all of the complexes. This may be due to a combination of lattice packing effects, and solid phase hydrogen bonding. In addition to this, for the oxamide and thiooxamide ligands, complexation produces a geometry in which the whole $(\text{SCN})_2$ system becomes coplanar, thus leading to geometric isomerism of the N alkyl groups, Fig. 6.2.2.

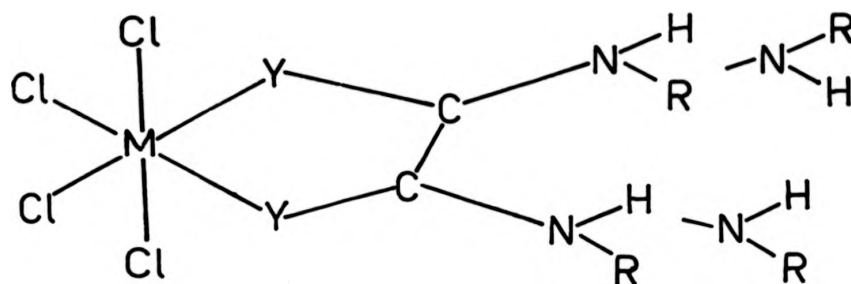


Fig. 6.2.2 Possible Isomers of $\text{MCl}_4(\text{Y}_2\text{C}_2\text{N}_2(\text{NR})_2)$

A third possible isomer to those shown in Fig. 6.2.2 in which the two alkyl groups are adjacent is, unlikely, due to steric crowding. The malonamide derivatives may also have additional isomers due to several different configurations of the six-membered MOCCCO ring, which is not necessarily planar. $\text{TiCl}_4 \cdot \text{DEM}$, $\text{TiCl}_4 \cdot \text{DMDTO}$ and $\text{SnCl}_4 \cdot \text{DMDTO}$ exhibit single intense N-H stretches, which may be due to either several N-H bands being coincidentally isoenergetic, or the ligand adopting a particular thermodynamically favoured configuration.

The ^1H NMR spectra of the $\text{MCl}_4 \cdot \text{L}$ complexes, Table 6.2.2, were found to be consistent with the proposed solid state structures, although in some cases, resolution was limited due to poor complex solubility.

Compound	δMe	$\delta\text{CH}_2\text{Et}$	δCH_2 (back bone)	δNH
DMO	2.83(a)	-	-	7.59(b)
$\text{TiCl}_4\cdot\text{DMO}$	3.26(c)	-	-	9.12(b)
$\text{SnCl}_4\cdot\text{DMO}$	3.32(a)	-	-	8.80(b)
DEO	1.15(d)	3.30(e)	-	7.71(b)
$\text{TiCl}_4\cdot\text{DEO}$	1.39(d)	3.74(e)	-	8.86(b)
DEM	1.09(d)	3.21(e)	3.40(f)	6.99(b)
$\text{TiCl}_4\cdot\text{DEM}$	1.27(d)	3.49(e)	3.88(f)	7.66(b)
$\text{SnCl}_4\cdot\text{DEM}$	1.27(d)	3.53(e)	4.02(f)	7.97(b)
DMDTO	3.27(a)	-	-	10.39(b)
$\text{TiCl}_4\cdot\text{DMDTO}$	3.40(c)	-	-	9.91(b)
$\text{SnCl}_4\cdot\text{DMDTO}$	3.33(c)	-	-	10.28(b)
DEDTO	1.33(d)	3.74(e)	-	10.35(b)
$\text{TiCl}_4\cdot\text{DEDTO}$	1.34(d)	3.76(g)	-	10.29(b)
$\text{SnCl}_4\cdot\text{DEDTO}$	1.45(d)	3.91(g)	-	10.00(b)

(a) doublet

(b) broad singlet

(c) poorly resolved doublet

(d) triplet

(e) two superimposed quartlets (pseudo pentaplet)

(f) sharp singlet

(g) poorly resolved 'pseudo pentaplet'

Table 6.2.2 ^1H NMR Spectra of $\text{MCl}_4\cdot\text{B}$, CDNO_2/TMS (90 MHz)

For the same reasons ^{13}C measurements of the complexes were unobtainable, although no such restriction was found for the ligands, Table 6.2.3. No obvious pattern for differences between the SnCl_4 and TiCl_4 adducts was observable. A general downfield shift for all the resonances indicates

that electron density is transferred from the alkyl groups into the CNO(S) moiety. The magnitude of this shift is considerably greater for the O donors (e.g. $\text{SnCl}_4 \cdot \text{DMO}$, $\Delta\delta 0.49$) than for the S donors ($\text{SnCl}_4 \cdot \text{DMDTO}$, $\Delta\delta 0.08$), suggesting that this effect is more pronounced for the amide complexes than the thioamide complexes.

Ligand	$(\text{S})\text{O}=\text{C} \begin{array}{l} \text{R} \\ \text{R}' \end{array}$	$\text{R}-\text{NHMe}$	$\begin{array}{c} \text{H} \\ \\ \text{R}-\text{N}-\text{CH}_2\text{Me} \end{array}$	$\begin{array}{c} \text{H} \\ \\ \text{R}-\text{N}-\text{CH}_2\text{Me} \end{array}$	$\text{R}-\text{C}-\text{CH}_2-\text{C}-\text{R}$
DMO(a)	162.36	26.39	-	-	-
DEO(b)	161.64	-	35.36	14.69	-
DEM(b)	167.75	-	34.45	14.43	43.09
DMDTO(a)	132.53	34.12	-	-	-
DEDTO(b)	184.32	-	42.37	12.61	-

Table 6.2.3 ^{13}C NMR Shift Data of the Ligands (a) CD_3OD and
(b) CDCl_3

This is partially reflected in the predominantly $\nu(\text{C}-\text{N})$ IR stretching mode, where $\Delta\nu(\text{C}-\text{N})$ is slightly higher for the O-bonded systems than for the S-bonded systems. The implication that the bond order in the C-N bond is maintained mainly by delocalisation from the NHR groupings rather than by loss of $\text{C}=\text{O}$ or $\text{C}=\text{S}$ bond density is evidence that the large difference between $\Delta\nu(\text{C}=\text{O})$ ($17\text{--}24\text{ cm}^{-1}$) and $\Delta\nu(\text{C}=\text{S})$ ($47\text{--}100\text{ cm}^{-1}$) is, in fact, a true indication of the relative donor properties of the two sets of ligands, and that the S donors are more strongly bonded to the metal atom than the corresponding O donors. This is in accordance with the general picture for MCl_4 systems ($\text{M} = \text{Ti}, \text{Zr}, \text{Hf}$) and that sulphur is a better donor than oxygen (60, 62).

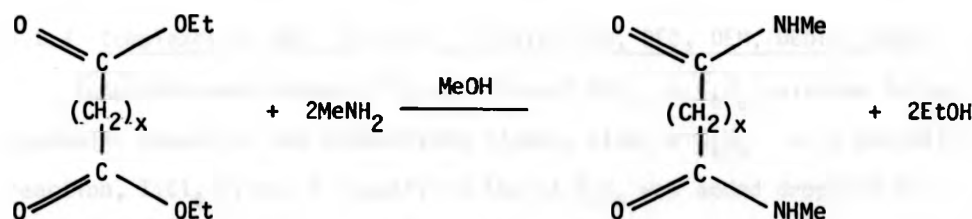
No evidence was found that the geometric isomers seen in the solid state spectra, persist in solution. It can only be presumed here that some

rotation about the C-N bond is still possible, despite the increased bond order in the adducts. The ^1H NMR spectrum of $\text{TiCl}_4\cdot\text{DEM}$ showed in addition to the resonances expected for the complex, a well defined triplet ($\delta 1.45$) and quartet ($\delta 4.94$) that was shown to be independent of the $\text{TiCl}_4\cdot\text{DEM}$ system by the integrated intensity. A large downfield shift for the methylinic quartet pointed to a situation where the nitrogen atom environment had been drastically altered. Two models for this behaviour are aminolysis to give a Ti-N linkage with expulsion of HCl , and reaction with the MeNO_2 solvent giving protination of the N atom (and consequently produced a quartet for the methylene group due to a reduction in $^3\text{J}(\text{H-H})$). The former seems the most likely prospect as a single N-H resonance is observable, and the intense brown colour of the nitromethane anion, which would have to be present if protination had taken place, was noticeably absent.

6.3 Experimental

6.3.1 Preparation of DMO, DEO, DMDTO, DEDTO and DEM

$\text{N,N}'$ -dimethyloxamide (DMO) and $\text{N,N}'$ -dimethylmalonamide (DEM) were prepared by direct addition of three-fold excess of aqueous 25% MeNH_2 solution to solutions of the appropriate ethyl ester in MeOH .



The white precipitate formed was recrystallised in high yield from $\text{MeOH}/\text{EtOH}/\text{Et}_2\text{O}$.

N,N' -diethyloxamide (DEO) was prepared in an analogous manner to DMO by distilling a 2:1 excess of anhydrous EtNH_2 onto a solution of diethyloxamide in MeOH at 77 K in vacuo. Warming the resultant mixture to room temperature and leaving to stand for several hours produced large colourless plates of DEO which was recrystallised from hot MeOH.

N,N' -dimethyldithiooxamide (DMDTO) and N,N' -diethyldithiooxamide (DEDTO) were prepared from the corresponding oxamides by a slightly modified method to that of Hurd *et al* (383, 397). To a refluxing solution/suspension of finely ground DEO or DMO in toluene was added a three-fold excess of solid P_4S_{10} in small portions. The reaction was exothermic. On completion of addition, the mixture was maintained at reflux for a further 6 to 8 hours, producing an orange brown solution and an intractable black solid. The solution was decanted and the solid residue washed with 3 x 100 ml portions of toluene. Combining the solution and washings and removal of solvent gave an orange/brown oil, which was dissolved in MeOH and refluxed with activated charcoal for 2 hours. Filtration through a celite-bedded sinter and concentration of the resultant clear orange solution gave orange crystals of DMDTO or DEDTO, which were recrystallised from hot MeOH (overall yield 40-50%).

6.3.2 Complexes of MCl_4 ($\text{M} = \text{Sn}, \text{Ti}$) with DMO, DEO, DEM, DEDTO, DMDTO

Complexes were prepared by addition of MCl_4 in C_6H_6 solution to an equimolar amount of the appropriate ligand, also in C_6H_6 . In a typical reaction, TiCl_4 (1 ml, 9.1 mmol) in 150 ml C_6H_6 was added dropwise to a solution of DEDTO (1.60 g, 9.1 mmol) in C_6H_6 (200 ml) producing an immediate colour change. On stirring for several hours, an orange precipitate of $\text{TiCl}_4\cdot\text{DEDTO}$ separated from solution, which was collected, washed with C_6H_6 (2 x 100 ml portions), hexane (2 x 100 ml portions) and dried in vacuo. Yields were virtually quantitative in all cases. Analytical data and physical properties are summarised in Table 6.3.1.

	mp ^a	colour	Δ_M^b	%C		%H		%N		%Cl	
				Calc	Obs	Calc	Obs	Calc	Obs	Calc	Obs
TiCl ₄ .DMO	>543	yellow	0.93	15.7	15.7	2.6	2.8	9.2	9.1	46.4	45.9
SnCl ₄ .DMO	>524	white	0.77	12.8	13.0	2.2	2.2	7.4	7.6	37.7	37.6
TiCl ₄ .DEO	>493	yellow	1.41	21.6	21.7	3.6	3.8	8.4	8.4	42.4	41.1
TiCl ₄ .DEM	>419	pale yellow	0.09	24.2	24.0	4.1	4.0	8.1	7.9	40.8	40.1
SnCl ₄ .DEM	>473	white	0.44	20.1	20.0	3.4	3.4	6.7	6.5	33.8	32.8
TiCl ₄ .DMDTO	>458	orange	1.07	14.2	14.6	2.4	2.7	8.3	7.9	42.0	41.7
SnCl ₄ .DMDTO	>466	pale yellow	1.31	11.8	12.0	2.0	2.1	6.9	6.9	34.7	34.1
TiCl ₄ .DEDT0	>413	orange	0.66	19.7	19.9	3.3	3.3	7.7	7.9	38.7	38.3
SnCl ₄ .DEDT0	>458	pale yellow	0.82	16.5	16.1	2.8	3.1	6.5	6.3	32.5	31.8

Table 6.3.1 Analytical Data of MCl₄.B Complexes^amelting with decomposition, (K) uncorrected^b($\Omega^{-1} \text{mole}^{-1} \text{cm}^2$) in 10^{-3}M solutions in CH_3NO_2

100

APPENDIX A

APPENDIX A

STARTING MATERIALS AND ANALYTICAL METHODS

(a) Starting Materials

Acetonitrile was obtained from Fisons Scientific Apparatus Ltd., Loughborough, and prior to use was refluxed over CaH_2 and distilled under a normal pressure of dry nitrogen.

Aluminium powder was obtained from BDH Chemicals Ltd., Poole. Prior to use it was washed with dry Et_2O , and stored in an oven at 393 K.

Aluminium trichloride was obtained as the anhydrous material from BDH Chemicals Ltd., Poole, and freed from FeCl_3 by repeated fractional sublimation in vacuo.

Antimony pentachloride was obtained by distillation of the technical grade material in high vacuum.

Antimony trichloride (AR grade) was obtained from BDH Chemicals Ltd., Poole, and purified by sublimation in vacuo.

Antimony tribromide was obtained from BDH Chemicals Ltd., Poole. It was recrystallised from C_6H_6 , and sublimed in vacuo prior to use.

Arsenic tribromide was obtained from Pfaltz and Bauer Ltd., Stamford, Conn., and distilled in vacuo prior to use.

Arsenic trichloride was obtained from Hopkin and Williams Ltd., Essex, and distilled over Na metal in vacuo.

Benzene (AR grade) was obtained from BDH Chemicals Ltd., Poole, and stored over Na wire. Prior to use it was distilled over CaH_2 under a normal pressure of nitrogen.

Bis(cyclopentadienyl)Hafnium (IV) dichloride was obtained from Strem Chemicals Inc., Newburyport, Mass.

Bis(cyclopentadienyl)Titanium (IV) dichloride was obtained from Strem Chemicals Inc., Newburyport, Mass., or synthesised from TiCl_4 and NaCp by the method of Wilkinson and Birmingham (398).

Bis(cyclopentadienyl)Zirconium (IV) dichloride was obtained from Aldrich Chemical Co. Inc., Milwaukee, Wis., or from Alfa (Ventron), Danvers, Mass.

Bis(dimethylamino)dimethylsilane was prepared according to the method of Washburne and Peterson (399).

Bis(diphenylphosphino)methane (dpm) was obtained from BDH Chemical Ltd., Poole, and recrystallised from C_6H_6 .

Butyl lithium was obtained as a 1.6 M solution in n-hexane from the Aldrich Chemical Co. Inc., Milwaukee, Wis., and syringed directly out of the bottle as required.

Carbon tetrachloride was obtained from BDH Chemical Ltd., Poole, and distilled from CaH_2 under a normal pressure of N_2 prior to use.

Chlorobenzene was obtained from Hopkin and Williams Ltd., Essex, and distilled from P_2O_5 under a normal pressure of nitrogen prior to use.

Chloroform was obtained from BDH Chemicals Ltd., Poole. It was freed from ethanol by stirring 800 ml portions with P_2O_5 for two hours, followed by distillation from CaH_2 under a normal pressure of nitrogen.

Chromium trichloride was obtained as metallic purple platelets of the anhydrous material from ICN Pharmaceuticals, Inc., Plainview, New York.

Deuterated solvents were distilled on a closed section of the vacuum line over the same desiccant as was used for the proteo analogue.

Dichloromethane was obtained from BDH Chemical Ltd., Poole, and distilled from P_2O_5 under a normal pressure of nitrogen prior to use.

Dichlorodimethylsilane was obtained from Midland Silicones Ltd., and distilled under nitrogen before use.

Dichloro-bis(dimethylamino)silane and Dichloro-bis(dimethylamino)germane were prepared from Me_2NH and the appropriate tetrahalide by the method of Cass and Coates (400).

Diethylether was obtained from BDH Chemical Ltd., Poole, and stored over Na wire.

Dimethylamine was obtained as the anhydrous material from BDH Chemicals Ltd., Poole. It was distilled in vacuo, and stored in a re-sealable glass ampoule in vacuo.

Dimethylsulphoxide (DMSO) was obtained from Fisons Scientific Apparatus Ltd., Loughborough, and stored over Linde-type 4A molecular sieves.

Germanium tetrachloride was obtained from BDH Chemicals Ltd., Poole. It was distilled in vacuo, and stored in a re-sealable glass ampoule under vacuum.

Gold trichloride was prepared by passing chlorine over finely divided metallic gold at 413 K. The anhydrous material was obtained as shining red platelets.

Hafnium metal 99.9% was obtained as a fine powder ($<40\mu$) from Goodfellow Metals, Cambridge.

Hafnium tetrabromide was prepared using the apparatus illustrated in Fig. A1. A stream of dry nitrogen was passed over the metal in a silica tube, and the furnace temperature was gradually raised to ~ 750 K. The nitrogen stream was gradually replaced by a mixture of Br_2 and N_2 produced by passing N_2 over previously dried liquid bromine. The product sublimes out of the

furnace tube and is collected in trap A. The product was pumped in vacuo for several hours before being sealed in glass ampoules under nitrogen.

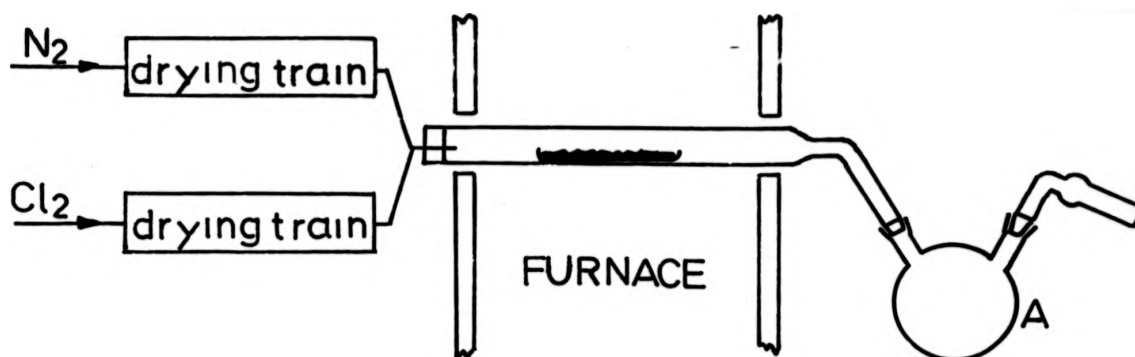


Fig. A1 Apparatus for the Preparation of MX_4 ($M = \text{Hf}, X = \text{Cl}, \text{B},$
 $M = \text{Zr}, X = \text{Cl}$)

Hafnium tetrachloride was prepared directly from the elements using the apparatus in Fig. A1.

Hafnium tetraiodide was prepared from the elements. Finely divided hafnium was mixed with a four-fold excess of resublimed iodine, and placed in a heavy walled furnace tube, Fig. A2.

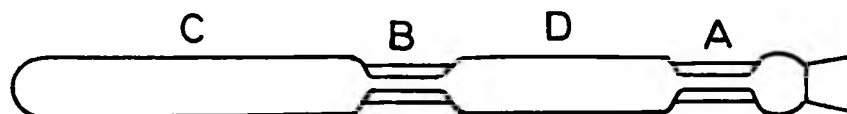


Fig. A2 Furnace Tube

The tube was attached to the vacuum line, and cooled to 77 K to prevent I_2 subliming out of the reaction mixture. The tube was sealed at A, and placed in a furnace at 523 K. Daily rotation of the tube over a 4 day period ensured that the reactants remained in the hot zone of the furnace. After reaction was complete, the products were sublimed into section D, and on careful warming at D, excess iodine was resublimed back into C to give HfI_4 as bright orange crystals at D. The product was then isolated by closing the seal at B.

Hexamethylcyclotrisiloxane was obtained from Alfa, Danvers, Mass.

n-Hexane was obtained from May and Baker Ltd., Dagenham, and distilled from CaH_2 under a normal pressure of nitrogen.

Molybdenum pentachloride, Molybdenum tetrachloride, Molybdenum trichloride, Molybdenum oxytetrachloride and Molybdenum oxytrichloride were all obtained from the Climax Molybdenum Co., New York.

Octamethylcyclotetrasiloxane was obtained from Alfa, Danvers, Mass.

Phenyl phosphine was obtained from Strem Chemicals Inc., Newburyport, Mass.

Pyridine was obtained from Fisons Scientific Apparatus Ltd., Loughborough, and prior to use was distilled from KOH under an N_2 atmosphere.

Silicon tetrachloride was distilled in vacuo from the technical grade material, and stored in a re-sealable glass ampoule under vacuum.

Tetrachloro-bis(trimethylamine)Hafnium (IV) was prepared from HfCl_4 and NMe_3 by the method of Willey (144).

Tetrachloro-bis(trimethylamine)Zirconium (IV) was prepared by the method of Hughes and Willey (141).

$\text{N},\text{N},\text{N}',\text{N}'$ -tetramethyldiaminomethane was obtained from the Aldrich Chemical Co. Inc., Milwaukee, Wis., and was purified by distillation from KOH in vacuo.

Tetrahydrofuran was obtained from May and Baker Ltd., Dagenham, and was distilled prior to use from CaH_2 under a normal pressure of nitrogen.

Tin metal was obtained from BDH Chemicals Ltd., Poole. It was washed with Et_2O , 2% HCl and EtOH before being dried in vacuo.

Tin tetrabromide and Tin tetrachloride were obtained from BDH Chemicals Ltd., Poole, and distilled in vacuo before use.

Tin tetraiodide was prepared from Iodine and an excess of Sn metal in boiling CCl_4 . The product was recrystallised from CCl_4 to give deep orange crystals.

Titanium tetrachloride was obtained from Hopkin and Williams Ltd., Essex. It was stored over Cu turnings, and syringed directly from the bottle as required.

α -Titanium trichloride was obtained as the anhydrous resublimed product from ICN Pharmaceuticals Inc., Plainview, New York.

Trichloro-bis(trimethylamine)M (III), $M = \text{Ti, V, Cr}$ were prepared from anhydrous metal trichlorides and NMe_3 by the method of Fowles and Hoodless (68).

Trichloro-(dimethylamino)germane and Trichloro-(dimethylamine)silane were prepared by the method of Cass and Coates (400).

Trichloro-tris(ligand)M (III), $M = \text{Ti, V, Cr}$, Ligand = THF, MeCN were prepared by extraction of the anhydrous metal halide with the appropriate ligand in a Soxhlet apparatus similar to the method of Kern (401).

Trimethylamine was obtained from BDH Chemicals Ltd., Poole. It was dried by distilling in vacuo onto P_2O_5 at 195 K, and after stirring for two hours was distilled in vacuo into a resealable glass ampoule.

s-Trioxan and s-Trithiane were obtained from the Aldrich Chemical Co. Inc. Milwaukee, Wis., and purified by sublimation in vacuo.

Tris(2-aminoethyl)amine, tren was obtained from Strem Chemicals Inc., Newburyport, Mass., and distilled under reduced pressure from KOH prior to use.

Tris(2-dimethylaminoethyl)amine, (Me_6tren) was prepared from tren by the method of Ciampolini and Nardi (402). Prior to use it was distilled under reduced pressure from KOH.

Tris(dimethylamino)phosphine oxide (HMPA) was obtained from the Aldrich Chemical Co. Inc., Milwaukee, Wis. Prior to use it was distilled under reduced pressure from KOH.

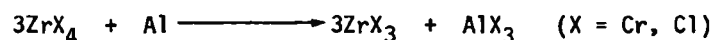
Tris(trimethylsilyl)phosphine was prepared from PCl_3 and Me_3SiMgCl in boiling THF according to the method of Schumann and Rösch (403).

Vanadium trichloride was obtained from ICN Pharmaceuticals Inc., Plainview, New York, as the anhydrous material.

Zirconium metal was obtained from Cerac/Pure Inc., Menomonee Falls, Wisconsin.

Zirconium tetrachloride was prepared from the elements in a similar manner to that used for HfBr_4 .

Zirconium tribromide and Zirconium trichloride were prepared by reduction of the tetrahalide with Al powder, i.e.



The Al powder was mixed with a 3.1 fold excess of ZrX_4 , and placed in a furnace tube (Fig. A2). The tube was pumped in vacuo, and sealed at A. It was then placed in a tube furnace at ~ 500 K. The tubes were removed each day and the fused mass formed by the reaction broken up and remixed. Reaction was complete after ~ 2 weeks, at which time careful heating of the tube at C sublimed excess ZrX_4 and AlX_3 into D. The ZrX_3 was then isolated by sealing the tube at B.

(b) Analytical Methods

Chlorine, Bromine and Iodine were determined by the Volhard method. A small quantity of the test sample (0.1 - 0.15 g) was hydrolysed in dilute aqueous HNO_3 and the solution made up to 100 ml. Determinations were carried out on 25 ml aliquots of the test solution, which were titrated against standard KSCN with $\text{NH}_4\text{Fe}(\text{SO}_4)_2/\text{HNO}_3$ as indicator. The end point was indicated

by the formation of blood-red $\text{Fe (III)(SCN)}_6^{3-}$. For chloride determinations, 4 ml PhNO_2 was added to each test aliquot to coagulate the AgCl precipitate. The AgNO_3 solution was standardised against NaCl with K_2CrO_4 as indicator.

Titanium was determined by Atomic Absorption. Typically, 0.2-0.3 g of sample were dissolved in dilute HCl , and the solution made up to 50 ml. The solutions were run on a Varian AA6 Spectrophotometer using a nitrous oxide/acetylene flame at 364.3 nm. The spectrophotometer was standardised before each determination with a standard solution of $\text{Ti(SO}_4)_2$ in H_2SO_4 (1 mg/ml)

Zirconium was determined gravimetrically following combustion to the oxide. 0.05-0.1 g sample was placed in a platinum crucible, which had previously been heated to constant weight, and was spotted with a few drops of 50% HNO_3 . The sample was gently heated until combustion occurred, after which it was heated strongly. The spotting/heating cycle was repeated until the crucible was at constant weight, and the residues weighed as ZrO_2 .

Carbon, Hydrogen, Nitrogen, Phosphorus and Sulphur were determined professionally by Butterworth Laboratories Ltd., Teddington, Middlesex.

APPENDIX B

APPENDIX B

EXPERIMENTAL TECHNIQUES AND INSTRUMENTATION

(a) Experimental Techniques

The majority of the compounds described in this thesis were air/moisture sensitive. To overcome this problem, special anaerobic techniques were used, the compounds being handled under an inert atmosphere (N_2 or Ar) or in high vacuum.

The Dry Box

Loading of reaction vessels, and the preparation of samples for spectroscopic analysis was carried out in a steel gloved box, which was constantly flushed with dry nitrogen. The internal atmosphere of the box was desiccated by two dishes of P_2O_5 which were regularly stirred and replaced. Entrance to the box was achieved via an 'airlock' type entry port, which was flushed with an independent supply of dry nitrogen.

The Vacuum Line

Preparation and isolation of products was carried out using a standard all glass vacuum line. The vacuum was produced and maintained with a Genevac double stage rotary pump, type G.R.D. 2 or G.R.S. 2, and an electrically heated mercury diffusion pump. Using this system a vacuum of 10^{-3} mmHg was obtainable (Fig. B1).

Solvent Drying

Solvent drying was carried out under a dry nitrogen atmosphere using a specially designed solvent still (Fig. B2). Batches of solvent (~400 ml) was refluxed ca 1 hour over the appropriate desiccant (See Appendix A), and then collected on the sintered frit. The solvent was de-gassed either by

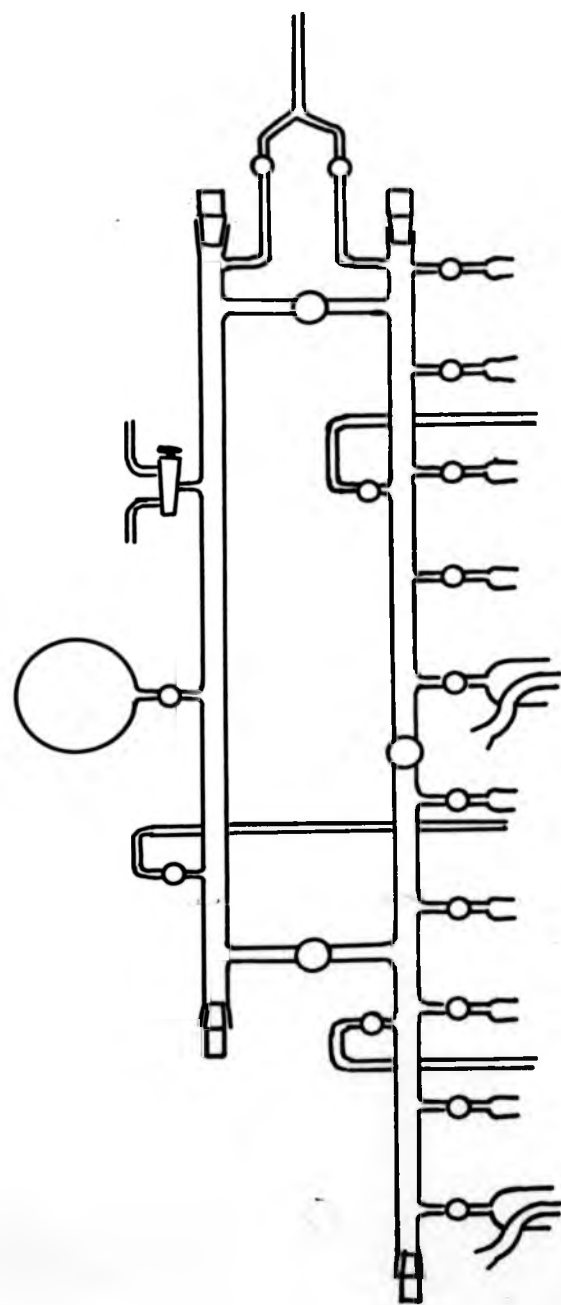


Fig. B1 The Vacuum Line

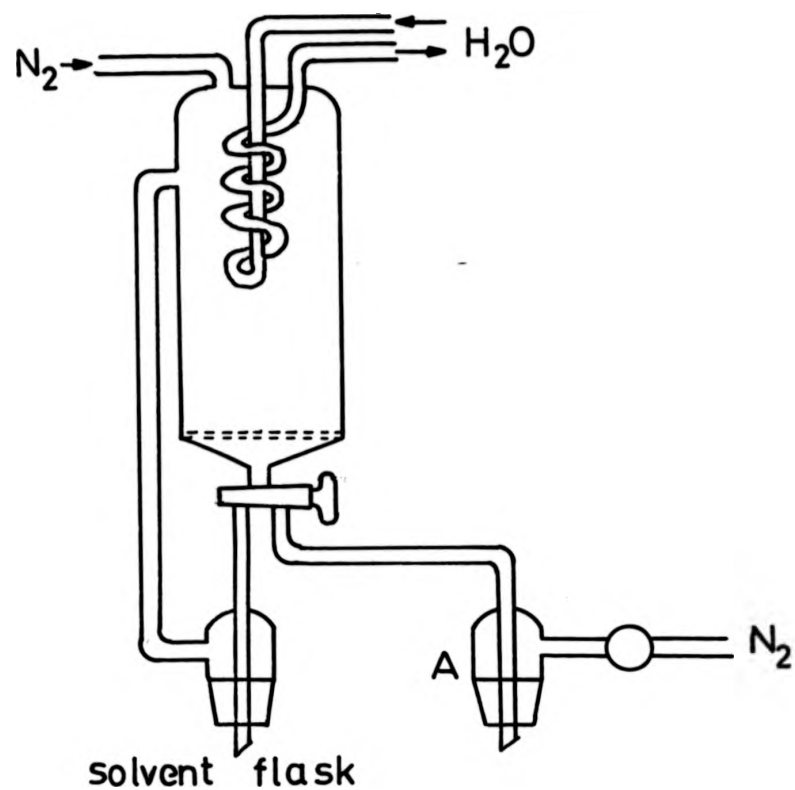


Fig. B2 Solvent Still

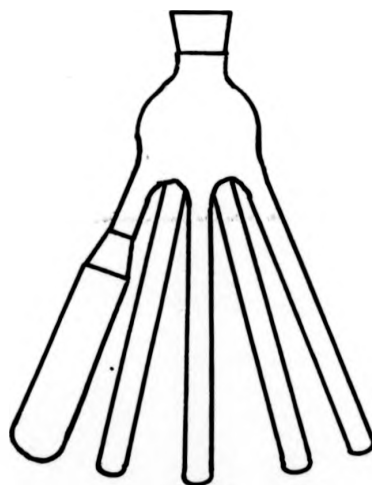


Fig. B3 a 'pig'

applying a positive pressure of dry nitrogen at the solvent collection point A, or more routinely by freeze/pump/thaw cycles on the vacuum line or by merely pumping off a small fraction of the solvent in vacuo.

Product Storage

After washing in vacuo with the appropriate solvent and pumping in vacuo for several hours, products were introduced to a pre-flamed glass 'pig' (Fig. B3). The pig was then transferred to the vacuum line, evacuated and the atmosphere replaced with dry nitrogen. Each 'leg' was then sealed under a normal pressure of nitrogen, thus encapsulating the sample.

Preparation of Complexes

(a) Reactions involving soluble metal halides, e.g. TiCl_4 , SnX_4 ($\text{X} = \text{Cl}$, Br , I), SbCl_5 , AuCl_3

Complexes were prepared by dropwise addition of a solution of the metal halide in a non-coordinating solvent (e.g. C_6H_6 , n-hexane, CCl_4 , etc) to a well stirred solution of the appropriate ligand in the same solvent. Experiments were either performed in a dry box or, where cooling of the reaction vessel was required, under a constant head of dry nitrogen.

(b) Reactions involving insoluble metal halides, e.g. ZrCl_4 , HfCl_4

Reactions in which an insoluble metal halide was used, or where prolonged reaction times were required, were carried out by sealing the reactants in a single ampoule bomb (Fig. B4a). The bomb was loaded using the apparatus shown in Fig. B5a. The metal halide was placed in a pre-flamed single ampoule bomb (A) and the appropriate ligand in a dry flask (B). These were attached to the apparatus and evacuated. Dry solvent is then condensed into both A and B at 77 K. On warming to room temperature, the solution in flask A was poured into B by rotating the glass arm. The reaction mixture was degassed, the bomb sealed, and placed on a mechanical shaker or in a water bath until reaction was complete.

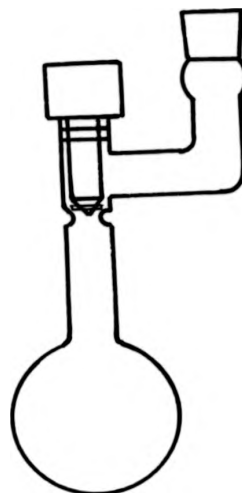


Fig. B4a Single Ampoule Reaction Vessel

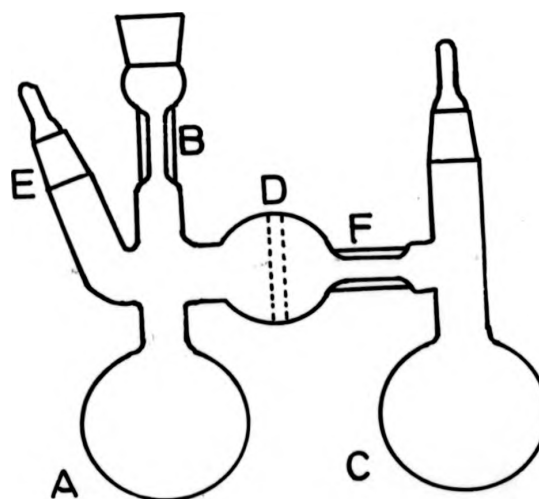


Fig. B4b Double Ampoule Reaction Vessel

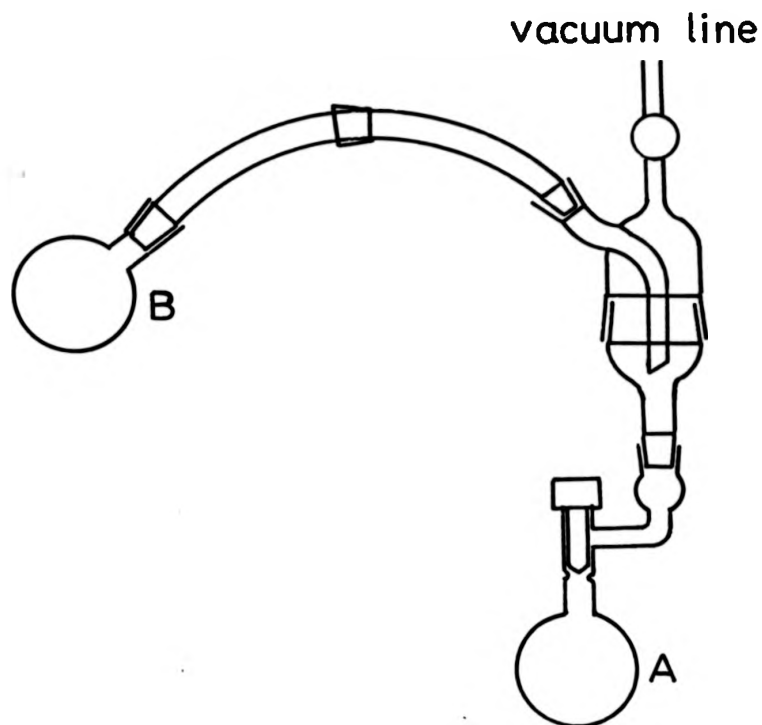


Fig. B5a Loading on the Vacuum Line

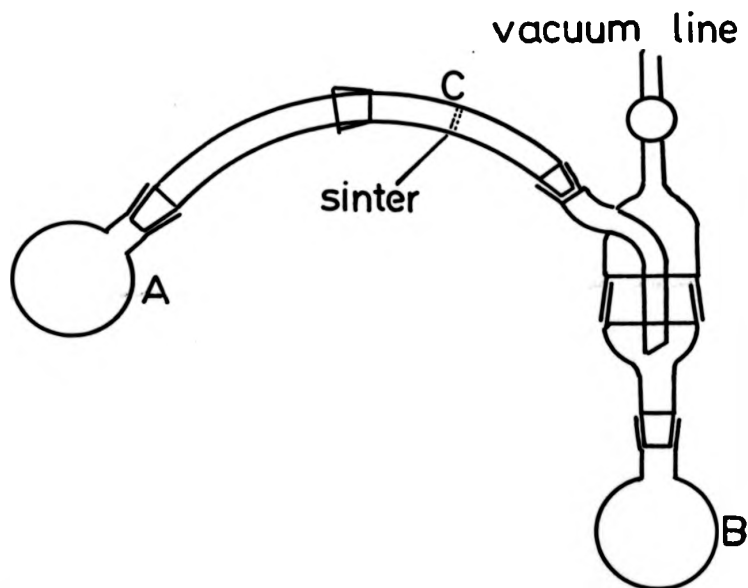


Fig. B5b Extraction on the Vacuum Line

- (c) Reactions involving soluble trimethylamine complexes as intermediates,
i.e. $\text{MCl}_3 \cdot 2\text{NMe}_3$, ($\text{M} = \text{Ti, V, Cr}$), $\text{MCl}_4 \cdot 2\text{NMe}_3$, ($\text{M} = \text{Zr, Hf}$)

Reactions of this type were carried out using the apparatus in Fig. B5b. The NMe_3 complex and ligand were placed in flasks A and B respectively, and the apparatus evacuated. Dry benzene was then condensed into A and B at 77 K. On warming to room temperature, the solution in flask A was decanted from the decomposition product through sinter C into flask B by rotating the glass arm. The reaction mixture was then degassed, and liberated NMe_3 trapped out at 77 K, and identified by its gas phase IR spectrum.

- (d) Reactions involving liquid NMe_3

These reactions were carried out using a double ampoule bomb (Fig. B4b). The solid reactant was introduced to bulb A via seal B, and the bomb evacuated on the vacuum line. Dry NMe_3 was then condensed into A at 77 K, and the bomb sealed at B in vacuo. On warming to room temperature, the NMe_3 solution was tipped into bulb C via sinter D, and the NMe_3 back-distilled by cooling bulb A to 273 K. This process was repeated until complete extraction had been achieved. NMe_3 was removed from the system via E, and the product isolated by sealing the bomb at F.

Product Isolation

Workup of products was achieved using the apparatus shown in Fig. B5b. The crude products are placed in flask A, and the system is evacuated. Dry solvent is distilled into A at 77 K, and when the flask has warmed to room temperature, the solvent is decanted through the frit C into flask B. This process is continued until all soluble products have been extracted, and the insoluble product is then pumped in vacuo for several hours.

(b) Instrumentation and Physical Measurements

Infra Red Spectra

Infra red spectra ($4000\text{--}200\text{ cm}^{-1}$) were recorded on Perkin-Elmer 621 or 580 B Grating Infra Red Spectrophotometers. Spectra run on the PE 621 instrument were calibrated at 2855 , 1601 and 1028 cm^{-1} using a 0.05 mm polystyrene film. Solid samples were investigated as Nujol or hexachlorobutadiene mulls sandwiched between CsI plates. Gaseous samples were condensed into a gas cell, fitted with NaCl windows and run on a PE 457 instrument. Spectra in the $400\text{--}50\text{ cm}^{-1}$ region were recorded on a RIIC FS-720 Spectrophotometer as Nujol mulls held between polythene plates.

Nuclear Magnetic Resonance Spectra

Proton NMR spectra were recorded on Perkin-Elmer R12 (60 MHz), Brücker WH 90 (90 MHz), Perkin-Elmer R34 (220 MHz) or Brücker WH 400 (400 MHz) spectrometers. The field at which each spectrum was measured is indicated in the text. Tetramethylsilane (TMS) was used as a reference. ^{13}C and ^{31}P spectra were recorded on a Brücker WH 90 instrument at 22.63 MHz and 36.44 MHz respectively. ^{13}C spectra were referenced using TMS, and ^{31}P spectra with 40% H_3PO_4 (glass capillary).

Electronic Spectra

Ultra violet and visible spectra were measured on a Carey 14 spectrophotometer using the apparatus shown in Fig. B6. Routine spectra were run on a Unicam SP 800 instrument. Solid samples were introduced into bulb A in the dry box, and the cell was then removed to the vacuum line and evacuated. The appropriate solvent was then distilled into bulb A at 77 K, and on warming to room temperature, the solution was tipped into the cylindrical quartz UV cell B. The sample could be diluted by distilling on additional solvent from bulb A.

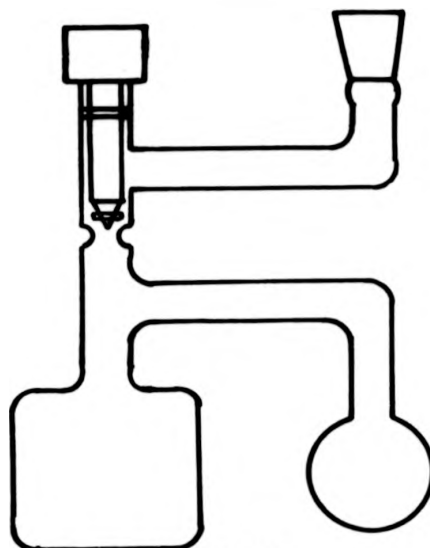


Fig. B6 UV Cell

Conductivity Measurements

Conductivities were measured using the apparatus shown in Fig. B7.

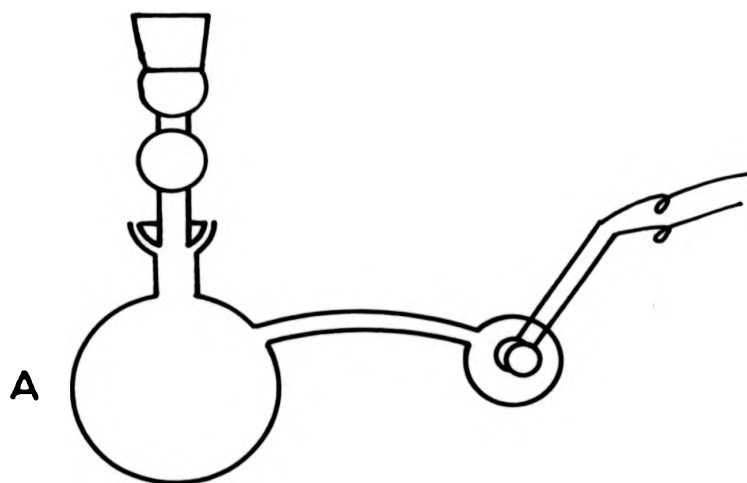


Fig. B7 Conductivity Cell

An accurately weighed small amount of sample was placed in bulb A, and the apparatus evacuated. The appropriate solvent was then condensed into A at 77 K, and the weight of solvent determined by difference. The apparatus

was placed in a thermostated bath at 298 K for 30 mins to equilibrate, and sufficient solution was then poured into cell B to cover the platinum electrodes. The resistance of the solution was then measured using a Phillips PR 9500 bridge. Further readings were taken at different concentrations by removing some of the solvent in vacuo and repeating the above procedure. A plot of concentration of sample versus resistance gives the solution resistance at $10^{-3}M$ by extrapolation. The conductivity can now be calculated by,

$$\Lambda_m = \frac{1000 C}{C_m R}$$

where Λ_m = molar conductivity.

C = Cell Constant, calculated as 0.308 cm^{-1} using a standard 0.1 M KCl solution.

C_m = molar Concentration of solute

R = Resistance

Experimentally determined values were compared to values obtained for non-conducting, 1:1 and 1:2 electrolytes in the same solvent (222).

REFERENCES

1. R. Colton and J. H. Canterford, 'Halides of the first row transition metals', Wiley, NY (1969).
2. J. H. Canterford and R. Colton, 'Halides of the second and third row transition metals', Wiley, NY (1969).
3. D. L. Kepert, 'The Early Transition Metals', Academic Press, London (1972).
4. R. J. H. Clark, 'The Chemistry of Titanium and Vanadium', Elsevier, Amsterdam (1968).
5. D. A. Johnson 'Some Thermodynamic aspects of Inorganic Chemistry', C.U.P. (1968).
6. D. O. Kepert and K. Vrieze, 'Compounds of the transition elements involving metal-metal bonds', Pergamon Press (1975).
7. D. Kepert and R. Mandyczewsky, Inorg. Chem., 1968, 7, 2091.
8. H. J. Gardner, Nature, 1964, 204, 282.
9. A. G. Sharpe, Adv. Fluorine Chem., 1960, 1, 29.
10. R. D. Peacock, Prog. Inorg. Chem., 1960, 2, 193.
11. R. D. W. Kemmitt and D. W. A. Sharp, Prog. Fluorine Chem., 1965, 4, 142.
12. D. Babel, Structure and Bonding, 1967, 3, 1.
13. R. D. Peacock, Adv. Fluorine Chem., 1973, 7, 113.
14. A. W. Strauss and J. D. Corbett, Inorg. Chem., 1969, 8, 227.
15. R. L. Daake and J. D. Corbett, Inorg. Chem., 1978, 17, 1192.
16. A. Cisar, J. D. Corbett and R. L. Daake, Inorg. Chem., 1979, 18, 836.
17. J. C. Taylor and P. W. Wilson, Acta Crystallogr., Sect. B, 1974, 30, 1216.
18. E. A. Allen, B. J. Brisdon and G. W. A. Fowles, J. Chem. Soc., 1964, 4531.
19. G. W. A. Fowles and J. L. Frost, J. Chem. Soc. (A), 1967, 671.
20. A. Zalkin and D. E. Sands, Acta. Crystallogr., 1958, 11, 615.
21. D. E. Sands and A. Zalkin, Acta. Crystallogr., 1959, 12, 723.

22. P. M. Boorman, N. N. Greenwood, M. A. Hildon and H. J. Whitfield, J. Chem. Soc.(A), 1967, 2017.
23. W. Littke and G. Brauer, Z. Anorg. Allg. Chem., 1963, 325, 122.
24. A. J. Edwards and G. R. Jones, J. Chem. Soc.(A), 1969, 1651.
25. I. R. Beattie and G. A. Ozin, J. Chem. Soc.(A), 1969, 1691.
26. M. F. A. Dove, J. A. Creighton and L. A. Woodward, Spectrochim. Acta., 1962, 18, 267.
27. M. W. Lister and L. E. Sutton, Trans. Faraday. Soc., 1941, 37, 393.
28. J. E. Griffiths, J. Chem. Phys., 1968, 49, 642.
29. P. Brand and J. Schmidt, Z. Anorg. Allg. Chem., 1966, 348, 257.
30. R. F. Rolsten and H. M. Sisler, J. Am. Chem. Soc., 1957, 79, 5891.
31. J. H. Simons and M. G. Powell, J. Am. Chem. Soc., 1959, 12, 719.
32. R. B. Johannesen, G. A. Candela and T. T. Sang, J. Chem. Phys., 1968, 48, 5544.
33. B. Krebs, Angew. Chem. Int. Ed., 1969, 8, 146.
34. B. Krebs, Z. Anorg. Allg. Chem., 1970, 378, 263.
35. R. D. Burbank and F. N. Bensey, U.S. At. Energy Comm., 1956, K-1280.
36. A. Büchler, J. B. Berkowitz-Mattuck and D. H. Dugre, J. Chem. Phys., 1961, 34, 2202.
37. Z. E. Zarsorin, V. G. Girichev, V. P. Spiridonov, K. S. Krasnov and V. I. Tsirel'Nikov, Izv. Vyssh. Uchebn. Zaved., Khim. Khim. Tekhnol., 1973, 16, 802. Chem. Abs., 1973, 79, 71111.
38. G. V. Girichev, E. Z. Zasorin, N. I. Krasnov and V. P. Spiridonov, Izv. Vyssh. Uchebn. Zaved., Khim. Khim. Tekhnol., 1975, 18, 1647. Chem. Abs., 1976, 84, 52478.
39. T. M. Brown and E. L. McCann, Inorg. Chem., 1968, 7, 1227.
40. L. F. Dahl and D. L. Wampler, Acta Crystallogr., 1962, 15, 903.
41. H. Schaeffer, H. G. v. Schnering, J. Tillack, F. Kuhnen, H. Woehrlé and H. Baumann, Z. Anorg. Allg. Chem., 1976, 353, 281.
42. G. Natta, P. Corradini and G. Allegra, J. Polymer. Sci., 1961, 51, 399.
43. J. A. Watts, Inorg. Chem., 1966, 5, 281.

44. J. Kleppinger, J. C. Calabrese and E. M. Larsen, *Inorg. Chem.*, 1975, 14, 3128.
45. L. F. Dahl, T-I. Chiang, P. W. Seabaugh and E. M. Larsen, *Inorg. Chem.*, 1964, 3, 1236.
46. B. Morosin and A. Narath, *J. Chem. Phys.*, 1964, 40, 1958.
47. H. G. v. Schnering and H. Wöhrle, *Angew. Chem. Int. Ed.*, 1963, 2, 558.
48. H. Schäfer and H. G. v. Schnering, *Angew. Chem.*, 1964, 76, 833.
49. D. Babel, *J. Solid State Chem.*, 1972, 4, 410.
50. R. Siepmann, H. G. v. Schnering and H. Schäfer, *Angew. Chem. Int. Ed.*, 1967, 6, 637.
51. R. Siepmann and H. G. v. Schnering, *Z. Anorg. Allg. Chem.*, 1968, 357, 289.
52. R. B. Jackson and W. E. Streib, *Inorg. Chem.*, 1971, 10, 1760.
53. J. W. Tracy, N. W. Gregory, E. C. Lingafelter, J. D. Dunitz, H. C. Mez, R. E. Rundle, L. Scheringer, H. L. YakeI jr. and M. K. Wilkinson, *Acta Crystallogr.*, 1961, 14, 927.
54. J. D. Corbett, R. L. Daake, K. R. Poeppelmeier and D. H. Guthrie, *Inorg. Chem.*, 1978, 100, 652.
55. D. G. Adolphson and J. D. Corbett, *Inorg. Chem.*, 1976, 15, 1820.
56. N. V. Sidgwick, *J. Chem. Soc.*, 1941, 433.
57. S. Ahrland, J. Chatt and N. R. Davies, *J. Chem. Soc. Quart. Rev.*, 1958, 12, 265.
58. R. J. Pearson, *J. Chem. Educ.* 1968, 45, 581.
59. R. J. Pearson, *J. Chem. Educ.*, 1968, 45, 643.
60. F. M. Chung and A. D. Westland, *Can. J. Chem.*, 1969, 47, 195.
61. J. Chatt, *J. Inorg. Nucl. Chem.*, 1958, 8, 515.
62. G. W. A. Fowles and R. A. Walton, *J. Chem. Soc.*, 1964, 4331.
63. A. T. Casey and R. J. H. Clark, *Inorg. Chem.*, 1968, 7, 1598.
64. D. E. Scaife, *Aust. J. Chem.*, 1967, 20, 845.
65. M. Antler and A. W. Laubengayer, *J. Am. Chem. Soc.*, 1955, 77, 5250.

66. G. W. A. Fowles and C. M. Pleass, *J. Chem. Soc.*, 1957, 1674.
67. G. W. A. Fowles and R. A. Hoodless, *J. Chem. Soc.*, 1963, 33.
68. M. W. Duckworth, G. W. A. Fowles and P. T. Greene, *J. Chem. Soc.(A)*, 1967, 1592.
69. G. W. A. Fowles, P. T. Greene and J. S. Wood, *J. Chem. Soc., Chem. Commun.*, 1967, 971.
70. R. J. H. Clark and G. Natile, *Inorg. Chim. Acta*, 1970, 4, 533.
71. C. D. Schmulbach, C. L. Kolich and C. C. Hinkley, *Inorg. Chem.*, 1972, 11, 2841.
72. K. Watenpaugh and C. N. Caughlan, *Inorg. Chem.*, 1966, 5, 1782.
73. E. C. Alyea and P. H. Merrell, *Inorg. Nucl. Chem. Lett.*, 1973, 9, 69.
74. I. R. Beattie and T. Gilson, *J. Chem. Soc.*, 1965, 6595.
75. P. C. Crouch, G. W. A. Fowles and R. A. Walton, *J. Chem. Soc.(A)*, 1968, 2172.
76. P. T. Greene and P. L. Orioli, *J. Chem. Soc.(A)*, 1969, 1621.
77. B. J. Russ and J. S. Wood, *J. Chem. Soc., Chem. Commun.*, 1966, 745.
78. P. T. Greene, B. J. Russ and J. S. Wood, *J. Chem. Soc.(A)*, 1971, 3636.
79. E. L. Muetterties and R. A. Schunn, *J. Chem. Soc. Quart. Rev.*, 1966, 20, 245.
80. C. Furlani, *Coord. Chem. Rev.*, 1968, 3, 141.
81. J. S. Wood, *Progr. Inorg. Chem.*, 1972, 16, 227.
82. C. I. Bränden and I. Lindquist, *Acta Chem. Scand.*, 1961, 17, 353.
83. C. I. Bränden, *Acta Chem. Scand.*, 1962, 16, 1806.
84. J. V. Brenčič, B. Čeh and P. Segedin, *Z. Anorg. Allg. Chem.*, 1979, 454, 181.
85. R. A. Walton, *J. Chem. Soc. Quart. Rev.*, 1965, 19, 126.
86. R. S. P. Coutts and P. C. Wailles, *Adv. Organomet. Chem.*, 1970, 9, 135.
87. C. I. Bränden and I. Lindquist, *Acta Chem. Scand.*, 1960, 14, 726.
88. M. Boyer, Y. Jeanin, C. Rocchiccioli-Deltcheft and R. Thouvenot, *J. Coord. Chem.*, 1978, 4, 219.
89. L. Brun, *Acta Crystallogr.*, 1966, 20, 739.

90. M. G. B. Drew, G. W. A. Fowles, D. A. Rice and N. Rolfe, *J. Chem. Soc., Chem. Commun.*, 1971, 231.
91. B. P. Susz and D. Cassimatis, *Helv. Chim. Acta*, 1961, 44, 395.
92. D. G. Holah and J. P. Fackler, *Inorg. Chem.*, 1965, 4, 1112, 1721.
93. N. Tanaka and K. Nagase, *Bull. Chim. Soc. Jpn.*, 1969, 42, 2854.
94. J. Hughes and G. R. Willey, *Inorg. Chim. Acta*, 1974, 11, L25.
95. D. A. House, *Inorg. Nucl. Chem. Lett.*, 1967, 3, 67.
96. R. J. H. Clark, D. L. Kepert and R. S. Nyholm, *J. Chem. Soc.*, 1965, 2877.
97. D. G. Blight, D. L. Kepert, R. Mandyczewsky and K. R. Trigwell, *J. Chem. Soc., Dalton Trans.*, 1972, 313.
98. R. J. H. Clark, M. L. Greenfield and R. S. Nyholm, *J. Chem. Soc.(A)*, 1966, 1254.
99. B. J. Brisdon, G. W. A. Fowles and B. P. Osborne, *J. Chem. Soc.*, 1962, 1330.
100. G. W. A. Fowles and C. M. Pleass, *J. Chem. Soc.*, 1957, 2078.
101. P. J. H. Carnell and G. W. A. Fowles, *J. Chem. Soc.*, 1959, 4113.
102. D. A. Edwards and G. W. A. Fowles, *J. Chem. Soc.*, 1961, 24.
103. R. J. H. Clark, J. Lewis, R. Nyholm and P. Pauling, *Nature*, 1961, 192, 222.
104. R. J. H. Clark, J. Lewis and R. Nyholm, *J. Chem. Soc.*, 1962, 2460.
105. R. J. H. Clark, D. L. Kepert, R. Nyholm and J. Lewis, *Nature*, 1963, 99, 599.
106. R. J. H. Clark, W. Errington, J. Lewis and R. Nyholm, *J. Chem. Soc.(A)*, 1966, 989.
107. R. J. H. Clark, R. H. Negrath and R. Nyholm, *J. Chem. Soc., Chem. Commun.*, 1966, 486.
108. W. P. Crisp, R. L. Deutscher and D. C. Kepert, *J. Chem. Soc.(A)*, 1970, 2199.
109. R. J. H. Clark, *J. Chem. Soc.*, 1965, 5699.
110. J. Chatt and R. G. Hayter, *J. Chem. Soc.*, 1963, 1343.
111. E. G. Rochow and E. W. Abel, 'The Chemistry of Germanium, Tin and Lead', Pergamon Press, Oxford (1975).

112. E. G. Rochow, 'The Chemistry of Silicon', Pergamon Press, Oxford (1975).
113. I. R. Beattie, J. Chem. Soc. Quart. Rev., 1963, 17, 382.
114. M. Webster and H. E. Blaydon, J. Chem. Soc.(A), 1969, 2443.
115. I. Lindquist, 'Inorganic adducts of oxo molecules', Springer, Berlin (1963).
116. Y. Hermodsson, Acta Crystallogr., 1960, 13, 656.
117. G. G. Mather, G. M. McLaughlin and A. Pidcock, J. Chem. Soc., Dalton Trans., 1973, 1823.
118. L. A. Aslanov, V. M. Ionov, W. M. Attia, A. B. Permin and V. S. Petrosyan, J. Organomet. Chem., 1978, 144, 39.
119. M. Nardelli and G. Fava, Acta Crystallogr., 1959, 12, 727.
120. J. D. Smith, 'The Chemistry of Arsenic, Antimony and Bismuth', Pergamon Press, Oxford (1975).
121. R. D. Schmulbach, Inorg. Chem., 1965, 4, 1232.
122. A. Lipka, Acta Crystallogr., Sect. B, 1979, 35, 3020.
123. M. Webster, Chem. Rev., 1966, 66, 87.
124. V. Gutmann and E. Wychera, Inorg. Nucl. Chem. Lett., 1966, 2, 257.
125. D. H. Boal and G. A. Ozin, J. Chem. Soc., Dalton Trans., 1972, 1824.
126. M. Webster and S. Keats, J. Chem. Soc.(A), 1971, 836.
127. R. Hulme, D. Mullen and J. C. Scruton, Acta Crystallogr., Sect. A, 1969, 25, 5171.
128. T. Bjorvatten, Acta Chem. Scand., 1966, 20, 1863.
129. L. P. Battaglia, A. Bonamartini Corradi, G. Pelizzi and M. E. Vidoni Tani, J. Chem. Soc. Dalton Trans., 1977, 1141.
130. M. J. Deveney and M. Webster, J. Chem. Soc.(A), 1970, 1643.
131. K. E. Kim and G. W. Chang, Can. J. Microbiol., 1974, 20, 1754.
132. P. H. Clippard, J. C. Hanson and R. C. Taylor, J. Cryst. Mol. Struct., 1971, 1, M363.
133. D. D. Eley and H. Watts, J. Chem. Soc., 1952, 1914.
134. W. Strohmeier, J. F. Guttenberger, H. Blumenthal and G. Albert, Chem. Ber., 1966, 99, 3419.

135. R. Kurze and R. Paetzold, *Z. Anorg. Allg. Chem.*, 1972, 387, 367.
136. J. J. Watkins, M. D. Sefcik and M. A. Ring, *Inorg. Chem.*, 1972, 11, 3146.
137. C. C. Hsu and R. A. Geanagel, *Inorg. Chem.*, 1977, 16, 2529.
138. J. G. Drake and G. W. A. Fowles, *J. Chem. Soc.*, 1960, 1498.
139. R. F. Trandell and G. Urry, *J. Inorg. Nucl. Chem.*, 1978, 40, 1305.
140. K. G. Huggins, F. W. Parrett and H. A. Patel, *J. Inorg. Nucl. Chem.*, 1969, 31, 1209.
141. J. Hughes and G. R. Willey, *Inorg. Chim. Acta*, 1976, 20, 137.
142. J. Hughes and G. R. Willey, *Inorg. Chim. Acta*, 1977, 24, L81.
143. J. Hughes, Ph.D. Thesis, University of Warwick (1975).
144. G. R. Willey, *Inorg. Chim. Acta*, 1977, 21, L12.
145. L. S. Jenkins and G. R. Willey, *Inorg. Chim. Acta*, 1978, 29, L201.
146. T. A. Lane and J. T. Yoke, *Inorg. Chem.*, 1976, 15, 484.
147. R. Kiesel and E. P. Schram, *Inorg. Chem.*, 1973, 12, 1090.
148. K. Kiesel and E. P. Schram, *Inorg. Chem.*, 1974, 13, 1313.
149. R. J. H. Clark, *Spectrochim. Acta*, 1965, 21, 955.
150. M. L. H. Green and C. R. Lucas, *J. Chem. Soc., Dalton Trans.*, 1972, 1000.
151. P. C. Wailes, R. S. P. Coutts and H. Weigold, 'Organometallic Chemistry of Ti, Zr and Hf', Academic Press, New York (1974).
152. J. J. Saltzmann, *Helv. Chim. Acta*, 1968, 51, 526.
153. R. R. Holmes and E. F. Bertaut, *J. Am. Chem. Soc.*, 1958, 80, 2980.
154. N. Menshutkin, *Z. Physik. Chemie*, 1890, 5, 589.
155. G. Y. Ahliah and M. Goldstein, *J. Chem. Soc.(A)*, 1970, 326, 2590.
156. A. K. Biswas, J. R. Hall and D. P. Schweinsberg, *Inorg. Nucl. Chem. Lett.*, 1978, 14, 275.
157. D. J. Williams and K. J. Wynne, *Inorg. Chem.*, 1978, 17, 1108.
158. D. J. Williams, C. O. Quicksall and K. J. Wynne, *Inorg. Chem.*, 1978, 17, 2071.

159. D. A. Edwards and G. W. A. Fowles, *J. Less-Common Met.*, 1962, 4, 512.
160. E. A. Allen, K. Feenan and G. W. A. Fowles, *J. Chem. Soc.*, 1965, 1636.
161. J. Lewis, R. S. Nyholm and P. W. Smith, *J. Chem. Soc.*, 1962, 2592.
162. C. Djordjević, R. S. Nyholm, C. S. Pande and M. H. B. Stiddard, *J. Chem. Soc.(A)*, 1966, 16.
163. W. M. Carmichael and D. A. Edwards, *J. Inorg. Nucl. Chem.*, 1967, 29, 1535.
164. P. C. H. Mitchell, *J. Chem. Soc. Quart. Rev.*, 1966, 20, 103.
165. C. D. Garner, P. Lambert, F. E. Mabbs and T. J. King, *J. Chem. Soc., Dalton Trans.*, 1977, 119.
166. M. Cousins and M. L. H. Green, *J. Chem. Soc.*, 1964, 1567.
167. P. C. H. Mitchell, *J. Inorg. Nucl. Chem.*, 1964, 26, 1967.
168. E. M. Larson and T. E. Henzler, *Inorg. Chem.*, 1974, 13, 581.
169. G. W. A. Fowles, B. J. Russ and G. R. Willey, *J. Chem. Soc., Chem. Commun.*, 1967, 646.
170. G. W. A. Fowles and G. R. Willey, *J. Chem. Soc.(A)*, 1968, 1435.
171. E. M. Larson, *Adv. Inorg. Chem. Radiochem.*, 1970, 13, 1.
172. D. A. Miller and R. D. Bereman, *Coord. Chem. Rev.*, 1972, 9, 107.
173. R. J. Puddephatt, 'The Chemistry of Gold', Elsevier, Amsterdam (1978).
174. G. W. A. Fowles, P. T. Greene and T. E. Lester, *J. Inorg. Nucl. Chem.*, 1967, 29, 2365.
175. M. Ciampolini, *Structure and Bonding*, 1969, 6, 52.
176. M. Ciampolini, *J. Chem. Soc., Chem. Commun.*, 1966, 47.
177. J. Hughes and G. R. Willey, *J. Coord. Chem.*, 1974, 4, 33.
178. J. Hughes and G. R. Willey, *Inorg. Chim. Acta*, 1975, 13, L1.
179. J. T. Braunscholtz, E. A. V. Ebsworth, F. G. Mann and N. Sheppard, *J. Chem. Soc.*, 1958, 2780.
180. M. E. Baldwin, *J. Chem. Soc.*, 1960, 4369.
181. D. A. Buckingham and D. Jones, *Inorg. Chem.*, 1965, 4, 1387.

182. S. K. Madan and J. Peone jr, *Inorg. Chem.*, 1967, 6, 463.
183. P. Paoletti, L. F. Fabbrizzi and R. Barbucci, *Inorg. Chim. Acta. Rev.*, 1973, 7, 43.
184. S. B. Hartley, W. S. Holmes, J. K. Jacques, M. F. Mole and J. C. Coubrey, *J. Chem. Soc. Quart. Rev.*, 1963, 17, 204.
185. J. R. Van Wazer, *J. Am. Chem. Soc.*, 1956, 78, 5709.
186. G. M. Phillips, J. S. Hunter and L. E. Sutton, *J. Chem. Soc.*, 1945, 146.
187. J. V. Bell, J. Heisler, H. Tannenbaum and J. Goldenson, *J. Am. Chem. Soc.*, 1954, 76, 5184.
188. R. Dorschner, F. Choplin and G. Kaufmann, *J. Mol. Struct.*, 1974, 22, 421.
189. R. Dorshner and G. Kaufmann, *Inorg. Chim. Acta*, 1975, 15, 71.
190. G. J. Bullen. F. S. Stephens and R. J. Wade, *J. Chem. Soc.(A)*, 1969, 1804.
191. C. Rønning and J. Songstad, *Acta Chem. Scand., Sect. A*, 1979, 33, 187.
192. W. McFarlane and D. S. Rycroft, *J. Chem. Soc. Commun.*, 1972, 902.
193. N. M. Karayannis, C. M. Mikuiski, L. L. Pytlewski, *Inorg. Chi. Acta. Rev.*, 1971, 69.
194. H. Teichmann and G. Hilgetag, *Angew. Chem. Int. Ed.*, 1967, 6, 1013.
195. V. Gutmann and G. Beer, *Inorg. Chim. Acta.*, 1969, 3, 87.
196. C. I. Bränden, *Acta Chem. Scand.*, 1963, 17, 759.
197. L. A. Aslanov, V. M. Attiya, M. V. Ionov, A. B. Permin, V. S. Petrosyan, *Tezisy Dokl-Vres. Soveshch. Org. Kristallokhim. 1st Ed., Riga. USSR*, 1974. *Chem. Abs.*, 1977, 87, 61106.
198. J. F. de Wet and S. F. Darlow, *Inorg. Nucl. Chem. Lett.*, 1971, 7, 1041.
199. J. C. Russell, M. P. du Plessis, L. R. Nassimbeni, B. J. Gellatly, *Acta Crystallogr., Sect. B*, 1977, 33, 2062.
200. R. Julien, N. Rodier and P. Khodadad, *Acta. Crystallogr., Sect. B*, 1977, 33, 2411.
201. J. M. LeCarpentier, R. Schlupp and R. Weiss, *Acta. Crystallogr., Sect. B*, 1972, 28, 1278.

202. J. A. Tiethof, J. K. Stalick and D. W. Meek, *Inorg. Chem.*, 1973, 12, 1171.
203. Von F. I. Vilesov, S. N. Lopatin, V. I. Vivna, R. Paetzold and
k. Niendorf, *Z. Phys. Chem. (Liepzig)*, 1974, 255, 661.
204. F. Lux, F. I. Vilesov, S. N. Lopatin, V. I. Vovna and R. Paetzold,
Z. Phys. Chem. (Liepzig), 1977, 258, 593.
205. E. le Coz and J. E. Guerchais, *Bull. Soc. Chim. Fr.*, 1971, 80.
206. R. A. Zingaro and R. M. Hedges, *J. Phys. Chem.*, 1961, 65, 1132.
207. M. W. G. de Bolster and W. L. Groeneveld, *Recl. Trav. Chim. Pays-Bas*,
1971, 90, 477.
208. J. G. H. du Preez and F. G. Sadie, *J. S. Afr. Chem. Inst.*, 1966, 19, 73.
209. J. T. Donoghue and D. A. Peters, *J. Inorg. Nucl. Chem.*, 1969, 31, 467.
210. N. B. Mikheeva, A. N. Kamenskaya, N. A. Konovalova, T. A. Bibakova and
Mikheeva, *Russ. J. Inorg. Chem.*, 1977, 22, 1766.
211. M. Valloton and A. E. Merbach, *Helv. Chim. Acta*, 1975, 58, 2272.
212. W. E. Slinkard and D. W. Meek, *Inorg. Chem.*, 1969, 8, 1811.
213. P. M. Boorman, S. A. Clow, D. Potts, H. Wieser, *Inorg. Nucl. Chem.*
Lett., 1973, 9, 941.
214. J. A. Tiethof, A. T. Hetey and D. W. Meek, *Inorg. Chem.*, 1974, 13, 2505.
215. P. Bruno, M. Caselli, C. Gragale and S. Magrino, *J. Inorg. Nucl. Chem.*,
1977, 39, 1757.
216. C. M. P. Favez and A. E. Merbach, *Helv. Chim. Acta*, 1977, 60, 2695.
217. H. Teichmann and G. Hilgetag, *Chem. Ber.*, 1965, 98, 856.
218. T. A. Mastryukova and M. I. Kabachnik, *J. Org. Chem.*, 1971, 36, 1201.
219. W. van der Veer and F. Jellinek, *Recl. Trav. Chim. Pays-Bas*, 1968, 87, 367.
220. R. F. Zahrobsky, *J. Am. Chem. Soc.*, 1971, 93, 3313.
221. P. M. Boorman and K. J. Riener, *Canad. J. Chem.*, 1971, 49, 2926.
222. W. J. Geary, *Coord. Chem. Rev.*, 1971, 7, 81.
223. Von D. Kottgen, H. Stoll, A. Lente, R. Pantzer and J. Goubeau, *Z. Anorg.*
Allg. Chem., 1971, 385, 56.

224. Y. Kawano, Y. Gushikem and Y. Hase, *J. Coord. Chem.*, 1978, 4, 227.
225. Yu. A. Lysenko, O. A. Osipov and E. E. Kravtsov, *Russ. J. Inorg. Chem.*, 1971, 33, 3313.
226. W. van der Veer and F. Jellinek, *Recl. Trav. Chim. Pays-Bas*, 1966, 85, 842.
227. T. J. Kistenmacher and G. D. Stucky, *Inorg. Chem.*, 1971, 10, 122.
228. J. L. Templeton, W. L. Dorman, J. C. Dorman, J. C. Clardy and R. E. McCarley, *Inorg. Chem.*, 1978, 17, 1263.
229. J. L. Templeton and R. E. McCarley, *Inorg. Chem.*, 1978, 17, 2293.
230. I. R. Beattie, T. Gilson, K. Livingston, V. Fawcett and G. A. Ozin, *J. Chem. Soc.(A)*, 1967, 712.
231. P. Reich and W. Wieker, *Z. Naturforsch., B.*, 1968, 23, 739.
232. I. R. Beattie and G. A. Ozin, *J. Chem. Soc.(A)*, 1970, 370.
233. M. Becke-Goehring and A. Slawisch, *Z. Anorg. Allg. Chem.*, 1966, 346, 295.
234. J. L. Burdett and L. L. Burger, *Canad. J. Chem.*, 1966, 44, 111.
235. M. Zeldin, P. Mehta and W. D. Vernon, *Inorg. Chem.*, 1979, 18, 463.
236. G. Roland, B. Gilbert, J. Decerf and G. Duykaerts, *Spectrochim. Acta, Part A*, 1973, 29, 879.
237. G. W. A. Fowles, P. T. Greene and T. E. Lester, *J. Inorg. Nucl. Chem.*, 1967, 29, 2365.
238. E. W. Ainscough and A. M. Brodie, *Coord. Chem. Rev.*, 1978, 27, 59.
239. J. Kincaid, K. Nakamoto, J. A. Tiethof and D. W. Meek, *Spectrochim. Acta, Part A*, 30, 2091.
240. E. A. C. Lucken and M. A. Whitehead, *J. Chem. Soc.*, 1961, 2459.
241. D. Ya. Osokin, I. A. Safin and I. A. Nuretdinov, *Org. Magn. Reson.*, 1972, 4, 831.
242. A. J. Banister and N. N. Greenwood, *J. Chem. Soc.*, 1965, 1534.
243. H. Hess, *Z. Kristallogr.*, 1963, 118, 361.
244. K. Moedritzer and J. R. van Wazer, *Inorg. Chem.*, 1973, 12, 2856.
245. J. P. Costes, G. Cros and J. P. Laurent, *J. Inorg. Nucl. Chem.*, 1978, 40, 829.

246. F. C. Gunderloy and C. E. Erickson, *Inorg. Chem.*, 1962, 1, 349.
247. H. Bürger and W. Sawdony, *Inorg. Nucl. Chem. Lett.*, 1966, 2, 209.
248. H. Bürger, H. Stammreich and Th. Teixeira Sans, *Monatsh. Chem.*, 1966, 97, 1276.
249. D. C. Bradley and M. H. Gitlitz, *Nature*, 1968, 218, 353.
250. H. Bürger and W. Sawdony, *Spectrochim. Acta*, Section A, 1967, 23, 2827.
251. D. C. Bradley and M. J. Hillyer, *Trans. Faraday Soc.*, 1966, 62, 2374.
252. U. Wannagat, *Adv. Inorg. Chem. Radiochem.*, 1965, 6, 225.
253. J. G. A. Luijten, F. Rijkens and G. J. M. van der Kerk, *Organomet. Chem. Rev.*, 1965, 3, 393.
254. W. P. Neumann and K. Kühlein, *Organomet. Chem. Rev.*, 1968, 7, 241.
255. H. Bürger and H. J. Neese, *Chimia*, 1970, 24, 209.
256. D. C. Bradley, *Adv. Inorg. Chem. Radiochem.*, 1972, 15, 259.
257. D. C. Bradley and M. H. Chisholm, *Acc. Chem. Res.*, 1976, 9, 273.
258. E. W. Abel, D. A. Armitage and G. R. Willey, *Trans. Faraday Soc.*, 1964, 60, 1257.
259. J. Mack and C. H. Yoder, *Inorg. Chem.*, 1969, 8, 278.
260. A. W. Jarvie and D. Lewis, *J. Chem. Soc.*, 1963, 1673.
261. C. H. Yoder, D. R. Griffith and C. D. Schaeffer jr., *J. Inorg. Nucl. Chem.*, 1970, 32, 3689.
262. C. H. Yoder and J. J. Zuckerman, *Inorg. Chem.*, 1967, 6, 103.
263. E. W. Randall and J. J. Zuckerman, *J. Am. Chem. Soc.*, 1968, 90, 3167.
264. L. V. Vilkov, N. A. Tarasenko and A. K. Prokof'ev, *Zh. Struct. Khim.*, 1970, 11, 129.
265. D. C. Bradley, M. H. Chisholm, C. E. Heath and M. B. Hursthouse, *J. Chem. Soc., Chem. Commun.*, 1969, 1261.
266. C. Heath and M. B. Hursthouse, *J. Chem. Soc., Chem. Commun.*, 1971, 143.
267. M. H. Chisholm, F. A. Cotton and M. W. Extine, *Inorg. Chem.*, 1978, 17, 1329.
268. J. Fayos and D. Mootz, *Z. Anorg. Allgem. Chem.*, 1971, 380, 196.

269. D. C. Bradley, M. Hursthouse and C. N. Newing, *J. Chem. Soc., Chem. Commun.*, 1971, 411.
270. D. C. Bradley and I. M. Thomas, *J. Chem. Soc.*, 1960, 3857.
271. M. F. Lappert and A. R. Sanger, *J. Chem. Soc.(A)*, 1971, 1314.
272. G. Chandra and M. F. Lappert, *Inorg. Nucl. Chem. Lett.*, 1965, 83.
273. G. Chandra and M. F. Lappert, *J. Chem. Soc.*, 1968, 1940.
274. M. F. Lappert and A. R. Sanger, *J. Chem. Soc.(A)*, 197-, 874.
275. A. D. Jenkins, M. F. Lappert and R. C. Srivastava, *J. Organomet. Chem.*, 1970, 23, 165.
276. H. Schumann, W. W. Du Mont and H. J. Kroth, *Chem. Ber.*, 1976, 109, 237.
277. H. M. J. C. Creemers, F. Verbeek and J. G. Noltes, *J. Organomet. Chem.*, 1968, 15, 125.
278. T. A. George and M. F. Lappert, *J. Chem. Soc., Chem. Commun.*, 1966, 463.
279. T. A. George and M. F. Lappert, *J. Chem. Soc.(A)*, 1969, 992.
280. K. Moedritzer and J. R. van Wazer, *Inorg. Chem.*, 1964, 3, 268.
281. G. M. Burch and J. R. van Wazer, *J. Chem. Soc(A)*, 1966, 586.
282. E. Benzing and W. Kornicker, *Chem. Ber.*, 1961, 94, 2263.
283. H. Bürger and H. J. Neese, *Z. Anorg. Allgem. Chem.*, 1969, 370, 275.
284. H. Bürger, C. Kuess and H. J. Neese, *Z. Anorg. Allgem. Chem.*, 1971, 381, 198.
285. H. Bürger and K. Wiegel, *Z. Anorg. Allgem. Chem.*, 1973, 398, 257.
286. T. Gasparis, H. Nöth and W. Storch, *Angew. Chem. Int. Ed.*, 1979, 18, 326.
287. E. W. Abel, D. A. Armitage, R. P. Bush and G. R. Willey, *J. Chem. Soc.*, 1965, 57.
288. K. Moedritzer, *Organomet. Chem. Rev.*, 1966, 1, 179.
289. G. Chandra, A. D. Jenkins, M. F. Lappert and R. C. Srivastava, *J. Chem. Soc.(A)*, 1970, 2550.
290. W. S. Moore and C. H. Yoder, *J. Organomet. Chem.*, 1975, 87, 389.
291. D. C. Bradley and M. H. Gitlitz, *J. Chem. Soc.(A)*, 1969, 1152.
292. T. A. George and M. F. Lappert, *J. Organomet. Chem.*, 1968, 14, 327.

269. D. C. Bradley, M. Hursthouse and C. N. Newing, J. Chem. Soc., Chem. Commun., 1971, 411.
270. D. C. Bradley and I. M. Thomas, J. Chem. Soc., 1960, 3857.
271. M. F. Lappert and A. R. Sanger, J. Chem. Soc.(A), 1971, 1314.
272. G. Chandra and M. F. Lappert, Inorg. Nucl. Chem. Lett., 1965, 83.
273. G. Chandra and M. F. Lappert, J. Chem. Soc., 1968, 1940.
274. M. F. Lappert and A. R. Sanger, J. Chem. Soc.(A), 197-, 874.
275. A. D. Jenkins, M. F. Lappert and R. C. Srivastava, J. Organomet. Chem., 1970, 23, 165.
276. H. Schumann, W. W. Du Mont and H. J. Kroth, Chem. Ber., 1976, 109, 237.
277. H. M. J. C. Creemers, F. Verbeek and J. G. Noltes, J. Organomet. Chem., 1968, 15, 125.
278. T. A. George and M. F. Lappert, J. Chem. Soc., Chem. Commun., 1966, 463.
279. T. A. George and M. F. Lappert, J. Chem. Soc.(A), 1969, 992.
280. K. Moedritzer and J. R. van Wazer, Inorg. Chem., 1964, 3, 268.
281. G. M. Burch and J. R. van Wazer, J. Chem. Soc(A), 1966, 586.
282. E. Benzing and W. Kornicker, Chem. Ber., 1961, 94, 2263.
283. H. Bürger and H. J. Neese, Z. Anorg. Allgem. Chem., 1969, 370, 275.
284. H. Bürger, C. Kuess and H. J. Neese, Z. Anorg. Allgem. Chem., 1971, 381, 198.
285. H. Bürger and K. Wiegel, Z. Anorg. Allgem. Chem., 1973, 398, 257.
286. T. Gasparis, H. Nöth and W. Storch, Angew. Chem. Int. Ed., 1979, 18, 326.
287. E. W. Abel, D. A. Armitage, R. P. Bush and G. R. Willey, J. Chem. Soc., 1965, 57.
288. K. Moedritzer, Organomet. Chem. Rev., 1966, 1, 179.
289. G. Chandra, A. D. Jenkins, M. F. Lappert and R. C. Srivastava, J. Chem. Soc.(A), 1970, 2550.
290. W. S. Moore and C. H. Yoder, J. Organomet. Chem., 1975, 87, 389.
291. D. C. Bradley and M. H. Gitlitz, J. Chem. Soc.(A), 1969, 1152.
292. T. A. George and M. F. Lappert, J. Organomet. Chem., 1968, 14, 327.

293. M. F. Lappert and B. Prokai, *Adv. Organomet. Chem.*, 1967, 5, 225.
294. S. Sujishi and S. Witz, *J. Am. Chem. Soc.*, 1954, 76, 4631.
295. H. M. Manasevit, U. S. Department Commun., P. B. Report 143, 572. *Chem. Abs.*, 1961, 55, 17333.
296. B. J. Aylett and L. K. Peterson. *J. Chem. Soc.*, 1965, 4043.
297. E. A. V. Ebsworth and H. J. Emeléus, *J. Chem. Soc.*, 1958, 2150.
298. M. F. Lappert and G. Srivastava, *Inorg. Nucl. Chem. Lett.*, 1965, 53.
299. G. R. Willey, *J. Am. Chem. Soc.*, 1968, 90, 3362.
300. J. Hughes and G. R. Willey, *J. Am. Chem. Soc.*, 1973, 95, 8758.
301. D. C. Bradley and M. H. Gitlitz, *J. Chem. Soc.(A)*, 1969, 980.
302. C-C. Hsu and R. A. Geanagel, *Inorg. Chim. Acta*, 1979, 34, 241.
303. D. C. Bradley and A. S. Kasenally, *J. Chem. Soc., Chem. Commun.*, 1968, 22, 1430.
304. R. Tabacchi, L. Vuitel and A. Jacot-Guillarmod, *Helv. Chim. Acta*, 1970, 53, 1495.
305. A. Storr and B. S. Thomas, *Can. J. Chem.*, 1970, 48, 3667.
306. L. J. Bellamy, 'The Infra red spectra of complex molecules', Methuen, London. (1964).
307. A. D. Westland and L. Westland, *Can. J. Chem.*, 1965, 43, 426.
308. A. J. Carty and R. K. Hariss, *J. Chem. Soc., Chem. Commun.*, 1967, 234.
309. M. G. B. Drew, A. P. Wolters and I. Barry Tomkins, *J. Chem. Soc., Dalton Trans.*, 1977, 974.
310. H. Vahrenkamp and H. Nöth, *J. Organomet. Chem.*, 1968, 12, 281.
311. S. Chan, S. Di Stefano, F. Fong, H. Goldwhite, P. Gysegem. and E. Mazzola, *Inorg. Chem.*, 1973, 12, 51.
312. J. R. van Wazer and K. Moedritzer, *J. Inorg. Nucl. Chem.*, 1964, 26, 737.
313. W. Noll. *Ger. Pat.* 825087, *Chem. Abs.*, 1955, 49, 11703.
314. H. Jenker, *Ger. Pat.* 965328, *Chem. Abs.*, 1959, 53, 13065.
315. P. D. Zemaný and F. P. Price, *J. Am. Chem. Soc.*, 1948, 70, 4222.
316. K. Moedritzer, *Adv. Organomet. Chem.*, 1968, 6, 171.

317. K. Schaarshmidt, Z. Anorg. Allgem. Chem., 1961, 310, 69.
318. G. S. Kyker and E. P. Schram, J. Am. Chem. Soc., 1968, 90, 3672.
319. H. Bürger and H. J. Neese, Z. Anorg. Allgem. Chem., 1969, 365, 243.
320. L. H. Sommer, J. D. Citron and G. A. Parker, J. Am. Chem. Soc., 1969, 91, 4729.
321. I. Haiduc, 'The Chemistry of Inorganic Ring systems', Volume 1, Wiley-Interscience, London, (1970).
322. I. Haiduc, 'The Chemistry of Inorganic Ring systems', Volume 2, Wiley-Interscience, London, (1970).
323. B. J. Rowbotham and T. Schaef, Can. J. Chem., 1974, 52, 489.
324. D. R. Armstrong and D. T. Clark, J. Chem. Soc., Chem. Commun., 1970, 99.
325. H. R. Allcock, Chem. Rev., 1972, 72, 315.
326. D. P. Craig and K. A. R. Mitchell, J. Chem. Soc., 1965, 4682.
327. K. Lienhard and E. G. Rochow, Z. Anorg. Allgem. Chem., 1964, 331, 307.
328. K. Baker and G. W. A. Fowles, J. Less-Common Met., 1965, 8, 47.
329. J. A. W. Dalziel, T. G. Hewitt and S. D. Ross, Spectrochim. Acta, 1966, 22, 1267.
330. J. A. W. Dalziel and T. G. Hewitt, J. Chem. Soc.(A), 1968, 93.
331. W. R. Costello, A. T. McPhail and G. A. Sim, J. Chem. Soc(A), 1966, 1190.
332. M. Schmidt and W. A. Schenk, Naturwissenschaften, 1971, 58, 96.
333. W. A. Schenk and M. Schmidt, Z. Anorg. Allgem. Chem., 1975, 416, 311.
334. A. Luttringhaus and W. Killick, Tetrahedron Lett., 1959, 13.
335. J. J. Lagowski, Coord. Chem. Rev., 1972, 22, 185.
336. G. Huttner and B. Krieg, Angew. Chem. Int. Ed., 1971, 10, 512.
337. J. L. Adcock and J. J. Lagowski, Inorg. Chem., 1973, 12, 2533.
338. F. A. Cotton, G. A. Rusholme and G. A. Shaver, J. Coord. Chem., 1973, 99.
339. J. Trotter and S. H. Whitlow, J. Chem. Soc.(A), 1970, 455.
340. W. C. Marsh, N. L. Paddock, C. J. Stewert and J. Trotter, J. Chem. Soc., Chem. Commun., 1970, 1190.

317. K. Schaarshmidt, Z. Anorg. Allgem. Chem., 1961, 310, 69.
318. G. S. Kyker and E. P. Schram, J. Am. Chem. Soc., 1968, 90, 3672.
319. H. Bürger and H. J. Neese, Z. Anorg. Allgem. Chem., 1969, 365, 243.
320. L. H. Sommer, J. D. Citron and G. A. Parker, J. Am. Chem. Soc., 1969, 91, 4729.
321. I. Haiduc, 'The Chemistry of Inorganic Ring systems', Volume 1, Wiley-Interscience, London, (1970).
322. I. Haiduc, 'The Chemistry of Inorganic Ring systems', Volume 2, Wiley-Interscience, London, (1970).
323. B. J. Rowbotham and T. Schaef, Can. J. Chem., 1974, 52, 489.
324. D. R. Armstrong and D. T. Clark, J. Chem. Soc., Chem. Commun., 1970, 99.
325. H. R. Allcock, Chem. Rev., 1972, 72, 315.
326. D. P. Craig and K. A. R. Mitchell, J. Chem. Soc., 1965, 4682.
327. K. Lienhard and E. G. Rochow, Z. Anorg. Allgem. Chem., 1964, 331, 307.
328. K. Baker and G. W. A. Fowles, J. Less-Common Met., 1965, 8, 47.
329. J. A. W. Dalziel, T. G. Hewitt and S. D. Ross, Spectrochim. Acta, 1966, 22, 1267.
330. J. A. W. Dalziel and T. G. Hewitt, J. Chem. Soc.(A), 1968, 93.
331. W. R. Costello, A. T. McPhail and G. A. Sim, J. Chem. Soc(A), 1966, 1190.
332. M. Schmidt and W. A. Schenk, Naturwissenschaften, 1971, 58, 96.
333. W. A. Schenk and M. Schmidt, Z. Anorg. Allgem. Chem., 1975, 416, 311.
334. A. Luttringhaus and W. Killick, Tetrahedron Lett., 1959, 13.
335. J. J. Lagowski, Coord. Chem. Rev., 1972, 22, 185.
336. G. Huttner and B. Krieg, Angew. Chem. Int. Ed., 1971, 10, 512.
337. J. L. Adcock and J. J. Lagowski, Inorg. Chem., 1973, 12, 2533.
338. F. A. Cotton, G. A. Rusholme and G. A. Shaver, J. Coord. Chem., 1973, 99.
339. J. Trotter and S. H. Whitlow, J. Chem. Soc.(A), 1970, 455.
340. W. C. Marsh, N. L. Paddock, C. J. Stewert and J. Trotter, J. Chem. Soc., Chem. Commun., 1970, 1190.

341. H. P. Calhoun, N. L. Paddock, J. Trotter and J. N. Wingfield, J. Chem. Soc., Chem. Commun., 1972, 875.
342. N. K. Hota and R. O. Harris, J. Chem. Soc., Chem. Commun., 1972, 407.
343. H. Schumann and H. Benda, Angew. Chem. Int. Ed., 1970, 9, 76.
344. D. Neubauer and S. Weiss, Z. Anorg. Allgem. Chem., 1960, 303, 28.
345. M. G. B. Drew, D. H. Templeton and A. Zalkin, Inorg. Chem., 1967, 6, 1906.
346. K. W. Bartz, U. S. Pat. 2,947,727, Chem. Abs., 1960, 54, 25976.
347. S. Coffey, (ED.), 'Rodd's Chemistry of Carbon Compounds, Vol. IC', 2nd Edit., Elsevier, Amsterdam, (1965) p.21.
348. I. S. Morozova, G. M. Tarasova, V. V. Ivanovov, E. Bryukova and N. S. Enikolopyan, Dokl. Akad. Nauk. SSSR, 1971, 199, 654. Chem. Abs., 1971, 75, 139907.
349. W. R. Ward, Spectrochim. Acta, 1965, 21, 1311.
350. M. Schmidt, R. Bender, J. Ellerman and H. Gäblein, Z. Anorg. Allgem. Chem., 1977, 437, 149.
351. W. Lindeman, R. Wögerauer and P. Berger, Z. Anorg. Allgem. Chem., 1977, 437, 155.
352. G. Valle, G. Carrazzolo and M. Mammi, Ricerca Scientifica Rendiconti, 1965, 8, 1469.
353. J. R. Ferraro, 'Low-frequency Vibrations of Inorganic and Coordination Compounds', Plenum Press, New York (1971) p. 156.
354. I. R. Beattie and M. Webster, J. Chem. Soc., 1963, 38.
355. M. Schmidt, R. Hender and C. H. Burshka, Z. Anorg. Allgem. Chem., 1979, 454, 160.
356. E. Campaigne, N. F. Chamberlain and B. E. Edwards, J. Org. Chem., 1962, 27, 135.
357. E. W. Abel, M. Booth and K. G. Orrell, J. Chem. Soc., Dalton Trans., 1980, 1582.

358. K. A. Andrianov and A. J. Petrashko, Dokl. Akad. Nauk, SSSR, 1960, 131, 561. Chem. Abs., 1960, 54, 16375.
359. K. A. Andrianov, T. V. Vasil'eva and S. Kh. Korotkevich, Zh. Obsch. Khim., 1962, 32, 2311.
360. H. Nöth, G. Schmidt and Y. Chung, Proc. 8th Int. Conf. on Coordination Chem., (Vienna), 1964, p.180.
361. G. A. Anderson and J. J. Lagowski, Inorg. Chem., 1971, 10, 1910.
362. H. Watanabe, M. Narisada, T. Nakagawa and M. Kubo, Spectrochim. Acta, 1960, 16, 78.
363. L. A. Melcher, J. L. Adcock and J. J. Lagowski, Inorg. Chem., 1972, 11, 1247.
364. N. W. Alcock, M. Pierce-Butler and G. R. Willey, J. Chem. Soc., Dalton Trans., 1976, 707.
365. K. Issleib, G. Wille and F. Krech, Angew. Chem. Int. Ed., 1972, 11, 527.
366. E. M. Ayerst and J. R. C. Dukes, Acta Crystallogr., 1954, 7, 588.
367. B. Long. P. Markey and P. J. Wheatley, Acta Crystallogr., 1954, 7, 140.
368. P. J. Wheatley, J. Chem. Soc., 1965, 396.
369. D. D. Daviel and R. A. Pasternak, Acta Crystallogr., 1956, 9, 334.
370. A. Christensen, H. J. Geise and B. J. van der Veken, Bull. Soc. Chim. Belg., 1975, 84, 1173.
371. D. Rinne and U. Thewalt, Z. Anorg. Allgem. Chem., 1978, 443, 185.
372. J. Archambault and R. Rivest, Can. J. Chem., 1958, 36, 1461.
373. A. Clearfield and E. J. Malkiewicz, J. Inorg. Nucl. Chem., 1963, 25, 237.
374. W. Gerrard, M. F. Lappert and J. W. Wallis, J. Chem. Soc., 1960, 2141.
375. W. E. Bull, S. K. Madan and J. E. Willis, Inorg. Chem., 1963, 2, 303.
376. C. S. Kraihanzel and S. C. Grenda, Inorg. Chem., 1965, 4, 1037.
377. E. L. Meutterties and E. G. Rochow, J. Am. Chem. Soc., 1953, 75, 490.
378. M. Martinette, S. Mizushima, C. Curran and J. V. Quagliano, Spectrochim. Acta, 1959, 11, 77.

379. W. Gerrard, M. F. Lappert, M. Pyszora and J. W. Wallis, *J. Chem. Soc.*, 1960, 2144.
380. E. L. Meutterties, *J. Am. Chem. Soc.*, 1960, 82, 1082.
381. S. C. Jain and R. Rivest, *J. Inorg. Nucl. Chem.*, 1967, 29, 2787.
382. G. Peyronel, A. C. Fabretti and G. C. Pellacani, *Spectrochim. Acta*, Part A, 1974, 30, 1723.
383. S. O. Wandiga, L. S. Jenkins and G. R. Willey, *J. Inorg. Nucl. Chem.*, 1979, 41, 941.
384. G. C. Pellacani, G. Peyronel, W. Malavasi and L. Menabue, *J. Inorg. Nucl. Chem.*, 1977, 39, 1855.
385. G. Peyronel, G. C. Pellacani, A. Pignedoll and G. Benetti, *Inorg. Chim. Acta*, 1971, 5, 263.
386. G. Peyronel, G. C. Pellacani, G. Benetti and G. Pollacci, *J. Chem. Soc.*, Dalton Trans., 1973, 879.
387. G. C. Pellacani, G. Peyronel and W. Malavasi, *Inorg. Chim. Acta*, 1974, 8, 49.
388. G. Peyronel, G. C. Pellacani and G. Pignedoll, *Inorg. Chim. Acta*, 1971, 5, 627.
389. G. C. Pellacani, *Can. J. Chem.*, 1974, 52, 3454.
390. A. J. Aarts, H. O. Desseyn and M. A. Herman, *Inorg. Chim. Acta*, 1978, 29, L197.
391. A. C. Fabretti, G. C. Pellacani and G. Peyronel, *J. Inorg. Nucl. Chem.*, 1971, 33, 4247.
392. G. Peyronel, A. C. Fabretti and G. C. Pellacani, *J. Inorg. Nucl. Chem.*, 1973, 35, 973.
393. G. C. Pellacani and W. Malavasi, *J. Inorg. Nucl. Chem.*, 1975, 37, 477.
394. R. Rivest, *Can. J. Chem.*, 1962, 40, 2234.
395. H. O. Desseyn and M. A. Herman, *Spectrochim. Acta*, Part A, 1967, 23, 2457.
396. H. O. Desseyn, W. A. Jacob and M. A. Herman, *Spectrochim. Acta*, Part A, 1969, 25, 1685.

397. R. N. Hurd, G. de la Mater, G. C. McElheny, R. J. Turner and V. H. Wallingford, *J. Org. Chem.*, 1961, 26, 3980.
398. G. Wilkinson and J. M. Birmingham, *J. Am. Chem. Soc.*, 1954, 76, 4281.
399. J. S. Washburne and W. R. Peterson, *J. Organomet. Chem.*, 1970, 21, 59.
400. R. Cass and G. E. Coates, *J. Chem. Soc.*, 1952, 2347.
401. R. J. Kern, *J. Inorg. Nucl. Chem.*, 1962, 24, 1105.
402. M. Ciampolini and N. Nardi, *Inorg. Chem.*, 1966, 5, 41.
403. H. Schumann and L. Rösch, *Chem. Ber.*, 1974, 107, 854.